2017

GENETIC ANALYSIS OF *SERF* GENE FUNCTION IN *Drosophila melanogaster* AND ITS CONTRIBUTION TO A FLY MODEL OF SPINAL MUSCULAR ATROPHY

Swagata Ghosh
University of Kentucky, reach.swagatag2016@gmail.com
Digital Object Identifier: https://doi.org/10.13023/ETD.2017.034

STUDENT AGREEMENT:

I represent that my thesis or dissertation and abstract are my original work. Proper attribution has been given to all outside sources. I understand that I am solely responsible for obtaining any needed copyright permissions. I have obtained needed written permission statement(s) from the owner(s) of each third-party copyrighted matter to be included in my work, allowing electronic distribution (if such use is not permitted by the fair use doctrine) which will be submitted to UKnowledge as Additional File.

I hereby grant to The University of Kentucky and its agents the irrevocable, non-exclusive, and royalty-free license to archive and make accessible my work in whole or in part in all forms of media, now or hereafter known. I agree that the document mentioned above may be made available immediately for worldwide access unless an embargo applies.

I retain all other ownership rights to the copyright of my work. I also retain the right to use in future works (such as articles or books) all or part of my work. I understand that I am free to register the copyright to my work.

REVIEW, APPROVAL AND ACCEPTANCE

The document mentioned above has been reviewed and accepted by the student's advisor, on behalf of the advisory committee, and by the Director of Graduate Studies (DGS), on behalf of the program; we verify that this is the final, approved version of the student's thesis including all changes required by the advisory committee. The undersigned agree to abide by the statements above.

Swagata Ghosh, Student

Dr. Brian C. Rymond, Major Professor

Dr. David Westneat, Director of Graduate Studies

GENETIC ANALYSIS OF *SERF* GENE FUNCTION IN *Drosophila melanogaster* AND ITS CONTRIBUTION TO A FLY MODEL OF SPINAL MUSCULAR ATROPHY

DISSERTATION

A dissertation submitted in partial fulfillment of the requirements for the degree of Doctor of Philosophy in the College of Arts and Sciences at the University of Kentucky

By

Swagata Ghosh

Lexington, Kentucky

Director: Brian C. Rymond

Lexington, Kentucky

2017

ABSTRACT OF DISSERTATION

GENETIC ANALYSIS OF *SERF* GENE FUNCTION IN *Drosophila melanogaster* AND ITS CONTRIBUTION TO A FLY MODEL OF SPINAL MUSCULAR ATROPHY

The *Serf* gene is evolutionarily highly conserved but its biological function is not known in any organism. In human, *SERF1/H4F5* was first identified as a modifier of the disease Spinal Muscular Atrophy (SMA). SMA is caused by mutations in the Survival Motor Neuron 1(*SMN1*) gene leading to diminished levels of the *Smn* protein. More than 90% of patients with the most severe form of SMA have deletions that remove *SERF1* as well as mutaions within *SMN1*. Hence, loss of *Serf* activity is hypothesized to exacerbate SMA disease progression. The primary motivation of this thesis was to test this intriguing but yet unverified hypothesis using a model organism, *Drosophila melanogaster*.

To genetically manipulate *Serf* activity I created deletion, overexpression and knockdown alleles of *Serf*. I found that *Serf* is non-essential for viability in *Drosophila* and that null mutants have no obvious developmental defects. However, the loss of *Serf* gene activity results in diminished adult locomotion. In addition, *Serf* null mutants show lower *Smn* protein abundance. As *Smn* mRNA levels do not change with *Serf* manipulation, regulation likely occurs at the level of *Smn* protein translation or stability.

I tested the impact of *Serf* in SMA by altering *Serf* expression in a fly SMA model harboring equivalent *Smn* point mutations as those that cause SMA in human patients. I found that diminished *Serf* levels exacerbate the observed mutant phenotype in growth, development and viability which correlates with decreased *Smn* protein abundance. Importantly, the simple overexpression of *Serf* in certain *Smn* mutant backgrounds increases the *Smn* protein abundance, which in some cases, correlates with a partial rescue of the associated phenotypic defects. In addition to being required for maximal *Smn* abundance, I found that *Serf* gene expression directly correlates with the abundance of toxic α-synuclein protein seen in a fly Parkinson's disease model. These data support a role for *Serf* in protein homeostasis relevant to proteins active in at least two distinct neurodegenerative diseases.

My study has also revealed that *Serf* influences lifespan in *Drosophila*. Loss of *Serf* reduces lifespan by 20-30% whereas ubiquitous overexpression of *Serf* results in an equivalent extension of the normal lifespan. Lifespan extension occurs even when *Serf* overexpression is restricted to muscles, neurons or only adult tissues. Change in lifespan with *Serf* manipulation inversely correlates with the accumulation of poly-ubiquitinated protein aggregates, a marker of tissue aging. These aggregates are marked with Ref(2)p/p62, a target of autophagy. Analysis of expression of several genes in the

autophagy pathway suggests that *Serf* expression may promote longevity, at least in part, by upregulating the life-extending autophagy pathway. *Serf* gene expression also correlated with a modest resistance to oxidative stress and changes in the abundance of a mitochondrial marker protein, mitofusin, suggesting the possibility that *Serf* activity may impact mitochondrial function. Taken together, these studies establish *Serf* as a modifier of the *Smn*-limited SMA phenotype and reveal previously unknown roles for the *Serf* gene in *Drosophila* mobility and lifespan.

Key words: *Serf*, *Smn*, Spinal Muscular Atrophy, Lifespan, Protein abundance.

SWAGATA GHOSH

03/06/2017
Date

GENETIC ANALYSIS OF *SERF* GENE FUNCTION IN *Drosophila melanogaster* AND ITS CONTRIBUTION TO A FLY MODEL OF SPINAL MUSCULAR ATROPHY

By

Swagata Ghosh

Brian C. Rymond
Director of Dissertation

David F. Westneat
Director of Graduate Studies

03/06/2017
Date

This dissertation is dedicated to my mother Mrs. Suparna Ghosh, my father Mr. Kamal Kanti Ghosh, my husband Dr. Daipayan Banerjee and my daughter Aarini Banerjee.

ACKNOWLEDGEMENTS

This dissertation would not be complete without the continuous help and support of many. I would like to express my heartfelt appreciation to all of them who helped me in this journey.

I am very grateful to my advisor Dr. Brian C. Rymond for his continuous support towards my intellectual growth and development during my graduate education. Without his guidance and training, I would not be able to achieve a successful completion of my dissertation. I would also like to thank my committee members, Drs Douglas Harrison, Pete Mirabito and Arthur Hunt, for their thoughtful insights into my dissertation work all along. Also, I am very grateful to Dr. Bruce Downie for his time and help in my doctoral examination.

I have been very fortunate to be a part of the Biology department which literally served as my second home in a foreign country. The great team of biology faculty have always been extremely resourceful in my graduate educations. My heartfelt gratitude towards Dr. Douglas Harrison for his endless help with *Drosophila* laboratory resources and scientific feedbacks. Also, Drs. Ann Morris, Robin Cooper, Vincent Cassone, Jakub Famulski, Edward Rucker, Jeremiah Smith and Bruce O'Hara deserve special mention for helping me with various scientific methods. The present and past biology staff members including Jacquie Burke, Jacqueline Lee, Seth Taylor, Beverly Taulbee and Cheryl Edwards have been the pillars of our department and made it a little easier for me to survive through the stressful days of graduate school.

My dissertation would not have been possible without the contribution of a number of undergraduate students. I would like to thank Alice Blevins, Katie Thacker, Mason Johnson, Matthew Antel, Riley Cutler, Sarah Milian, Heather Feese, Grace Babbs, Karen Lyle and Nathan Horrel for their effort and enthusiasm towards my research. I would also like to mention the contribution of my fellow graduate student colleagues and friends Dr. Josh Titlow and Cole Malloy in my research. My graduate life would not be happier without the love and support of my friends in the department, Drs. Min Chen, Qian Chen, Lakshmi Pillai, Wenwen Wen, Stephen Wilson, Amber Hale to name a few.

Finally, the support of my mother Suparna Ghosh and my father Kamal Kanti Ghosh has been the constant source of strength and inspiration all throughout my Ph.D. They always believed in me and inspired me to overcome the difficulties that came along the way. They travelled across thousands of miles to help me reach the finish line during my final days of Ph.D. I will be ever grateful to them for all their sacrifices for giving me a brighter future. Last but not the least, I could not have made it if I did not have my husband Dr. Daipayan Banerjee standing beside me through thick and thin of life. His love, support, faith and patience were the source of my motivation towards chasing my dreams. I also thank him for giving me such loving and caring parents in laws who always supported me in reaching my academic goals. I could not be more complete at the end of this journey without our beautiful daughter, Aarini Banerjee, who taught me how to become a mother, above and beyond everything. She is the ultimate reward of my graduate life.

TABLE OF CONTENTS

LIST OF TABLES

LIST OF FIGURES

Chapter 1: Introduction

1.1 Spinal Muscular Atrophy: Spinal Muscular Atrophy (SMA), the leading genetic cause of human infant (*Homo sapiens*) mortality is caused by homozygous loss of the gene Survival Motor Neuron 1 (*SMN1*). This disease affects one in every 10,000 livebirths, one in every 50 being a carrier (Pearn 1980, Ogino, Leonard *et al*. 2002). It is characterized by the loss of motor neurons in the anterior horn region of the spinal cord leading to progressive muscle atrophy, paralysis and death. To date, there is no effective treatment for this debilitating disease. However, advances in medical technology and the molecular understanding of the disease pathogenesis has expanded the scope of therapy. Addressing critical unanswered questions in the biology of the disease is necessary for further therapeutic development.

1.1.1 Clinical manifestation and molecular pathogenesis

SMA is clinically divided into four types based on the age of disease onset and extent of motor functions loss: 1) type I (severe); 2) type II (intermediate); 3) type III (mild); 4) type IV (very mild) (Russman 2007, Wang, Finkel *et al*. 2007). About 50% of patients diagnosed with SMA have the most severe form, type I, which is also known as Werdnig-Hoffman-disease (Markowitz, Tinkle *et al*. 2004). Type I SMA affects patients before 6 months of age and death occurs within first 2 years of life. Patients have no control of head movement and are unable to sit without support. Difficulty in breathing, poor feeding capabilities combined with decreased airway protection and increased risk of aspiration pneumonia are major causes of morbidity and mortality. Type II, the intermediate form, shows onset by 7 to 18 months of age. Patients can sit without aid but unable to walk and death occurs during adolescence. Type III, the mild Kugelberg-

Welander disease, starts after 18 months of age where patients usually attain maximum motor milestones including walking and live up to adult age. The adult onset type IV is the mildest form that begins in the second or third decade of life and shows mild motor impairment without respirational and nutritional problems.

SMN was first identified as the SMA disease causing gene in 1995 (Lefebvre, Burglen *et al*. 1995), soon after the disease locus was mapped to chromosome 5q13 (Brzustowicz, Lehner *et al*. 1990, Melki, Abdelhak *et al*. 1990). There are two versions of the SMN gene, *SMN1* (Telomeric) and *SMN2* (Centromeric). There is always one copy of the *SMN1* gene per haploid genome, although the copy number of the *SMN2* gene is variable (1-6 copies) in the human population due to duplication and gene conversion events (Lunn and Wang 2008). The *SMN1* and *SMN2* genes differ by 5 nucleotides only one of which resides in the 1.7 kb coding region. This coding sequence change does not, however, alter the amino acid sequence (Lefebvre, Burglen *et al*. 1995, Burglen, Lefebvre *et al*. 1996). Both genes contain 9 exons and 8 introns and code for a 38 kD protein with 294 amino acid. The *SMN1* gene is expressed ubiquitously in all somatic tissues and is highly phylogenetically conserved (Schrank, Gotz *et al*. 1997, Miguel-Aliaga, Culetto *et al*. 1999, Paushkin, Charroux *et al*. 2000).

In spite of the presence of multiple *Smn* coding genes in the human genome, homozygous loss of *SMN1* has been shown to cause SMA in 98% cases (Hahnen, Forkert *et al*. 1995, Lefebvre, Burglen *et al*. 1995).These patients always retain at least one copy of *SMN2*. However, SMN2 transcripts undergo alternative splicing due to a C to T transition at position six of exon seven resulting in exon skipping, giving rise to a truncated protein (fig. 1.1)(Lorson, Hahnen *et al*. 1999, Lorson and Androphy 2000). A**s**

only about 10% of *SMN2* pre-mRNA is properly spliced to produce the functional full length SMN protein (Lefebvre, Burglen *et al*. 1995)**,** *SMN2* alone cannot compensate for the loss of the *SMN1* gene.

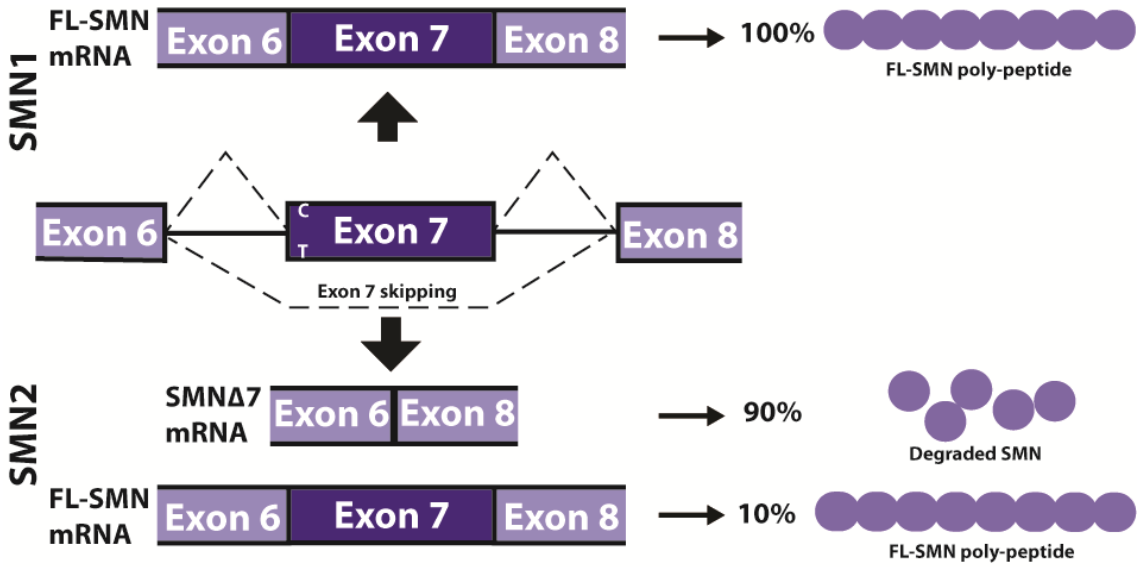

Figure 1.1 Schematic representation of SMN1 and SMN2 splicing and its impact at the protein level. Magnified view of exon 6-8 of *SMN1* and *SMN2* pre-mRNA. The C-T transition in *SMN2* favors exon 7 skipping (90%) while 10% full length *SMN2* is formed. Therefore, 90% of SMN2 protein is truncated and is rapidly degraded. SMN1 pre-mRNA on the other hand is properly spliced and produces 100% functional protein.

SMN is a multi-domain protein (figure 1.2) consisting of an N terminal lysine (K)-rich domain, a central Tudor domain, a C-terminal tyrosine-glycine (YG)-box and the exon 7 encoded domains (Renvoise, Khoobarry *et al*. 2006). The Tudor domain, highly conserved among different RNA binding proteins, mediates SMN's interaction with arginine-glycine (RG)-motifs of several proteins including the Sm core proteins of UsnRNP complexes [Reviewed in (Meister and Fischer 2002, Gubitz, Feng *et al*. 2004)]. LSm/Sm proteins constitute the core of the spliceosomal U rich snRNP complexes by binding onto their target snRNA molecules in the form of a heptameric ring (Hermann, Fabrizio *et al*. 1995, Salgado-Garrido, Bragado-Nilsson *et al*. 1999).

Although the LSm/Sm ring structure assembles spontaneously in presence of their target snRNA *in vitro* (Raker, Plessel *et al*. 1996, Raker, Hartmuth *et al*. 1999), inside cells it is tightly regulated by a large macromolecular entity, called the SMN complex. The SMN protein interacts with itself and eight other proteins including Gemin 2-8 and Unrip to form this huge 1MDa complex (Meister, Buhler *et al*. 2000, Otter, Grimmler *et al*. 2007). In this complex SMN directly binds Gemin 2, 3, 5 and 7 whereas Gemin 4, 6,8 and Unrip interacts indirectly with Smn (Baccon, Pellizzoni *et al*. 2002, Paushkin, Gubitz *et al*. 2002, Pellizzoni, Baccon *et al*. 2002, Gubitz, Feng *et al*. 2004). In addition to the SMN complex components, SMN protein directly interacts with many other proteins that serve as substrates for the complex. The Gemin5 protein is known to contain 13 WD-repeat domains and hence is thought to serve as a platform for direct interaction among the substrates, like the set of seven LSm/Sm proteins and the SMN core in the complex (Paushkin, Gubitz *et al*. 2002). The Sm proteins are known to be methylated by the methylosome which produces symmetrical dimethyl arginines that directs them to the

SMN complex (Meister, Buhler *et al*. 2001); (Friesen, Paushkin *et al*. 2001). The SMN complex binds the LSm/Sm proteins to promote the formation of the heptameric ring structure of the Sm-core proteins. (Meister, Buhler *et al*. 2001, Meister and Fischer 2002, Pellizzoni, Yong *et al*. 2002). Newly transcribed (m^7G)-capped U rich snRNAs are exported to the cytoplasm where they bind to the SMN complex containing the Sm-core proteins. The SMN complex then transfers the Sm-core onto the UsnRNAs to generate the UsnRNP particle. This step is required for cap hyper-methylation of UsnRNAs to form the (m3G)-cap structure necessary for its nuclear import. The SMN complex remains bound to the UsnRNP particles until they are imported back to nucleus, thus assisting in essentially all steps of UsnRNP biogenesis (Paushkin, Gubitz *et al*. 2002). The assembly of the functional U rich snRNP complex involved in pre-mRNA splicing is the best characterized housekeeping function of the SMN protein.

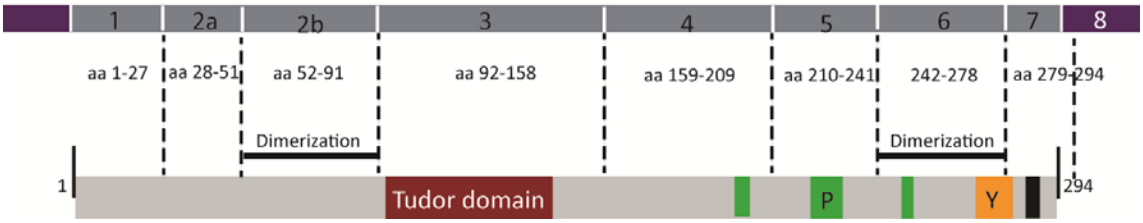

Figure 1.2 The exon boundaries of the *SMN1* gene and domain structure of the SMN protein. Top: SMN protein is encoded by 9 exons, the coding region is shown in grey and the untranslated regions in purple. **Bottom**: The black bars indicate the domains required for oligomerization of SMN; the Tudor domain is shown in brown; the poly-proline domains are in green, the orange box represents YG box domain and the cytoplasmic targeting motif is shown in black.

Inhibited snRNP assembly due to SMN deficiency has been shown in SMA patients and disease models (Pellizzoni, Yong *et al*. 2002, Gabanella, Butchbach *et al*. 2007). With the help of biochemical *in vitro* assay for ATP dependent snRNP assembly and changes in the relative levels of snRNAs have been shown to occur with reduced SMN abundance, a change that is believed to underlie the splicing defects. (Pellizzoni, Yong *et al*. 2002, Gabanella, Butchbach *et al*. 2007). SMA patient derived cell lines show reduced accumulation of a subset of UsnRNPs (major class- U1, U2 and U4 snRNPs) correlated with diminished SMN levels (Wan, Battle *et al*. 2005). This feature is recapitulated in the brain and spinal cord of a mouse SMA model, such that the degree of snRNP assembly impairment correlates with the disease severity (Gabanella, Butchbach *et al*. 2007). Here, the level of radiolabeled U1-snRNA, immune-precipitated from *in vitro* U1-snRNP assembly reaction mix was shown to reduce in the tissue extracts of SMA mice (*Mus musculus*) as compared to the control mice. Inhibited snRNP biosynthesis has also been shown to cause specific loss of motor neurons in *Xenopus* and zebrafish embryonic model (Winkler, Eggert *et al*. 2005). Moreover, restoration of normal snRNP levels by injecting purified UsnRNPs into *SMN* or *Gemin-2* deficient embryos, provides phenotypic rescue in both *Xenopus tropicalis* and zebrafish (*Danio rerio*) models. Similarly genetic introduction of a functional SMN derivative capable of snRNP assembly rescued the SMA phenotype with correlated increase in the snRNP and snRNA levels in mice (Winkler, Eggert *et al*. 2005, Workman, Saieva *et al*. 2009). Consistent with inhibited spliceosomal snRNP biosynthesis, widespread changes in the alternate splice forms in various tissues of SMA mice, not just neuronal tissue, were observed (Zhang, Lotti *et al*. 2008). However, another study concluded SMN deficiency

appears to preferentially reduce the assembly of minor U12 dependent snRNPs (Gabanella, Butchbach *et al*. 2007, Zhang, Lotti *et al*. 2008). For instance, altered splicing and mRNA expression of a U12 intron containing SMN target, Stasimon, is seen in the motor circuit of SMA mice (Lotti, Imlach *et al*. 2012). This target gene is necessary for SMN dependent motor circuit function in flies (*Drosophila melanogaster*) and Zebrafish, thereby postulating a mechanistic basis for motor neuron selectivity in SMA (Lotti, Imlach *et al*. 2012).

Other functions of *SMN* critical for motor neuron survival have also been postulated. It has been shown that SMN localizes in the ribonucleoprotein granules within the growth cones and neurites of cultured primary or ES cell derived motor neurons (Fan and Simard 2002, Zhang, Xing *et al*. 2006). The observation that these granules undergo bidirectional transport to the neuronal processes and growth cones (Zhang, Xing *et al*. 2006) leading to the hypothesis that SMN is necessary for localized RNA processing and translation of proteins within long neurons. Evidence in support of this idea comes from the finding that diminished SMN level reduces β-actin mRNA and protein titers in the axons and growth cones, possibly by inhibiting transportation of β-actin containing ribonucleoprotein complexes containing SMN (Rossoll, Kroning *et al*. 2002, Rossoll, Jablonka *et al*. 2003). The deficiency of β-actin causes axonal outgrowth and pathfinding defect in SMA cell culture (Zhang, Pan *et al*. 2003) and the zebra fish model system (McWhorter, Monani *et al*. 2003). In addition, SMN interacts with Profillin IIa (Lambrechts, Braun *et al*. 2000), the predominant neuronal isoform of an actin binding protein (Sharma, Lambrechts *et al*. 2005) in distinct granules within the neurites and growth cones. Neuronal Profillin IIa regulates actin dynamics and axonal outgrowth.

Mutant SMN fails to interact with Profillin IIa(Sharma, Lambrechts *et al*. 2005). A number of *Drosophila melanogaster* models of SMA have also demonstrated defective neuromuscular junction and skeletal muscle features (Chan, Miguel-Aliaga *et al*. 2003, Gunadi, Sasongko *et al*. 2008) thereby postulating specific roles for SMN protein in maintaining the integrity of neuromuscular junctions.

While the SMN1 transcript is efficiently spliced to produced full-length SMN protein, the major product of SMN2 pre-mRNA splicing is a truncated SMNΔ7 transcript (Lorson, Hahnen *et al*. 1999, Lorson and Androphy 2000) which gives rise to a smaller protein lacking YG-box domain responsible for self-association (Talbot, Ponting *et al*. 1997, Lorson, Strasswimmer *et al*. 1998, Martin, Gupta *et al*. 2012) (Lorson, Strasswimmer *et al*. 1998). SMN self-association and integration into the larger SMN-Gemin complex stabilizes the SMN protein by inhibiting its degradation via the ubiquitin proteasome pathway (Chang, Hung *et al*. 2004, Burnett, Munoz *et al*. 2009). Consequently the SMNΔ7 protein is very unstable and cannot protect motor neurons from *SMN1* loss (Burnett, Munoz *et al*. 2009). In addition to the SMN2 product, there are a number of SMA disease states arising from deletion or point mutation of the YG box domain of SMN1 (Burghes 1997) that diminishes SMN self-association, complex formation and hence its stability (Praveen, Wen *et al*. 2014, Gupta, Martin *et al*. 2015).

1.1.2 Genetic modifiers of SMA

Genetic modifiers of a disease reflect allelic distinctions in the genetic background of individuals that enhance or suppress the primary phenotype (Suzuki, Kashiwagi *et al*. 2004). Certain modifiers protect the affected individual from expressing the full disease phenotype, a phenomenon known as incomplete penetrance (of the

primary mutant allele). There are several different ways by which genetic modifiers can influence the primary disease gene. They can directly alter the expression of the disease causing gene by affecting mRNA/protein synthesis, processing or stability. Alternatively the modifier protein can impact different aspects of the biological function of the causative protein relevant to the disease pathogenesis. SMA is a monogenic human disorder with a wide range of severity. The identification of novel genetic modifiers modulating the SMA phenotype can expand our understanding of this devastating genetic disorder and may lead to the development of novel screening or therapeutic approaches.

The *SMN2* gene is the main modifier of SMA severity identified to date and hence the primary target of therapy. While all SMA patients carry homozygous loss of *SMN1* gene function, the *SMN2* copy number varies from at least one up to six within European population because of gene duplication or conversion (Wirth, Brichta *et al*. 2006, Wirth, Brichta *et al*. 2006, Khoo and Krainer 2009, Alias, Bernal *et al*. 2011). As the SMN2 gene produces a small amount of functional SMN protein it is not surprising that disease severity reduces with *SMN2* dosage (Feldkotter, Schwarzer *et al*. 2002, Wirth, Brichta *et al*. 2006). Within certain populations, sequence variations within the *SMN2* cis-regulatory elements influence the *SMN2* gene transcription or exon 7 splicing increase or decrease the amount of full length *SMN2* product and hence modify the disease phenotype (Wirth, Brichta *et al*. 2006). In addition, changes in the expression of trans-regulatory factors like splice enhancers (SF2/ASF) or repressors (hnRNP A1) also act on *SMN2* expression by influencing *SMN2* splicing (Nlend Nlend, Meyer *et al*. 2010) thereby modifying the disease. The expression of *SMN2* transcript also depends on the level of methylation and acetylation found on the CpG islands within *SMN2* promoter which varies and negatively

correlates with the disease severity in patients with identical *SMN2* copy number (Wirth, Brichta *et al*. 2006, Hauke, Riessland *et al*. 2009).

Increasing the expression of full length SMN protein from the *SMN2* gene, has been the major focus of SMA therapeutics. It has been targeted by promoting appropriate splicing of the *SMN2* transcript by technologies involving small RNA based reprogramming of splicing; for example- antisense oligonucleotide, bidirectional RNA technology and trans-splicing (Skordis, Dunckley *et al*. 2003, Baughan, Shababi *et al*. 2006, Dickson, Osman *et al*. 2008, Khoo and Krainer 2009, Coady and Lorson 2010). The use of small molecules in increasing exon 7 inclusion during *SMN2* splicing, although found to be beneficial *in vitro*, did not have much effect *in vivo* (Arnold and Burghes 2013). However, small molecules like quinazoline derivatives have been shown to act as a *SMN2* promoter activating compound that successfully increases SMN levels *in vitro* and in SMNΔ7 mouse model (Cai, Ash *et al*. 2005, Butchbach, Singh *et al*. 2010). In addition, inhibitors of histone deacetylase (HDACi) like VPA that upregulate *SMN2* transcription *in vitro* have been shown to improve motor function and increase survival by 15-30% in animal models (Brichta, Hofmann *et al*. 2003, Sumner, Huynh *et al*. 2003, Hahnen, Eyupoglu *et al*. 2006, Riessland, Brichta *et al*. 2006, Avila, Burnett *et al*. 2007, Garbes, Riessland *et al*. 2009, Riessland, Ackermann *et al*. 2010).

An analysis of the transcriptome of siblings with identical *SMN1/SMN2* genetic make-up but different phenotypic expression, one being affected and the other asymptomatic, revealed another protective modifier of SMA in human, *Plastin3*. *Plastin 3* or *PLS3*, an F actin bundling protein that influences the G/F actin ratio is necessary during axonal growth and pathfinding (Dent and Gertler 2003, Oprea, Krober *et al*.

2008). Genetic interaction between *PLS3* and *SMN* have been shown to be conserved in *Caenorhabditis. elegans* and *Drosophila* where RNAi mediated knockdown of *PLS3* enhanced *SMN* loss of function defects in both invertebrate systems (Chang, Dimlich *et al*. 2008, Dimitriadi, Sleigh *et al*. 2010). *PLS3* overexpression has been shown to rescue the axonal growth defect in Zebrafish SMA model with diminished SMN level (Oprea, Krober *et al*. 2008, Hao le, Wolman *et al*. 2012) as well as in cultured motor neurons from SMA mouse embryo (Oprea, Krober *et al*. 2008). A mouse model of SMA overexpressing *PLS3* revealed that the NMJs of SMA mice are defective in F-actin associated cellular processes like axonal connectivity at the NMJ, which is rescued by *PLS3* overexpression. *PLS3* overexpression counteracts the poor axonal connectivity observed in SMA NMJs and facilitates maturation of the neuromuscular junctions (NMJs) (Ackermann, Krober *et al*. 2013). Thus *PLS3* establishes a classic example of a genetic modifier, the discovery of which significantly expanded the knowledge about molecular pathogenesis of the disease.

In addition to identifying modifier genes from patient population, unbiased genetic screens were also undertaken in an attempt to uncover new modifiers in powerful invertebrate models. Both *Drosophila* and *C. elegans* have one copy of *SMN* ortholog, the loss of which causes larval lethality, positively correlated with alterations in the architecture and activity of the neuromuscular junctions (Miguel-Aliaga, Culetto *et al*. 1999, Chan, Miguel-Aliaga *et al*. 2003, Rajendra, Gonsalvez *et al*. 2007, Chang, Dimlich *et al*. 2008, Dimitriadi, Sleigh *et al*. 2010). In *Drosophila* neuronal or muscle specific expression of *SMN* is sufficient to significantly rescue larval lethality with correlated improvement in the neuromuscular phenotypes (Chang, Dimlich *et al*. 2008). Similarly in

C. elegans loss of function of *SMN* causes larval lethality and neuromuscular defects. The neuromuscular defects are rescued by expressing transgenic SMN in the neurons but muscle specific expression of SMN does not rescue them as effectively (Briese, Esmaeili *et al*. 2009). Loss of function alleles in both of these systems therefore serve as very good models to screen for genetic modifiers. A P element insertion screen in *Drosophila* revealed 17 enhancers and 10 suppressor of SMA, a subset of which were shown to affect SMN dependent NMJ phenotype (Chang, Dimlich *et al*. 2008). Among these was a type II receptor of BMP signaling pathway, *wishful thinking (wit)*, the insertion mutant of which enhanced SMA NMJ defects (Chang, Dimlich *et al*. 2008). They further showed that altered expression of other members of the BMP pathway, *Mad* and *Dad*, which increase BMP signaling rescues NMJ defects associated with *SMN* loss of function (Chang, Dimlich *et al*. 2008). A subsequent genome-wide RNAi screen in *C. elegans* identified four new modifier genes namely *ncbp-2* (Cap binding protein 20), *flp4-* (FARFamide family neuropeptide protein), *grk-2* (G protein coupled receptor kinase), and *T02G5.3* (gene of unknown function) the knockdown of which enhanced the growth defect associated with *SMN* loss of function allele (Dimitriadi, Sleigh *et al*. 2010). Moreover depletion of *ncbp-2* and *flp-4* showed conservation in enhancing SMA defects in the *Drosophila* system (Dimitriadi, Sleigh *et al*. 2010). Conversely many SMA enhancing modifiers initially identified in the *Drosophila* P element insertion screen (Chang, Dimlich *et al*. 2008) were found to enhance the growth and neuromuscular function defect of a SMN loss of function allele in *C. elegans* (Dimitriadi, Sleigh *et al*. 2010). The *C. elegans* study on SMA modifiers (Dimitriadi, Sleigh *et al*. 2010) also proposed an interaction map of SMA modifiers showing two basic biological processes

impacting the SMA state. These are endocytosis and translational control and are hypothesized to coordinate synaptic activity and receptor signaling with local translation during neuronal development and maintenance (Kong, Wang *et al*. 2009, Dimitriadi, Sleigh *et al*. 2010). Impaired synaptic vesicles release consistent with defects in synaptic vesicle endocytosis at the NMJs has been documented in severe SMA mice (Kong 2009). However, what features of SMN function are responsible for these defects and whether SMN is involved in the possible functional interaction of endocytosis and local translational regulation is not yet known.

1.1.3 The *SERF* gene- A candidate modifier of SMA

In spite of the advances made in understanding SMA, some critical questions remain to be answered. Why are reduced SMN levels specifically detrimental for motor neuron survival? Does *SMN* have a non-snRNP assembly function critical for motor neuron maintenance or activity? What is the mechanistic basis for variable severities seen in SMA?-Genetic studies, such as candidate modifier genes identification and analysis offers the means to address some of these questions.

The *SERF* coding gene in humans, *H4F5*, was first discovered in a population genetic screen for genetic modifiers of SMA (Scharf, Endrizzi *et al*. 1998). *SERF*/*H4F5* is located adjacent to the *SMN* locus within a 500 kb inverted duplication of chromosome 5 (Fig 1.3). Two copies are present, 6.5 kb upstream of both *SMN1* (telomeric copy) and *SMN2* (centromeric copy) (Scharf, Endrizzi *et al*. 1998). The majority of type I SMA patients have deletions in the 5q13 locus that remove *SMN1* and adjacent sequences leaving *SMN2* and adjacent markers intact. Marker C212, used to define SMA deletion is located 13kb upstream of *SMN* exon1 (Scharf, Endrizzi *et al*. 1998). Scharf *et al*. showed

that this marker is embedded within the last intron of *SERF/H4F5*, 3 kb upstream of *H4F5* exon 3b. They showed that 94% of the type I SMA patients carried *SMN1* deletions extending through C212 and hence including part or all of *H4F5*. Exon3b of *H4F5* is actually 5 kb closer to *SMN1* than C212 and therefore the frequency of *H4F5* is possibly under-represented in this study. Deletions within another neighboring gene *NAIP*, were not correlated with the SMA phenotype. Based on these observations *SERF/H4F5* was proposed to be a significant candidate modifier of SMA severity (Scharf, Endrizzi *et al*., 1998).

The *SERF* gene is phylogenetically highly conserved. *SERF* gene codes for two alternate isoforms due to alternate splicing. In human the larger 1.8 kb isoform codes for 110 amino acids protein whereas the shorter 0.7 kb codes for a protein 62 amino acid long. The shorter isoform, more commonly found across species, is ubiquitously expressed including the central nervous system in humans (Scharf *et al*., 1998). The longer isoform also shows similar expression profile (Scharf *et al*., 1998). Based on a Kyte-Doolittle secondary protein structure analysis program, they predicted that the *SERF* protein forms a helix-turn-helix structure rich in lysine and arginine residues and potentially has nucleic acid binding properties. This protein does have a low level of homology with the RNA binding domain of matrin-cyclophilin, a protein known to co-localize with spliceosomal snRNPs and other components of splicing machineries (Mortillaro and Berezney 1998) and the yeast SERF protein co-purifies with two known splicing factors, Prp8 and Brr2. To date, however, no biological function is known or predicted for *SERF* in any organism. It is not uncommon to find genes in eukaryotic

organisms that encode conserved proteins with no known biological function. *SERF* encodes one of these mysterious proteins possibly important for human health.

Figure 1.3 Genetic map of the SMA locus. The chromosomal 5q13 region containing two large inverted chromosomal fragment (black horizontal bar). The telomeric copy contains the SMN1 gene (shown in blue) and the centromeric copy contains the SMN2 gene. The *SERF1* genes (shown in red) are located adjacent to *SMN1* and *SMN2*. The multicopy microsatellite markers are shown in red.

1.2 *SERF* function in protein homeostasis

Apart from *Serf*'s connection with SMA, it was found to be implicated in the 'protein misfolding diseases', in which mutations within a specific peptide or protein leads to its improper folding and aggregation into highly organized aggregates called amyloids (Chiti and Dobson 2006, Vendruscolo, Knowles *et al*. 2011). In an attempt to identify positive regulators of amyloid protein aggregation, Van-Ham *et al*. used a *C.elegans* model of poly-Q expansion disease and performed a chemical mutagenesis screen to identify loss of function mutations that suppress aggregate formation and related toxicity (van Ham, Holmberg *et al*. 2010). They found that point mutation and deletion mutation of the *C. elegans* ortholog of human *SERF, MOAG-4,* greatly reduced the amount of the Poly-Q aggregates and the locomotion defect, associated with Poly-Q toxicity in these worms (van Ham, Holmberg *et al*. 2010). Two other disease related proteins, amyloid-β (Alzheimer's disease) and α-synuclein (Parkinson's disease), showed reduced amount of aggregated proteins in *MOAG-4* mutant worms. In addition, they analyzed the different oligomeric states of the Poly-Q aggregates that differed in size and SDS solubility in wild type and *MOAG-4* mutants and found that soluble compact aggregate intermediates are significantly reduced in the mutant worms (van Ham, Holmberg *et al*. 2010). In a follow-up study by Falsone *et al*., 2012, the shorter isoform of *SERF* was shown to promote amyloid assembly of diverse structurally unrelated aggregation prone proteins in an *in-vitro* system. Presence of *SERF* was shown to accelerate the process of initial nucleation of the fibers and also to increase the accumulation of large aggregated species (Falsone, Meyer *et al*. 2012). Thus, together these studies propose that *SERF* functions in promoting

amyloid aggregation, however, *SERF*'s natural function in the absence of these exogenous disease causing proteins remained largely unexplored.

One hypothesis is that the SERF protein functions within the cellular protein homeostasis network, since a growing pool of evidence supports the idea that amyloid aggregation is an active cell surveillance mechanism that protects cells from toxic misfolded proteins (Chen, Retzlaff *et al*. 2011). It has been shown, for instance, that soluble misfolded oligomers of amyloid-β peptide, but not the larger aggregates, confer cytotoxicity possibly initiated by membrane permeabilization (Glabe 2006). Moreover, cytoplasmic inclusions of mutant androgen receptor protein (AR) involved in spinobulber muscular atrophy was shown to confer a cytoprotective role (Taylor, Tanaka *et al*. 2003). Terminal aggregation of misfolded proteins is thought to be necessary for their autophagy mediated removal from cells (Welchman, Gordon *et al*. 2005). In fact, soluble and insoluble protein aggregates have been shown to partition between distinct subcellular compartments,- that specify their subsequent proteolytic degradation by either the ubiquitin proteasomal system (UPS) or autophagy, respectively (Kaganovich, Kopito *et al*. 2008). Thus factors involved in the process of protein aggregation and turnover might functionally interact to maintain the quality of the cellular proteome. Given SERF's hypothesized function in amyloid aggregation, it is conceivable that SERF could influence other aspects of protein homeostasis.

1.3 SERF's genetic interaction with Ubiquitin Proteasome pathway factors in yeast:

Saccharomyces cerevisiae does not have a *SMN* homologue but contains a single copy of the *SERF* gene which codes for a small protein, 69 aa in length. In yeast the *SERF* gene (*ySERF*) is non-essential and has been found to co-purify with two essential

splicing factors Ppr8p, Brr2p (Krogan, Cagney *et al*. 2006). The y*SERF* protein's association with Prp8p and Brr2p implies its potential role in modulating their function and hence in cellular splicing. However, based on our previous analysis we think, *ySERF* has only a minor, if any, role in cellular splicing (Ghosh & Rymond unpublished). A systematic genome wide screen to identify *ySERF*'s genetic interactions revealed previously unknown genetic associations of *ySERF* with a Ub protease and a Ub-protease cofactor, *UBP6* and *BRE5,* respectively (Rymond & Boone, unpublished). *UBP6* is a ubiquitin protease that physically associates with the proteasome and functions to recycle and maintain the cellular free pool of ubiquitin (Hanna, Leggett *et al*. 2003). *BRE5* and its associated ubiquitin protease *UBP3* is required for selective autophagic degradation of ribosomes under nutrient starvation. (Kraft, Deplazes *et al*. 2008). Interestingly, Prp8p is the only known spliceosomal component undergoing ubiquitination (Bellare, Kutach *et al*. 2006). Its Ub conjugation is known to stabilize the U4/U6-U5 tri-snRNP level by suppressing Brr2p mediated U4/U6 unwinding (Bellare, Small *et al*. 2008). The recovery of *ySERF* with these Ub-sensitive effectors of post-transcriptional regulatory factors and its genetic interactions with cellular proteolytic factors suggest a possible role in ubiquitin-proteasome system (UPS) or other ubiquitin-sensitive steps in protein function or removal.

1.4 Hypotheses about *SERF* gene function:

The primary motivation behind my dissertation project is to provide the very first test of the hypothesis that *SERF* is an authentic modifier of the SMA phenotype. Given SERF's hypothesized function in protein homeostasis pathways (protein aggregation and degradation), it is conceivable that SERF could be relevant to the stability of the Smn

protein, which depends upon oligomerization to prevent its ubiquitin-directed protein degradation by the proteasome (Burnett, Munoz *et al*. 2009). To test this idea, I will use the *Drosophila melanogaster* model system and, in my studies, also investigate the uncharacterized biological function of eukaryotic SERF protein. *Drosophila melanogaster* provides an excellent invertebrate model system to address these questions as it is readily amenable to genetic manipulation. Moreover, unlike human cells, *SMN* and *SERF* are single copy genes in *Drosophila* (henceforth, *Smn* and *Serf*, according to established fly nomenclature rules). Also, the established fly SMA model display conserved features of the disease pathogenesis and provides an ideal system for genetic interaction studies. With this study I hope to shed light on how SMN activity may be regulated in SMA and potentially add to the clinical targets used for disease screening or intervention. In addition, investigation of the natural function of Serf protein in *Drosophila* could potentially provide insight into the evolutionary significance of its conservation.

Hypothesis 1: The phylogenetically conserved *Serf* gene is important for the normal growth, development or physiology of *Drosophila melanogaster.*

Hypothesis 2: The *Serf* gene modulates SMA severity by stabilizing *SMN* protein abundance.

Specific Aims: The major specific aims of my dissertation are to determine: i) if altered *Serf* expression(deletion, overexpression and knock down) effect *Drosophila* viability, development, locomotion behavior, adult lifespan and stress response; ii) if *Serf* genetically interacts with Smn in the Smn-limited fly model of SMA.

Chapter 2: The *Serf* gene in *Drosophila* is non-essential for viability or fertility.

2.1 Introduction

The putative modifier of SMA, *SERF1*, is conserved across species but the natural biological function is not known in any organism. What we know from studies in human patients and the *C. elegans* model of human neurodegenerative diseases is that *SERF* might have a potential role in SMA pathogenesis and protein homeostasis (Scharf, Endrizzi *et al*. 1998, van Ham, Holmberg *et al*. 2010). Although in *S. cerevisiae* (Kastenmayer, Ni *et al*. 2006) and *C. elegans*, *SERF* is non-essential for viability (van Ham, Holmberg *et al*. 2010), whether it is essential in insects or higher organisms is not known. Therefore, the logical question to ask was- is the *Serf* gene essential for viability or development in *Drosophila melanogaster*? A standard reverse genetic approach was used to answer this question. This required the creation of null mutants of *Serf* in *Drosophila*. The likely Serf ortholog was first identified by sequence comparison and then deletion alleles were created by imprecise P element excision (O'Brochta *et al*., 1991). To complement the *Serf* deletion study I created a *Serf* cDNA transgenic for UAS-GAL4 based mis-expression studies. In addition, a UAS-*Serf* RNAi construct was also used for knocking down *Serf* in GAL4 driven manner. This chapter is focused on describing the generation and preliminary characterization of these various *Serf* alleles. Specifically, the molecular analyses at the transcript and protein expression levels are presented along with quantitative analysis of viability and locomotor activity of the mutants at various developmental stages.

2.2 Results

2.2.1 Identification of the Serf orthologue in *Drosophila melanogaster*

The **s**mall **E**DRK **r**ich **f**actor or **Serf** family of proteins is highly conserved across phylogeny. There are 2 copies of the *SERF1* gene in humans- *SERF1A* and *SERF1B.* Both genes encode two protein products due to alternative splicing, a longer isoform (Accession number: NP_001171558), 110 amino acids in length, and a shorter isoform (Accession number: NP_075267), 62 amino acids in length. We sought to identify the *Drosophila* ortholog of SERF1 by searching for homology with both the long and the short isoforms of human SERF1 protein sequence using BLASTP. We identified a *Drosophila* gene, CG17931 (FlyBase ID: FBgn0038421, Accession number: NM_001300436.1), that encodes a protein showing maximum homology with the shorter isoform of SERF1 protein. The existence of this gene product is also reported in the FlyBase EST cDNA clones (FBtr0083323). This protein shows 81% sequence similarity and 65% sequence identity with the human presumptive ortholog over 80% of the sequence Fig. 1A. The longer isoform of the human SERF1, when aligned with the protein sequence of CG17931, showed 78% similarity and 65% identity over 60% of the sequence – the reduced homology is due to the missing carboxyl terminal amino acids in the fly protein.

Given this sequence similarity with the human SERF1 protein, we named the gene encoded by CG17931 as *Serf*. Shown in the figure below (Fig 1A) is the deep conservation in the protein sequences of the Serf orthologs from different eukaryotic species. As shown in the representative sequence alignment, the N terminal segment of

this small protein is highly conserved among species ranging from budding yeast (*S. cerevisiae*), to plants (*Arabidopsis thaliana)* to humans (*Homo sapiens*).

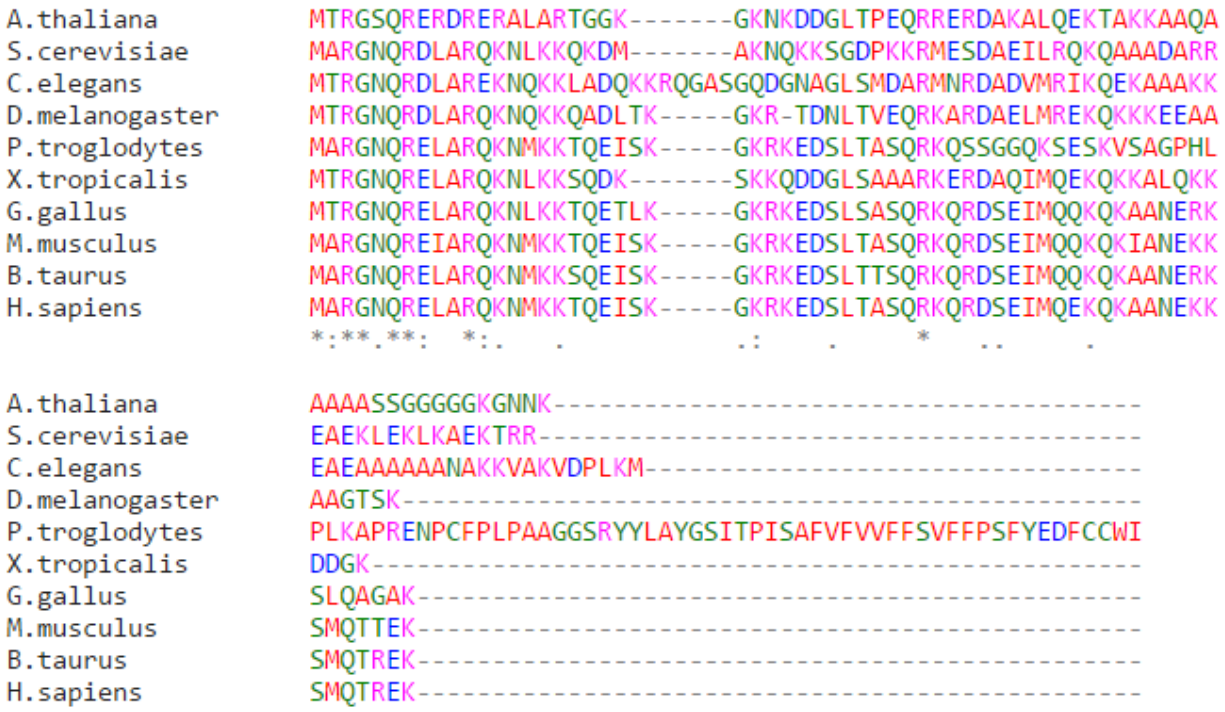

Fig 2.1. The *SERF1* gene is phylogenetically highly conserved. Multiple sequence alignment of the *Drosophila* Serf protein with orthologs from different taxa using Muscle multiple alignment program that uses log-expectation scoring function. Alignment shows the deepest evolutionary conservation within the N terminal region. '*' (Asterisk) indicates identical residues; ':' (Colon) indicates conservation among groups with strongly similar properties; '.' (Period) indicates conservation among groups with weakly similar properties. Color code: Red- Small hydrophobic; Blue-Acidic; Magenta- Basic-H; Green- Hydroxyl, Sulfhydryl, Amine, G.

2.2.2 Generation of the *Serf* deletion allele by P-element excision

The *Serf* deletion mutants were created by a P-element mobilization screen (O'Brochta, Gomez *et al*. 1991). P elements are natural autonomous transposable elements in *Drosophila*, 2907 bps in length with 31 bp terminal inverted repeats and 11 bp sub-terminal inverted repeats. Collections of fly strains are available with P-element insertions at specific sites covering much of the fly genome (Bellen, Levis *et al*. 2011). When mobilized by co-expression of functional P-transposase, the P-element can be precisely excised, leaving a wildtype gene copy or imprecisely excised, resulting in local deletions or partial element excisions or other chromosomal rearrangements.

The P-element insertion line CG17931^{EY09918}, obtained from the Bloomington Stock Center, harbors an insertion in the 5' untranslated region, 150 bases upstream of the transcription start site of the CG17931/*Serf* gene (Fig 2.2B). The scheme of crosses that served to mobilize this P element is described in figure 2.2A. The mobilization screen is based on the loss of y+ and w+ marker genes carried by the P element which, when excised, changes the body color and eye color from wild type brown and red to yellow and white, respectively. First, at the P_0 generation the transposase expressing Δ2-3 line was crossed with the P element insertion line, CG17931^{EY09918}, to create progeny expressing the active transposase carrying the P-element. The P element mobilizes in the somatic and germline cells of these progeny. Several males from this progeny displaying mottled red and white eyes due to somatic excision events and a few balancer females (yw, Ly/TM3 Sb) were crossed at the P_1 generation. Four hundred such bulk P_1 crosses with multiple males in each were set. Excision alleles were identified in the progeny of the P_1 crosses by the simultaneous loss of y+ and w+ markers. For each P_1 vial, three

excision flies (male or female) were isolated and individually crossed with balancer flies, thus establishing the F_1 generation. A total of three hundred and forty eight P_1 vials were screened to establish 2 or 3 F_1 crosses for each vial named as A, B and C. Balanced siblings from each F_1 cross were then mated to establish the stocks of individual excision events at the F_2 generation. Two hundred and ninety six F_2 stocks were established to screen for *Serf* deletion and precise excision lines.

DNA was extracted from homozygous P-element excision adult fly lines to score for *Serf* deletion by the polymerase chain reaction (PCR) using primers flanking the native *Serf* locus. Figure 2.2B describes the location of these primers on the scale map of the *Serf* gene. A description of the primer pairs and their predicted amplicon sizes based on the genotypes are described in table 2.1. For each primer set, DNA isolated from a completely wild type line (WT) and the initial P element insertion line (EY09918) were used as controls. A control pair of primers from a different locus (*Unpaired3* gene) was used to test the quality of the genomic DNA extracted from each of the lines. Different sets of *Serf* specific primers were used (see Table 2.1) for identification of potential deletions, cross-verification of the results from each primer set and isolating deletions that are contained within the gene coding region. The primer set 2 (A+C) and 3 (A+B) were used for preliminary screening candidate deletions. 'A' binds to the first intron within the *Serf* gene. Paired with primer C that binds to the first exon, it amplifies a region spanning the P element insertion site and paired with B which binds within the first intron amplifies from the first intron most proximal to the transcription initiation site. Absence of an amplicon for both sets of primers would be suggestive of a deletion event causing loss of one or both primer binding sites.

Figure 2.2C shows a representative gel image of the PCR based screen. Analysis of this figure is summarized in Table 2.2. Using primer pair A+C and A+B, here I determine that the DNA corresponding to lane 10 or 16 (same DNA samples in both lanes but used in PCR with different sets of primers) and 12 or18 are potential precise excisions while DNA that corresponds to lanes 9 or 15 and 11 or 17 with no amplicons for either primer sets represent potential *Serf* deletions. In summary I identified 12 potential deletions, 56 potential precise excisions and 4 lines with left-over P element at the insertion site (Example not shown here).

Further characterization with primer pairs 4, 5 and 6 (See Table 2.1) reveals that only 2 out of the 12 lines contained the deletion within Serf coding region. One example is shown in figure 2.2C (lane 20) where a candidate deletion produced a band of 500 bps, instead of 1500 bps with primer set C+H (H binds to a region beyond *Serf* gene) suggesting that the deletion within this line is possibly confined within the *Serf* region and takes out most of the coding region ($Serf^{\Delta 10a}$, also called 10a). The other smaller deletion produced about 1000 bps amplicon with C+H (data not shown), instead of 1500 bps, suggesting about 500 bps within the *Serf* coding region is possibly lost in this line ($Serf^{\Delta 6c}$, also called 6c).

Next we sequenced 5 lines, 2 candidate deletions (10a, 6c) and 3 candidate precise excisions (8b, 13a, 26b) to identify the deletion boundaries and verify wildtype *Serf* sequence in the candidate precise excision lines. As predicted by our PCR analysis the mutant 6c was found to be a 571 bps deletion within the *Serf* locus that includes the *Serf* transcription start site, the first intron and most of the second exon which codes for most of the Serf protein (Fig 2.2B). Mutant 10a is similar but deletes 1051 bps within the *Serf*

gene including the start codon, the whole of the coding region and a portion of the 3' untranslated region (Fig 2.2B). Given the loss of much/all of the Serf coding sequence, the 6c and 10a alleles were chosen as null alleles for subsequent development and behavior studies. In the precise excision controls, the Serf coding region is intact and as commonly seen with P-element excision, a12 bps P-element derived inverted repeat is present at the site of the original insertion. The precise excision line PE26B was chosen as an isogenic control for the null alleles in our subsequent experiments. Since the two Serf deletion mutants are viable and fertile I conclude that *Serf* is not an essential gene of *Drosophila melanogaster*.

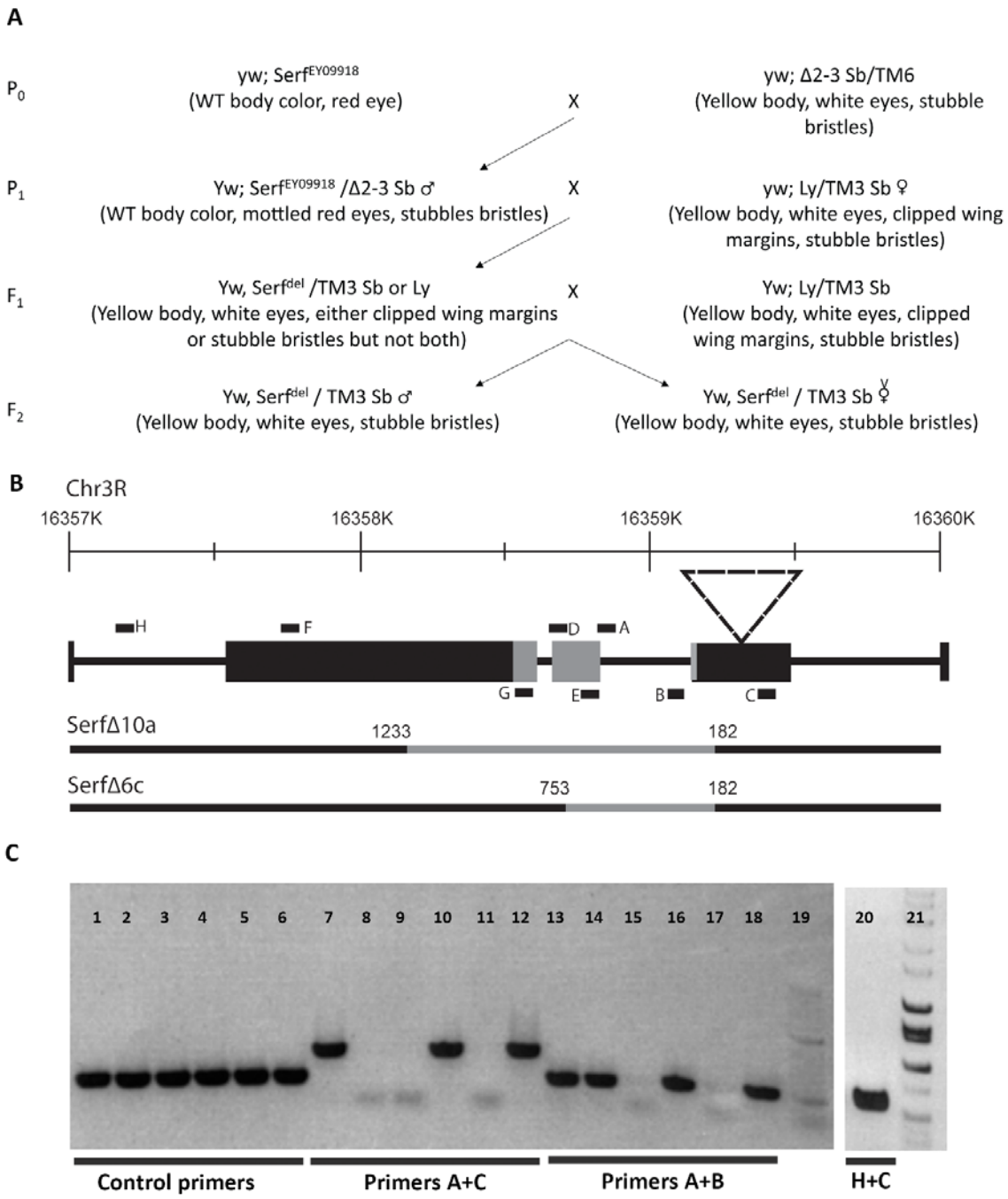

Fig 2.2. Generation of the *Serf* deletion lines by P element excision screen: (A) The scheme of crosses to drive P element excision and generate potential excision lines for screening. (B) Illustration of the Serf gene structure, mapped to the scale on chromosome 3, right arm. The *Serf* gene is located at 3R: 16357535..16359466 in the minus orientation

and contains 3 exons, shown in boxes and 2 introns shown in bars. The gray region within the boxes indicate protein coding sequence. The small bars indicate the primer binding sites for PCR based screening. The triangle indicate the site (3R: 16359291) of P element insertion. The bars below correspond to the Serf deletions 10a and 6c, the two independently derived lines. The deleted region for each mutant is shown by the gray bar and the numbers flanking them indicate the nucleotide positions within the Serf genomic locus- the 1st nucleotide of the 1st exon being positioned at chromosomal co-ordinate 16359466. (B) Representative agarose gel image showing PCR based screening. Amplifications with different sets of primers are indicated below the lanes. Lanes 1, 7 and 13 contains the wild type control (yw); lanes 2, 8 and 15 contains the P element insertion line Serf^{EY09918} ; Lanes 3-6, 9-12 and 15-18 contains test samples in the same order for 3 different primer sets. Lane 20 shows amplification from *Serf*$^{\Delta 10a}$ locus with primer set C+H; lane 21 shows molecular weight marker.

Table 2.1 describes the primer pairs used in the excision screen with predicted amplicon sizes for the respective genotypes (EY00918 represents the initial *Serf*^{EY09918} P element insertion line). For preliminary screening (representative shown in figure 2.2C) primer set 2 and 3 were used. Primer set 3, 4 and 5 were used for further characterization of the potential deletions identified from the preliminary screens. '-' represents absence of a band and '+/-' represents absence or presence of a band for which the amplicon size cannot be predicted.

Set	Primer Pair	Spanned region contains	Predicted Size (bps)			
			WT	**EY09918**	**Precise Excision**	***Serf* Deletion**
1	Control	*Unpaired 3* region	**300**	**300**	**300**	**300**
2	A+C	P element insertion site	**500**	**-**	**500**	**-**
3	A+B	1st intron	**328**	**328**	**328**	**-**
4	D+E	2nd exon	**106**	**106**	**106**	**+/-**
5	G+F	3rd exon	**460**	**460**	**460**	**+/-**
6	C+H	Entire coding region	**1500**	**-**	**1500**	**+/-**

Table 2.2 summarizes the analysis of the representative gel image in figure 2.2C showing a preliminary PCR based screen. '+' & '-' represents presence and absence of an amplicon, the predicted sizes of which are described in table 2.1. Amplifications from the control and test DNA samples were run in the same order for all three primer pairs. Lanes for the corresponding genotypes are indicated in parenthesis. Test DNA samples corresponding to the lanes 10 & 16 and 12 & 18 produce band predicted for precise excision with both primer sets, hence these are strong candidates for precise excision alleles. Similarly, the test DNA samples corresponding to the lanes 9 & 15 and 11 & 17 fails to produce a band with either primer set as expected for the potential deletion mutants. Hence, these two DNA samples are strong candidates for *Serf* specific deletion.

Primer Pair	**Control DNA Samples**		**Test DNA Samples**	
	WT	**EY09918**	**Potential Precise excision**	**Potential *Serf* deletions**
Control (lanes 1-6)	+ (lane 1)	+(lane 2)	+	+
A+C (lanes 7-12)	+(lane 7)	-(lane 8)	+(lanes 10,12)	-(lanes 9,11)
A+B (lanes 13-18)	+(lane 13)	+(lane14)	+(lanes 16,18)	-(lanes 15,17)

2.2.3 Generation of *Serf* cDNA expression alleles

Apart from the null mutants we also created a *Serf* cDNA expression allele in flies. This line was not only necessary to complement our genetic studies with the null mutant, but also served as a rescue line for complementation experiments. Moreover, we wanted to know if tissue or developmental stage specific mis-expression of the *Serf* cDNA construct would produce a mutant phenotype. In order to do so, we employed the standard UAS-GAL4 bipartite gene expression tool in *Drosophila*.

The UAS-GAL4 system takes advantage of the GAL4 based transcriptional regulation of galactose inducible genes like GAL10 and GAL1 in yeast, which depends on the binding of GAL4 transcription factor to four related 17 bps sequences collectively known as the Upstream Activating Sequences (UAS). Here the expression of the gene of interest, the responder, is controlled under the UAS element, which in this case is five tandemly arrayed and optimized GAL4 binding sites. The GAL4 gene is expressed in a separate transgenic, the driver, where it's expression in spatially and temporally controlled. Crossing these two lines would produce progeny where the responder gene will be expressed in a pattern that matches the GAL4 expression pattern in the respective driver (Figure 2.3). One of the major strengths of this approach is the astounding array of the driver lines that have been created by the enhancer-trap GAL4 construct generated by Brand and Perrimon, 1993. This allows us to use a wide diversity of genomic regulatory sequences to drive gene expression in almost every major tissue type in *Drosophila*. A number of modifications were done to the UAS-GAL4 system to increase the specificity of the spatial and temporal regulation of gene expression. In our study (described in chapter 3) we have also used the Geneswitch-GAL4 drivers that use a GAL4-progesteron

receptor human p65 activation domain chimera, where the GAL4 activity is induced upon binding to an appropriate ligand and the UAS-responder is subsequently expressed (Han *et al*., 2000;Osterwalder etal.,2001;Roman etal.,2001) (Figure 4) .

We created the UAS-Serf cDNA transgenic line by cloning and genomic insertion. The *Serf* cDNA clone (SD16330: was obtained from Bloomington stock center, FlyBaseID: FBcl0276419) as a clone within the pOT2 vector. I sub-cloned the *Serf* cDNA sequence into the pUAST vector (described in materials and methods) which was then used for embryo injection by Duke University Model System Genomics. We used the AttB40 fly line for targeted injection at the 25C6 site (Bateman *et al*., 2008), located on the right arm of the 2nd chromosome.

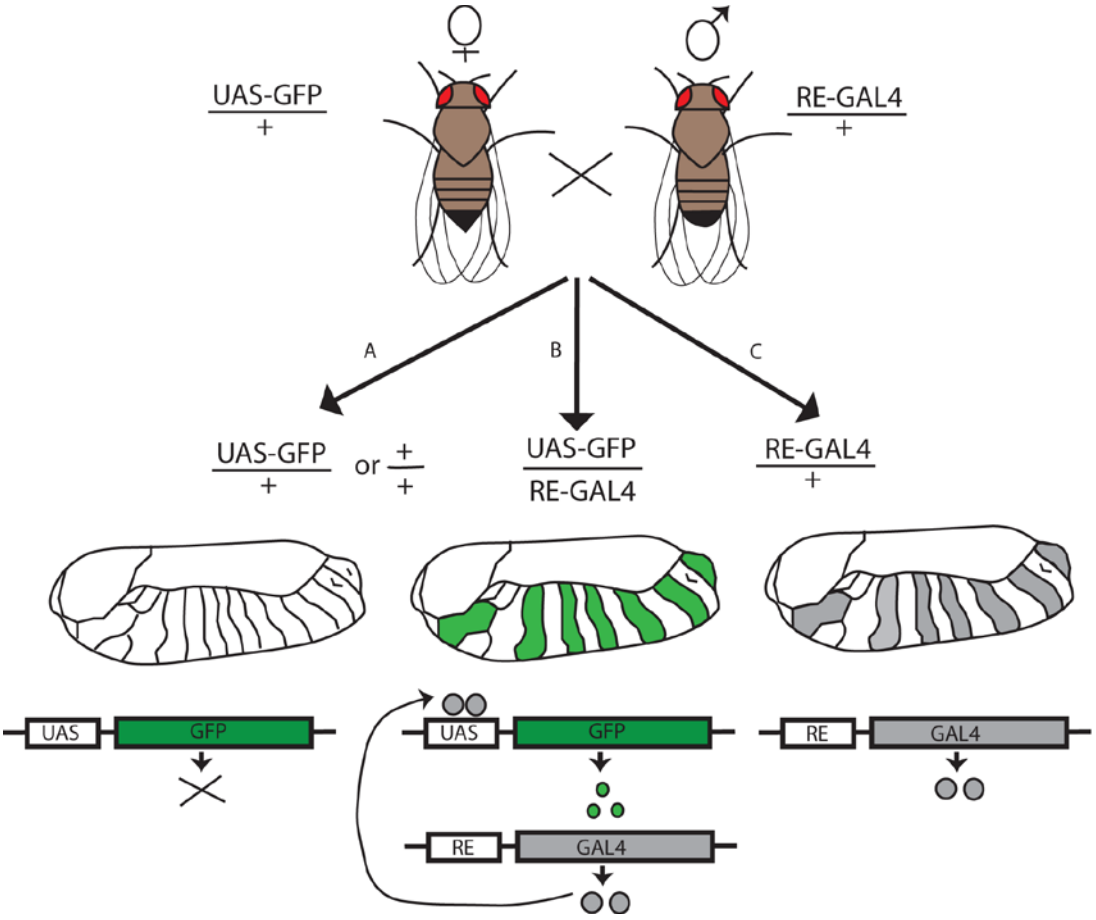

Fig 2.3. Schematic representation of the UAS-GAL4 system (Adapted and modified from Duffy 2002)**.** Females carrying the UAS responder gene (UAS-GFP), when mated with males carrying the GAL4 driver (RE-GAL4) produces the following progeny. A) The progeny with either wild type chromosomes or one copy of UAS-GFP, do not express GFP as there is no GAL4 protein to turn on the UAS-GFP transgene. B) The progeny carrying both the driver and responder elements express GFP, as the GAL4 protein binds UAS and activates GFP transcription. The GFP is expressed in a segmental pattern in the depicted embryo as GAL4 protein expression is restricted within the corresponding segments by the regulatory element (RE). C) The progeny with only the

RE-GAL4 driver transgene expresses GAL4 in a segmental pattern in the depicted embryo, but does not have the UAS-GFP to activate.

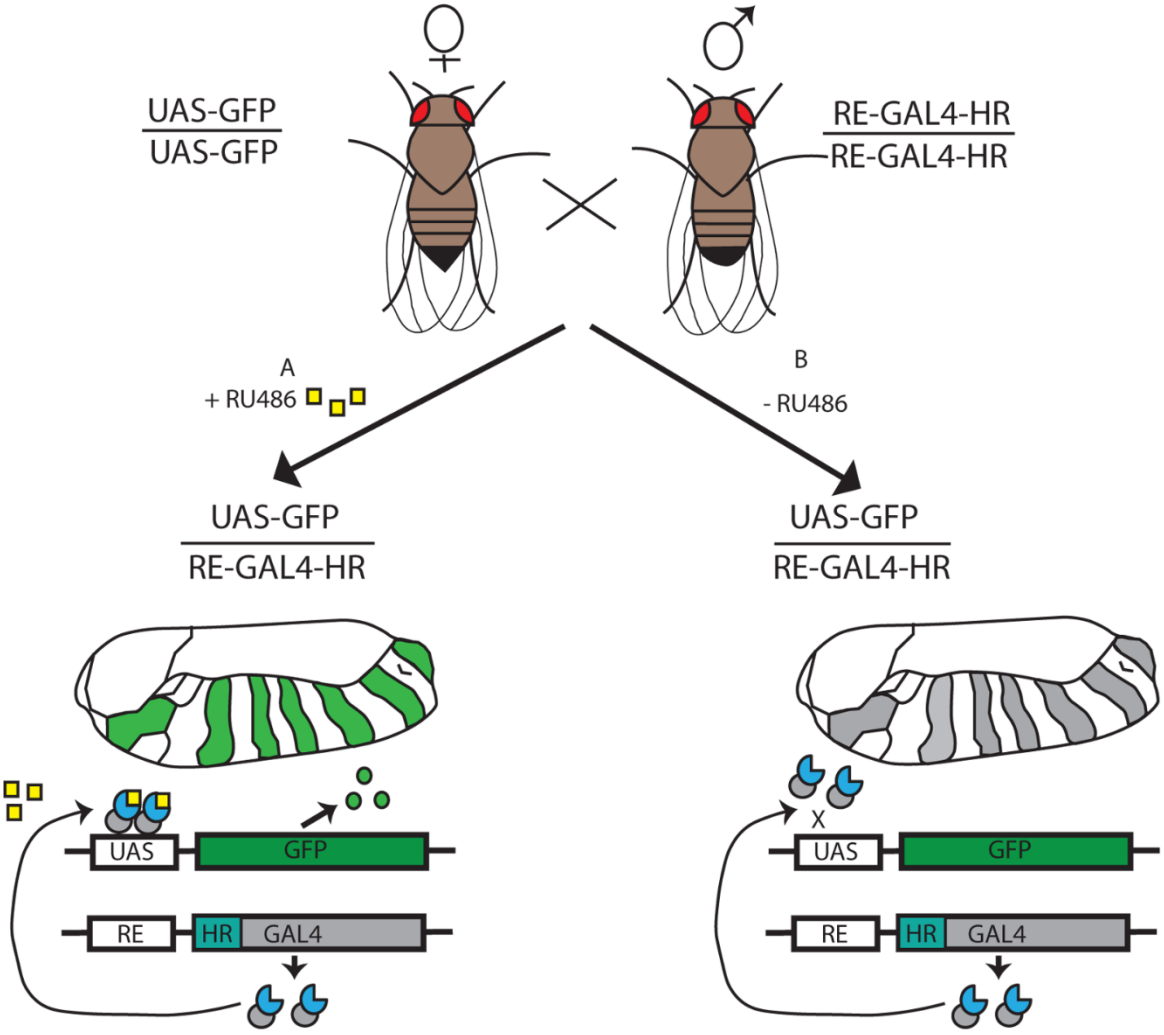

Fig 2.4 Schematic representation of the Geneswitch GAL4 system (Adapted and modified from Duffy 2002)**.** A slight modification to the standard UAS-GFP system, where the GAL4 is fused with a hormone responsive element. (A) In the presence of the drug RU486 the fusion GAL4 protein can bind to the UAS and activate the responder gene. (B) In the absence of the drug RU486 the fusion GAL4 protein is incapable of

binding to UAS and hence cannot activate the responder. This modification fine tunes the temporal regulation of gene expression.

2.2.4 Validation of the *Serf* deletion and cDNA expression alleles

Next I validated the *Serf* alleles by assessing transcript and protein expression in flies that contain the null allele or that express the *Serf* cDNA. To assess the levels of *Serf* mRNA I used northern blotting. Fifteen µg of total RNA extracted from whole flies were analyzed for the presence of *Serf* transcript. Figure 2.5A shows the results of the northern blot analysis with radiolabeled probe complementary to regions in the second exon of the *Serf* transcript which constitutes bulk of the *Serf* coding region. The level of ribosomal RNA in 15µg of total RNA is presented to show the quality of RNA yield for each line, also used as loading control. Here I detect a band for the wild type control w^{1118} (lane 1) and the precise excision control PE26B (lane 3) which disappears in the P-element insertion mutant $Serf^{EY09918}$ (lane 2) and in both of our *Serf* deletion mutants $Serf^{\Delta 10a}$ (lanes 4 & 7) and the $Serf^{\Delta 6c}$ (lane 5). Since, this particular band diminishes to a level below detection in the *Serf* deletion and insertion mutants and is restored in the precise excision line (while ribosomal RNA is present in all samples), I conclude that this band represents the *Serf* transcript.

In a similar way I compare *Serf* expression in flies containing wildtype levels of *Serf* mRNA with wildtype flies containing a second, cDNA copy of *Serf* driven by the Act5c-GAL4 driver. This widely used driver appears to provide high level gene expression in essentially all tissues throughout development (Duffy 2002). Compared to the driver only control lacking the *Serf* cDNA (lane 6) the two independent *Serf* cDNA expression

lines 6c and 27a (Lane 8 & 9, respectively) produced 3.2 fold and 2.55 fold more *Serf* mRNA, respectively, after normalization for loading differences using the rRNA control.

To assay for protein expression from each of our *Serf* mutants, I extracted total protein from whole flies and performed western blots using a polyclonal antibody against the N-terminus of the human Serf protein which cross-reacts with the fly protein. In both of the *Serf* deletion mutants I have created, the translational start codon is lost along with either bulk of the coding sequence ($Serf^{\Delta 6c}$) or essentially all of it ($Serf^{\Delta 10a}$). Therefore, I expect these two deletion mutants to be complete null alleles. As shown in the figure (Figure 2.5B) the lower band of the doublet for the YW, Act5c GAL4 and the PE26B lines (Lanes 1, 2 & 4), which runs below 15 KD band in a 15% polyacrylamide gel, corresponds to Serf, since it becomes undetectable in the P element insertion line $Serf^{EY09918}$ and the two *Serf* deletion lines 10a and 6c (Lanes 3, 6 & 7). The Serf protein is not highly abundant in adult wild type flies but gets 4.1 fold overexpressed (compare lane 1 and 4) when the UAS-*Serf* cDNA is trans-activated under the ubiquitous Act5c-GAL4 driver (Lane 5). Similar levels of the β-tubulin band is observed across all the *Serf* lines.

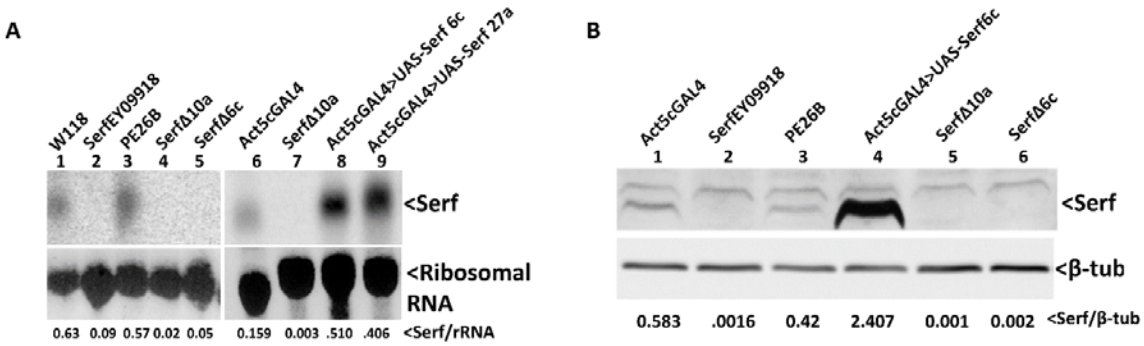

Fig 2.5 Molecular analysis of *Serf* alleles. (A) Northern blot probed against *Serf* 2nd exon in *Serf* alleles. Ribosomal RNA shown as a loading control. Relative levels of *Serf* transcript is indicated below each lane. (B) Western blot with anti- human Serf peptide antibody in *Serf* alleles. -tubulin is shown as a loading control. Relative levels of Serf protein in indicated below each lane.

2.2.5 Generation and validation of a *Serf* RNAi knockdown allele

In addition to the *Serf* deletion allele, we created an RNA interference (RNAi)-mediated conditional knockdown of *Serf* using the same UAS-GAL4 system as described above. We obtained the UAS-hp-CG17931 (*Serf*) construct from the Vienna Drosophila RNAi center, a publicly available genome-wide library of *Drosophila* RNAi transgenes (Dietzl *et al*., 2007). The strategy is to express short inverted repeat segments of a target gene's transcript under the control GAL4 so as to target the RNA interference pathway. We expressed the UAS-hp-*Serf* construct under the ubiquitous Actin5c-GAL4 driver. Figure 6a shows the *Serf* transcript in the Act5c-GAL4 driver only control line which decreases to the level below detection upon ubiquitous expression of the UAS hp-*Serf* construct. Figure 6B shows Serf protein levels expressed in the GAL4 driver control and knockdown lines (Lane 1 & 2). The Serf protein level relative to a nonspecific band in the same blot decreases about 10 fold in the knockdown line compared to the control.

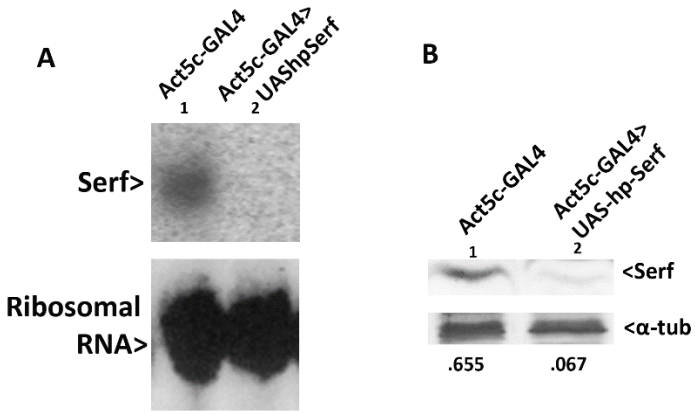

Fig 2.6. Molecular analysis of Serf RNAi mediated knockdown line. (A) Northern blot of *Serf* transcript probed against sequences from *Serf* 2nd exon. Ribosomal RNA is shown as a loading control. (B) Western blot showing Serf protein levels. A non-specific band (ns) in the same blot in the corresponding wells has been used for normalization.

2.2.6. Viability during development is unaltered in flies with different *Serf* alleles.

The first thing we learned by generating the *Serf* null mutants is that *Serf* in *Drosophila* is non-essential for viability and fertility. Indeed, the deletion, the global knockdown or the global overexpression of *Serf* did not cause any obvious defect during development. However, reduced viability can be masked by the large number of flies used in our standard propagation. Therefore, to be more quantitative, I measured the viability of the different *Serf* lines in terms of percentage of pupation and adult eclosion.

Figure 2.7A describes the comparison of the percentages of pupation and pupal eclosion between the *Serf* deletion ($Serf^{\Delta 10a}$) and precise excision control (PE26B). Data shows that the PE26B and $Serf^{\Delta 10a}$ lines form 68% and 64% pupae respectively which is not statistically different (P value=.5899, n=310 for PE26B and 326 for $Serf^{\Delta 10a}$). However, a laboratory wild type control line w^{1118} shows 90% pupation in this assay confirming that other factors (like handling) do not influence the viability observed in our experimental lines. Measurement of percentage of pupal eclosion however showed that very similar proportion of pupae eclosed into adults for all the lines; 96%, 100% and 99% for the w^{1118}, PE26B and $Serf^{\Delta 10a}$ respectively. Overall, it appears that genetic differences between the w^{1118} and the other two possibly contributes to the reduced larval viability, but their difference does not correlate with presence or absence of *Serf*. Therefore I conclude that the loss of *Serf* gene function is of little or no consequence to viability up to the point of eclosion.

Figure 2.7 B shows the viability of ubiquitous *Serf* knockdown (Act5c GAL4> UAS-hp-*Serf*) and overexpression flies (Act5c GAL4> UAS *Serf*) in comparison to an isogenic GAL4 driver control. Here I see that the GAL4 driver control shows 68%

pupation while 98% of those pupae form adults. Compared to that, in the *Serf* knockdown flies 86% larvae form pupae, out of which 90% eclose as adults. In the *Serf* overexpression flies on the other hand 89% larvae form pupae and a 100% of those eclose as adults. Although, there is no statistical difference in the percentage pupation and pupal eclosion between the knockdown and overexpression group (P value >.05, n=186), percentage pupation is significantly reduced in the Act5c-GAL4 control (P value=.001) This result is surprising and one possibility is that the GAL4 protein might interfere with other cellular processes in the absence of a UAS responder within the driver only line. Overall these data show that global knockdown or overexpression of *Serf* does not cause viability defect in flies which is consistent with the results from *Serf* deletion flies. However, percentage pupation is significantly different between the deletion and *Serf* knockdown flies (P value<.0001), but these two lines are derived from two completely different genetic backgrounds and hence cannot be compared directly to each other.

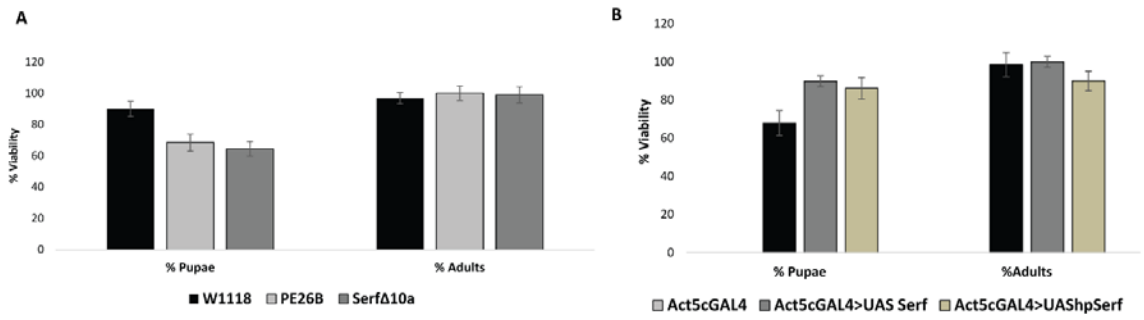

Figure 2.7: Viability of *Serf* mutants during development is not impaired. (A) Percent pupation (% pupae) and percent pupal eclosion (% adults) in the *Serf* deletion flies (SerfΔ10a) vs the precise excision flies (PE26B). The w^{1118} line is used as a laboratory wild type control. More than 300 larvae per genotype were scored in groups of 20.(B) Percent pupation and percent adult eclosion in the Act5cGAL4 driven Serf overexpression (Act5cGAL4>UAS *Serf*) flies and *Serf* knockdown (Act5cGAL4>UAShp*Serf*) flies in comparison to Act5cGAL4 driver only control and a laboratory wild type control (w^{1118}). One hundred and eighty six larvae were scored for the knockdown and overexpression lines and one hundred and thirty seven larvae for the Act 5c GAL4 control.

2.2.7 Flies with various *Serf* alleles do not show mobility defect at larval stage.

As one feature of health and neuromuscular function, we measured locomotion in flies with normal, elevated or abolished *Serf* expression. In larvae, locomotion is a complex behavior, commonly assayed by measuring numbers of peristaltic waves generated in the larva per unit time as they move forward. For this assay we used early 3rd instar larvae (i.e., obtained 96hrs post egg laying). As shown in the figure (Fig 8A) the average body wall contraction per minute is 48.61 for the precise excision line and 48.88 for the *Serf*$^{\Delta 10a}$ line. Obviously, these two lines were not significantly different from each other (P value=.9126, Unpaired student t-test). These results are similar to what has been reported by other groups for wild type laboratory strains (Heckscher, Lockery *et al*. 2012, Nichols, Becnel *et al*. 2012).

In Fig 2.8, we compared the Actin5c GAL4 driven ubiquitous Serf overexpression line and Serf RNAi knockdown line with the Act5cGAL4 driver only control for average body wall contractions per minute. We find that all three lines showed similar mobility, scoring 58.53, 59.46 and 58.00 contractions per minute in the driver only, *Serf* RNAi knock down and *Serf* overexpression backgrounds, respectively. While these genetically related lines are indistinguishable, these do differ significantly from the values seen above for the precise excision mutant (P value=.0013, unpaired t-test), indicating that genetic features other than *Serf* expression influence larval mobility. Nevertheless, based on our observations we conclude that neither the absence of *Serf* nor its global overexpression have a readily detectable impact on larval mobility.

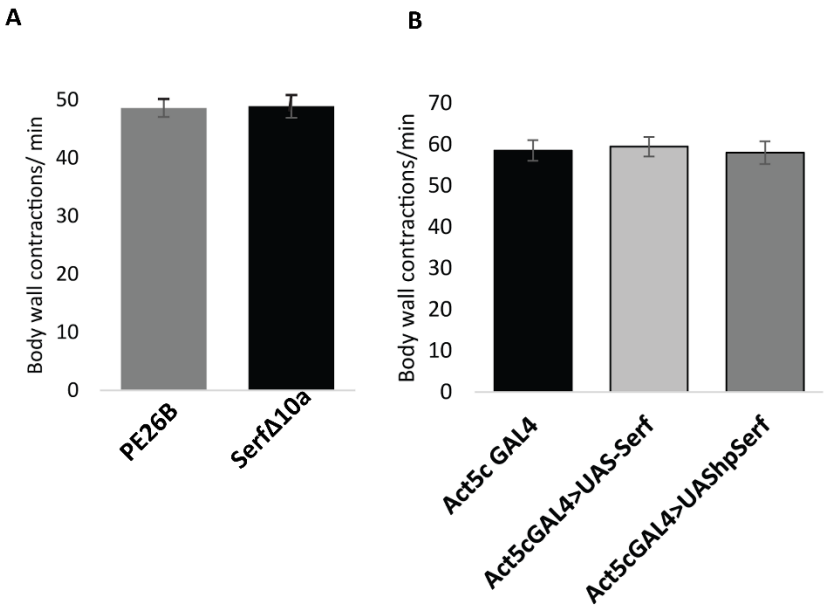

Figure 2.8: *Serf* mutants do not show larval body wall contraction defects. (A) Average body wall contractions per minute in *Serf* deletion ($Serf^{\Delta 10a}$) larvae vs the precise excision (PE26B) larvae. There is no significant difference between the two groups (P value=.9126, n=20 for each genotype, Unpaired student t-test). (B) Average body wall contractions per minute in ubiquitous *Serf* overexpression (Act5cGAL4>UAS *Serf*) larvae and *Serf* knockdown (Act5cGAL4>UAS-hp-*Serf*) larvae in comparison to the driver only control (Act5c GAL4). There is no significant difference between the control and the overexpression group (P value=0.7883, n=15 for each genotype, Unpaired t-test) or the control and the knockdown group (P value=0.8871, n=15 for each genotype, Unpaired t-test).

2.2.8 Loss of *Serf* gene activity causes climbing impairment in adult flies.

Fly climbing activity is known to be compromised with adult age and in mutants with neuromuscular defects (Martinez, Javadi *et al*. 2007). Since the loss of *Serf* activity is implicated as exacerbating a neuromuscular disease, SMA, we performed climbing assays to learn whether changes in Serf gene expression affected the fly climbing behavior. In essence,12-flies were placed in a graduated cylinder, tapped to drop them to the bottom, and the time required for 50% of the group to climb 17.5 cms from the bottom of the cylinder was measured at three different age groups (1 week. 2 week and 4 week post eclosion). At least 100 male flies of each genotype were assayed at each time point, grouped into 10 cohorts.

For all genotypes tested the time for climbing increases with age showing a decline in the climbing performance with age (Figure 9). The w^{1118} line served as the fully wildtype control. This line takes an average of around 10 seconds to climb the specified distance when 1 week old and increases up to about 45 seconds when 4 week old. The Act5c-GAL4 driver only control behaved similarly to the w^{1118} line, a mean of around 14 seconds to climb when 1 week old which increases to an average of around 43 seconds at 4 week old age, showing that the GAL4 expression by itself did not impact the climbing behavior. The ubiquitous *Serf* overexpression flies (Act5cGAL4>UAS *Serf*) performed very similar to the driver only control. Interestingly, when *Serf* is deleted (Act5cGAL4;$Serf^{\Delta 10a}$) the average time required for climbing increased significantly in all three age group flies, averaging around 30 seconds at 1 week old age and about 105 secs when 4 week old (P value<<.0001, unpaired student t-test), indicating that the *Serf* null flies are impaired in locomotor function. To confirm that the climbing impairment is

solely caused by loss of the Serf gene, we expressed the *Serf* cDNA in the Serf deletion background (Act5cGAL4>UAS *Serf, Serf*$^{\Delta 10a}$) and asked if the climbing defect could be reverted. We indeed found that the climbing performance in the Serf null flies reverted back to wild type levels upon ubiquitous expression of the *Serf* cDNA construct (P value<.0001, unpaired student t-test). At 1 week old age the average time required for climbing was restored back to 12 secs, which at 4 week old age increases to 30 secs similar to the wild type. Therefore, we concluded that *Serf* gene in *Drosophila* is critical for sustaining normal locomotor function in adults while it does not appear to impact locomotion at the larval stage. This is the first report in any organism of a *Serf*-dependent biological function.

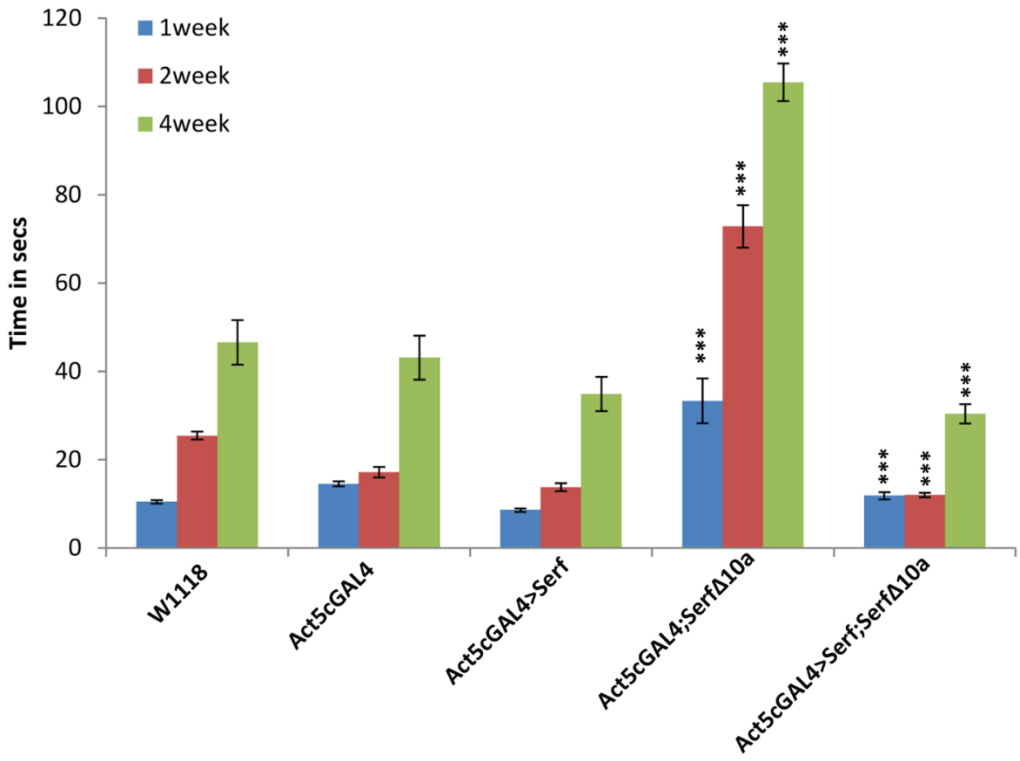

Fig 2.9. *Serf* deletion causes impairment of climbing performance in adult Drosophila. Graph showing the average time required by 50% of flies in each cohort to climb 17.5 cms at three different ages. For each genotype at each time point n=10 (10 cohorts, each consists of 12-15 flies). The w^{1118} line serves as a completely wild type control. The Act5c GAL4 line is the driver only control. The *Serf* deletion flies (Act5cGAL4; $Serf^{\Delta 10a}$) require significantly longer time to climb the specified distance at all time points (P value <.0001, unpaired Student's t test), which is then rescued to normal by Act5c-GAL4 driven *Serf* cDNA expression in these flies (Act5c GAL4>*Serf*, $Serf^{\Delta 10a}$).

2.3 Conclusions and discussion

In summary, my initial studies revealed several important things about the *Serf* gene in *Drosophila melanogaster*. Here I show that the *Serf* gene is non-essential for *Drosophila* development and viability, similar to *C. elegans* and *S. cerevisiae*. Altered Serf levels do not impact the locomotion behavior at the larval stage, however, adult climbing ability is impaired with loss of *Serf*. Thus, for the first time *Serf* is being described as having a biological impact in any model system, since loss of *Serf* has been shown to be benign in *C. elegans* and is not reported to cause any growth defect in yeast. Climbing ability of flies gradually declines with age and has long been used as measure for age related changes in *Drosophila* (Ganetzky and Flanagan 1978, Martinez, Javadi *et al*. 2007). Genetic alterations causing alteration in the locomotor phenotype of flies involve pathologies of muscle, peripheral neuron or central nervous system (Scholz and Singleton 2008). Therefore, the impaired locomotor phenotype is often documented in neuromuscular or age related neurodegenerative disease models in flies (Feany and Bender 2000); (Sofola, Kerr *et al*. 2010, Pandey and Nichols 2011). Since *Serf* is implicated in SMA and neurodegenerative diseases, the finding that loss of *Serf* diminishes climbing ability in flies, might point to *Serf*'s importance in maintaining neuronal, muscular or neuromuscular functioning in *Drosophila* possibly relevant in SMA pathogenesis. Thus despite its non-essential role for development and viability, here I identify, for the first time, an important function of *Serf* in *Drosophila* physiology. It also opens up the possibility that *Serf* might have other necessary function during adult life in flies.

Molecular analysis suggests that *Serf* is not a particularly abundant protein in flies. The mod-encode tissue RNA-seq data from *Drosophila* also reports moderate level of expression of the *Serf* transcript, although expressed ubiquitously (Gelbert, W.M, 2013, Flybase high-throughput expression Pattern). However, when trans-activated under the Act5c promoter in a UAS-GAL4 system, I could not drive more than a 2-3 fold overexpression of this gene. This suggests that the *Serf* promoter is also almost equally active as the Act5c. In contrast about 5 fold overexpression was achieved with the same driver at the protein level. It is possible that *Serf* mRNA is differentially translated in different tissues, therefore the total transcript levels might not be directly correlated with the total protein levels expressed within tissues. In fact human studies have shown that alternate *SERF* isoforms differentially express in different tissues (Scharf *et al*., 1998).

With the creation of different *Serf* alleles in flies I have also created tools for dissecting *Serf*'s role in modulating SMA phenotype in *Drosophila*, which is the major goal of my thesis. The SMA disease model in flies is known to display viability defects, growth defect, developmental arrest or larval locomotion defect in flies (Chan *et al*.,, 2003, Chang *et al*., 2008; Garcia, E.L 2013, RNA; Praveen *et al*., 2014). Here I show that flies with alternate alleles of *Serf* do not show major developmental defects or larval locomotion problem. It will be interesting to look at, when combined with *Smn* mutants *Serf* alleles can modify *Smn* dependent mutant phenotypes in flies or not. Any potential exacerbation or amelioration of SMA related phenotypes would clearly reflect genetic interaction of *Serf* with *Smn,* since a mutant *Serf* allele, by itself, do not cause any problem. A hypomorphic allele of *Smn* (Smn^{e33}) that shows muscle specific reduction in the *Smn* protein level, has been shown to display flightlessness while development and

viability is not impacted (Rajendra *et al*., 2007). The fact that *Serf* null mutant is deficient of climbing without affecting viability during early development, therefore, could be related to subtle changes in Smn protein abundance pointing to the relevance of *Serf* in SMA pathogenesis. Thus my initial finding is consistent with Serf's predicted impact in SMA.

2.4 Materials and methods

2.4.1 Fly strains and maintenance

The following genotypes are used in this chapter: (i) w^{1118}; (Xia, Fakler *et al*.) y w; {Act5C-GAL}25FO1/ CyO, y+ (Xia, Fakler *et al*.) [(i) & (Xia, Fakler *et al*.) are obtained from Bloomington Stock Center] ; (iii) {UAS-hp-SERF}100894 (Xia, Fakler *et al*.) (*SERF* RNAi line- Vienna *Drosophila* RNAi Center); (Ruan, Tang *et al*.) UAS-*SERF* cDNA; (v) $Serf^{\Delta 10a}$ (vi) Precise excision 26B. Flies were cultured in 25℃ humidified chamber under constant light condition. Vials or bottles containing semi defined medium, as described by Bloomington *Drosophila* Stock Center (Backhaus *et al*.,, 1984), were used for all experiments in this study. The specific crosses performed in this chapter to obtain the progeny (larvae or adults) of required genotypes are described in table 2.3.

Table 2.3 describes the specific crosses performed, to obtain the progeny of required genotypes for different assays conducted in this chapter.

Stage collected	Cross description	Progeny genotype collected
1st instar larva	Act5c GAL4/TM3 Ser GFP x w^{1118}	Act5c GAL4/+
	Act5c-GAL4/TM3 Ser GFP x UAS-Serf (cDNA)	UAS-Serf (cDNA)/+, Act5c-GAL4/+
	Act5c-GAL4/TM3 Serf GFP x UAS-hp-Serf (RNAi)	UAS-hp-Serf(RNAi)/+, Act5c GAL4/+
Adult	Act5c-GAL4/Cyo x w^{1118}	Act5c-GAL4/+
	Act5c-GAL4/Cyo x UAS-Serf (cDNA)	UAS-Serf (cDNA)/Act5c-GAL4
	Act5c-GAL4/Cyo x UAS-hp-Serf (RNAi)	UAS-hp-Serf(RNAi)/ Act5c GAL4
	Act5c-GAL4/Cyo GFP x w^{1118}	Act5c-GAL4/+
	Act5c-GAL4/Cyo GFP, $Serf^{\Delta 10a}$ x $Serf^{\Delta 10a}$	Act5c-GAL4/+, $Serf^{\Delta 10a}$
	Act5c-GAL4/Cyo GFP, $Serf^{\Delta 10a}$ x UAS-Serf cDNA, $Serf^{\Delta 10a}$	Act5c-GAL4/UAS-Serf (cDNA), $Serf^{\Delta 10a}$

2.4.2 Cloning of UAS-*Serf*-cDNA construct

The *Serf* cDNA clone (SD16330) was obtained from Bloomington stock center (FlyBaseID FBcl0276419). The full length cDNA was cloned in pOT2 vector within 5'EcoRI and 3' XhoI site. The cDNA construct was amplified from this vector including the 3' XhoI site from the vector backbone and a 5' BamH1 site was introduced through the 5'oligo. These two sites were used to insert the PCR product into the pUAST vector (Brand, A.H. 1993 Development) which was then used for embryo injection by Duke University Model System Genomics Center injection facility. Oligonucleotides used in this cloning are described in table 2.4.

Table 2.4 describes the oligonucleotides used for amplifying the Serf-cDNA from pOT2 vector for cloning into pUAST vector.

Oligo name	Sequence
5'SERFcDNAoligo	AAAAAAGGATCCAAAAATGACACGCGGCAAC
3'SERFcDNAoligo	ATTTAGGTGACACTATAGAACTCGAG

2.4.3 Northern blot

Total RNA was extracted from 20 adult flies (equal number of males and females in each set) by homogenizing them in TRIzol reagent (Ambion, Life Technologies) using plastic pestles and appropriate micro-centrifuge tubes (GeneMate Microtubes, Bio Express). Homogenization was done keeping the samples on ice, followed by 2 consecutive chloroform extraction and precipitation using isopropanol. 15ug of total RNA was

resolved on a 1% agarose-formaldehyde gel followed by transfer onto Immobilon NY+ membrane (Millipore) and hybridization with random prime labeled probes (Invitrogen) against *Serf* (See Table 2.5 for specific probe information). The radioactive signals were visualized with a Typhoon 8600 Phosphoimager and quantified with ImageQuant 5.2 software (GE Healthcare Life Sciences, Pittsburgh,PA). Ribosomal RNA on the membrane after transfer was scanned and used as loading controls.

Table 2.5 describes the oligonucleotides used for amplifying segments of Serf gene used for synthesizing radiolabeled probes for northern blot experiment.

Template	Primer pairs for amplifying probe template	Size of probe template
Serf Exon1(CG17931 Exon1Fw+Rv)	5'- CATTTTTAAGGCTCCTTCTTGG-3' and 5'-CAACTTCGAATGCTCGAAAAG-3'	136 bps
Serf Exon2(D&E)	5'-CTGGCCTTCCTTTGCTCCA- 3' and 5'-GCGGCAACCAACGAGACCT- 3'	106 bps
Serf Exon3(F&G)	5'- CTTTCTGTCGGCTGCATATTATG- 3' and 5'- AGTTAATGCGGGAGAAGCAGA- 3'	460 bps

2.4.4 SDS PAGE and western blots

Protein extracts were made from 1 week old adult flies, 12-14 flies for each extract with equal numbers of males or females, by grinding them in 1X Lamelli buffer (2% SDS; 10% Glycerol; 60 mM Tris-Cl pH 6.8; 0.01% w/v bromophenol blue), 20µl per fly. Grinding is done on ice for 3-4 minutes until cuticle remains, followed by heating at 90°C

for 10 minutes. Supernatant were collected after spinning the samples at full speed for 5 minutes in a table top centrifuge and stored at -80℃. Equal amount of protein in terms of volume of extract per fly (usually 1 fly worth of protein i.e. 20µl), were resolved on 15% SDS-PAGE for detecting Serf and β-tubulin. The gels were blotted on .45µ PVDF membrane (Millipore Corp. MA) and membranes were probed with rabbit polyclonal antisera against Serf (1:1000 dilution; generated against human N terminal human SERF peptide, gift from Dr. Stefan Stamm, University of Kentucky) and mouse monoclonal anti-β tubulin (1:1000 dilution; Developmental Studies Hybridoma Bank, E7-s). The primary antibodies were detected with alkaline phosphatase conjugated goat anti-mouse IgG antibodies (1:5000 dilution; Life Technologies) or goat anti-rabbit IgG (1:5000 dilution; Sigma). Detection of alkaline phosphatase based signals is done either using BCIP/NBT substrate (Promega) followed by scanning the colored blot using HP G4050 scanning machine or Amersham^{TM} ECF substrate for western blotting (GE Healthcare, Life Sciences) followed by scanning of the fluorescent signal by the typhoon scanner (Emission Filter526 SP Fluorescein, Cy2, AlexaFluor 488, PMT-600, Sensitivity-high). Densitometric analysis of the blots were done with Image Quant 5.2 software.

2.4.5 Viability and growth Assay

Viability assay was also performed as previously described (Praveen et,al 2014). Synchronized eggs were collected on apple juice agar plates (1:3 diluted frozen apple juice concentrate, 2.2% *Drosophila* agar, 2.5% sucrose in dH_2O) where they hatch to the 1st instar larval stage (24 hrs). First instar larvae were either directly picked (when all larvae are of identical genotype) under dissecting microscope (Leica) or screened for the absence of GFP (when the population has mixed genotypes) and picked under a light

microscope attached with a UV lamp. Specific numbers of larvae were picked and transferred in a scoop of cornmeal food (semi defined medium, as described by Bloomington *Drosophila* Stock Center, Backhaus *et al*.,, 1984) which is then carefully placed inside the standard food vials (same composition). Small vials containing 15-20 larvae were placed in 25C temperature and humidity controlled chambers and monitored for pupae formation and adult eclosion, until at least 100 larvae were scored. The number of pupae formed and adults eclosed were counted. Percent larvae pupated and percent pupae eclosed into adults were measured for each line and statistically analyzed as described in 2.4.8.

2.4.6 Larval mobility Assay

Body wall contractions per minute (Nichols, C.D. 2012 J. Vis. Exp; Heckscher, E.S. 2012, J. Neuroscience) were measured in 96 hrs post egg laying larvae. Collection of synchronized 1st instar larvae was done as described for viability assay (2.4.5). The food containing the staged larvae were scooped out from the vials with a spatula, 72 hours after collection (96 hrs post egg laying). The larvae were then carefully separated from the food on a small Petri dish, washed in 1X PBS briefly and placed on fresh apple juice plates warmed to room temperature. After acclimatization for 1 minute the body wall contractions were counted under a light dissecting microscope (Leica) for one minute. Twenty larvae for each genotype were assayed like this. Mean body wall contractions for each genotype were then analyzed for statistical significance as described in 2.4.8.

2.4.7 Adult Climbing assay

The gross locomotor function of adult flies were assessed by climbing assay as previously described (Martinez, V.G. 2007, Developmental Neurobiology). This assay

was performed at room temperature in a glass cylinder placed underneath a light source. About 100 flies for each genotype grouped into 10 cohorts of 10-12 male flies per genotype were placed in a 250 ml glass cylinder and gently tapped to the bottom. The time taken by 50% flies to climb 150 ml mark (17.5 cms from the bottom) of the cylinder was recorded and compared between the experimental and the control groups. 5 repeated measurements were taken with at least 10 cohorts from each genotype. Means of the 5 repeats from each cohort were obtained to calculate the average between the cohorts for statistical analysis (described in 2.4.8).

2.4.8 Statistical analyses

The viability assay dataset were analyzed for statistical significance by the two sample t-test between percentages. Rest of the data in this chapter are analyzed for statistical significance using two-tailed Unpaired Student's *t*-test. For all statistical tests $P<0.05$ were considered significant. For all graphs, data are represented as the mean ± the standard deviation of mean (Becker, Semler *et al*.) and significant difference is expressed as: '*'- P value between 0.01-0.05; '**'- P value between 0.001-0.01; '***' P value<.001.

Chapter 3: *Drosophila* lifespan is sensitive to the levels of *Serf* expression

3.1 Introduction

So far, I have shown that the *Serf* gene in flies is non-essential for viability. Flies with altered levels of Serf progress through all developmental stages although the adults show reduced climbing ability. The next question I wanted to ask is whether adult flies with alternate alleles of *Serf*- wild type, deletion and overexpression, have comparable lifespans. Adult lifespan is commonly assayed as a measure of organismal aging. Genetic intervention of the lifespan of an organism can provide insight into the gene function in the age-related changes of cellular processes.

Aging, although most commonly defined as a progressive and irreversible decline in organismal performance, is not just a build-up of detrimental changes over time but a dynamic and well-regulated process. Research over the past 100 years has, however, shed some light onto the biological processes that impact aging at a cellular- and organismic-level. For instance, restriction of nutrient intake is known to enhance longevity in many species (Guarente and Kenyon 2000, Partridge and Gems 2002). Inhibition of different nutrient sensing signaling pathways like Insulin/IGF signaling (IIS) and target of rapamycin (TOR) has been shown to extend organismal lifespan in a manner similar to dietary restriction (Guarente and Kenyon 2000, Partridge and Gems 2002, Tatar, Bartke *et al*. 2003, Kapahi, Zid *et al*. 2004). The IIS pathway negatively regulates a plethora of factors involved in oxidative, thermal and metabolic stress resistance which are shown to mediate the lifespan extension caused by mutations that reduces IIS pathway activity (Giannakou and Partridge 2007). Both the IIS and TOR pathways inhibit autophagy, a known quality control process that promotes the clearance of damaged proteins and

damaged cytoplasmic organelles. Genetic inhibition in autophagy is seen to reduce lifespan and enhanced autophagy is associated with increased lifespan (Madeo, Zimmermann *et al*. 2015).

Here I examine the contribution of the *Serf* gene to adult lifespan in *Drosophila melanogaster*. I also test *Serf*'s impact on the oxidative stress response and, a known marker of mitochondrial function that declines during aging (Wallace 2005).

3.2 Results

3.2.1 Life-span is shortened in *Serf* deletion flies.

I used a standard *Drosophila* lifespan assay to determine if the loss of the Serf protein altered adult lifespan. The *Serf* deletion flies ($Serf^{\Delta 10a}$) were compared with an otherwise isogenic precise excision line, called PE26B, containing a functional *Serf* gene. Age matched male and female PE26B and $Serf^{\Delta 10a}$ flies were maintained under optimized culture conditions and the number of viable flies recorded each day until 100% of the flies were dead. Each line had 100 flies of each sex in 5 cohorts (20 flies per cohort) and maintained in a temperature controlled room under a 12 hr-12hr light/dark cycle. In figures 3.1A and D, I present the survival curves of *Drosophila* females and males, respectively. I find that the maximum survival of the control group is 53 days for females and 57 days for males, with a 50% survival of 43 days in males and 35 days in females. In comparison, the lifespans of both females and males of the $Serf^{\Delta 10a}$ line were significantly shorter (P value < .0001), the maximum lifespan and 50% survival time being 36 days and 27 days in females and 49 days and 29 days in males, respectively. Figure 3.1 B, E shows the mean 50% survival between the 5 cohorts in females and males

respectively. Here, the mean 50% survival of the female *Serf*$^{\Delta 10a}$ flies were reduced by 22.15% whereas that of male mutants were reduced by 35.48%. Figure 3.1 C and F shows the average lifespan which is the mean of the maximum survival obtained from each cohort. The female deletion mutants showed reduction in average lifespan by 20.25% whereas the male mutants showed 20.81% reduction. These results show that while *Serf* activity is not required for viability, it is needed to maintain the typical lifespan of *Drosophila melanogaster*, thus providing the first indication for a biological importance of this highly conserved protein in normal aging.

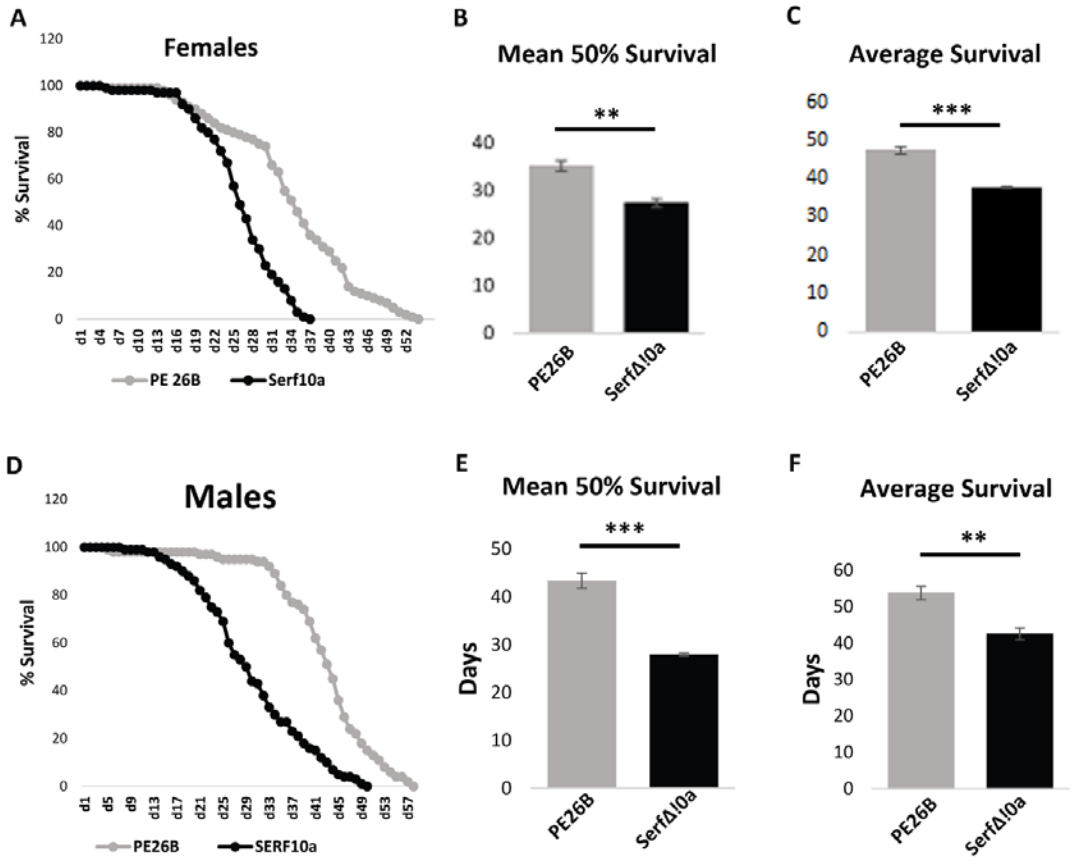

Fig. 3.1 *Serf* null flies show reduced lifespan. (A, D) Survival curves for female and male *Serf*$^{\Delta 10a}$ flies in comparison to the PE26B age matched controls. Percent survival is plotted on the Y axes and age in days on the X axes. Survival curves of the *Serf*$^{\Delta 10a}$ flies, both females and males, are significantly different from the PE26B controls (P<.0001 for both females and males, Kaplan Meier survival analysis,). (B, E) Graph representing the mean 50% survival of the *Serf*$^{\Delta 10a}$ and PE26B flies, females and males respectively. For both sexes the mean 50% survival of the deletion group is significantly reduced as compared to the controls (Females- P value=.0007, n=5, unpaired student t-test; Males- P value<.0001, n=5, unpaired student t-test). (C, F) Graph representing the average survival of the *Serf*$^{\Delta 10a}$ and PE26B flies, females and males respectively. For both sexes the average survival of the deletion is significantly reduced as compared to the controls

(Females- P value<.0001, n=5, unpaired student t-test; Males- P value=.0018, n=5, unpaired student t-test).

3.2.2 Global overexpression of *Serf* increases lifespan.

In the previous chapter, I showed that expression of the UAS-SERF cDNA with the ubiquitous Actin5c-GAL4 driver increased *Serf* expression by approximately 4 fold (Fig2.5). Prior to using this derivative for our longevity assay we backcrossed this strain and the Actin-5c GAL4 control line with w^{1118} for 5 generations to limit genetic background differences (Spencer, C.C. 2003 Aging Cell). More than 150 flies with genotype Actin5c-GAL4>UAS-*Serf* (*Serf* overexpression) and Actin5c-GAL4/+ (negative control) were collected and grouped into cohorts of 10-12. In figure 3.2 A and D, I present the survival curve showing that the maximum lifespan of the control group is 70 days in females and 75 days in males, whereas the 50% survival is 53 days in females and 50 days in males. When *Serf* is overexpressed both females and males lived significantly longer (p value< .0001) with maximum length of survival increasing to 83 days in females and 85 days in males and 50% survival going up to 69 days in females and 62 days in males. We observe an increase in the 50% survival among females by 30.09% and that among males by 25.46% (Figure 3.2 B, E). The average survival is also increased in the overexpression group (Figure 3.2 C and F), where the females showed an increase by 22.79% and males by 11.6%. These results complement the *Serf* deletion line study and established Serf's impact in fruit fly physiology as a longevity promoting factor.

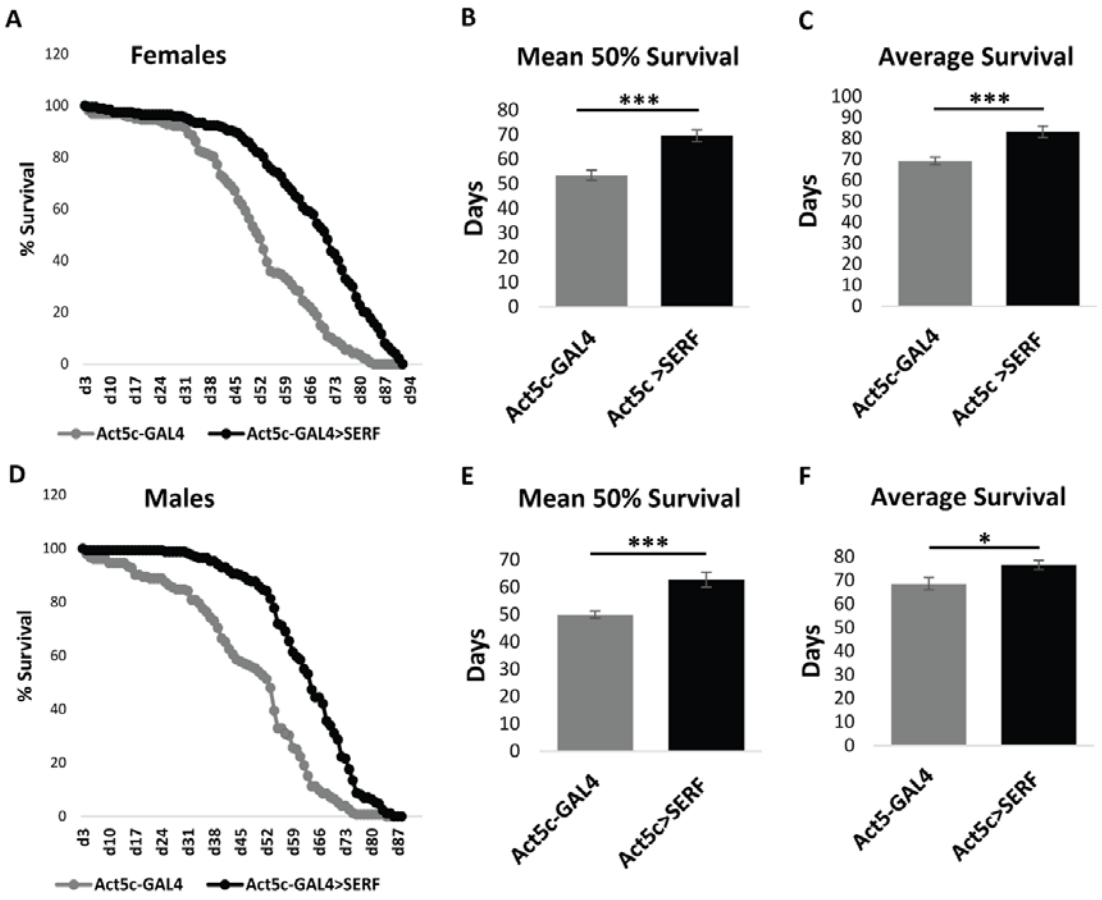

Fig. 3.2 Ubiquitous *Serf* overexpression increases lifespan (A, D) Survival curves for female and male Act5c GAL4 driven *Serf* over-expression flies respectively, in comparison to the age matched Act5c GAL4 driver only controls. Percent survival is plotted on the ordinates and age in days on the abscissa. Survival curves of the Act5c GAL4>*Serf* flies, both females and males, are significantly different from the Act5c GAL4 driver only controls (P<.0001 for both females and males, Kaplan Meier survival analysis) (B, E) Graph representing the mean 50% survival of the Act5c GAL4>*Serf* and Act5c-GAL4 flies, females and males respectively. For both sexes the mean 50% survival of the overexpression group is significantly increased as compared to the controls (P value<.0001, unpaired student t-test; females: n=15 for control; n=16 for overexpression

and males n=14 for both control and overexpression). (C, F) Graph representing the average survival of the Act5c GAL4>*Serf* and Act5c-GAL4 flies, females and males respectively. For both sexes the average survival of the overexpression group is significantly increased as compared to the controls (Females- P value<.0001, unpaired student t-test; Males- P value=.0033 females: n=15 for control; n=16 for overexpression and males n=14 for both control and overexpression).

3.2.3 Tissue specific overexpression of *Serf* and its impact on fly longevity.

In order to refine our understanding of *Serf*'s impact in fly longevity I overexpressed the cDNA under tissue specific drivers and measured their lifespan in comparison to isogenic driver only controls. Muscles and neurons were particularly interesting to us because- i) activation of cellular processes impacting longevity has been well characterized within these tissues; and ii) *Serf* 's implication in the neuromuscular and neurodegenerative diseases, raises its potential importance within these tissues.

3.2.3.1 Serf overexpression in muscles increases lifespan.

I used isogenized Mhc-GAL4 driver flies (Demontis and Perrimon 2010) to overexpress *Serf* in all muscles throughout development and adult life. Analysis of *Serf* protein expression by western blot of adult thoracic muscles shows 1.97 and 2.78 fold increased expression in males and females respectively (Fig 3.3G). The lifespan assays for females and males were done with more than 150 flies for each genotype grouped into 12 cohorts each with 10-12 flies. From the survival curves as shown in Figure 3.3 A and D, we can see that the maximum and the 50% survival of the overexpression females is significantly (P value <.0001) increased to 82 days and 49 days as compared to 61 days and 39 days in the control females. The impact was less obvious but statistically significant (P

value=.00347) in males where the maximum and 50% survival are increased from 64 days and 42 days in controls to 72 days and 46 days in the overexpression group. Figure 3.3 C and F shows the average lifespan which is the mean of the maximum survival obtained from each cohort. I found 24.57% increase in the 50% survival among female overexpression flies whereas 9.26% increase among males when compared with respective controls. The average lifespan of the overexpression group increased by 32.52% in females and 14.86% in males. These results show that *Serf* overexpression only in muscles is sufficient to mediate lifespan extension in adult flies, suggesting a role for *Serf* in influencing the cellular processes in muscles involved in determining lifespan.

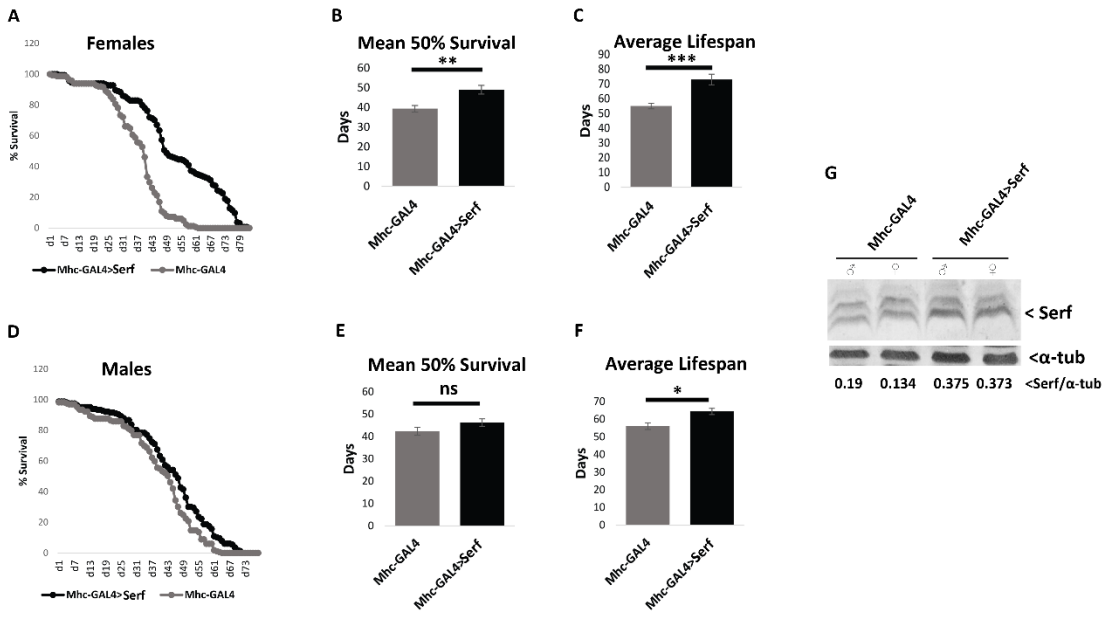

Fig. 3.3 Muscle specific *Serf* overexpression increases lifespan. (A, D) Survival curves for female and male Mhc-GAL4 driven *Serf* over-expression flies respectively, in comparison to the age matched Mhc-GAL4 driver only controls. Percent survival is plotted on Y axes and age in days on X axes. Survival curves of the Mhc-GAL4>*Serf* flies, both males and females, are significantly different from the Mhc-GAL4 driver only controls (Females-P<.0001; Males-P<.004 Kaplan Meier survival analysis.) (B, E) Graph representing the mean 50% survival of the Mhc-GAL4>SERF and Mhc-GAL4 flies, females and males respectively. The mean 50% survival of the female overexpression group is significantly increased as compared to the controls (P value=.0018, n=12, unpaired student t-test), however, it is not statistically significant in males (P value=.1655, n=12, unpaired student t-test). (C, F) Graph representing the average survival of the Mhc-GAL4>*Serf* and Mhc-GAL4 flies, females and males respectively. For both sexes the average survival of the overexpression group is significantly increased as compared to the controls (Females- P value<.0001, n=12, unpaired student t-test;

Males- P value=.0043, n=12 unpaired student t-test). (G) Western blot analysis of Serf protein in adult thoracic muscles of Mhc-GAL4>*Serf* and Mhc-GAL4 flies. The α-tubulin protein is used as loading control and Serf levels relative to α-tubulin is indicated below each lane.

3.2.3.2 *Serf* overexpression in neurons increases lifespan.

Isogenized Elav-GAL4 driver flies and UAS-*Serf* cDNA flies were crossed to drive pan-neuronal overexpression of *Serf* throughout development and adult life. Analysis of *Serf* protein expression by western blotting of protein extracts prepared from adult brains shows 2.27 fold and 2.59 fold overexpression in males and females respectively (Fig 3.4G). The lifespan assays for females and males were done with more than 180 flies for each genotype grouped into 15 cohorts each with 10-12 flies. From the survival curves (Fig 3.4 A&D) we can see that the lifespan of the overexpression group is significantly increased in both females and males (Females: P value <.0001; Males- P value<.0001) compared to the controls. The control flies show a maximum lifespan and 50% survival of 68 days and 45 days respectively in females and that for the males are 75 days and 46 days, respectively. In the overexpression group the maximum lifespan increases to 83 days in females and 87 days in males while the 50% survival increases to 60 days in females and 54 days in males. The mean 50% survival increases in the overexpression flies by 33.18% in the females (Fig 3.4B) and 17.06% in the males (Fig 3.4E), whereas, the average lifespan of the overexpression females and males increases by 21.67% (Fig. 3.4 C) and 19.18% in males (Fig. 3.4 F). Therefore, it is obvious from the results that *Serf* overexpression only in neurons is sufficient to mediate lifespan extension suggesting a potential role of *Serf* in longevity determining cellular activities within neuronal tissue.

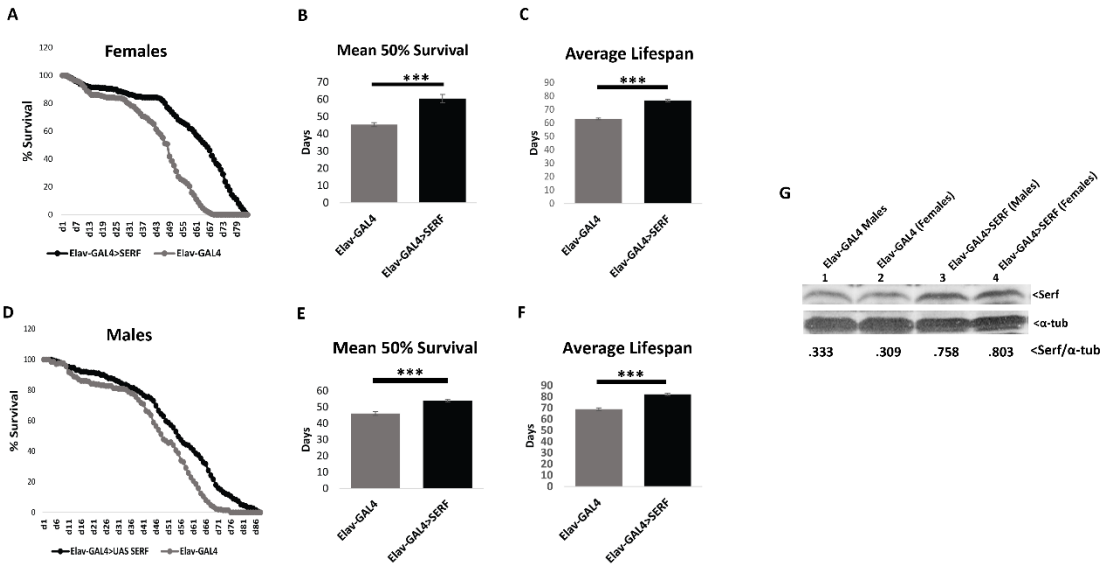

Fig. 3.4 Neuronal specific *Serf* overexpression increases lifespan. (A, D) Survival curves for female and male Elav-GAL4 driven *Serf* over-expression flies respectively, in comparison to the age matched Elav-GAL4 driver only controls. Percent survival is plotted on the Y axes and age in days on the X axes. Survival curves of the Elav-GAL4>*Serf* flies, both males and females, are significantly different from the Elav-GAL4 driver only controls (Females-P<.0001; Males-P<.0001 Kaplan Meier survival analysis.) (B, E) Graph representing the mean 50% survival of the Elav-GAL4>*Serf* and Elav-GAL4 flies, females and males respectively. The mean 50% survival of the overexpression group is significantly increased, in both females and males, as compared to the respective controls (P value<.0001, n=15, unpaired student t-test). (C, F) Graph representing the average survival of the Elav-GAL4>*Serf* and Elav-GAL4 flies, females and males respectively. For both sexes the average survival of the overexpression group is significantly increased as compared to the controls (P value<.0001, n=15, unpaired student t-test) (G) Western blot analysis of *Serf* protein in adult brain of Elav-GAL4>*Serf*

and Elav-GAL4 flies. The α-tubulin protein is used as loading control and Serf levels relative to α-tubulin is indicated below each lane.

3.2.4 *Serf* overexpression during adult life and its impact on longevity.

Our results indicate that flies show lifespan extension with both global and tissue-specific enhanced expression of Serf throughout development. To investigate *Serf*'s influence when overexpressed only in adult tissues I used the gene-switch system. The GeneSwitch system is a modified version of the standard UAS-GAL4 system where the GAL4 activator is replaced by a GAL4-progesteron receptor fusion protein which trans-activates target genes in a RU486 (Mifepristone) dependent manner, imparting temporal regulation on gene expression. The fusion GAL4 is now called a gene-switch protein and is expressed under a tissue specific enhancer/promoter for spatially controlled gene expression. In our experiments we expressed the UAS-*Serf* cDNA only in adult tissues by feeding the adult flies RU486 throughout life (See figure 2.4 for illustration). We compared genetically identical flies fed with either the drug or the vehicle and compared their lifespans. We used a ubiquitous daughterless GeneSwitch driver and a fat-body specific GeneSwitch driver to examine the impact of *Serf* overexpression in all adult tissues and in only adult fat bodies in determining lifespan.

3.2.4.1 Global *Serf* overexpression exclusively in adult tissues is sufficient to extend lifespan.

The daughterless-GAL4 geneswitch driver line (DaGS-GAL4) was isogenized with w^{1118} line, the same way as all other by back-crossing for 5 generations. The driver flies were crossed with the UAS-*Serf* cDNA flies and the progeny containing both of these elements were collected. More than 150 males and females were grouped into 12 cohorts with 12-

13 flies in each and reared on food containing RU486 or the vehicle. In order to make sure that the drug is turning on *Serf* overexpression I looked at the *Serf* protein levels in the drug treated and vehicle treated groups by western blot. Protein analysis shows an average of 3.31 fold and 2.89 fold overexpression in drug-fed males and females relative to respectively (Fig 3.5 D & H, respectively). Figure 3.4 A and D shows the survival curves combining all the cohorts of females and males respectively. Here the untreated controls show a maximum lifespan of 51 days in females and 61 days in males with 50% survival of 30 days in females and 41 days in males. Lifespan analysis showed that the RU486 treated females lived significantly longer as compared to the vehicle treated group (P value<.0001) where their maximum lifespan and 50% survival increased to 61 days and 39 days, respectively . The males of the overexpression group on the other hand showed a more mild impact (maximum lifespan 70 days, 50% survival 45 days) , although statistically significant (P value=.00189). Figure 3.5 B and F shows the average 50% survival between the cohorts from the two groups where the drug treated females show an increase of 19.24% and the males showed an 11.56% increase. Moreover, the average lifespan of the overexpression group increased both in females (fig. 3.5 C) and males (fig 3.5 G) by 15.41% and 11.94% respectively. These data showed that increased *Serf* expression in adult tissues during aging is beneficial and is sufficient for promoting longer lifespan, suggesting a potential function of the *Serf* gene in influencing the onset or the process of aging.

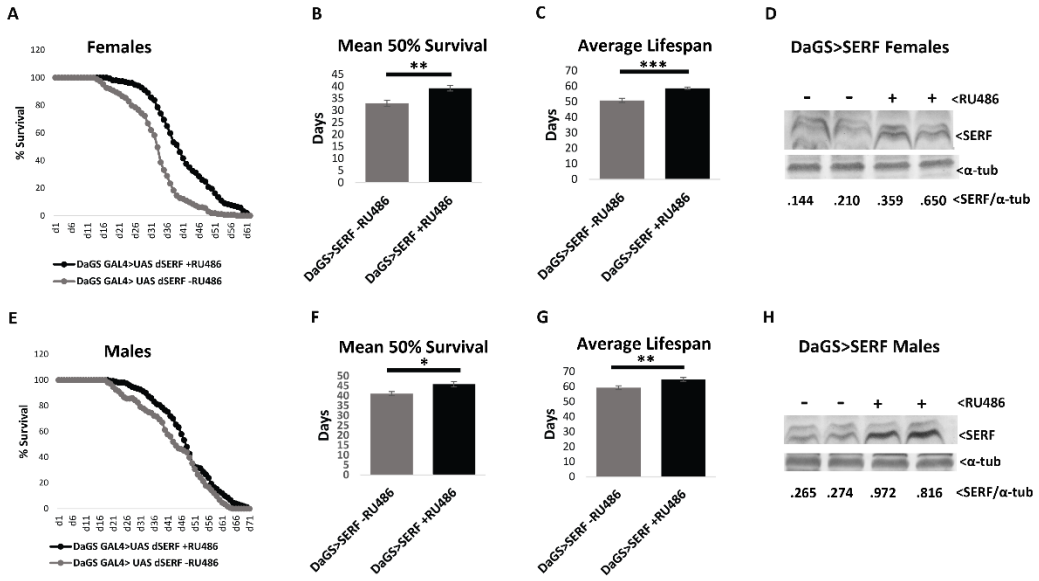

Fig.3.5 Global *Serf* overexpression in only adult tissues extend lifespan. (A, D) Survival curves of DaGS-GAL4>SERF flies with and without RU486 treatment in females and males respectively. Percent survival is plotted on the Y axes and age in days on the X axes. Survival curves of the drug treated flies, both males and females, are significantly different from the vehicle treated controls (Females-P<.0001; Males-P=.00189 Kaplan Meier survival analysis.) (B, E) Graph representing the mean 50% survival of the RU486 treated and vehicle treated DaGS-GAL4>*Serf* flies, females and males respectively. The mean 50% survival of the overexpression group, both females and males, is significantly increased as compared to the controls (Females: P value=.0014; Males: P value=.011; n=12; unpaired student t-test). (C, F) Graph representing the average survival of the RU486 treated and vehicle treated DaGS-GAL4>Serf flies, females and males respectively. For both sexes the average survival of the overexpression group is significantly increased as compared to the controls (Females- P value<.0001, n=12, unpaired student t-test; Males- P value=.0033, n=12 unpaired

student t-test). (G, H) Western blot analysis of SERF protein in adult extracts of DaGS-GAL4>Serf flies with and without RU486 treatment in females and males respectively. The α-tub band is shown as a loading control. Relative level of Serf with respect to α-tub is indicated below each lane.

3.2.5.2 Mis-expression of *Serf* in only adult fat bodies does not alter life-span.

The adult fat body in *Drosophila* performs a plethora of functions that includes energy homeostasis, storage and immune functions. Moreover, fat bodies form a non-autonomous circuit with the brain in which the insulin like signaling factors secreted by the fat body function to modulate adult longevity in a diet dependent manner (Bai *et al*.,, 2012). Therefore, the adult fat bodies were of particular interest to investigate a possible cell-non-autonomous effect of Serf in mediating lifespan extension. We used isogenic fat body GeneSwitch driver line (FBGS-GAL4) to cross with the UAS-*Serf* cDNA line and the progeny collected were either fed a diet that contained RU486 or only the drug vehicle. About 150 flies, females and males each, were examined in groups of 12-15 in 10 sex-specific cohorts. Consistent with the whole body study, the analysis of Serf protein levels shows 5.48 fold and 4.68 fold overexpression in the abdominal extracts (highly enriched with fat-bodies) of females and males respectively. Figure 3.6 A & E shows the survival curves of females and males, respectively. Here the untreated control flies show a maximum lifespan of 71 days in females and 72 days in males with a 50% survival of 47 days in both. The drug fed experimental group, both females and males, survived very similar to the controls where the maximum lifespan is 72 days for females and 75 days for males while the 50% survival is 46 days in males and 47 days in females. We observed no statistical difference in the average 50% survival (Fig. 3.6 B and F) and

average lifespan (Fig 3.6 C and G) between the two groups. These results suggest that the effect of *Serf* in promoting longevity in adult flies is not cell-autonomous or in other words it is important in which cells or tissues Serf activity is enhanced in order to assure longevity.

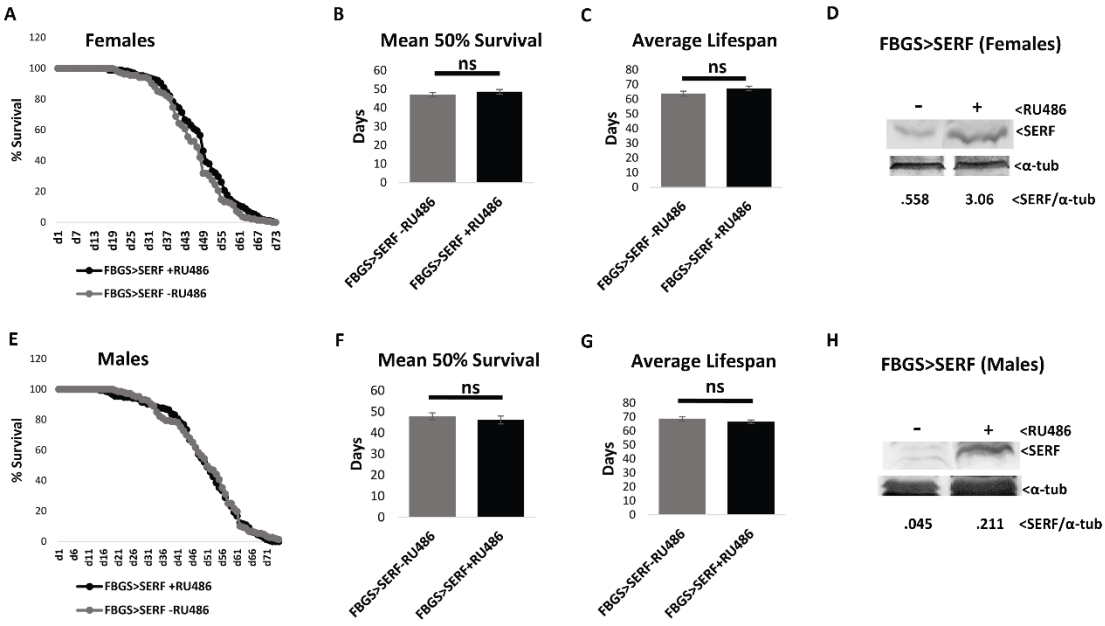

Fig.3.6 *Serf* overexpression only in adult fat bodies does not impact lifespan (A, D) Survival curves of FBGS-GAL4>*Serf* flies with and without RU486 treatment in females and males respectively. Percent survival is plotted on the Y axes and age in days on the X axes. Survival curves of the drug treated flies, both males and females, are statistically indistinguishable from the vehicle treated controls. (P value>.05 Kaplan Meier survival analysis.) (B, E) Graph representing the mean 50% survival of the RU486 treated and vehicle treated FBGS-GAL4>Serf flies, females and males respectively. The mean 50% survival of the overexpression group, both females and males, does not differ

significantly from the controls (P value>.1 n=12; unpaired student t-test). (C, F) Graph representing the average survival of the RU486 treated and vehicle treated FBGS-GAL4>Serf flies, females and males respectively. For both sexes the average survival of the overexpression group is not significantly different from the controls (P value>.1, n=12, unpaired student t-test). (G, H) Western blot analysis of Serf protein in the abdominal extracts of FBGS-GAL4>Serf flies with and without RU486 treatment in females and males respectively. Data shows about 2 fold and 5 fold overexpression upon RU486 feeding in females and males respectively. The α-tub band is shown as a loading control. The relative level of Serf with respect to α-tub is indicated below each lane.

3.2.6 Impact of altered *Serf* on survival under oxidative stress

Increased load of oxidative damage is one of the several factors that drives the organismal decline observed with aging (Pacifici and Davies 1991). In many instances longevity extending genetic interactions operate by providing resistance against increased oxidative stress. For example in most mammalian models lifespan extension achieved by calorie restriction is associated with reduced levels of oxidized protein, lipid, DNA, reduced rate of reactive oxygen species (ROS) production and increased resistance to oxidative stress (Sun, Muthukumar *et al*. 2001, Bokov, Chaudhuri *et al*. 2004, Richardson, Liu *et al*. 2004, Harper, Salmon *et al*. 2006). My data so far is consistent with Serf acting as a longevity promoting factor. I next investigated whether the changes in lifespan observed with manipulation of *Serf* gene expression operate under conditions of free radical mediated oxidative damage. If so, the *Serf* deletion flies might be expected to show hypersensitivity to this stress while flies that expressed excess *Serf* might show increased resistance to induced oxidative damage. Paraquat feeding is an established

method of inducing free radical driven oxidative damage (Rzezniczak, Douglas *et al*. 2011). Paraquat interferes with mitochondrial electron transport chain complex-I to increase ROS production which then cyclically causes more mitochondrial damage and more ROS production.

3.2.6.1 *Serf* deletion flies show shortened lifespan even under paraquat induced oxidative stress.

Flies, 24 hours old from the $Serf^{\Delta 10a}$ and PE26B adult flies were fed paraquat containing food their sensitivity to oxidative stress. Approximately 100 flies of each genotype and sex were grouped into 10 independent cohorts of 10-11 flies each and the number of dead flies was counted every 12 hours until all had died. Figure 3.7 A and B shows the survival curves under oxidative stress in females and males respectively. The lifespan of wildtype adults flies is reduced from about 60 days to 10 days with paraquat treatment. I found that in the *Serf* deletion group, both females and males the maximum survival time is slightly reduced to 164-176 hrs (6-7 days). In addition, the 50% survival time is reduced in the deletion group by 33.77% in females and 20% in males as compared to the respective controls. Statistical analysis of the survival curves show that the *Serf* deletion flies are significantly more sensitive to oxidative stress (P value<.0001 for females, P value=.0019 for males) when compared to the wildtype.

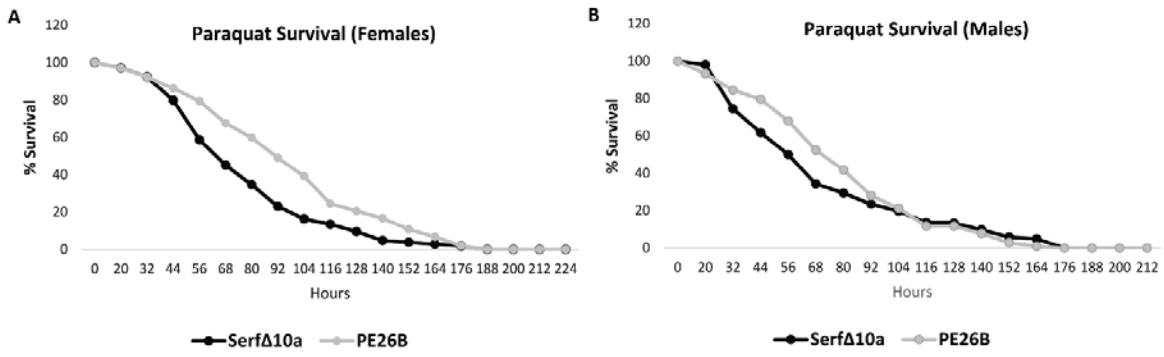

Fig. 3.7 Survival under paraquat induced oxidative stress is reduced in *Serf* deletion flies. (A) Survival curve for *Serf*$^{\Delta 10a}$ females in comparison to PE26B controls upon paraquat feeding. Survival under oxidative stress is significantly reduced in deletion females (P value<.0001, Kaplan Meier survival analysis). (B) Survival curve for *Serf*$^{\Delta 10a}$ males in comparison to PE26B controls upon paraquat feeding. Under oxidative stress male survival in modestly but significantly reduced (P value=.0019, Kaplan Meier survival analysis).

3.2.6.2 Global *Serf* overexpression females show modest increase in lifespan under paraquat induced oxidative stress.

We performed the complementary experiment to test the effect of *Serf* overexpression on longevity under paraquat induced oxidative stress. This was done using Act5c GAL4 driven cDNA *Serf* overexpression as previously described (section 3.2.6.1). The 50% survival under oxidative stress in females was increased by 11.11 % in the overexpression group compared to the controls. Statistical analysis of the survival curves show that the female *Serf* overexpression group lives modestly but significantly longer (P value=.0157) compared to the control. The change observed in males was not significant (P value =0.56). To our surprise I found that in males paraquat toxicity completely abolished the lifespan extension we had observed previously upon *Serf* overexpression under normal condition. While the increased lifespan observed with global overexpression of *Serf* under normal conditions is considerable, the increased survival under these genotoxic conditions was negligible. Nevertheless, the decrease in survival noted in the Serf mutant in the presence of paraquat and the weakly enhanced survival in the female flies that overexpress Serf under this condition suggest a contribution of the Serf protein to the animal viability under stress conditions.

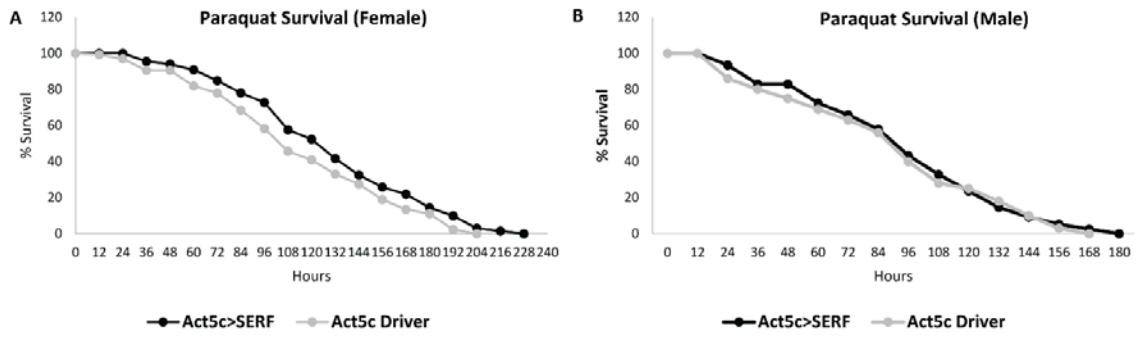

Fig. 3.8 Survival under paraquat induced oxidative stress is modestly increased in global *Serf* overexpression females but not in males. (A) Survival curve for Act5c-GAL4>*Serf* females in comparison to Act5c-GAL4 driver only controls upon paraquat feeding. Survival under oxidative stress is modestly but significantly increased in deletion females (P value= .0157, Kaplan Meier survival analysis). (B) Survival curve for Act5c-GAL4>*Serf* males in comparison to Act5c-GAL4 driver only controls upon paraquat feeding. Survival under oxidative stress is not changed in overexpression males compared to the controls.

3.2.7 The ubiquitous *Serf* overexpression flies show increased abundance of a mitochondrial marker protein, mitofusin.

The observation that the *Serf* deletion and overexpression flies show altered sensitivity to paraquat suggests that mitochondrial activity might be altered in these flies, since mitochondria are responsible for mediating the effect of paraquat induced toxicity. Rana *et al*., 2012 has shown that the overexpression of an E3 ubiquitin ligase, Parkin, in adult flies extends normal lifespan that correlates with increased mitochondrial activity (Rana, Rera *et al*. 2013). Parkin plays a role in mitochondrial quality control by enhancing the fission/fragmentation of damaged organelles for their subsequent degradation by autophagy (Youle and van der Bliek 2012, Ashrafi and Schwarz 2013). In order to do so, Parkin ubiquitinates a mitochondrial outer membrane protein, mitofusin (Mfn- a mitochondrial fusion promoting factor) for its degradation by the proteasome promoting, fragmentation of the dysfunctional mitochondria. In their study Rana *et al*., found that the steady state levels of Mfn are reduced in both young and old Parkin overexpression flies and that this increased expressed correlates well with increased mitochondrial activity (Rana *et al*., 2012). Figure 3.9 shows the western blot analysis of Mfn protein in *Serf* overexpression flies in comparison to the control in adults at 1 week and 5 weeks of age. The neuronal Elav protein was used for normalization. Mfn protein abundance increases between 1 week and 5 weeks independent of genotype, consistent with earlier reports (Rana *et al*., 2012). However, the relative abundance of Mfn protein (Mfn/Elav) is greater by about 2.5 fold at 1 week in the Serf overexpression line compared to the GAL4 driver control (compare lanes 1 and 3). This difference is also seen at 5 weeks, where the *Serf* overexpression group shows about 2 fold increase compared to the control (compare

lanes 2 and 4). These results contrast with what was seen with Parkin overexpression, where Mfn levels were reduced (Rana *et al*., 2012). Nonetheless, the data indicates possible alteration in the structure or activity of mitochondria in the *Serf* overexpression flies, which might relate to their oxidative stress response and longevity.

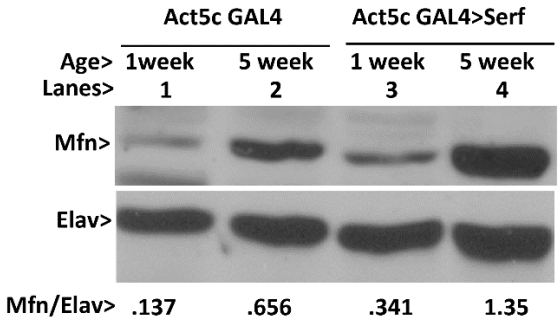

Fig. 3.9 Mitofusin (Mfn) protein abundance increases in ubiquitous *Serf* overexpression flies. Western blot analysis of adult whole female fly extracts at 1 week and 5 week old ages with rabbit anti-mitofusin and rat anti-Elav (loading control) antibodies in GAL4 driver control (Act5c-GAL4, Lanes 1 & 2) and *Serf* overexpression (Act5c GAL4>Serf, Lanes 3 & 4) flies. Relative levels of Mfn with respect to Elav is indicated below each lanes.

3.3 Conclusions and discussion

The major take home message from this portion of my study is that increased *Serf* gene expression promotes longevity while loss of *Serf* reduces lifespan in *Drosophila*. The data suggest that Serf may act in a non-autonomous manner to promote life-span extension. Genetically imposed changes in *Serf* expression resulted in modest changes in oxidative stress resistance that may correlate with alteration in mitochondria structure.

I observed that females were more sensitive to Serf-dependent lifespan changes than males. Such sex-specific differences are commonly reported in the literature (Lints, Bourgois *et al*. 1983). I also found that the different wildtype control strains used in my *Serf* deletion and overexpression studies showed *Serf*-independent differences in lifespan. Specifically the precise excision control showed a 30% decrease in longevity compared with the Act5c-GAL4 control. Previous studies have shown similar ill-defined lifespan differences (ranges between 60-80 days) among multiple wildtype *Drosophila* strains (Lints, Bourgois *et al*. 1983, Orr and Sohal 2003). Therefore, as done here, it is critical to use near isogenic lines for comparison when scoring for the impact of a specific gene (e.g., Serf) on lifespan. The reciprocal effect of loss of *Serf* or overexpression of *Serf* on lifespan compared with isogenized controls strongly supports my contention that Serf is a longevity factor in *Drosophila melanogaster.*

Since *Serf* has been implicated in neuromuscular and neurodegenerative diseases (Scharf *et al*.,, 1998, Van-Ham *et al*., 2010, Falsone *et al*.,, 2012) and loss of muscles and neuronal activity are important features of aging (Mattson and Magnus 2006, Demontis, Piccirillo *et al*. 2013), it was interesting to learn that *Serf* overexpression in muscles and

neurons was sufficient for lifespan extension. However, I cannot rule out the non-cell-autonomous or systemic effect of muscle or neuronal specific serf overexpression in other tissues, which could be relevant to the increased lifespan in these flies. For instance, enhanced FOXO signaling in muscles systemically increase the expression of its target 4E-BP in other tissues by regulating food intake and insulin release. The systemic enhancement of 4E-BP activity reduces the accumulation of poly-ubiquitinated protein aggregates in brain, retina, adipose tissues, which is linked to the lifespan extension observed in these flies (Demontis & Perrimon, 2010). Another example is the neuronal upregulation of the AMP activated protein kinase, which induces autophagy in the brain and also non-cell autonomously in the intestinal epithelium thereby improving protein homeostasis during aging and extending lifespan (Ulgherait, Rana *et al*. 2014). These instances point to the possibility that muscle or neuronal overexpression of *Serf* might exert non-cell-autonomous effect in other tissues to mediate its lifespan extending impact. However, the finding that overexpression of *Serf* in adult fat-bodies does not influence lifespan, bolsters the fact that it is important which tissues have the enhanced levels of Serf so as to exert its beneficial effect in longevity.

Among the best characterized pathways having major contribution in lifespan determination are the nutrient sensing IIS and TOR signaling pathways (Kenyon 2010, Evans, Kapahi *et al*. 2011). These pathways, the central regulators of metabolism, interact with each other to control various cellular processes including cell growth, mRNA translation, ribosome synthesis, expression of metabolism related and stress response genes and autophagy in response to environmental cues like availability of nutrients (Kenyon 2005);(Schmelzle and Hall 2000, Karpac and Jasper 2009). Since,

these signaling pathways govern the metabolic adaptation of an organism to environmental changes, they play a crucial role in determining organismal lifespan (Karpac and Jasper 2009, Evans, Kapahi *et al*. 2011). The activation of the evolutionarily conserved stress responsive Jun-N terminal Kinase (JNK) pathway has also been shown to exert protective effect under normal physiological condition and also under oxidative stress by extending lifespan (Wang, Bohmann *et al*. 2003, Libert, Chao *et al*. 2008). The finding that JNK activation operates by reducing IIS signaling, at multiple levels of the IIS pathway, provides a link between the environmental challenges (stress inducers that activate JNK) and cellular metabolic regulation (mediated by IIS) in the determination of organismal lifespan. Among several other major known determinants of lifespan is the G-protein coupled receptor *methuselah*, the loss of which extends lifespan by imparting resistance to paraquat driven oxidative stress, starvation stress and tolerance to high temperature (Lin, Seroude *et al*. 1998). Upregulation of the histone deacetylase Sir2 (Rogina and Helfand 2004) and loss of mitochondrial co-transporter Indy (Rogina and Helfand 2013) also extends lifespan that involves the calorie restriction pathway (Rapaport, Brunner *et al*. 1998, Rogina and Helfand 2004, Wang, Neretti *et al*. 2009). Whether these perturbations interact with IIS to mediate their effect on longevity is still unclear (reviewed in (He and Jasper 2014)).

Whether *Serf* function in lifespan extension is dependent on any of these known longevity pathways is not known. The extent to which these major ‘aging genes’ extend lifespan is comparable with that found in the case of enhanced Serf activity. For example the loss of function of *Chico* (IIS receptor substrate) and methuselah causes 48% (Clancy, Gems *et al*. 2001) and 35% (Lin, Seroude *et al*. 1998)increase in lifespan in females. In

my study I have seen a 33.18%, 32.52% and 30% increase in female lifespan with *Serf* overexpression in neurons, muscles and globally, respectively. Given such robust effect of *Serf* overexpression it is conceivable that Serf activity interacts with major lifespan determining pathways. Muscle specific overexpression of FOXO, the transcription factor negatively regulated by the IIS pathway, increases *Drosophila* lifespan (Demontis and Perrimon 2010) similar to *Serf*. Therefore, one possibility is that *Serf* functions downstream of IIS pathway. The *C. elegans* study has shown that *Serf* driven changes in the level of amyloid aggregation does not depend on DAF-16/FOXO in a Poly-Q expressing neurodegenerative disease model (Van-Ham *et al*., 2010), suggesting Serf might act either downstream to FOXO or in a parallel pathway to regulate amyloid aggregation. Importantly, *Serf* in *C. elegans* does not influence the normal lifespan. Therefore, if the lifespan extending effect of *Serf* is mediated by reduced IIS pathway remains to be an open question in *Drosophila*.

In contrast to the lifespan extending interventions that impart robust resistance to paraquat induced oxidative stress including reduced IIS signaling, enhanced JNK activity and loss of methuselah, Serf overexpression correlated with only a modest protection against the oxidative damage caused by paraquat feeding. Antioxidants like copper-Zn Superoxide Dismutase and Catalase increase *Drosophila* lifespan by directly imparting protection against free radical damage and therefore provides robust resistance against oxidative damage (Kirby *et al*.,, 2002; Missirlis, *et al*., 2001, Parkes *et al*.,, 1998). Our data therefore indicates that Serf is possibly not a direct mediator or regulator of oxidative stress response in flies. However, modest improvement in the free radical

induced stress management could partially contribute in the lifespan extending effect of Serf.

The finding that the level of mitofusin (Mfn) protein abundance increase in the long lived *Serf* overexpression flies, indicates an alteration in the mitochondrial structure and function possibly pertaining to the improvement in their oxidative stress response during normal course of aging. In contrast to our finding, Rana *et al*., has shown before that the lifespan extending effect of Parkin overexpression in adult tissues correlates with reduced accumulation of the Parkin substrate, Mfn, in aging flies, suggesting enhanced turnover of damaged mitochondria from cells with enhanced Parkin activity (Rana, Rera *et al*. 2013). Our finding that Mfn abundance increases in *Serf* overexpressing flies apparently suggesting that damaged mitochondria accumulates in these flies. However, it is important to mention that mitochondrial quality control is a complex phenomenon that depends on the level of mitochondrial fission and fusion (Youle and van der Bliek 2012). Mfn protein is known to function in and is required for the mitochondrial fusion reaction (Hales and Fuller 1997, Hermann, Thatcher *et al*. 1998, Rapaport, Brunner *et al*. 1998). Overexpression of Mfn in human cells has been shown to increase mitochondrial fusion and gives rise to long interconnected network of mitochondrial filaments (Santel and Fuller 2001). Therefore, increased level of Mfn in the *Serf* overexpression flies possibly relates to increased mitochondrial fusion and reduced fragmentation, which seems to be beneficial in the context of their longer lifespan. In fact, mitochondrial hyper-fusion has been shown to have cytoprotective roles under starvation stress and other physiological condition (Figge, Osiewacz *et al*. 2013). Moreover, according to a mathematical model predicted by systems biology age dependent adaptation to reduce mitochondrial fission

extends lifespan (Figge, Reichert *et al*. 2012). Together, these point to the possibility that the mitochondrial structure and function could be altered in the *Serf* overexpression flies which might relate to the longevity promoting effect of *Serf*.

3.4 Materials and methods

3.4.1 Fly strains and maintenance

The following genotypes are used in this chapter: (i) w^{1118}; (Xia, Fakler *et al*.) y w; {Act5C-GAL}25FO1/ CyO, y+ (Xia, Fakler *et al*.); (iii) elav-GAL (c155) (X); (Ruan, Tang *et al*.) Fat body-GS GAL4; [(i)-(Ruan, Tang *et al*.) obtained from Bloomington Stock Center] (v) daughterless-GS GAL4 (Obtained from Dr. David Walker laboratory, University of California, Loss Angeles); (vi) {mhcF3-580-GAL4} {mhcF3-580-RFP}/ SM6 (Xia, Fakler *et al*.) (Obtained from Dr. Thomas Gajewski lab, University of Chicago) (vii) {UAS-hp-Serf}100894 (Xia, Fakler *et al*.) (*SERF* RNAi line- Vienna *Drosophila* RNAi Center); (viii) UAS-*SERF* cDNA; (ix) $Serf^{\Delta 10a}$ (x) Precise excision 26B [(viii)-(x) generated in our lab; described in Chapter 2]. The fly strains (Xia, Fakler *et al*.)-(viii) were isogenized in the w^{1118} genetic background by backcrossing for 5 generations. Flies were cultured in 25C humidified chamber with 12 hours light dark cycle. Vials or bottles containing semi defined medium, as described by Bloomington *Drosophila* Stock Center (Backhaus *et al*.,, 1984), were used for all experiments in this study. The specific crosses performed in this chapter to obtain the progeny (larvae or adults) of required genotypes are described in table 3.1.

Table 3.1 describes the specific crosses performed, to obtain the progeny of required genotypes for the different assays conducted in this chapter.

Stage collected	Cross description	Progeny genotype collected
Adult	Act5c-GAL4/Cyo x w^{1118}	Act5c-GAL4/+
	Act5c-GAL4/Cyo x UAS-Serf (cDNA)	UAS-Serf (cDNA)/Act5c-GAL4
	Mhc-GAL4(Xia, Fakler *et al*.) x UAS-hp-Serf (RNAi)	UAS-Serf (cDNA)/Mhc-GAL4
	Mhc-GAL4(Xia, Fakler *et al*.) x w^{1118}	Mhc-GAL4/+
	Elav-GAL4(I) x UAS-Serf (cDNA)	Elav-GAL4/+, UAS-Serf (cDNA)/+
	Elav-GAL4(I) x w^{1118}	Elav-GAL4/+
	daGS-GAL4(Xia, Fakler *et al*.) x UAS-Serf (cDNA) (geneswitch driver)	UAS-Serf (cDNA)/daGS-GAL4
	FBGS-GAL4(Xia, Fakler *et al*.) x UAS-Serf (cDNA) (geneswitch driver)	UAS-Serf (cDNA)/FBGS-GAL4

3.4.2 Lifespan assay

Longevity measurements were performed as described by Demontis and Perrimon, 2011. Males and female flies of the correct genotype were collected separately within 24 hrs from eclosion and reared at a density of 10-15 flies per vial on standard food as described

before, at 25˚C humidified incubator with 12 hours light dark cycle. For our experiments with the GeneSwitch driver containing lines, adult flies were fed standard food containing 160µg/ml RU486 (Mifepristone, Sigma), prepared by adding 50ul of stock to the surface of freshly made food vials (Ren, C. 2009, Exp Gerontology). RU486 stock solution was prepared in ethanol and 50ul ethanol solvent was applied in the control food vials. All the food vials were air-dried for 48 hours for the ethanol to evaporate (Detailed protocol is available online at (http://towerlab.usc.edu/). Dead flies were counted every day and the food was changed every alternate day. For each experimental genotype and control group, at least two independent cohorts of flies, raised at different times from independent crosses, were analyzed.

3.4.3 Paraquat assay

The paraquat induced oxidative stress assay was performed as described previously by Cai *et al*.,, 2011. Male and female flies of the appropriate genotypes were collected and reared in the same manner as done for the lifespan assay except that the food was replaced with cellulose acetate plugs (Genesee Scientific, San Diego, CA) saturated with 2% sucrose plus 5 mM Paraquat. Flies were kept in a 25°C humidified incubator with 12 hrs light dark cycle. Viability was monitored every 12 hrs until all flies were dead.

3.4.4 Western blots

Protein extracts were made separately from 12 to 15 individuals at 1- and 5-weeks age (for Mfn protein analysis) for age matched, males or females by grinding them in 1X Lamelli buffer (2% SDS; 10% Glycerol; 60 mM Tris-Cl pH 6.8; 0.01% w/v bromophenol blue), 20µl per fly. Grinding is done on ice for 3-4 minutes until only the cuticle remains, followed by heating at 90℃ for 10 minutes. Supernatant were collected after spinning the

samples at 15,000 x g for 5 minutes in a table top centrifuge and stored at -80℃. Equal amounts of protein in terms of volume of extract per fly (usually 1 fly worth of protein i.e. 20µl), were resolved using 15% or 7.5% SDS-PAGE for detecting Serf or mitofusin (Mfn), respectively. The gels were blotted on .45µ PVDF membrane and membranes were probed with rabbit polyclonal antisera against human Serf (1:1000 dilution; generated against human N terminal Serf peptide, gift from Dr. Stefan Stamm, University of Kentucky), rabbit polyclonal anti-*Drosophila* Mfn (1:5000 dilution; generous gift from Dr. Alex Whitworth, University of California, LA) and rat anti- *Drosophila* Elav (1:5000 dilution, Developmental Studies Hybridoma Bank, 7E8A10). The rabbit primary antibody was detected using alkaline phosphatase conjugated goat anti-rabbit IgG (1:5000 dilution; Sigma). The rat antibody was detected using horseradish peroxidase conjugated goat anti-rat IgG (1:5000 dilution, Santa Cruz). Detection of alkaline phosphatase based signals involved colorimetric method using BCIP/NBT substrate (Promega) substrate. To detect the HRP based signals SuperSignal West Pico reagents were used (Thermo Fisher Scientific) followed by development on X-ray films (CL-XPosure^{TM} Film, 5 x 7 inches, Thermo Scientific). The colored blots and films were scanned using Kodak Image Station 2000R. The ImageQuant software was used to perform densitometry analysis of the scanned blots.

3.4.5 Statistical analyses

The lifespan data were analyzed using the R-survival package {Ziehm, 2013 #33}. The program utilizes Kaplan Meier curves and log rank tests {Rich, 2010 #34} to compare the survival curves between the experimental and control groups. For all other statistical analysis two tailed Unpaired Student's t-test was used. For all statistical tests $P<0.05$

were considered significant. For all graphs, data are represented as the mean ± the standard deviation of mean (Becker, Semler *et al*.) and significant difference is expressed as: ‘*’- P value between 0.01-0.05; ‘**’- P value between 0.001-0.01; ‘***’ P value<.001.

Chapter 4: The *Serf* gene in *Drosophila* enhances autophagy

4.1 Introduction

So far I have shown that *Serf* in *Drosophila* is required for normal adult fly climbing ability and lifespan. Climbing naturally declines with age due to combined loss of muscular and neuronal activity. The fact that loss of *Serf* impairs climbing performance at every age, combined with its impact on lifespan raises the possibility that *Serf* depletion enhances tissue aging. Gradual deterioration of protein quality control contributes to age related functional decline in tissues (Koga, Kaushik et al. 2011), at least in part due to the accumulation of toxic, poly-ubiquitinated protein aggregates (Lindner and Demarez 2009). These aggregates serve as a marker for tissue-aging and have been observed in organisms from flies to humans. These structures appear to accumulate due to decreased clearance efficiency by autophagy in aged tissue (Rubinsztein *et al.*, 2006). In fact, genetic enhancement of autophagy by transgenic overexpression of pro-autophagy gene ATG5 in mice (Pyo, Yoo et al. 2013) or autophagy stimulator HLH30 in *C. elegans* is sufficient to extend lifespan. This was observed by Demontis and Perrimon in *Drosophila* where lifespan extension was partially achieved by promoting autophagy and subsequent clearance of the poly-ubiquitinated protein aggregates from the adult muscles (Demontis and Perrimon, 2010). Since Serf is predicted to play a role in the protein quality control, I hypothesized that the changes in lifespan observed with *Serf* gene manipulation might correlate with changes in autophagy. This chapter addresses this hypothesis.

4.2 Results

4.2.1 The Short lived *Serf* deletion mutants show increased accumulation of poly-ubiquitinated aggregates in adult thoracic muscles.

The *Serf* deletion flies show an average (between males and females) of about 28% reduction in the normal adult lifespan compared to the precise excision (i.e., wildtype) controls. The survival curves of the *Serf* deletion flies and the isogenic controls start to deviate between 3-4 weeks of age when the *Serf* deletion flies begin to die off at a high rate. To learn if there is a difference in the amount of poly-ubiquitinated aggregates in the muscles I imaged flies of both genotypes at 1 and 4 weeks after eclosion.

Figure 4.1A shows the representative fluorescent microscopic images of tissue sections from the precise excision control (PE26B) and *Serf* deletion ($Serf^{\Delta 10a}$) at one and four using an anti-ubiquitin primary antibody and an AF594-labeled secondary antibody. As expected, the amount of these aggregates increases over time in both the control and the deletion lines. However, the amount of aggregate is greater in the *Serf* deletion strain compared to the wildtype control at both time points.

Figure 4.1B shows quantification of the aggregate accumulation expressed in terms of the total aggregate area as a percentage of the total tissue surface area. The control line at 1-week of age shows an average of .07% of the surface area aggregates while in the *Serf* deletion this value by 5.05 fold to cover approximately 0.34% of the tissue surface (P=.0145, n=10). At 4 weeks, 0.55 % of the tissue surface in the wildtype is composed of poly-ubiquitinated aggregates and this value increases 2.78-fold to 1.54% in the *Serf* deletion background. This difference is reproducible and statistically significant (P=.0004, n=10).

Figure 4.1C presents a measure of aggregate size, the average number of pixels per particle. The average particle size increases in both genotypes between one week and four weeks. However, we do not observe any change in the average size of the particles between the two genotypes. Therefore, the total number of aggregates increase in the short-lived *Serf* deletion mutant background, but apparently not their average sizes.

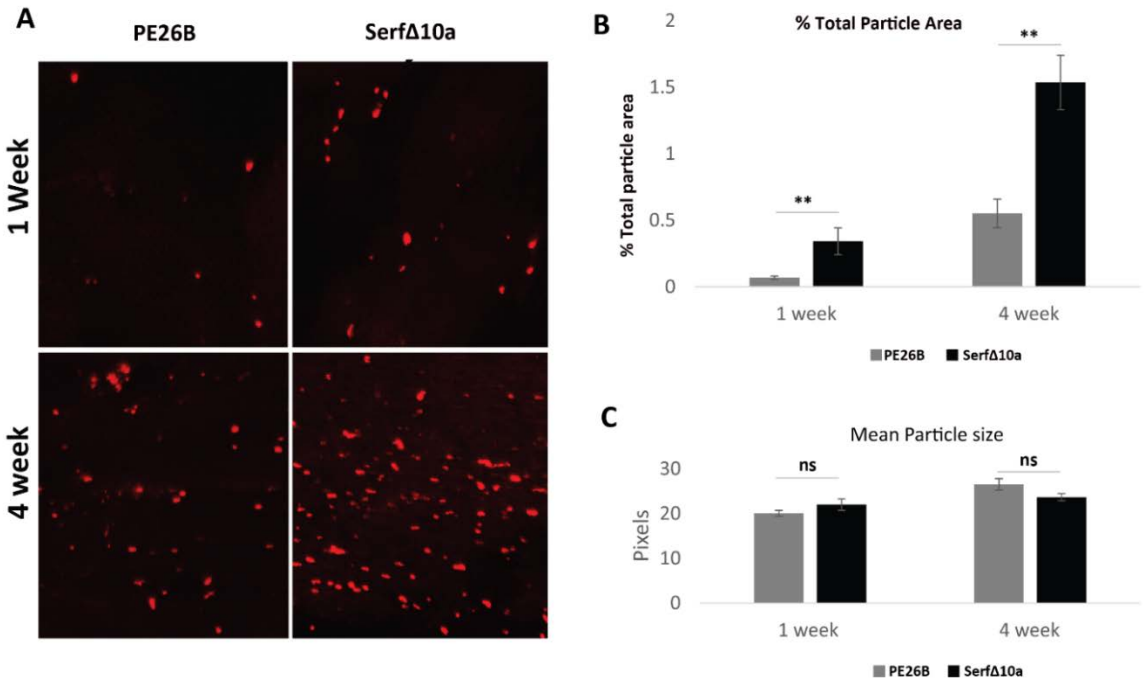

Fig 4.1. Serf deletion flies show increased accumulation of age related poly-ubiquitinated protein aggregates in flight muscles. A) Representative sections of adult flight muscles at 1 week and 4 week age from WT (precise excision line PE26B) and the *Serf*$^{\Delta 10a}$ mutant stained with flies stained with anti-ubiquitin antibody and detected with fluorescent conjugated secondary antibody. Protein aggregates are shown in red. B) Quantification of aggregate abundance in terms of total particle area as a percentage of the total muscle area. At both time points the *Serf*$^{\Delta 10a}$ mutant shows significant increase in the percentage of particle covered area compared to the control (P=.0145 at 1 week; P=.0004 at 4 weeks; Repeat measures ANOVA, n=10 flies per genotype per time point; at least 8 sections per fly were used). C) Quantification of aggregate size in terms of average pixels per particle. The mean particle size does not significantly differ between *Serf*$^{\Delta 10a}$ and the control group (P=.1972 at 1 week; P=.0726 at 4 week, Unpaired t-test, n=10 per genotype per time point).

4.2.2 *Serf* overexpression reduces accumulation of poly-ubiquitinated aggregates.

The ubiquitous overexpression of *Serf* increases fly lifespan by approximately 30%. The survival curves of the *Serf* overexpression flies and the isogenic controls start to separate out at around 35 days when the percentage of survival of the controls begins to decline rapidly. I wanted to know if there is a correlated distinction in the amount of poly-ubiquitinated aggregates in the muscles of these two groups and therefore I performed a time course study of this marker in 1 week, 4 week and 7 week old animals.

Figure 4.2A shows the representative fluorescent-microscopic images of tissue sections from the driver only control (Act5c GAL4) and ubiquitous *Serf* overexpression (Act5c GAL4>Serf) flies at 1 week, 4 week and 7 week old age. Numerous aggregates were found in both genotypes, however, the amount is reduced in the *Serf* overexpression background compared to the driver only control at every time point. As shown in figure 4.2B, the 1 week old Act5c-GAL4 control line shows an average of 0.139% surface area in aggregates which decreases in the *Serf* overexpression group to.07% , however not statistically significant (P=.3377, n=6). At 4 weeks of age1.02% of the control tissue area presents as aggregates while *Serf* overexpression group shows about a 40% decrease to an average of 0.59% of tissue surface. Again, however, this difference is not statistically significant (P=.3606, n=6. At 7 weeks the Act5c-GAL4 control accumulates a great load of aggregates covering an average of 2.5% of its tissue area, whereas, the *Serf* overexpression group shows by 2.45 fold and presents only 1.02% tissue surface with aggregates (Figure 4.2B). This difference is statistically significant (P value=.0121, n=9).

Figure 4.2C shows the average aggregate size in terms of the number of pixels per particle using these same animals Here I find that the average sizes of the protein

aggregates are slightly but significantly reduced in the *Serf* overexpression flies, both at 4 weeks (14.85%, P=.0379, n=6 per genotype) and at 7 weeks (14.57%, P=.0048, n=9 per genotype) compared to the driver only control. Together, these data show that *Serf* overexpression not only extends the lifespan of flies but reduces the accumulation of an accepted marker of tissue aging.

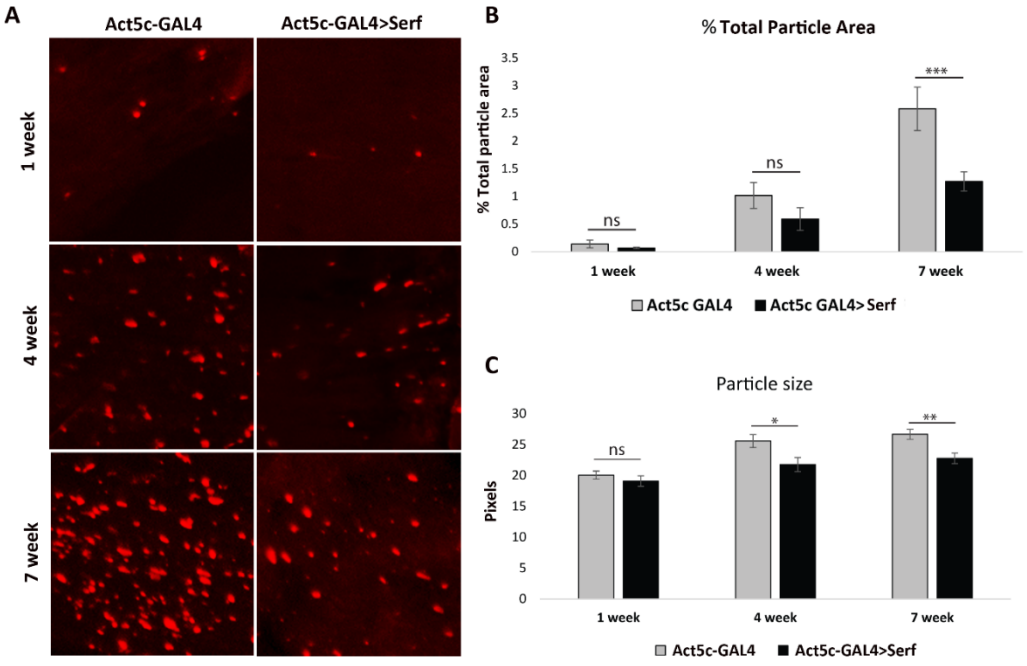

Fig 4.2.Ubiquitous *Serf* overexpression flies show reduced accumulation of age related ubiquitinated protein aggregates in the flight muscles. A) Representative immune-fluorescent images of adult flight muscle sections at 1 week, 4 weeks and 7 weeks age from the driver only control (Act5c GAL4) and *Serf* overexpression (Act5c GAL4>*Serf*) flies stained with anti-ubiquitin antibody and detected with fluorescent conjugated secondary antibody. Protein aggregates are shown in red. B) Quantification of aggregate abundance in terms of total particle area as a percentage of the total muscle area. The *Serf* overexpression group showed consistent decrease in the percentage of particle covered area as compared to the controls at all time points, however, it is statistically significant at 7 week old age (P=.0121; Repeated Measures ANOVA; n=9, at least 8 sections per fly were used). C) Quantification of aggregate size in terms of average pixels per particle. The mean aggregate size also decreases significantly in the 4

weeks (P=.0379, n=6, at least 8 sections per fly) and 7 weeks of age (P=.0048, n=9, at least 8 sections per fly) *Serf* overexpression flies as compared to the controls.

4.2.3 Total ubiquitinated protein amounts are increased in the *Serf* deletion and reduced in *Serf* overexpression adult flies.

Since we found that the poly-ubiquitinated aggregates, observed microscopically, are increased in the *Serf* deletion mutant and decreased in the overexpression flies, we wanted to know if this change reflected differences in the total ubiquitinated protein levels in adult tissues. Therefore, I isolated proteins from whole body extracts of 2 week and 4 week old flies and performed western blot using the anti-poly-ubiquitin antibody (Perrimon *et al*., 2010). I observe that the overall amounts of ubiquitination increases from 2 weeks to 4 weeks in both PE26B control (Fig. 4.3Acompare lanes 1-3 and 5-7, where 1 & 5 represents 2 weeks and 3 & 7 represents 4 weeks) and the $Serf^{\Delta 10a}$ mutant flies(compare lanes 2-4 and 6-8, where 2 & 6 represents 2 weeks and 4 & 8 represents 4 weeks). However, the deletion mutant group (Lanes 2, 4, 6 & 8) consistently showed greater anti-ub staining compared to the controls (Lanes 1, 3, 5 & 7) at both time points and for both the sexes. In contrast, the levels of α-tubulin loading control remain roughly similar under all conditions. This observation indicates that the absolute level of protein ubiquitination increases in the *Serf* deletion mutant.

In contrast to the *Serf* deletion results, I find that overexpression of *Serf* reduces the ubiquitinated protein accumulation that occurs in the older animals (Figure 4.3B). While it is true that both the control (lanes 1-3 and 5-7, where 1 & 5 represents 2 weeks and 3 & 7 represents 4 weeks) and *Serf* overexpression flies (lanes 2-4 and 6-8, where 2 & 6 represents 2 weeks and 4 & 8 represents 4 weeks) show an increase in ubiquitination at 4

weeks compared to two weeks, the increase is noticeably less in the *Serf* overexpression background regardless of the sex. In addition, we note a curious change in the pattern of ubiquitinated proteins when Serf protein levels vary. In the *Serf* deletion, not only is the overall anti-ubiquitin signal increased, but also more signal is found associated with the high molecular weight protein bands. Consistent with that, in overexpression flies, most of the high molecular weight protein bands diminish greatly along with the reduction of the overall ubiquitin signal. Another important point to note here is that the PE26B and the Act5c-GAL4 control flies show very obvious difference in the ubiquitin signal. The level of signal obtained from the Act5c-GAL4 control is equivalent to that of the *Serf* deletion line. One possibility is that different genetic background show differences in the level of total ubiquitinated protein and whether this observation is consistent between different experiments will be addressed in the discussion section for this chapter.

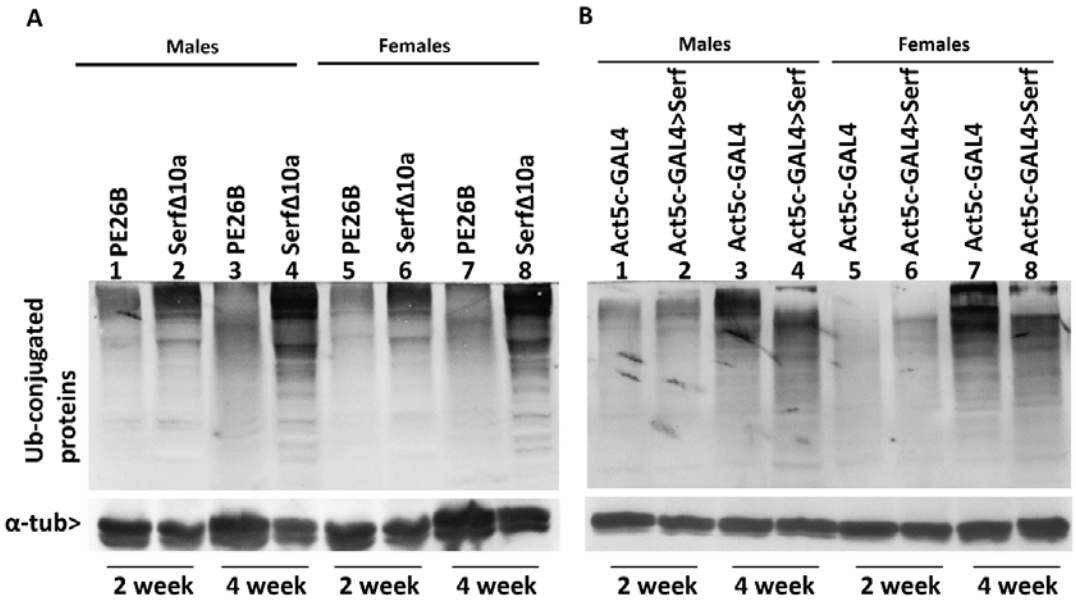

Figure 4.3 Total ubiquitinated protein levels are increased in *Serf* deletion and reduced in *Serf* overexpression adult flies. Western blot images of adult whole fly extracts at 2 week and 4 week old ages with anti-ubiquitin and anti-α-tubulin (Loading control) antibodies in males and females separately. A. The *Serf* deletion ($Serf^{\Delta 10a}$: Lanes 2, 4, 6 and 8) and precise excision (PE26B: lanes 1, 3, 5 & 7) control flies were compared for relative levels of total ubiquitinated proteins in males (Lanes 1-4) and females (Lanes 5-8). B. The *Serf* overexpression (Act5c GAL4>*Serf*: Lanes 2, 4, 6 and 8) and driver only controls (Act5c GAL4: lanes 1, 3, 5 & 7) flies were compared for relative levels of total ubiquitinated proteins in males (Lanes 1-4) and females (Lanes 5-8).

4.2.4 Impact of altered *Serf* expression on autophagy

The *Serf* deletion and overexpression flies showed increased and decreased abundance of poly-ubiquitinated protein aggregates in their muscles, respectively (Fig 4.1 & 4.2). Such complexes are cleared from fly tissues by autophagy (Perrimon 2010; Korolchuk *et al*., 2009; Rubinsztein, 2006.). Upregulation of autophagy is thought to extend normal lifespan, at least in part, by the efficient clearance of these potentially toxic aggregates (Perrimon 2010). Therefore, I investigated whether autophagy is altered with *Serf* deletion or overexpression.

I first asked if autophagy induction by starvation is altered with *Serf* deletion or overexpression. Induction of autophagy upon nutrient deprivation is a conserved life sustaining phenomenon across species (Reviewed in Mizushima, 2007). In *Drosophila*, larval fat-bodies undergo robust induction of autophagy in response to starvation as fat bodies readily sense nutrient availability (Reviewed in Mauvezine *et al*., 2014; Scott *et al*., 2004). Autophagy can be observed by the accumulation of Lysotracker+ vesicles (Neufeld *et al*., 2008) representing the final digestive compartments of the autophagy pathway (Scott *et al*., 2004). In contrast to "induced autophagy", the phenomenon of "basal autophagy" is different in its most simplistic view, by being a constitutive process which clears defective cytosolic components in adult muscles even in the absence of starvation (Reviewed in Mizushima, 2007). Therefore, while results from starvation induced autophagy cannot be directly correlated with protein aggregate accumulation in non-starved adult *Serf* tissues, it will give us an idea if *Serf* generally impacts the autophagic process. Later in this chapter I will address whether *Serf* influences "basal autophagy" in adult tissues.

4.2.4.1 The short lived *Serf* deletion flies show decreased abundance of Lysotracker positive autophagy-related vesicles in the larval fat bodies.

Since the *Serf* deletion mutant shows shortened lifespan and increased abundance of poly-ubiquitinated aggregates**,** autophagy may be less efficient in this genetic background. Here I test whether starvation induced autophagy is diminished in the *Serf* deletion mutant compared to the wildtype control. Figure 4.3A shows fluorescent microscopic images of representative larval fat body cells from the precise excision control (PE26B: panel a-c & a'-c') and the *Serf* deletion mutant (*Serf*$^{\Delta 10a}$*:* panel d-f & d'-f') at the 3rd instar stage. The Lysotracker positive yvesicles are shown in red and the nuclei in blue. The fat body cells undergo an abrupt switch from no Lysotracker positive puncta in fed state state (panel a-f) to numerous Lysotracker positive vesicles when starved (panel a'-f'), in both genotypes. Compared with the control, the *Serf* deletion line consistently shows fewer red punctate structures and the vesicles appear smaller in size. These data are quantified in figures 4.3B and C with abundance expressed as the number of visible puncta normalized per nuclei in the field. The average sizes are measured in pixels. I find that the control larvae form on average about 20.73 vesicles per nucleus, whereas the deletion mutant shows about 10.39 per nucleus. This 1.99 fold reduction in vesicle number after starvation is y6statistically significant (P value=.0351, n=5). The average particle size is also reduced by 2.59 fold in the deletion group compared to the control (P value=.0103, n=5). These data strongly suggest that, at least in larval fat bodies, the autophagy response to starvation is less robust in the *Serf* deletion mutant.

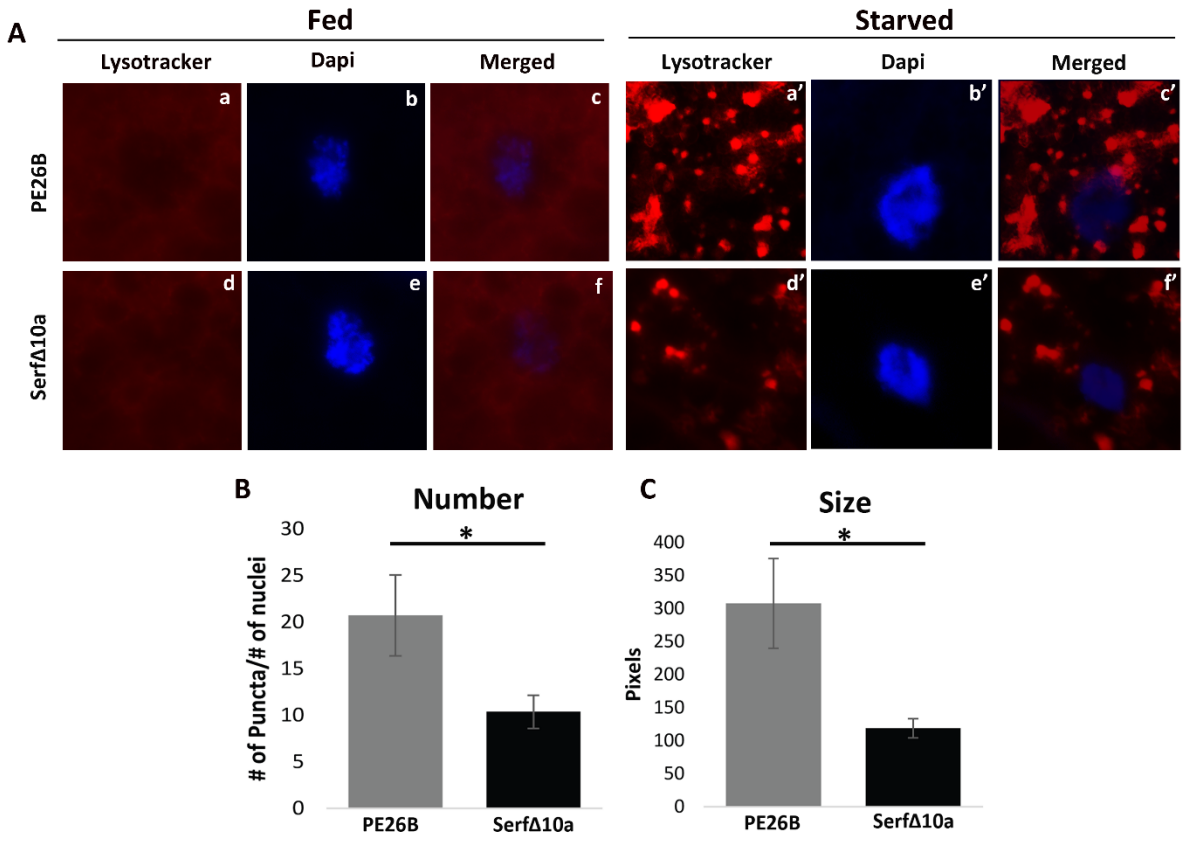

Fig 4.4. *Serf* deletion larvae show reduced size and abundance of lysotracker positive vesicles after induction of autophagy. A) Representative images from the precise excision control (PE26B) and the deletion (*Serf*$^{\Delta 10a}$) group. Red: Lysotracker; Blue: DAPI. B) Quantification of the abundance of Lysotracker positive puncta as measured by number of puncta per nucleus, which is significantly reduced in the deletion group compared to the controls (P value =.0351; n=5). C) Quantification of the size of the vesicles. The average size of the vesicles significantly reduces in the deletion group compared to the controls (P value =.0103; n=5 genotype).

4.2.4.2 The long lived *Serf* overexpression flies show an increased autophagic response to starvation.

Since the *Serf* overexpression flies show decreased abundance of poly-ubiquitinated aggregates, it is conceivable that the autophagic response is more robust in this background. Figure 4.4A shows the representative images of fat body cells documenting Lysotracker positive vesicles from the driver only control (Act5c-GAL4: panel a-c & a'-c') and the *Serf* overexpression line (Act5c-GAL4>*Serf:* d-f & d'-f'). Once again, we find few or no Lysotracker positive in the fed state, regardless of genotype, while starvation induces the autophagy resulting in the production of many Lysotracker positive vesicles. Figure 4.4B and C shows the quantification of the abundance of the Lysotracker positive vesicles and their average sizes respectively. The driver only control was found to form an average of 32.37 vesicles per cell, whereas the *Serf* overexpression line showed 43.73 vesicles per nucleus on an average. Although it appears that the number of Lysotracker stained vesicles increases slightly in the Serf overexpression line, the difference is not statistically significant (P value=.5056, n=5). The vesicle size does not differ significantly between the two genotypes. Taken together with the results presented above, it appears that while the absence of Serf dampens the autophagic response to starvation, excessive Serf is unlikely to stimulate autophagy much beyond that normally seen with nutrient deprivation in larval fat bodies.

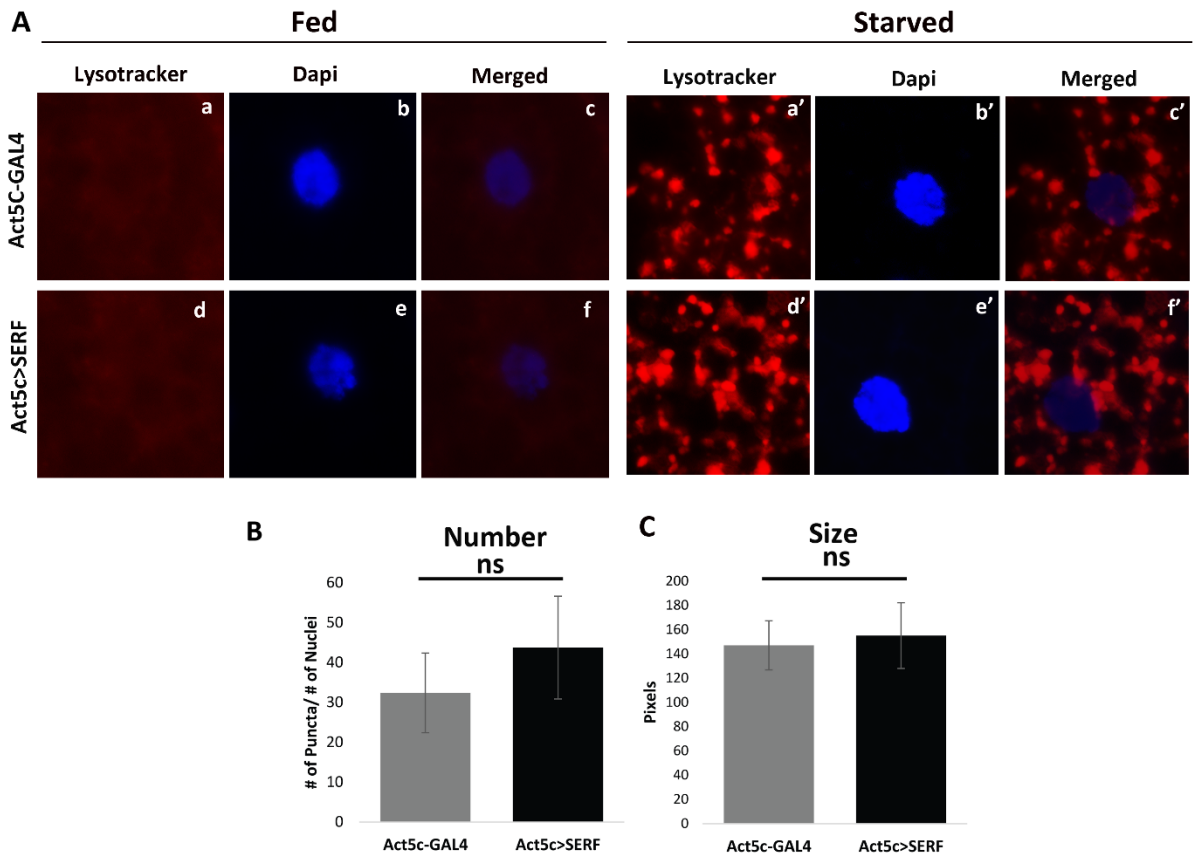

Fig 4.5. *Serf* overexpression has little impact on the number of Lysotracker positive vesicles upon starvation-induced autophagy in larval fat bodies. A) Representative images from the driver only control (Act5c-GAL4) and the *Serf* overexpression group (*Act5c-GAL4>Serf*) group. Red: Lysotracker; Blue: DAPI. B) Quantification of the abundance of Lysotracker positive puncta as measured by number of puncta per nucleus, which is slightly increased in the overexpression group compared to the controls but is not statistically significant (P value=.5056; Unpaired t test, n=5 per genotype). C) Quantification of the size of the vesicles. The average size of the vesicles did not change in the overexpression group as compared to the controls (P value=.8177; unpaired t test, n=5 genotype).

4.2.4.3 Increased Ref(2)P protein abundance indicates that autophagy is impaired in the absence of *Serf.*

The Lysotracker staining assay results strongly suggest that deletion of *Serf* reduces the autophagic response to starvation. I wanted to further validate this finding by assaying for the accumulation of a protein called Ref(2)P, a known target of autophagy (Mauvezin, Ayala et al. 2014). Ref(2)P is the *Drosophila* ortholog of human p62, a protein that binds to the poly-ubiquitinated proteins and the complex is recruited to the autophagosomes (Wooten *et al.*, 2006). While assisting in poly-ubiqutinated protein recruitment, p62/Ref(2)P is also degraded with the autophagosome cargo (Bjorkoy, Lamark et al. 2005) (Klionsky, Elazar et al. 2008). Since p62/Ref(2)P is constitutively expressed, this protein accumulates when autophagy is impaired by mutation to genes required for autophagy, such as $Atg6^{1}$(Shravage et al., 2013). Therefore, the accumulation of Ref(2)P is viewed as a reliable marker of reduced autophagic flux (Bjorkoy, Lamark *et al.*,2005; Klionsky, Elazar *et al.*, 2008).

I assayed the relative levels of Ref(2)P in the starved larval fat bodies of *Serf* deletion and overexpression flies in comparison to the controls. Figure 4.4A shows western blot images of Ref(2)P (and α-tubulin loading control) from the *Serf* deletion ($Serf^{\Delta 10\alpha}$) mutant and the precise excision (*PE26B*) control larvae. In this assay I used the $Atg6^{1}$mutant as a positive control for Ref(2)P accumulation. I looked at the Ref(2)P protein level both under fed (Lanes 1-3) and starved (Lanes 4-6) conditions. When fed, there is no induction of autophagy, and expect to see the 85 KD band for Ref(2)P protein. The Ref(2)P is observed in the wildtype (PE26B precise excision) preparation under fed conditions and, as expected, the abundance of this is greatly reduced after starvation (compare lanes 2 &

5). In contrast, when autophagy is arrested by the *Atg6*^{1}mutation, Ref(2)P levels are elevated and present under both fed and starved conditions (compare lanes 1 & 4). In contrast with this wildtype control strain, with the *Serf* mutant, we observe Ref(2)P in both the fed and starved animals (compare lanes 3 & 6), although the level of accumulation is much less than what is seen when autophagy is fully arrested with the *Atg6*^{1}mutant. These observations indicate that the level of Ref(2)P clearance and hence the efficiency of the autophagy pathway is reduced in the absence of *Serf.*

Figure 4.4B describes the results obtained with the *Serf* overexpression (Act5c GAL4>Serf) and control (Act5c-GAL4) larvae, under fed (Lanes 1-3) and starved (Lanes 4-conditions. Very low levels of Ref(2)p were detected in the Act5c-GAL4 flies with or without *Serf* overexpression under both fed and starved condition. Therefore no conclusion could be made about the impact of Serf overexpression on starvation induced autophagy.

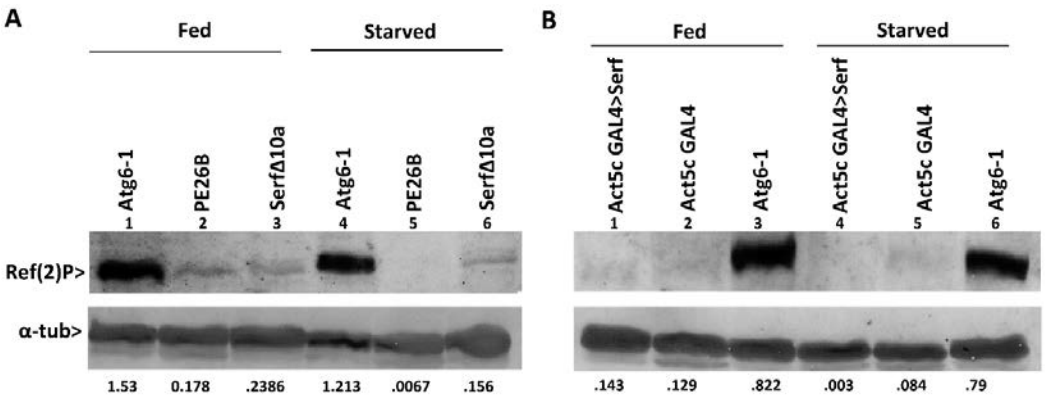

Figure 4.6 The relative levels of Ref(2)P protein increases in the starved *Serf* deletion larvae. Western blot images of larval protein extract with anti Ref(2)P and anti α-tubulin (loading control). A) *Serf* deletion ($Serf^{\Delta 10a}$: Lanes 3&6) and precise excision control (PE26B: Lanes 2&5) larvae are compared for relative Ref(2)P levels. The $Atg6^{1}$ group (Lanes 1&4) served as positive control for Ref(2)P accumulation. Lanes 1-3 shows fed group; lanes 4-6 shows starved group. The number under each lane indicates relative Ref(2)P levels with respect to α-tubulin. B) *Serf* overexpression ($Serf^{\Delta 10a}$: Lanes 1&4) and GAL4 driver control (PE26B: Lanes 2&5) larvae are compared for relative Ref(2)P levels. The $Atg6^{1}$ group (Lanes 3&6) served as positive control for Ref(2)P accumulation. Lanes 1-3 shows fed group; lanes 4-6 shows starved group.

4.2.4.4 *Serf* expression modulates the relative expression of several autophagy genes in young adult flies.

The *Serf* deletion flies are short-lived and accumulate more poly-ubiquitinated protein aggregates in the muscles whereas the *Serf* overexpression flies are long-lived and accumulate fewer poly-ubiquitinated aggregates compared to their respective isogenic controls. One explanation is that the basal level autophagy is either reduced in the deletion flies or enhanced in the overexpression flies leading to increased or decreased aggregate accumulation. To test, I studied the relative expression of *Atg1, Atg5, Atg6, Atg7* and *Atg8a* in these flies at four different ages in their adult life. The evel of autophagy gene expression has previously been shown to change with animal age and in absence of autophagy inducing stimulus such starvation. The basal level of autophagy correlates with the clearance of protein aggregates from multiple types of adult tissue (Simonsen *et al*., 2008; Perrimon *et al*.,2010; reviewed in Rubinsztein *et al*., 2011). Therefore, I predict that relative expression of autophagy genes in adult tissues will decrease with *Serf* deletion and increase with Serf overexpression.

Adult flies from both the experimental and control genotypes at four different ages were used to prepare cDNA for quantitative PCR analysis. The α tubulin transcript was used as an internal control for mRNA abundance. Figure 4.5A shows the fold change in the relative expression of the 5 autophagy genes in the *Serf* deletion group ($Serf^{\Delta 10a}$) compared with the precise excision control (PE26B) at weeks one, two, three and five. The *Atg5*, *Atg7* and *Atg6* genes show a trend of reduction in the relative expression in the mutant. The *Atg5* gene shows an average of 27.42%, 21.71%, 12.4% and 28.82% reduction at the four respective ages, however, the reduction is statistically significant at

only 1 week old time point (P value<.05, n=3). Similarly, the *Atg7* gene shows decreases by 34.01%, 33.35%, 40.7% and 32.86% at the respective time points. The decrease is statistically significant at 1 week (P<.05, n=3) and 3 week (P<.05, n=2) old age. The change in relative expression for the *Atg6* gene is less obvious. Only at 5 weeks is expression significantly reduced (20.25% (P<.01, n=2). In contrast, the Atg1 gene shows a trend of increased relative expression by 22.6%, 16.18%, 21.4% and 19.85% for the 4 age groups, however, none of these are statistically significant. The Atg8a gene stayed relatively unaltered, except at 3 weeks where it showed significant increase by 28.1% (P value<.01, n=2). Taken together, the data suggest that the absence of *Serf* impacts expression of certain autophagy genes, with the messages of two, *Atg5* and *Atg7* providing the best evidence for consistent under-representation in the mutant background.

In the *Serf* overexpression line I find that 4 out of 5 genes, *Atg1, Atg5, Atg6* and *Atg7* show significant upregulation in the relative gene expression levels at weeks one and two (Figure 4.5B). As shown in the figure, the relative expression of *Atg1, Atg5, Atg6* and *Atg7* genes increases by 56.75% (P values<.0001, n=3), 112.6% (P value<.01, n=3), 52.3% (P values<.0001, n=3) and 107.65% (P values<.0001, n=3), respectively at 1 week old age, and 40.4% (P value<.0001,n=2), 143.4% (P value<.01, n=2), 58% (P values<.05, n=2) and 114.4% (P value<.0001, n=2), respectively at 2 week old age. However, this increase in expression is no longer obvious after 2 weeks. Moreover the expression of autophagy genes are generally found to decrease as the flies get older, irrespective of the genotype. In summary, four out of the five *Atg* genes tested show significant increases in mRNA abundance in with *Serf* overexpression, suggesting an enhancement of basal level

autophagy during early life consistent with the decreased abundance of poly-ubiquitinated protein aggregates seen above.

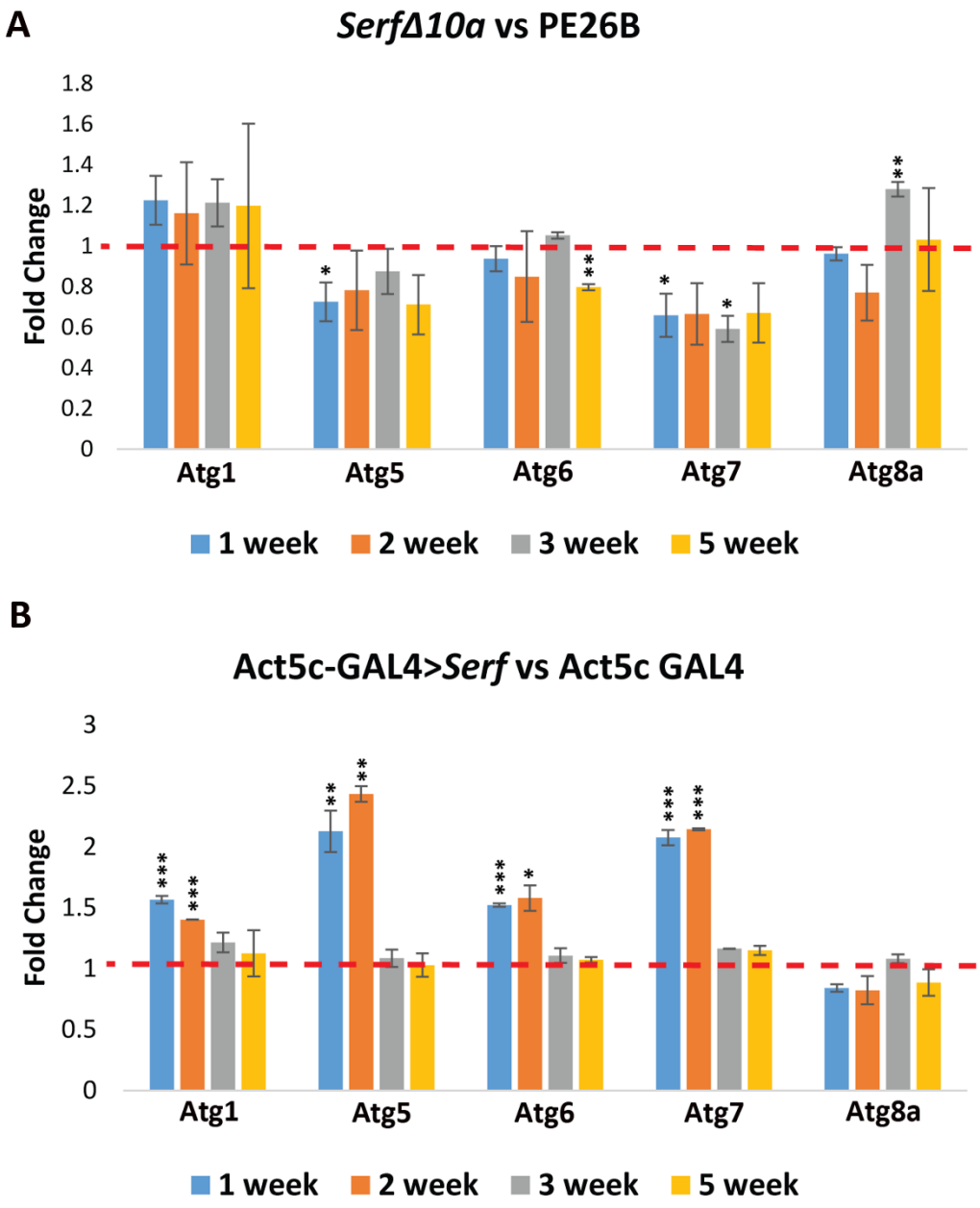

Fig 4.7: Autophagy genes are differentially expressed in *Serf* deletion and overexpression flies. Real time PCR of autophagy gene transcripts (*Atg1*, *Atg5*, *Atg6*,

Atg7 and *Atg8a*) performed at 4 different time points. Relative expression levels are calculated by normalizing with alpha tubulin expression level. Fold changes of relative transcript levels in the experimental group are quantified with respect to the control group as shown in the bars. Significance of fold change is calculated with respect to no change in expression between the two groups i.e fold change =1 (shown by the red dashed line). A) Fold change of relative expression in the *Serf* deletion ($Serf^{\Delta 10a}$) flies with respect to the precise excision control (PE26B). The Atg5 and Atg7 genes show a consistent trend of reduced expression at all time points in the *Serf* deletion flies however it is statistically significant at only certain time points indicated by the stars. (‘*’ P value <.05; ‘**’ P value <.01; Unpaired t test, n=3 for 1week, n=2 for the rest). B) Fold change of relative expression in the *Serf* overexpression (Act5c-GAL4>*Serf*) flies with respect to the driver only control (Act5c-GAL4). The *Atg1, Atg5*, *Atg6* and *Atg7* genes show a consistent and significant upregulation of relative expression at 1 week and 2 week time points in the *Serf* overexpression flies, however, no difference is observed at the 3 week and 5 week time points between the two groups. (‘*’ P value <.05; ‘**’ P value <.01; ‘***’ P value <.001, Unpaired t test, n=3 for 1week, n=2 for the rest).

4.2.4.5 The autophagy substrate Ref(2)P tags the poly-ubiquitinated protein aggregates in muscles and its accumulation increases and decreases with *Serf* deletion and overexpression, respectively.

So far, my data show that the expression of several autophagy genes is enhanced in adult flies with *Serf* overexpression while the *Serf* deletion flies show modest reduction in the expression of a couple of genes. To learn whether this change correlates with altered basal level autophagy in adults muscles, here I test for co-localization of Ref(2)P with the poly-ubiquitin protein aggregates as well as the overall Ref(2)P accumulation in this tissue. Since Ref(2)P is a known target of autophagy that binds and recruits poly-ubiquitinated autophagy substrates into autophagosomes (Wooten *et al.,* 2006), its co-localization with protein aggregates would indicate that the aggregates are autophagy substrates (Mauvezin *et al.,* 2014; Perrimon *et al.,* 2010). In, addition accumulation of Ref(2) eP is indicative of reduced autophagic flux (Mauvezin *et al.,* 2014).

Figure 4.8 shows confocal images of anti-Ref(2)P and anti-Ubiquitin (Ub) antibody stained adult thoracic muscles where Ref(2)P and Ub proteins are visualized with green and red fluorescent conjugated secondary antibodies, respectively. Here I used young (1 week old) and old (5 week old) muscles from both *Serf* deletion ($Serf^{\Delta 10a}$, panel A) and *Serf* overexpression (Act5c-GAL4>Serf, panel B) flies along with their respective age-matched isogenic controls. Several points can made based on these images. First, most of the Ub-positive aggregates in red co-localize with Ref(2)P signals in green in both genotypes at both time points (Merged panels in fig 4.8A and 4.8B). However, the number of particles that do not overlap increases at 5 week old time point for both genotypes. Second, for both the *Serf* deletion mutant (Fig 4.8A) and overexpression flies

(Fig. 4.8B) there is an increase in green and red puncta from 1 week to 5 week aged muscles, similar to what has been shown before (Fig 4.1A and Fig 4.2A). Third, the muscles of the *Serf* deletion strain (*Serf*$^{\Delta 10a}$) show greater numbers of green and red puncta at both time points compared to the precise excision control (PE26B) (Fig 4.8A). In contrast, while the 1 week old muscles look very similar, the *Serf* overexpression (Act5c>GAL4) muscles show an obvious decrease in the number of both types of puncta at 5 week old age, compared to the driver only control (Act5c-GAL4), (Fig 4.8B).

Figure 4.6C and D shows the quantification of Ref (2)P positive aggregates for *Serf* deletion and overexpression groups, respectively. As shown in the figure (Fig 4.8C) the percentage of total Ref(2)P positive particle area significantly increases in *Serf*$^{\Delta 10a}$ compared to the PE26B control at both 1 week (0.02% in PE26B and 0.197% in *Serf*$^{\Delta 10a}$; P value= 0.0074; n=5 per genotype) as well as 5 week old age (0.48% in PE26B and 1.139% in *Serf*$^{\Delta 10a}$; P value= .0062; n=5 per genotype). On the other hand, while the 1 week old *Serf* overexpression flies show reduction in the of aggregates containing the Ref(2)P signal compared to the GAL4 control (Fig 4.8D) this difference is not statistically significant (0.01% in Act5c>*Serf* and 0.04% in Act5c GAL4, P value=.5866; n=5 per genotype). However, the reduction becomes significant at 5 week old age when the *Serf* overexpression flies show 0.31% of the tissue area as Ref(2)P positive, compared to 0.627% in the GAL4 control group (P value=.0323; n=5 per genotype). These data support that Ref(2)P turn-over in adult muscles is reduced in the *Serf* deletion flies while increased in the *Serf* over-expression flies. The fact that the poly-ubiquitinated protein aggregates are tagged with Ref(2)P indicates that the autophagic clearance of these

aggregates is decreased in *Serf* deletion and increased in *Serf* overexpression flies compared with wildtype flies.

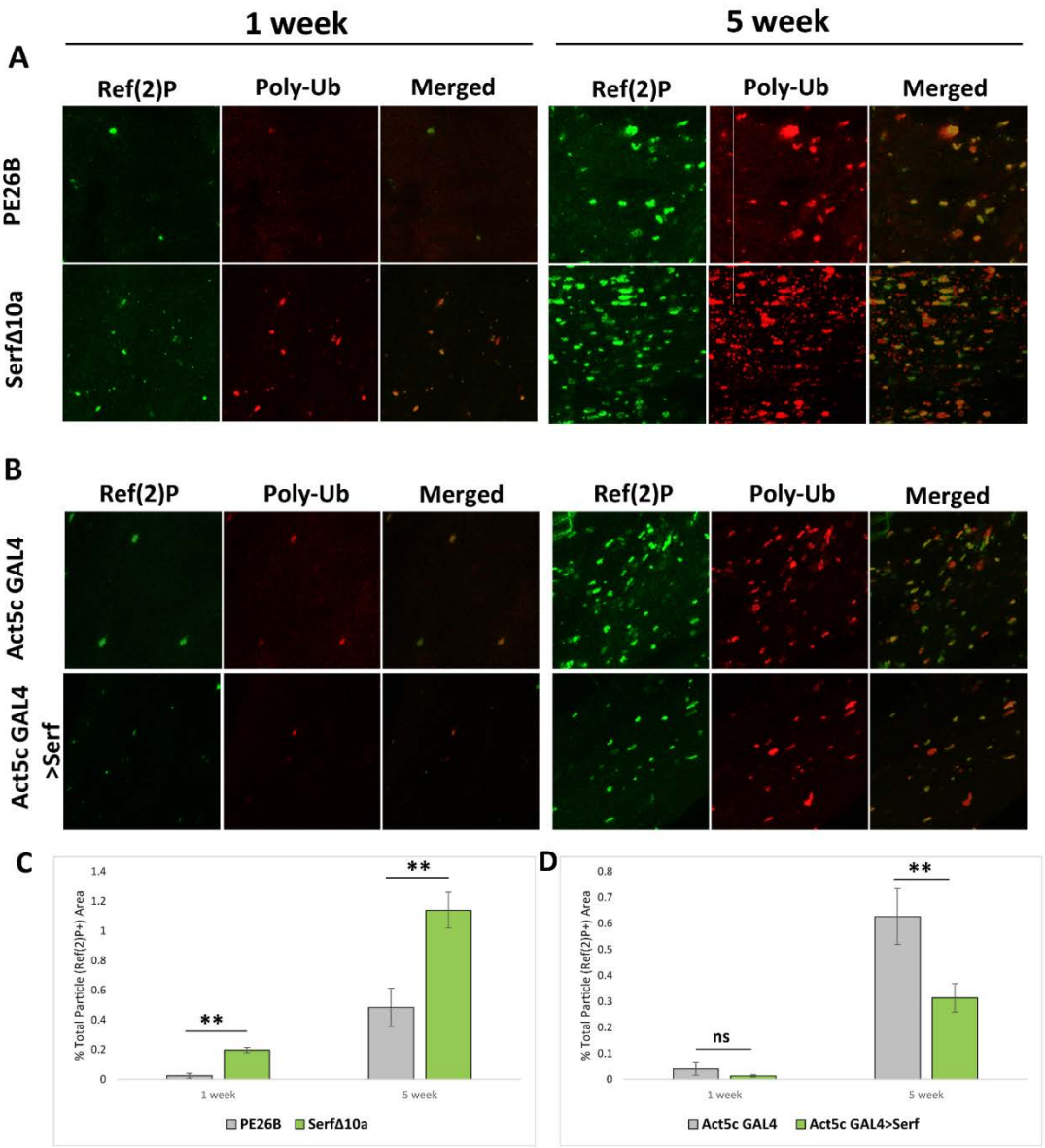

Figure 4.8 The accumulation of Ref(2)P positive protein aggregates in the adult thoracic muscles increases in Serf deletion and decreases in *Serf* overexpression flies. Adult muscles tissues immunostained with rabbit anti-Ref(2)P and mouse anti-poly-

ubiquitin antibodies that are detected with goat anti-rabbit FITC conjugated (Krogan, Cagney et al., 2008) and goat anti-mouse AF594 conjugated (Vernace, Arnaud et al., 2007) secondary antibodies. A) Representative confocal images of the precise excision control (PE26B) and *Serf* deletion ($Serf^{\Delta 10a}$) muscles showing Ref(2)P positive aggregates in green, poly-Ub positive aggregates in red and co-localization of both as yellow signal in the merged panel. B) The same as described in 'A' for the Act5c-GAL4 control and *Serf* overexpression muscles (Act5c GAL4>Serf). C) and D) Quantification of Ref(2)P positive aggregates in terms of total aggregate covered area as a percentage of the total tissue surface area for the *Serf* deletion and *Serf* overexpression group respectively.

4.3 Conclusions and discussion

The major conclusions from this portion of my study are- i) the abundance of a tissue aging marker, the poly-ubiquitinated protein aggregates, increases and decreases in the *Serf* deletion and overexpression flies respectively; and ii) changes in the level of autophagy correlate with the increase and decrease of aggregate build up in flies with altered *Serf* expression. Both of these observations correlate with the reduction and extension of lifespan we observed with *Serf* deletion and overexpression, respectively (Chapter 3).

The accumulation of intracellular inclusions or aggregates of non-functional proteins is a characteristic feature of all aged organisms (Reviewed in Koga *et al.*, 2011). The autophagy/lysosome system is the major intracellular protein degradation system that removes aggregates of damaged proteins (Rubinsztein *et al.*, 2006). Decreased autophagic activity with age has been described in different animal models from invertebrate to mammals and contributes partly to the age dependent accumulation of protein aggregates in all tissues (Reviewed in Koga *et al.*, 2011). In fact, cellular functions that influence organismal lifespan have been shown to exert regulatory role on autophagy. For instance, functional autophagy is required for the lifespan extending effect of the mutations in the nutrient sensing TOR signaling pathway both in *C. elegans* and *Drosophila* (Hansen *et al.,* 2008; Katewa *et al.,* 2011). The expression of autophagy genes are shown to be necessary for maintaining the longer lifespan of the insulin/IGF signaling (IIS) pathways mutants, like *daf-2* in *C. elegans* (Hars, Qi et al. 2007) (Melendez et al., 2003). Muscle specific upregulation of the FOXO transcription factor, a downstream signaling component of the IIS pathway (Ortholog of *C. elegans* DAF-16) in

Drosophila, is sufficient to extend lifespan that correlates with enhancing the autophagic turnover of age related protein aggregates from muscles (Perrimon 2010). My observations that altered levels of Serf in flies correspond to the changes in autophagy in a manner that correlates with their lifespan, is consistent with the established role of autophagy in the determination of organismal lifespan. Moreover, it is also consistent with the fact that autophagy plays a role in the clearance of the age related poly-ubiquitinated aggregates. However, my study does not address whether *Serf* integrates with any other known pathways that modulate autophagy and lifespan. It will be intriguing to test if Serf driven changes in autophagy and lifespan could be influenced by mutations in the TOR or IIS pathway factors.

The magnitude of autophagy gene activation with *Serf* overexpression differed between the *Atg* genes assayed. The expression levels of *Atg5* and *Atg7* genes were most sensitive to altered levels of Serf, followed by *Atg6* and *Atg1*. The question that naturally arises is whether expression changes in a few genes in the pathway can bring about changes in the overall pathway. The proteins coded by these genes performs distinct function in the autophagy pathway. The different steps that comprise the autophagy pathway are induction, cargo recognition & selection, vesicle formation, autophagosome-vacuole fusion and cargo breakdown & release of the degradation products in the cytosol (Congcong, He 2009). The *Atg1* gene codes for a kinase, the activation of which is required for induction of autophagy. The Atg8 protein is the key component of the vesicle forming machinery that interacts with the cargo complex via the adaptor protein p62/SQSTM1 (*Drosophila* Ref(2)P) which binds to and selects the cargo for inclusion into the growing phagophore. Thus Atg8 is important for both cargo selection and

vesicle formation. Following the induction step Atg8 protein gets modified by lipidation required for its incorporation into the phagophore membrane. The Atg6 protein is the component of the class III phosphatidyl inositol complex required for Atg8 lipidation and the nucleation and assembly of the initial phagophore membrane. Atg5 is the core member of the ubiquitin like conjugation system that forms the Atg12-Atg5-Atg16 complex, essential for membrane elongation and expansion of the forming autophagosome. Atg12 is activated by Atg7 (E1 like activating enzyme), transferred to Atg10 (E2 like conjugating enzyme) and attached to the substrate protein Atg5. The Atg12-Atg5 complex then interacts with Atg16, a coiled coil protein that links this complex to the phagophore membrane.

All the *Atg* genes (includes many more not discussed here) are not subject to transcriptional regulation (Liang *et al.,* 2013). Transcriptional activation of specific set of *Atg* genes have been shown to be required for autophagy induction under different stress conditions (Congcong, He 2009). For instance, under starvation stress the *Atg8* gene expression is rapidly upregulated in yeast and in certain mammalian cells (Huang *et al.,* 2000; Egami *et al.,* 2005). Bernard *et al*., has shown that stimulation of autophagy under nutrient limiting condition requires transcriptional activation of *Atg1*, *Atg7* and *Atg8* genes (Bernard *et al.,* 2015. Moreover, it has been proposed that the amount of Atg7 protein is rate limiting in the Atg8-lipidation (Bernard *et al*., 2015). Also, the activation of autophagy downstream of the mTOR pathway has been shown to involve p73 mediated transcriptional upregulation of *Atg5*, *Atg7* and *UVRAG* genes (Rosenbluth et al., 2009)s. These data together supports the idea that selective transcriptional upregulation of

Atg genes is sufficient for induction of autophagy. Therefore, the changes in the Atg gene expression with altered levels of Serf is likely to influence the level of autophagy in cells.

While discussing the significance of this part of my study, it is also important to mention some peculiarities that I have observed in some of the assays. For instance the two different control genetic backgrounds used in our study, PE26B and Act5c-GAL4, show different levels of total ubiquitinated proteins. The intensity of the ubiquitin staining in the western blot assay is much higher in the Act5c-GAL4 line compared to the PE26B line. This observation is consistent in our other assays- immunostaining of age related protein aggregates with anti-poly-ubiquitin and anti-Ref(2)P antibodies. In both assays, the GAL4 driver control showed about 2 fold increase in the total aggregate covered tissue area when compared with the PE26B control. It is possible that the level of aggregate accumulation differ between different genetic backgrounds, may be because various other factors contribute to the rate of their formation and clearance and the limit to which the aggregates could be tolerated. Comparison of the experimental group with the corresponding isogenic control therefore becomes essential. Another noticeable point is that the amount of the age related protein aggregates observed by Ref(2)P staining is lower than that observed with poly-ubiquitin staining. This might suggest that all the poly-ubiquitinated bundles are not tagged with Ref(2)P. In fact, in older tissues I have observed poly-ubiquitin stained red puncta not overlapping with a green signal for Ref(2)P. Since, some of these poly-ubiquitinated protein bundles are extracellular whereas Ref(2)P is exclusively intracellular, Ref(2)P might not get access to the extracellular aggregates. Alternately, there may be simply more poly-ubiquitinated aggregates than available Ref(2)P, especially in the old tissue.

In summary, the data obtained from this chapter is consistent with Serf's predicted role in protein homeostasis. I show the first implication of Serf in a proteolytic process, autophagy. My data also show that *Serf* expression counteracts accumulation of age related protein aggregates, which could be achieved partly by enhancing autophagy. At a superficial level, this appears contradictory to *Serf*'s proposed role in promoting initial amyloid complex formation (Van-Ham 2010; Falsone 2012), however, it is hypothesized that formation of amyloid aggregates and their sub-compartmentalization in cell occurs to facilitate their subsequent degradation by autophagy (Kaganovich, Kopito *et al*. 2008). Therefore, it is possible that Serf's positive impact in complex formation favors autophagy, which in naturally aging tissue helps clearing up the toxic aggregates.

4.4 Materials and Methods

4.4.1. Fly strains and maintenance

The following genotypes are used in this chapter: (i) w^{1118}; (Xia, Fakler *et al*.) y w; {Act5C-GAL}25FO1/ CyO, y+ (Xia, Fakler *et al*.) [(i) & (Xia, Fakler *et al*.) are obtained from Bloomington Stock Center] (iii) UAS-*SERF* cDNA; (Ruan, Tang et al.) $Serf^{\Delta 10a}$; (v) PE26B [(iii)-(v) are generated in lab as described in chapter 2]. Flies were cultured in 25C humidified chamber with under 12 hr light/dark cycle. Vials or bottles containing semi defined medium, as described by Bloomington *Drosophila* Stock Center (Backhaus *et al*.,, 1984), were used for all experiments in this study. The specific crosses performed in this chapter to obtain the progeny (larvae or adults) of required genotypes are described in table 4.1.

Table 4.1 describes the specific crosses performed, to obtain the progeny of required genotypes for the different assays conducted in this chapter.

Stage collected	Cross description	Progeny genotype collected
1st instar larva	Act5c GAL4/TM3 Ser GFP x w^{1118}	Act5c GAL4/+
	Act5c-GAL4/TM3 Ser GFP x UAS-Serf (cDNA)	UAS-Serf (cDNA)/+, Act5c-GAL4/+
Adult	Act5c-GAL4/Cyo x w^{1118}	Act5c-GAL4/+
	Act5c-GAL4/Cyo x UAS-Serf (cDNA)	UAS-Serf (cDNA)/Act5c-GAL4

4.4.2 Tissue sectioning

For frozen/cryo sectioning of adult whole flies, wings and legs were clipped off while flies were anesthetized in CO_2 and immediately transferred into small amount of tissue embedding media (Tissue-TEK O.C.T. Compound, Sakura Finetek, CA) on a glass slide to coat each fly with the media evenly throughout the body minimizing bubble formation. The media coated flies were then transferred into Tissue-Tek cryomolds (Sakura Finetek, CA) containing the embedding media and placed in the base of the mold in appropriate orientation for longitudinal sectioning avoiding bubble formation. 5-6 flies were arranged side by side in each mold. The molds are then placed on a flat surface at -80℃ for immediate freezing. Frozen molds were stored in -80℃ freezer until sectioned. Tissue sectioning (7 µm each) was performed on Leica CM 1850 cryostat machine using gelatin coated (Coating solution: 0.1% gelatin and .001% chromium potassium sulfate in ddH_20)

glass slides (VWR Micro Slides, Superfrost plus 25 x 75). For whole mount experiments whole thoraces were cut off from the rest of the body of anesthetized flies in PBS in a dissecting dish (Pyrex spot plate: plate 9 cavity 85 × 100 mm Fisher Applied Scientific) followed by 5 minutes fixation in fixing solution (4% methanol free paraformaldehyde, 0.2% Triton-X 100 in PBS). The thoraces were then transferred into PBS and cut into two longitudinal halves, each half was cut into two smaller chunks (as previously described in Hunt L.C 2013, Nature Protocols). Dissected tissues were immediately transferred into 96 well plate to follow up with immunofluorescence procedure.

4.4.3 Immunofluorescence

Immunofluorescence was performed either on serial frozen sections or on whole mounts of adult thoracic muscles following the previously described procedure (Hunt L.C 2013, Nature Protocols). Tissues were fixed in fixing solution (4% methanol free paraformaldehyde, 0.2% Triton-X 100 in PBS) for 20-30 mins at room temperature followed by three 5 minutes washes in wash buffer (0.2% Triton-X 100 in PBS) and 30 minutes blocking in blocking buffer (5% BSA in wash buffer) at room temperature. Incubation in primary antibody is done for overnight at 4°C. Mouse anti mono and polyubiquitinated Conjugates, mAb (FK2) (1:1000 dilution, Enzo Lifesciences) and Rabbit anti-Ref(2)P (A generous gift from Dr. Whitworth, UCLA) primary antibodies were used at a dilution of 1:100 in the blocking buffer. After 4 washes each for 20 minutes, anti rabbit FITC conjugated and anti-mouse AF594 conjugated secondary antibodies (1:500 dilution in blocking buffer) were used for 5-6 hours at room temperature. Following incubation the samples are again washed 4 times 20 minutes each. The slides with tissue sections are mounted in 70% glycerol with antifade agent for

imaging in Nikon ECLIPSE E800 fluorescent microscope. The whole mounts tissues are mounted in 1% low melting agarose in imaging dish (Fluoro Dish^{TM}, WPI.Inc.) for imaging with Nikon ECLIPSE Ti confocal microscope.

4.4.4 SDS PAGE and Western Blotting

SDS PAGE and western blots were performed following the procedure as described in chapter 2 (section 2.4.4). Age matched adult flies, males and females separately (12-15 flies for each) and synchronized 3rd instar larvae were used for extracting total protein (for protein extraction details see chapter 2). Mouse anti mono and polyubiquitinated Conjugates, mAb (FK2) (1:1000 dilution, Enzo Lifesciences), mouse monoclonal α-tubulin (1:1000 dilution; Developmental Studies Hybridoma Bank 12G10 anti-alpha tubulin -s) and Rabbit polyclonal anti-Ref(2)P (A generous gift from Dr. Whitworth, UCLA)primary antibodies were used at a dilution of 1:1000 in the blocking buffer. Alkaline phosphatase conjugated polyclonal goat anti-mouse IgG (1:5000 dilution, Life Technologies) and goat anti-rabbit secondary IgG (1:5000 dilution, Sigma) were used for BCIP/NBT based detection. Membranes are scanned using HP G4050 scanning machine followed by analysis with Image Quant 5.2 software.

4.4.5 Lysotracker staining

Lysotracker staining was used to visualize induction of autophagy in larval fat bodies upon starvation. Larval starvation and Lysotracker staining was performed as previously described (Scott, R.C. 2004 Developmental Cell). About 20 second instar larvae were transferred to vials containing fresh fly food (Recipe: see Chapter 2, section 2.4.5) supplemented with yeast paste. 24 hours later larvae are either dissected immediately (fed) or after starving them for 4 hours (starved). For starvation larvae were transferred in

small petri plates (VWR Petri Dish, 60 x 15 mm) with 20% sucrose soaked filter paper on its base. Fat bodies from fed and starved larvae were dissected in PBS on glass slides (VWR Micro Slides 25 x 75 mm). Dissected fat bodies were then transferred on a fresh slide with a few drops of 100µM Lysotracker Red DND-99(Invitrogen) and 1µM DAPI in PBS. After incubation for 2 minutes fat bodies were transferred to PBS on a fresh slide, covered with glass cover slips (Electron Microscopy Sciences, 22 x 22 mm) and immediately photographed live on Nikon ECLIPSE E800 fluorescent microscope.

4.4.6 Real time quantitative RT-PCR

Total RNA was extracted from 12-14 adult flies (equal number of males and females in each) by homogenizing them with plastic pestles in appropriate micro-centrifuge tubes in TRIzol reagent (Ambion, Life Technologies) on ice followed by 2 consecutive chloroform extraction and precipitation using isopropanol. Total RNA was DNase treated prior to cDNA synthesis. 0.5-1.0 µg RNA was then used for cDNA synthesis using MMLV Reverse Transcriptase 1st-Strand cDNA Synthesis Kit (Epicentre) following manufacturer's guidelines. 45 cycle real time PCR was performed with 1:5 diluted cDNA using FastStart SYBR Green Master (Roche) on a LightCycler 96 Real-Time PCR System (Roche, Indianapolis, IN). For all experiments, three biological replicates were analyzed. The relative transcript abundance was normalized to expression of the housekeeping genes α-tubulin84B. The primers used in this study are described in table 4.2.

Table 4.2 describes the primers used in the q-RT-PCR experiments.

Genes	Primer Pairs
Alpha-Tubulin84B	5'-GCTGTTCCACCCCGAGCAGCTGATC-3' and 5'-GGCGAACTCCAGCTTGGACTTCTTGC-3'
Atg1	5'-CGTCTACAAAGGACGTCATCGCAAGAAAC-3' and 5'-CGCCAAGTCGCCGCCATTGCAATACTC-3'
Atg5	5'-CCTGCGAATCTATACAGACGATGAC-3' and 5'-AGCTCAGATGCTCGGACATCCATTG-3'
Atg6	5'-TGCACGCAATGGCGGAGTTATCTTTGC-3' and 5'-CAGCTCCGCTTTCAGCTTAAAAGCAGC-3'
Atg7	5'-TGCCTTTCTGCTTCAGCAATGTCC-3' and 5'-GGCCCCATTTTGCCATTTTTATTTAG-3'
Atg8a	5'-TCGCAAATATCCAGACCGTGTGCCCGTC-3' and 5'-GCCGATGTTGGTGGAATGACGTTGTTCAC-3'

4.4.7 Image J analysis

Fluorescent microscopic and confocal images were analyzed using Fiji-Image J software. For fluorescent microscopic images, each images were opened with Image-J followed by the series of actions as described below: open image>Convert to 8-bit> select the tissue by marking the outline with freehand selection tool> analyze> measure to obtain the tissue surface area measurements (used for normalization) in pixel units> edit to clear the outside> image> adjust> threshold-adjust the threshold so as to select the particles only and hit apply> analyze particles by setting limits for circularity and particle size which

then gives a data sheet with pixel unit measurements for each particle> save the sheet. For confocal image analysis the same set of actions were performed on a z-projected image of the series of images obtained for each tissue. To do that- open image> Stacks>Z-project with maximum intensity>color>split channels to obtain Z-projected image for each channel (blue, green and red)>save each as tiff file>open image again and conduct the analysis steps as described above.

4.4.8 Statistical analyses

Immunostaining results obtained from serial tissue sections were statistically analyzed for calculating significance using repeat measure ANOVA. Immunostaining results from confocal images and *Atg* gene expression data were analyzed for statistical significance calculations using two-tailed Student's *t*-test. For all statistical tests $P<0.05$ were considered significant. For all graphs, data are represented as the mean ± the standard deviation of mean (Becker, Semler *et al*.) and significant difference is expressed as: '*'- P value between 0.01-0.05; '**'- P value between 0.001-0.01; '***' P value<.001.

Chapter 5: The *Serf* gene modifies SMA in a *Drosophila* disease model.

5.1 Introduction

A major goal of my dissertation is to test the long existing hypothesis that *Serf* is a genetic modifier of the disease Spinal Muscular Atrophy (SMA). With establishing the set if alternative *Serf* alleles, I created tools to test this hypothesis in the *Drosophila* model of SMA. In humans, deletion of the *Serf* gene along with *Smn1* mutation correlates with the most severe form of SMA, Type I (Scharf *et al*., 1998). SMA severity is inversely related to *Smn* protein abundance (Lefebvre *et al*., 1997) which is regulated, at least in part, by the ubiquitin-proteasome pathway (Burnett *et al.*, 2008). Consequently, we hypothesize the loss of *Serf* activity enhances the disease phenotype by diminishing Smn protein abundance.

This chapter describes a series of genetic interaction studies using previously characterized *Smn* mutants in genetic backgrounds containing normal, diminished, or enhanced *Serf* protein abundance. We assessed viability at the larval and pupal stages and locomotion at the larval stage. Furthermore we investigated the impact of *Serf* expression on *Smn* protein abundance in the *Smn* mutant backgrounds to learn whether or not the presence or absence of *Serf* impacts the levels of the biologically limiting Smn protein.

5.2Results

5.2.1 Genetic interaction between *Serf* and *Smn*

Genetic interaction between *Serf* and *Smn* was tested by altering the levels of *Serf* expression in a previously described fly SMA model. Our study uses *Smn* missense mutants (Smn^{D20V}, Smn^{T205I}, Smn^{V72G}, Smn^{G206S}, Smn^{Y203C}) created by the Matera lab

(Praveen *et al*., 2014). Each of these mutations is equivalent to a mutational change within one copy of the human *SMN1* gene which causes SMA in patients who have lost the second functional *SMN1* copy (typically by deletion). Praveen *et al*., modeled this hemizygous mutant state by introducing the *Smn* point mutations in a single copy trans-gene in a genetic background homozygous for the *Smn* null allele, Smn^{X7}(Smn^{X7}, Flag – Smn^{Tg}; Tg: transgene). Smn^{X7} is a deletion mutant that removes the promoter region and the entire *Smn* open reading frame of the fly *Smn* gene (Change *et al*., 2008). The fact that the individual *Smn* point mutants show different degrees of phenotypic severity allows us to score for both enhancement or relief of the mutant phenotypes after manipulation of *Serf* gene expression.

For our overexpression studies, we constitutively expressed the UAS-*Serf* cDNA under a Act5c-GAL4 driver transgene in a background homozygous for the Smn^{X7} deletion and bearing a single copy of one of the *Smn* point mutations or an equivalent wild type *Smn* transgene. For the complementary *Serf* depletion experiments, we performed RNAi mediated knockdown of *Serf* using UAS-*Serf* RNAi (hp*Serf*) under Act5c-GAL4 driver in a hemizygous *Smn* mutant background. The RNAi knockdown approach was used rather than our *Serf* deletion mutant for practical reasons. The *Serf* gene and the *Smn* gene reside near one another on the right arm of third chromosome, making assembly of the double mutants technically difficult.

5.2.1.1 The larval and pupal viability of Smn missense mutants is reduced upon ubiquitous Serf knockdown.

The w^{1118} line served as a wild type control in my experiments (Fig. 5.1). Here approximately 90% of the larvae form pupae and essentially all pupae eclose to viable

adults. When *Serf* is ubiquitously knocked down in this background viability remains roughly similar, about 86% larvae form pupae and all of the pupae appear to eclose to adults. The Smn^{X7} homozygous flies are larval lethal. A single Smn^{WT} transgenic construct shows good rescue of Smn^{X7} lethality with 85% larvae surviving to the pupal stage and about 97% of the pupae eclosing into adults. Knocking down *Serf* in the Smn^{WT}/Smn^{X7}background shows a minor reduction in pupation, from 85% to 81%, however, pupae eclosion decreases considerably from 97% to 74%. Overall, percentage of adults produced from the Smn^{WT}/Smn^{X7}line reduces from 82% to about 65% upon *Serf* knockdown. Therefore, *Serf* knockdown in the hemizygous *Smn* flies significantly reduced the percentage of pupae eclosing into adults (P<.0001) and the overall proportion of adults produced in this line (P=.00614).

The viability of the *Smn* missense mutants vary considerably (Fig 5.1 A, B and C). To test whether *Serf* knockdown exacerbates the reduced viability observed in hemizygous *Smn* point mutants, we picked *Smn* mutants that show comparatively milder effect. As previously reported (Praveen *et al*.,2014) the *D20V* mutant is the weakest among all and shows comparable viability as the Smn^{WT} construct. In the hemizygous *D20V* line about 69% larvae forms pupae and 90% of the pupae eclose. Thus *D20V* line produces about 59% viable adults. When *Serf* is knocked down in the *D20V* mutant, it shows a robust effect of reducing the percentage of pupation from 69% to 47%, which is statistically significant (P<.001). More effectively the percentage of pupal eclosion significantly drops from 90% to about 4% (P<.0001), thereby giving rise to only about 2% viable adults instead of 59% (P<.0001).

Similar results were obtained with the *V72G* and *T205I* mutants. Without altering *Serf* expression levels, the *V72G* and *T205I* mutants shows 71% and 83% pupation respectively. Upon *Serf* knockdown the *V72G* line shows a further reduction in pupation, from 71% to 37%. Although the change is still statistically significant, the impact of *Serf* knockdown on *T205I* pupation was somewhat weaker as pupation was reduced from 83% to 70%. Both of these *Smn* mutants are severely impaired in adult eclosion. The *V72G* mutant by itself is pupal lethal and, consequently, no impact of reduced *Serf* abundance on pupal vitality could be measured. However, in the *T205I*mutant 28% of the pupae eclose as adults and this is completely abolished with *Serf* knockdown. Together, these results show that *Serf* knockdown in hemizygous *Smn* missense mutant background reduces viability supporting the hypothesis that loss of *Serf* exacerbates the SMA phenotype.

A. % Larvae Pupating

	WT *Serf*	Act5c GAL4>*Serf RNAi*	P value
Smn^{WT}/Smn^{WT}	90% (n=100)	86% (n=106)	.508
Smn^{WT}/Smn^{X7}	85% (n=101)	81% (n=160)	.303
Smn^{D20V}/Smn^{X7}	69% (n=115)	47% (n=111)	.00096
Smn^{T205I}/Smn^{X7}	83% (n=120)	70% (n=103)	.017
Smn^{V72G}/Smn^{X7}	71% (n=119)	37% (n=103)	<.0001

B. % Pupae Eclosing

	WT *Serf*	Act5c GAL4>*Serf RNAi*	P value
Smn^{WT}/Smn^{WT}	100% (n=90)	86% (n=91)	.303
Smn^{WT}/Smn^{X7}	97% (n=86)	74% (n=118)	<.0001
Smn^{D20V}/Smn^{X7}	90% (n=79)	4% (n=52)	<.0001
Smn^{T205I}/Smn^{X7}	11% (n=99)	0% (n=72)	<.0001
Smn^{V72G}/Smn^{X7}	0% (n=84)	0% (n= 38)	-

C. % Larvae reaching adulthood

	WT *Serf*	Act5c GAL4>*Serf RNAi*	P value
Smn^{WT}/Smn^{WT}	90% (n=100)	86% (n=106)	.303
Smn^{WT}/Smn^{X7}	82% (n=101)	65% (n=160)	.00614
Smn^{D20V}/Smn^{X7}	59% (n=115)	2% (n=111)	<.0001
Smn^{T205I}/Smn^{X7}	11% (n=120)	0% (n=103)	<.0001
Smn^{V72G}/Smn^{X7}	0% (n=119)	0% (n=103)	-

Fig. 5.1 Ubiquitous *Serf* knockdown reduces viability of *Smn* mutants. A) The percentage of 1stinstar larvae reaching up to pupal stage with normal *Serf* expression (WT *Serf*) or ubiquitous *Serf* knockdown (Act5c-GAL4>*Serf* RNAi) in WT *Smn* (*SmnWT/WT*), *Smn* hemizygous (*SmnWT/*Smn^{X7}) and hemizygous *Smn* missense mutant backgrounds (Smn^{D20V}/Smn^{X7} , Smn^{T205I}/Smn^{X7} , Smn^{V72G}/Smn^{X7}). B)The percentage of pupae eclosing as adults with and without Act5c-GAL4 driven *Serf* knockdown in the *Smn* mutants described in part A. C) The percentage of larvae reaching adulthood with

and without Act5c-GAL4 driven *Serf* knockdown in the different *Smn* mutants as described in A.

5.2.1.2 Serf knockdown in the mild Smn mutants reduces their larval body size.

The severe *Smn* mutants with a larval lethal phenotype also have small larval body size (Praveen *et al*., 2014). *Drosophila* bearing weaker *Smn* alleles such as *D20V, T205I* and *V72G* generally progress to the pupal stage and were not reported to have smaller body size. Since we observed exacerbation of the reduced viability of the *D20V, T205I* and *V72G* mutants after *Serf* knockdown, we were interested to know if the larval body size of these mutants was also reduced. To investigate this issue, I collected larvae from hemizygous *WT* (flies with Flag-Smn^{WT} transgene, also called Smn^{WT} *or WT*), *D20V,T205I* and *V72G* lines with and without *Serf* knockdown at 96 hrs and 120 hrs post egg laying and measured the two dimensional area of the larvae from pictures captured after killing them in ethanol. For comparison, normal larval sizes were measured from the homozygous Smn^{WT} (*WT/WT*) line. In addition, the impact of ubiquitous *Serf* knockdown (Act5c GAL4>*Serf* RNAi) on the larval body size was also tested by comparing them with the *WT/WT* larvae.

Figure 3A shows representative images of larvae for each genotype with and without *Serf knockdown*. Figure 3B shows quantification of the average body area at 96 hrs and 120 hrs post egg laying, respectively. As shown in the figure, *Serf* knockdown in a wild type *Smn* background does not influence the normal larval body size of the homozygous Smn^{WT} line (*WT/WT*). When the Smn level is reduced to half in the hemizygous Smn^{WT} larvae (*WT*/Smn^{X7}) at 96 hrs and 120 hrs post egg laying, the body sizes are reduced by 6.37% (P>.05) and 15.04% (P<.0001) compared to the *WT/WT*

larvae, respectively. However, with knocking down *Serf* in the *WT/Smn*^{X7} genetic background their size does not change significantly at either time point. The *Smn D20V* and *T205I* mutants show *WT/Smn*^{X7} larval sizes at both time points when *Serf* is present. However, after *Serf* knockdown both Smn mutants show significant reductions in average size (i.e., 24.05% and 22.29%, respectively (P value <.0001 and P<.001) at 96 hrs post egg laying. Surprisingly, the average body area of the strongest mutant, *V72G*, is not reduced with *Serf* depletion at 96 hr. After 120 hours, the Smn *D20V* and *T205I* larvae size differences look more similar to the *WT*/*Smn*^{X7}control, with 8.58% and 6.45% reductions respectively after *Serf* knockdown. This observation indicates that while growth appears to be slowed, the animals eventually "catch up" to approach normal size.

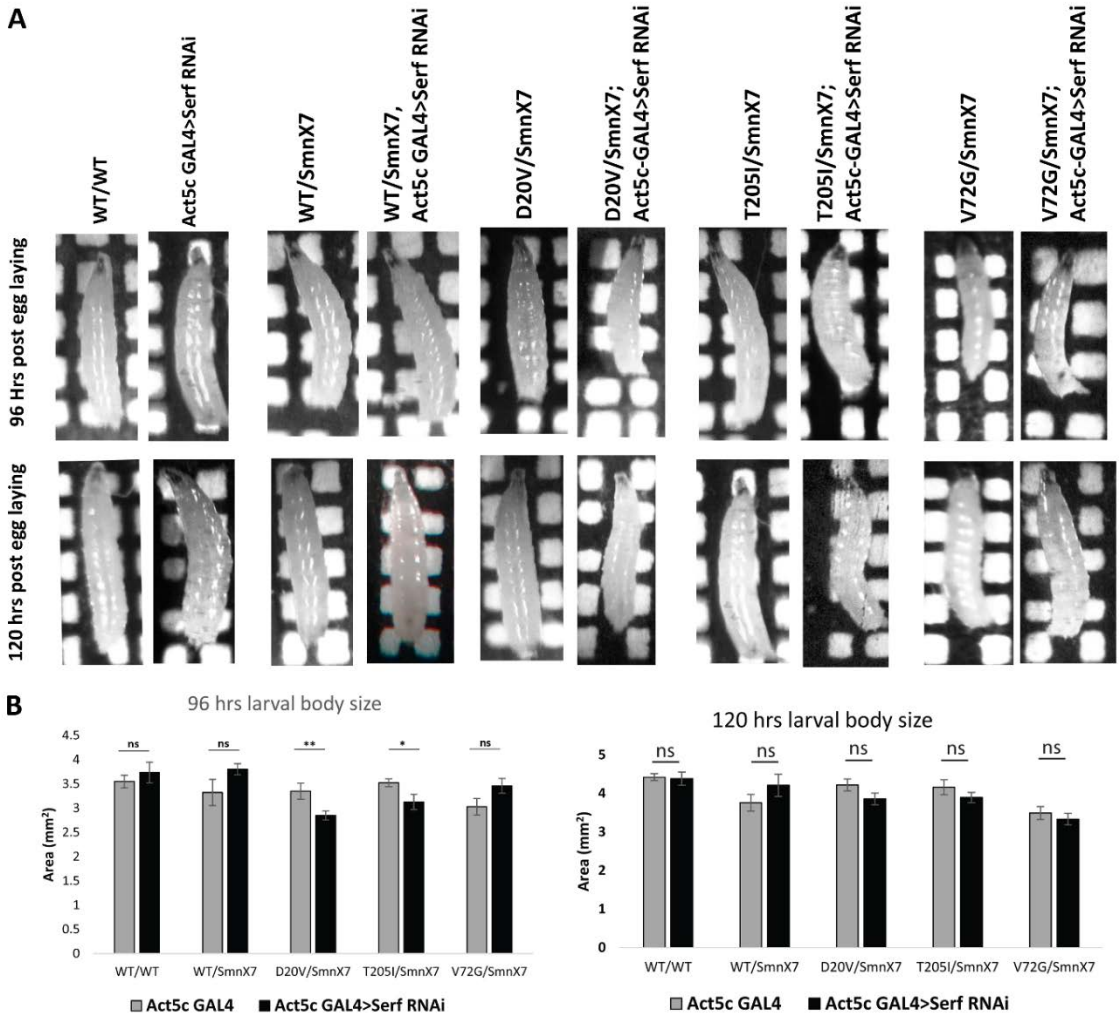

Fig. 5.2 Ubiquitous *Serf* knockdown in *Smn* mutant background results in reduced larval body area. A) Representative images showing average larval body sizes with and without *Serf* knockdown (Act5c GAL4>*Serf* RNAi) in the *Smn* mutant hemizygous backgrounds (*WT/Smn^{X7}*, *D20V/Smn^{X7}*, *T205I/Smn^{X7}*, *V72G/Smn^{X7}*) at 96 hrs and 120 hrs post egg laying. Larvae homozygous for the Flag-*Smn^{WT}* transgene (*WT/WT*) is compared with ubiquitous *Serf* knockdown larvae with wild type *Smn* (Act5c GAL4>*Serf* RNAi) showing no impact of *Serf* knockdown on larval body size. B) Quantification of the average body area at 96 hrs and 120 hrs post egg laying showing a decrease with *Serf*

knockdown in *D20V/Smn^{X7} and T205I/Smn^{X7}* lines .(At 96 hrs, *D20V/Smn^{X7}:*P value=.0133, Unpaired t-test, n=15; *T205I/Smn^{X7}:*P value =.0331 Unpaired t-test, n=15 for both genotype; At 120 hrs., *D20V/Smn^{X7}*: P value= 0.0994; *T205I/Smn^{X7}:*P value=0.268; Unpaired t-test, n=15 for each).

5.2.1.3 Serf knockdown in the Smn mutants does not impact the larval molting at 2nd-3rd instar transition.

The observation that *Serf* knockdown reduces larval body size of the *D20V* and *T205I* hemizygous mutants led us to ask whether this growth defect occurs due to developmental delay in which the mutant larvae are restricted to the second instar stage after depletion of *Serf*. The morphology of larval mouth hook is a standard means to stage larval development. The number and size of the teeth present on the mouth hook vary between different stages and does not overlap (Alpatov 1929, Okada 1963). In the first instar stage there are no teeth; in the second instar stage there are a few (3-4) teeth whereas numerous teeth on the mouth hook represents a third instar stage larva (Alpatov 1929).

I dissected mouth-hooks at 96 hrs post egg laying from the *WT*, *D20V*and *T205I* hemizygous larvae with and without ubiquitous *Serf* knockdown (n=10 per genotype). At this time point, all thewild type animals are in the 3rd instar stage. I found that 100% of the dissected *Smn^{WT}* hemizygous larvae show mouth-hooks typical for a 3rd instar larva (Fig. 3A). Likewise, *Serf* knockdown in this background does not arrest development and all the larvae dissected are at the 3rd instar stage (Fig 3A'). The *D20V* and *T205I* hemizygous larvae looks identical to the *Smn^{WT}* larvae, with mouth hook structures typical for a third instar stage larva (Fig 3B & 3C). This does not change with *Serf*

knockdown in these two mutants (Fig 3B' & 3C'), even though they show a much smaller body size at 96 hrs post egg laying compared with wildtype animals. Therefore I conclude that the reduction in the larval body size observed with *Serf* knockdown is due to growth impairment but is not due to failure to reach the 3rd instar stage. It is possible, however, that the larval molts of the mutant animals differ in timing with and without Serf depletion.

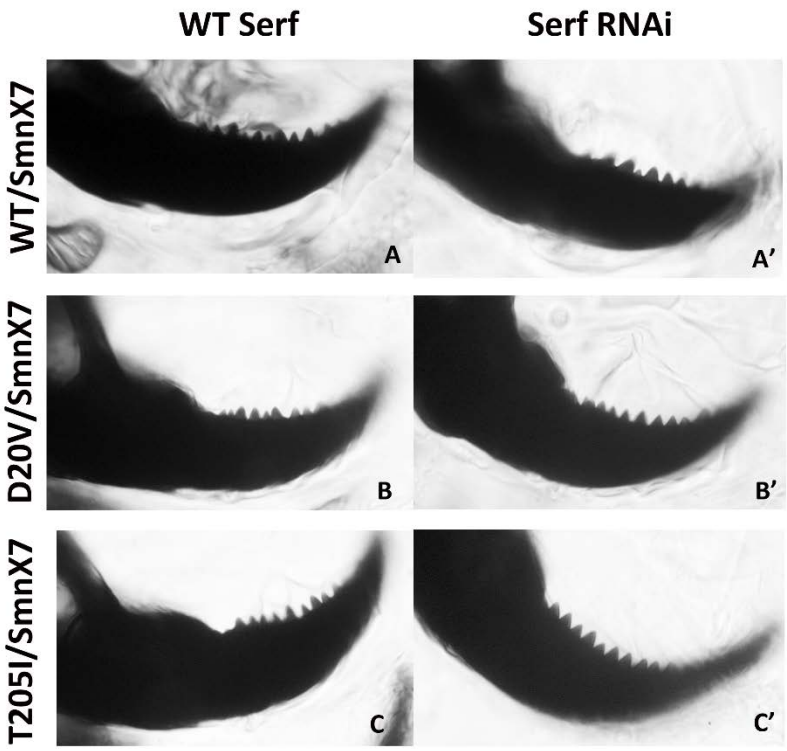

Fig 5.3: Representative larval mouth hook images from *WT/Smn^{X7}* (A-A'), *D20V/Smn^{X7}*(B-B'), *Y205I/Smn^{X7}* (D-D') lines at 96 hrs post egg laying with wild type levels of *Serf* (WT *Serf*: A,B,C) and ubiquitous *Serf* knockdown (Act5c GAL4>*Serf* RNAi: A',B',C'). Numerous teeth on the mouth hooks represents 3rd instar larval stage.

5.2.1.4 Knockdown of *Serf* does not impair larval locomotion in the mild *Smn* mutants.

Drosophila that express the weak *Smn* mutant alleles, *D20V*, *T205I* and *V72G*, do not show impaired larval locomotion. Since I found that *Serf* knockdown in these mutants reduces their viability (Fig. 5.1) and larval body size (Fig 5.2), I wanted to know whether or not larval locomotion is impaired after Serf deletion. Since the interpretation of simple mobility traces on an agar surface is complicated when body sizes differ, an alternative measure of larval mobility was used. Independent of size, forward progression occurs by a peristaltic pulse of body wall contraction and this can be used to score for locomotion (REF). For each genotype, 3rd instar larvae (96 hrs post egg laying) were used to determine the number of body wall contractions per minute.

As shown in the figure below (Fig.5.4), the *Flag-Smn*^{WT} homozygous larvae (*WT/WT*), with and without *Serf* knockdown show similar mobility. Animals with wild type and reduced levels of Serf average 58.5 and 58 contractions per minute, respectively. Similar to the homozygotes, the hemizygous *WT/Smn*^{X7} line also show equivalent larval movement with and without *Serf* knockdown, an average of 58 and 55 contractions/ minute (P value=.1002 n=15). However, it was surprising to note that 50% reduction of Smn in the hemizygous line did not reduce their locomotion performance. Likewise, all the *Smn* mutants with normal levels of *Serf* show similar range of average contractions like the homozygous of hemizygous *Smn*^{WT}. The *D20V*, *T205I* and *V72G* hemizygous mutants make an average of 55.87, 54 and 52.86 contractions per minute respectively. When *Serf* is knocked down in these mutants they make 60, 55.69 and 56.14 contractions per minute, on an average, respectively. The changes observed with and without *Serf*

knockdown are not statistically significant (P values= 0.1508, 0.5171 and 0.2830 for *D20V/X7*, *T205I/X7* and *V72G/X7* respectively, n=15 for each). Therefore I conclude that *Serf* knockdown in the mild *Smn* mutant flies does not cause a locomotion defect at the larval stage.

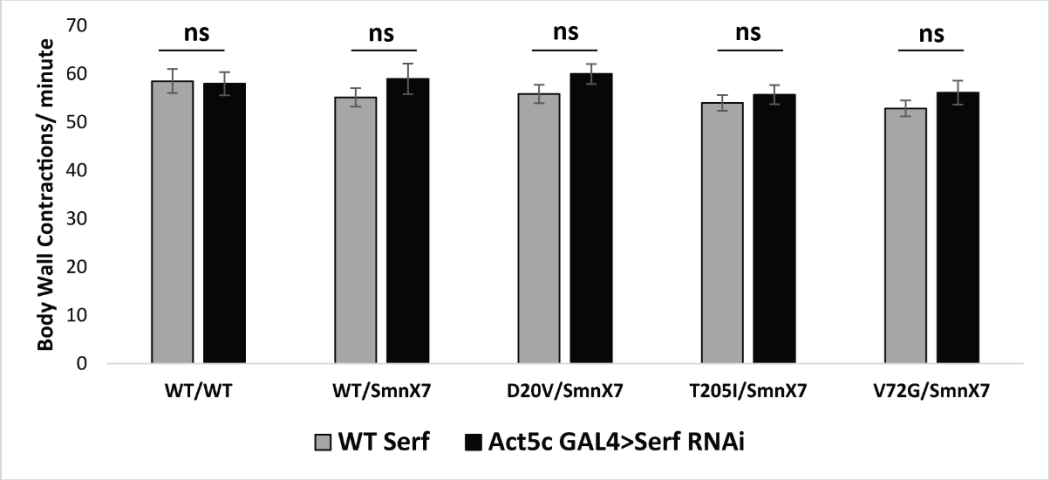

Fig 5.4. *Smn* mutants with ubiquitous *Serf* knockdown do not show larval locomotion defects. Average body wall contractions per minute were measured at 96 hrs post egg laying (n=15 for all genotypes) in *Smn* wild type homozygous (*WT/WT*), hemizygous (*WT/Smn^{X7}*) and missense mutant (*D20V/Smn^{X7}*, *T205I/Smn^{X7}*, *V72G/Smn^{X7}*) flies with wild type levels of *Serf* (WT *Serf*) or with ubiquitous *Serf* knockdown (Act5c GAL4>*Serf* RNAi). *Smn* mutants do not show significant differences in the average number body wall contractions per minute after *Serf* knockdown

5.2.1.5 Ubiquitous Serf overexpression does not rescue viability of majority of Smn mutants.

In the complimentary experiment I ubiquitously overexpressed *Serf* and asked whether the compromised viability of the *Smn* missense mutants could be rescued by the increased *Serf* abundance (Fig 5.4 A, B, C). In this experiment I included the two severe *Smn* mutants that are larval lethal, *G206S* and *Y203C* as well as the milder *D20V, T205I and V72G* mutants. *Serf* overexpression without any alteration to the *Smn* locus did not change the proportion of larvae producing pupae or the percentage of pupae eclosing as adults when compared with flies with wild type *Serf*. In both cases about 90% of the larvae forms pupae and all the pupae scored formed adults. The line hemizygous for the Smn^{WT} transgene (Smn^{WT}/Smn^{X7}) produces 85% pupae with 97% of the pupae eclosing as adults. When *Serf* is overexpressed in this line, I found that 86% of the larvae form pupae and 98% of the pupae eclose as adults. Thus, percentage of larvae reaching adulthood under normal *Serf* levels and with increased *Serf* in Smn^{WT}/Smn^{X7} background remains essentially the same, 82% and 84% respectively indicating that increased Serf protein abundance is not sufficient to suppress the reduced viability

. The larval lethality of the *G206S* and *Y203C* mutants could not be rescued with *Serf* overexpression. None of the mutant larvae, with or without *Serf* overexpression reach pupation. For the *V72G* mutant, equal proportion of larvae reach pupation (71%) with normal or elevated levels of *Serf* and none of these pupae eclose as adults. For the *T205I* mutant the percentages of pupae and adults also remained roughly the same with and without *Serf* overexpression. With normal *Serf* expression, the *T205I* mutant produces about 83% pupae with 28% of these pupae form viable adults. With *Serf*

overexpression the *T205I* mutant form 89% pupae with 20% of those eclose. Overall, larvae from the *T205I* line progress through development to form equivalent percentages of adults, 9% and 11%, with and without *Serf* overexpression respectively.

In contrast to the results presented above, the percentage of D20V that form pupae does increase from 69% to 82% with *Serf* overexpression which is subtle but statistically significant (P=.021, n=106). Unexpectedly, however, pupal eclosion in this background is significantly reduced with enhanced Serf expression (70% vs 90% with normal Serf levels, P value=.0013). Therefore, roughly equivalent proportion of larvae develop to adulthood in the D20V background (59% and 52%) with wild type and increased levels of *Serf* expression, respectively. This suggests that the increased proportion of pupae that form in the *D20V* background with overexpressed *Serf* probably do not emerge as adults. Overall, these data indicate that increased *Serf* expression is not sufficient to rescue the decreased viability of the majority *Smn* mutant flies, but, might have some beneficial effect in the weak *D20V* allelic background. This observation is indeed consistent with our *Serf* knockdown results where the *D20V* line was found to be most sensitive to reduced *Serf* levels and showed a robust exacerbation of decreased viability.

A. % Larvae Pupating

	WT *Serf*	Act5c GAL4>*Serf*	P value
Smn^{WT}/Smn^{WT}	90% (n=100)	90% (n=100)	-
Smn^{WT}/Smn^{X7}	85% (n=101)	86% (n=138)	-
Smn^{D20V}/Smn^{X7}	69% (n=115)	82% (n=106)	.021
Smn^{T205I}/Smn^{X7}	83% (n=120)	89% (n=179)	.170
Smn^{V72G}/Smn^{X7}	71% (n=119)	71% (n=136)	-
Smn^{G206S}/Smn^{X7}	0% (n=124)	0% (n=117)	-
Smn^{Y203C}/Smn^{X7}	0% (n=103)	0% (n=108)	-

B. % Pupae Eclosing

	WT *Serf*	Act5c GAL4>*Serf*	P value
Smn^{WT}/Smn^{WT}	100% (n=90)	100% (n=90)	-
Smn^{WT}/Smn^{X7}	97% (n=86)	98% (n=118)	-
Smn^{D20V}/Smn^{X7}	90% (n=79)	70% (n=87)	.0013
Smn^{T205I}/Smn^{X7}	28% (n=100)	20% (n=159)	.703
Smn^{V72G}/Smn^{X7}	0% (n=119)	0% (n=85)	-
Smn^{G206S}/Smn^{X7}	0%	0%	-
Smn^{Y203C}/Smn^{X7}	0%	0%	-

C. % Larvae reaching adulthood

	WT *Serf*	Act5c GAL4>*Serf*	P value
Smn^{WT}/Smn^{WT}	87% (n=100)	90% (n=100)	-
Smn^{WT}/Smn^{X7}	82% (n=101)	84% (n=138)	-
Smn^{D20V}/Smn^{X7}	59% (n=115)	52% (n=106)	.347
Smn^{T205I}/Smn^{X7}	11% (n=120)	9% (n=179)	.575
Smn^{V72G}/Smn^{X7}	0% (n=119)	0% (n=136)	-
Smn^{G206S}/Smn^{X7}	0% (n=124)	0% (n=117)	-
Smn^{Y203C}/Smn^{X7}	0% (n=103)	0% (n=108)	-

Fig.5.5 Ubiquitous *Serf* overexpression does not affect the viability of the *Smn* mutants. A) The percentage of 1st instar larvae reaching upto pupal stage normal *Serf* expression (WT *Serf*) or ubiquitous *Serf* overexpression (Act5c-GAL4> *Serf*) in WT *Smn*

($Smn^{WT/WT}$), *Smn* hemizygous (Smn^{WT}/Smn^{X7}) and hemizygous *Smn* missense mutant backgrounds (Smn^{D20V}/ Smn^{X7}, Smn^{T205I}/Smn^{X7}, Smn^{V72G}/Smn^{X7}, Smn^{G206S}/Smn^{X7}, Smn^{Y203C}/Smn^{X7}). B) The percentage of pupae eclosing as adults with and without Act5c-GAL4 driven *Serf* overexpression in the different *Smn* mutants as described in A. C) The percentage larvae that develop to adulthood with and without Act5c-GAL4 driven *Serf* overexpression in the different *Smn* mutants as described in panel A.

5.2.1.6 The reduced larval size phenotype of the severe *Smn* mutants is partially restored with *Serf* overexpression.

The severe *Smn* alleles, *G206S* and *Y203C*, show greatly reduced larval body size, similar to the homozygous null mutant Smn^{X7} (Praveen *et al*.,, 2014). This is expected since very little Smn protein can be detected in flies bearing these mutations. The introduction of the Smn^{WT} transgene into homozygous Smn^{X7}mutant flies significantly rescues this phenotype (Praveen *et al*.,, 2014). We were curious to know if *Serf* overexpression could improve growth in the hemizygous Smn *G206S* and *Y203C* mutant lines. Therefore, I overexpressed *Serf* in hemizygous *WT*, *G206S* and *Y203C* backgrounds and in the homozygous wildtype control and measured larval size as above. Figure 4A shows representative images of larval sizes which are quantified for the test population in Fig. 4B. I find that that the Smn^{WT}/Smn^{X7} larvae are 6.37% (P value=0.4575, n=15,) and 15.04% (P<.0001, n=15) smaller in size compared to the Smn^{WT}/Smn^{WT} larvae at 96 hrs and 120 hrs post egg laying, respectively. When *Serf* is overexpressed in Smn^{WT}/Smn^{X7} line, the larvae show 16.10% (P value=0.0718, n=15) and 23.97% (P value <.0001, n=15) body size increases at 96 hrs and 120 hrs, respectively, thereby becoming similar to the Smn^{WT}/Smn^{WT} group. However, *Serf* overexpression in a background a wildtype *Smn*

transgene does not change larval size when compared with the naturally Smn^{WT}/Smn^{WT} homozygous group.

The *G206S* and *Y203C* hemizygous larvae show 54.86% (P<.0001, n=15,) and 68.43% (P<.0001, n=15) reduction in the average body area compared to Smn^{WT}/Smn^{X7} larvae, respectively, consistent with a previous finding (Praveen *et al*.,, 2014). *Serf* overexpression in this hemizygous *G206S* background increases this size by 27.11% (P value>.05, n=15) and 39.83% (P value <.01, n=15) at 96 hrs and 120 hrs, respectively. A more robust impact of *Serf* overexpression can be seen with the *Y203C* mutant where *Serf* increases the relative body size by150.1% and 139.1% at 96 hrs and 120hrs, respectively (P value <0.0001 for both time points, n=15), respectively. Taken together, we find that ubiquitous overexpression of *Serf* partially restores the reduced larval size of *Smn* mutants.

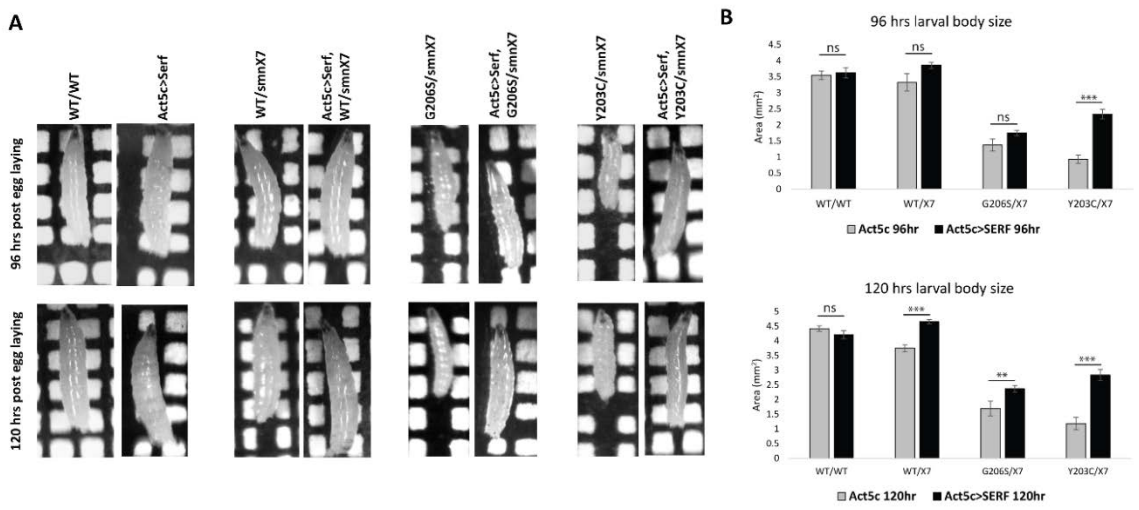

Fig. 5.6 Ubiquitous *Serf* overexpression in the severe *Smn* mutants increases larval body size. A) Representative images showing average larval body sizes with and without *Serf* overexpression (Act5c GAL4>*Serf*) in Smn^{WT} hemizygous ($Smn^{WT}/SmnX^{7}$) and *Smn* missense mutant hemizygous backgrounds (Smn^{G206S}/Smn^{X7}, Smn^{Y203C}/Smn^{X7}) at 96 hrs and 120 hrs post egg laying. Age matched larvae homozygous for the Flag-Smn^{WT} transgene (*WT/WT*) and unaltered *Smn* locus with ubiquitous *Serf* overexpression (Act5c GAL4>*Serf*) show normal larval body sizes at the respective time points. B) Quantification of the average body area at 96 hrs and 120 hrs post egg laying showing increase with *Serf* overexpression in $WT/SmnX^{7}$, $G206S/Smn^{X7}$ *and* $Y203C/Smn^{X7}$ lines. (At 96 hrs, $Y203C/Smn^{X7}$*:* P value <0.0001, Unpaired t-test, n=15; $WT/SmnX^{7}$& $G206S/Smn^{X7}$*:* P value >.05, Unpaired t-test, n=15 for both genotype; At 120 hrs, $WT/SmnX^{7}$ *&* $Y203C/Smn^{X7}$*:* P value <0.0001, Unpaired t-test, n=15 for both ; $G206S/Smn^{X7}$*:* P value <.005, Unpaired t-test, n=15).

5.2.1.7 *Serf* overexpression increases the body size of the severe Smn mutants but appears not to have a obvious impact on development.

As *Serf* overexpression partially restores the reduced body size of the *G206S* and *Y203C* hemizygous larvae, I wanted to know if this reflects simple growth improvement or rescue from a possible developmental delay in larval molts (Garcia, Lu *et al*. 2013). To address this question, I first asked if the small body size of the *G206S* and *Y203C* hemizygous mutants is consistent with the developmental stage predicted for larvae 96 hours after egg laying. As represented in the figure (Fig.5.6), at 96 hours post egg laying the mouth hooks of all the Smn^{WT} hemizygous larvae (Fig. 5.6A) dissected (n=10) display numerous teeth demonstrating that the 3rd instar stage has been reached. Likewise, *Serf* overexpression in the Smn^{WT} line (fig.6A') showed 100% of these larvae with 3rd instar specific mouth hook features. Although the *G206S* and *Y203C* hemizygous larvae are much smaller in size than the Smn^{WT} at 96 hrs post egg laying, most animals still display the mouth hook features of the 3rd instar stage (Fig 6B & 6D, respectively). However, 1 in 10 larvae for the *G206S* genotype (Fig 6C) and 2 in 10 for the *Y203C* genotype (Fig 6D) showed mouth hook structures more similar to the 2nd instar stage, likely indicating slowed development. As anticipated the developmentally delayed larvae showed the smallest body size in the population. Although *Serf* overexpression significantly improves the average larval body size of these two mutants, we still find 2nd instar stage larvae in similar proportions (1 in 10 larvae dissected) for both the *G206S* (fig 6C') and *Y203C* (fig 6E') mutants. Therefore, the 3rd instar larval molt delay observed in the *G206S* and *Y203C* hemizygous background is not greatly advanced by *Serf* overexpression.

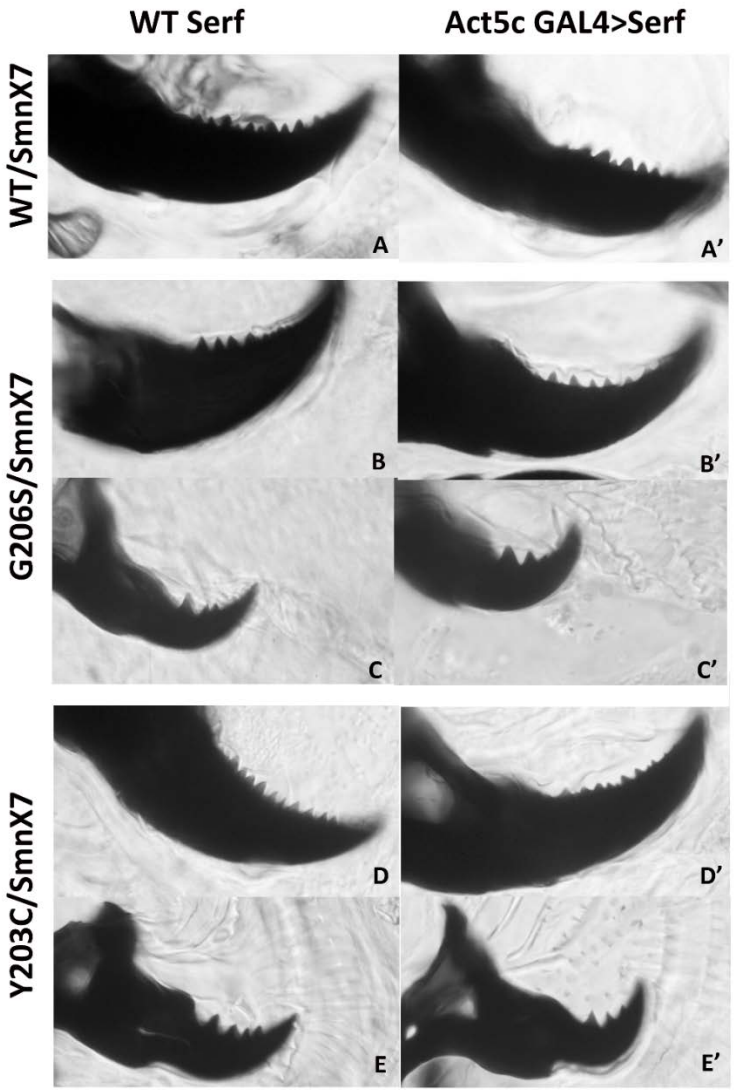

Fig 5.7. Representative larval mouth hook images from *WT/Smn^{X7}* (A-A'), *G206S/Smn^{X7}* (B-C'), *Y203C/Smn^{X7}* (D-E') lines at 96 hrs post egg laying with wild type levels of *Serf* (WT *Serf*: A,B,C,D,E) and ubiquitous *Serf* overexpression (Act5c GAL4>Serf: A',B',C',D',E'). Numerous teeth on the mouth hooks (A, A', B, B',D & D') represents 3rd instar larval stage and the smaller mouth hooks with 3-4 teeth (C,C',E & E') represents 2nd instar stage.

5.2.1.8 Overexpression of *Serf* improves locomotion in the severe *Smn* mutants.

The severe alleles of *Smn, G206S* and *Y203C,* cause severe larval locomotion defects (Praveen *et al*., 2014). As shown above (Fig 5.6) *Serf* overexpression in these mutants significantly increases their body size. I next wanted to determine whether *Serf* overexpression also improves locomotion of the mutant larvae.

As shown below (Fig. 5.8), the Smn^{WT} homozygous larvae (*WT/WT*), with and without *Serf* overexpression shows similar levels of crawling efficiency with 58.5 and 59.5 contractions per minute, respectively. The hemizygous line with 50% wild type *Smn* performs equally well as the homozygous wild type, with 55.36 contractions per minute and does not change with *Serf* overexpression (average at 54 contractions/minute). So, although Smn is present at only ½ the normal dosage, it does not affect the larval crawling efficiency and *Serf* overexpression in these animals does not appreciable influence this parameter. In contrast, the *Y203C* and *G206S* Smn mutants average at 13.9 and 13.75 contractions per minute, roughly $1/4^{th}$ the rate of the wildtype. This is consistent with the previous report (Praveen *et al*., 2014), however here the locomotion is assayed using a new method not used before. When *Serf* is overexpressed in *Y203C* and *G206S* mutant backgrounds mobility increases to 32.8 and 28 contractions per minute, respectively. This >2-fold increase in locomotion with enhanced *Serf* expression is statistically significant ($P<.0001$, $n=15$). Therefore I conclude that the simple increase in Serf abundance is sufficient to partially suppress two phenotypic defects of this Smn-limited SMA model, namely, larval size and locomotion.

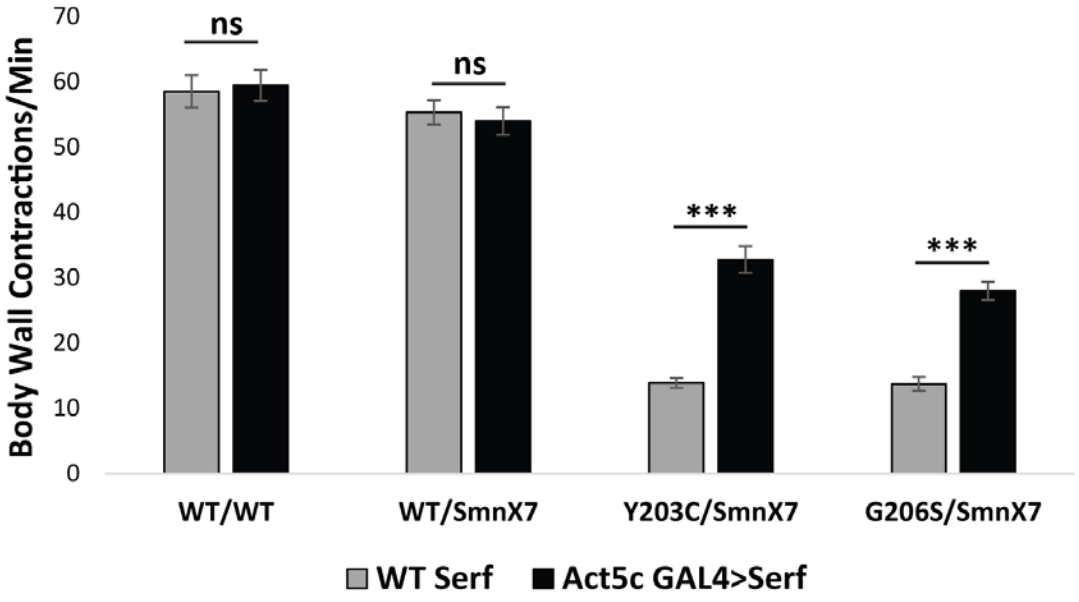

Fig 5.8 Ubiquitous *Serf* overexpression improves locomotion in the severe *Smn* mutants. Body wall contractions per minute were measured at 96 hrs post egg laying in homozygous (*WT/WT*) , hemizygous (Smn^{WT}/Smn^{X7}) and missense mutant (Smn^{Y203C}/Smn^{X7}, Smn^{G206S}/Smn^{X7}) flies with wild type levels of *Serf* (WT *Serf*) or with ubiquitous *Serf* overexpression (Act5c GAL4>*Serf*). The *Y203C* and *G206S* mutants are severely locomotion impaired. *Serf* overexpression in these mutants results in partial but statistically significant improvements in mobility (P<.0001, n=15, unpaired t test).

5.2.2 Impact of *Serf* on the *Smn* protein abundance

Together, our data so far reveal genetic interactions between *Serf* and *Smn* such that the altered *Serf* abundance modulates certain aspects of the *Smn* mutant phenotype. The Matera group previously showed that, similar to human SMA, the *Drosophila* multiple Smn mutants produce unstable Smn proteins. Since Serf has been implicated in protein homeostasis (Van-Ham *et al.*,2010), one possible explanation for our results is

that *Serf* expression stabilizes the residual *Smn* protein in the mutant background thereby reducing the severity of the SMA-like disease state.

5.2.2.1 The *Serf* deletion flies show reduced *Smn* protein abundance.

To test the impact of *Serf* on wild type *Smn* abundance, I compared the *Smn* protein levels in wildtype and *Serf* deletion flies. Figure 5.9A shows a representative Smn western blot image using endogenous β-tubulin as a normalization control. The *Serf* deletion mutant (Act5c-GAL4, SerfΔ10a: Lane 3) shows a 50.8% reduction in the relative *Smn* abundance as compared to the control (Act5c-GAL4: Lane 1). To know whether this reduction is due to the loss of *Serf* gene, I expressed the *Serf* cDNA in the *Serf* deletion mutant (Act5c-GAL4>*Serf, Serf*Δ*10a*: Lane 4) and asked if this is sufficient to recover normal *Smn* protein levels. I found that *Serf* cDNA expression indeed full restores *Smn* protein abundance in this genetic background. However, *Serf* cDNA expression in an otherwise wildtype background (Act5c-GAL4>Serf: Lane 2) does not elevate *Smn* protein levels above what is found in the control wildtype. Equivalent results were obtained with three independent replicates and the average changes in the *Smn* protein abundance are summarized in the table below (Table 5.1).

Table 5.1 Table shows average fold change in the relative *Smn* protein level in the *Serf* mutants from 4 biological replicates.

Genotypes	Average fold change in *Smn* level ± SEM	P values
Act5c-GAL4	**1**	
Act5c-GAL4>*Serf*	**1.05±0.078**	**.5452**
Serf*Δ*10a	**0.564 ± 0.048**	**<.0001**
Act5c-GAL4>*Serf*, *Serf*Δ*10a*	**0.925 ±0.032**	**.0575**

To determine whether the lower Smn abundance in the *Serf* deletion mutant is likely due to transcriptional differences, I performed semi-quantitative RT- PCR on the total RNA extracted from the adults of each genotype (Fig 5.9B). The *Smn* mRNA was normalized to α-tubulin mRNA and the fold change with *Serf* manipulation calculated. The Act5c-GAL4 driver line (Fig. 5.4B, Lanes 1 & 2) served as the negative control with unmanipulated *Serf* expression. Here I see that while the *Serf* deletion mutant (Fug. 5.4B, Lanes 5&6) showed a slight increase in *Smn* mRNA abundance (1.34 fold) the *Smn* protein level is actually reduced by half (Fig. 5.4A, Lane 3). With *Serf* overexpression in a wildtype background *Smn* protein essentially stays at normal levels (Fig 5.4A, Lane 2) while *Smn* mRNA is again slightly increased (1.21 fold). In the *Serf* deletion mutant with *Serf* overexpression (Fig.5.4B, Lane 7&8), the *Smn* mRNA remains unchanged while *Smn* protein is recovered to normal level (Fig. 5.4A, Lane 4). As *Smn* mRNA levels do not correlate with the observed *Smn* protein abundance changes, it appears likely that *Serf* primarily modulates *Smn* expression at the level of protein synthesis or stability.

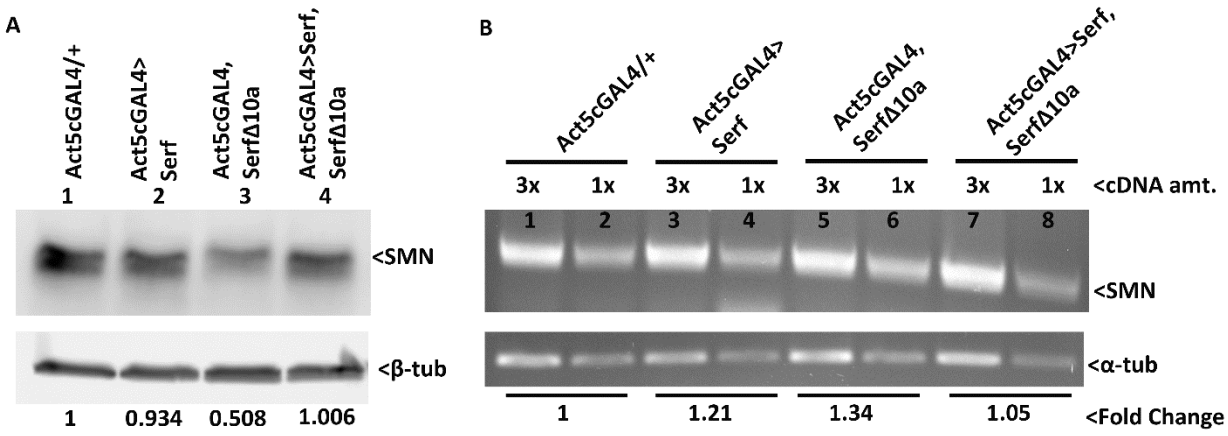

Fig 5.9. The relative *Smn* protein level is reduced in the *Serf* deletion flies without altering the relative *Smn* mRNA levels. A) Representative western blot showing *Smn* protein abundance in the Act5c-GAL4 driver control (Lane 1), *Serf* overexpression (Act5c GAL4>*Serf*; Lane 2), *Serf* deletion mutant (Act5c GAL4, *Serf*Δ*10a*; Lane 3) and the rescue line (Act5c GAL4>*Serf*, *Serf*Δ*10a*; Lane 4). The level of β-tubulin expression was used as a loading control. The fold change in relative *Smn* protein expression with respect to the WT is shown below the lanes. B. Semi-quantitative RT- PCR analysis of mRNA abundance in the respective lines tested for protein. 1x and 3x cDNA amounts were used for PCR from each genotype. The α-tubulin transcript was used as an internal control. Fold change in the relative *Smn* transcript abundance in *Serf* overexpression group (Lanes 3 &4), *Serf* deletion group (Lanes 5&6) and the rescue group (Lanes 7&8) with respect to the control group (Lanes 1&2) has been shown below the respective bands.

5.2.2.2 *Serf* knockdown in a *Smn* mutant line moderately reduces *Smn* protein abundance.

We were curious to know whether the reduction in the viability and larval growth observed in the *Smn* mutants with altered *Serf* expression correlates with changes in *Smn* protein abundance. To test, we assessed the relative level of *Smn* protein in larvae at 96 hrs post egg laying in the presence of normal *Serf* and after *Serf* knockdown.

Figure 5.10 shows the *Smn* protein levels in *Smn* mutants with and without *Serf* knockdown. Knocking down *Serf* in the Smn^{WT} hemizygous background (Lane 3) corresponds to a slight decrease in the Smn abundance (0.73 fold) as compared to those with normal amount of *Serf* (Lane 2). Similar to what was shown before (Praveen *et al*.,, 2014), the *D20V* Smn mutant line (Lane 4) shows normal levels of *Smn* protein. With *Serf* knockdown, I see a reduction in the *Smn* protein level (0.256 fold) in *D20V* background (Lane 5). This is consistent with the observed exacerbation of the *Smn* phenotype in these animals. Similarly, the *T205I* mutant also show reduction in the *Smn* protein levels (0.276 fold) with *Serf* knockdown, however, the variability of this reduction is much greater for this line. For the *V72G* mutant, the Smn protein level is already undetectable and therefore we could not measure further decrease with *Serf* knockdown. The variability of these results between 3 different biological replicates and the average values and statistical significance are summarized in the table below (Table 5.2).

Table 5.2 Table Shows average fold change in the relative *Smn* protein level in *Smn* missense mutants with and without *Serf* knockdown from 3 biological replicates.

Genotypes	Average fold change in *Smn* level ± SEM	P value
Smn^{WT}/Smn^{X7}	1	.1739
Act5c-GAL4>*SerfRNAi*, Smn^{WT}/Smn^{X7}	0.884± 0.07	
Smn^{D20V}/Smn^{X7}	1	.0036
Act5c-GAL4>*SerfRNAi*, Smn^{D20V}/Smn^{X7}	0.3963 ± .098	
Smn^{T205I}/Smn^{X7}	1	.519
Act5c-GAL4>*SerfRNAi*, Smn^{T205I}/Smn^{X7}	.8106 ± .268	

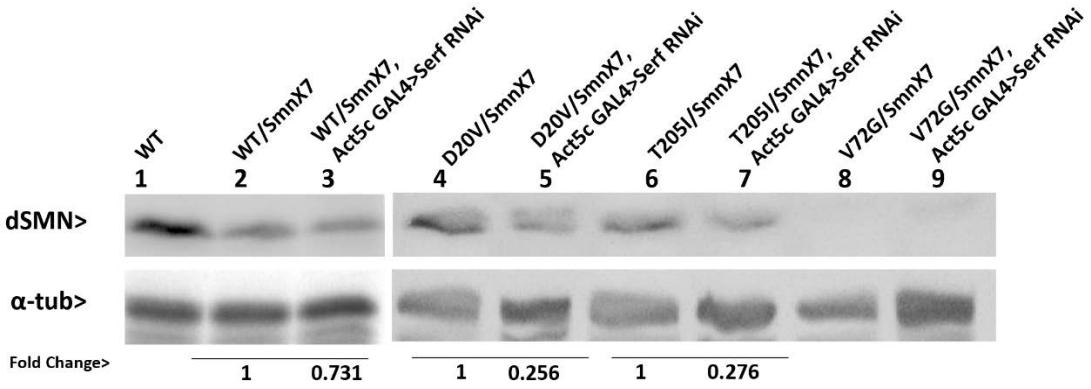

Fig 5.10 Ubiquitous *Serf* knockdown reduces *Smn* protein abundance in Smn^{D20V} mutant. Western blot analysis of *Smn* protein abundance in hemizygous *Smn* wild type ($Smn^{WT}/SmnX^{7}$) and mutant larvae (Smn^{D20V}/Smn^{X7}, Smn^{T205I}/Smn^{X7}, Smn^{V72G}/Smn^{X7}) with and without Act5c-GAL4 driven *Serf* knockdown. The Smn^{WT} transgenic homozygous is shown as a wild type control. The level of α-tubulin expression is shown as a loading control. The fold change of relative *Smn* protein expression in the *Smn* mutant larvae knocking down *Serf* with respect to those with wild type *Serf* is shown below each pair of lanes, except for *V72G* pair where the protein expression is diminished to undetectable levels.

5.2.2.3 *Serf* overexpression partially restores *Smn* protein abundance in certain *Smn* mutants.

While *Serf* overexpression in the *Smn* mutant background had little or no impact on adult viability, the most severe mutants, *G206S* and *Y203C*, showed significant improvement in larval size and locomotion with enhanced *Serf* expression. It is worthwhile mentioning here that, consistent with our observations, the milder *Smn* mutants including *D20V* and *T205I* were previously reported to have essentially wildtype

levels of Smn protein while the more severe mutants showed nearly undetectable levels of *Smn* protein (Praveen *et al*., 2014). In order to know whether the partial suppression of the SMA phenotype upon *Serf* overexpression was accompanied by an increase in *Smn* protein abundance, we assessed the whole series of *Smn* mutants by western blot (Fig 5.11).

Serf overexpression in a wild type *Smn* background does not alter *Smn* protein abundance (Fig 5.11A). However, when *Serf* is overexpressed in the hemizygous Smn^{WT} line (Lane 2), I see an increase in the *Smn* abundance by 1.53 fold (Lane 3). This trend is also seen with the T205I mutant (2.11fold increase, lane 4), the *D20V* mutant (2.19 fold increase, Lane 6) and the *G206S* mutant (1.93 fold, Lane 14). For the *V72G* and *Y203C* mutants, however, I could not reproducibly visualize the Smn protein band. The average fold differences observed in these mutants with *Serf* overexpression in three independent replicates are summarized in the table below (Table 5.3). While the exacerbation of the Smn mutant phenotype with Serf loss is strongly correlative, It increased Smn protein abundance with *Serf* overexpression does not tightly correlate with the degree of phenotypic restoration. That being said, the *G206S* mutant does show significant improvement in Smn protein abundance, size and larval locomotion with enhanced *Serf* levels. Also, the *D20V* mutant shows slight improvement in viability when *Serf* is over-expressed and Smn protein levels increase after Serf overexpression in this mutant background.

Table 5.3 Table shows average fold change in the relative *Smn* protein level in *Smn* missense mutants with and without *Serf* overexpression from at least 2 biological replicates.

Genotypes	Average fold change in *Smn* level ± SEM	P value
Smn^{WT}/Smn^{X7}	1	.0542
Act5c-GAL4>*Serf*, Smn^{WT}/Smn^{X7}	2.11 ± .9645	
Smn^{D20V}/Smn^{X7}	1	.0645
Act5c-GAL4>*Serf*, Smn^{D20V}/Smn^{X7}	1.94 ± .25206	
Smn^{T205I}/Smn^{X7}	1	.1213
Act5c-GAL4>*Serf*, Smn^{T205I}/Smn^{X7}	1.86 ±.439	
Smn^{G206}/Smn^{X7}	1	.0707
Act5c-GAL4>*Serf*, Smn^{G206S}/Smn^{X7}	2.82 ±.8898	

I also scored the Smn^{e33} for changes in Smn protein abundance with Serf overexpression. The Smn*e33* mutant is a hypomorphic *Smn* allele (Rajendra *Et al.* 2007) which causes severe atrophy of indirect flight muscles and motor neuron routing defects in adult flies rendering them flightless. The *Smne33* allele was generated by imprecise excision of a P element inserted 94 bps upstream of the *Smn* transcription start site. The *Smn* protein abundance in the *e33* mutant is specifically reduced in the thoracic muscles

for unknown reasons. We overexpressed *Serf* ubiquitously in the *Smn*^{e33} mutant and studied its impact on the *Smn* mRNA and protein expression within thoracic muscles.

Figure 5.11B shows the level of *Smn* protein abundance in the wild type (Act5c-GAL4 control; Lane 1), the *Smn*^{e33} mutant (Act5c-GAL4, *Smn*^{e33}; Lane 2) and *Smn*^{e33} with ubiquitous *Serf* overexpression flies (Act5c-GAL4>Serf,Smne33; Lane 3). Here I see reduction in the amount of Smn protein in *Smn*^{e33} muscle extract (0.43 fold) as compared to the driver only control. When I overexpressed *Serf* in these flies I found significant restoration to 0.74 fold of the normal level. This result was reproducible within 3 independent replicates and the average changes are summarized in the table below (Table 5.4). This change did not correlate with alterations in the Smn mRNA level as monitored by semi-quantitiative PCR.

Table 5.4 Table shows average fold change in the relative *Smn* protein level in *Smn*^{e33} with and without *Serf* overexpression.

Genotypes	Average fold change in *Smn* level
Act5c-GAL4	**1**
Act5c-GAL4, *Smn*^{e33}	**.528**
Act5c-GAL4>*Serf*, *Smn*^{e33}	**.983**

However, unlike the previous report (REF) I do not observed a reduction in Smn mRNA in the *Smne33* background. The basis for this discrepancy is unclear. We do note,

however, that increase Serf expression in not sufficient to restore flight to the *Smn* ^{e33} mutant flies (data not shown).

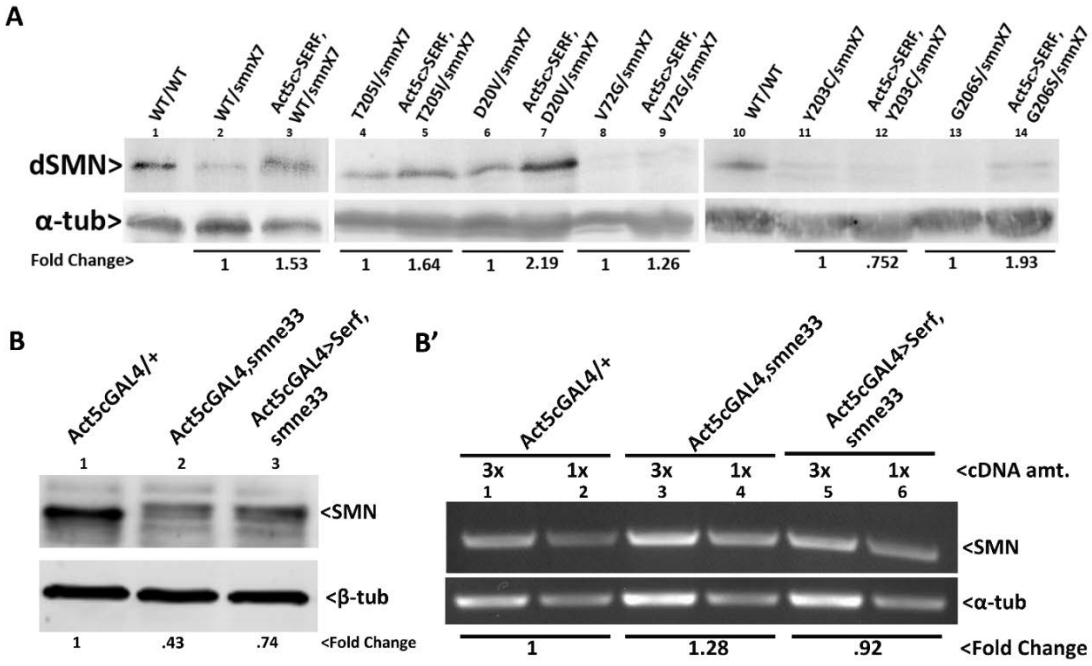

Fig 5.11. Ubiquitous *Serf* overexpression in a few *Smn* mutants shows moderate increase in the diminished *Smn* protein abundance. A) Western blot analysis of Smn protein abundance in hemizygous *Smn* wild type ($Smn^{WT}/SmnX^{7}$) and mutant larvae (Smn^{T205I}/Smn^{X7}, Smn^{D20V}/Smn^{X7}, Smn^{V72G}/Smn^{X7}, Smn^{G206S}/Smn^{X7}, Smn^{Y203C}/Smn^{X7}) with and without Act5c-GAL4 driven *Serf* overexpression. The Smn^{WT} transgenic homozygous is shown as a wild type control. The level of α-tubulin expression is shown as a loading control. The fold change of relative Smn protein expression in *the Smn* mutant larvae overexpressing *Serf* with respect to those with wild type *Serf* is shown below each pair of lanes. B) Western blot of Smn protein with extracts from adult thoracic segments of

Act5c-GAL4 driver control (Lane 1), *Smn^{e33}* mutant (Act5cGAL4, *Smn^{e33}*, Lane 2) and *Serf* overexpression in *Smn^{e33}* mutant (Act5cGAL4>Serf, *Smn^{e33}*,Lane 3) lines. β-tubulin levels are shown as loading control. Fold change of relative Smn protein levels in each genotype with respect to the control is shown below each lane. B') Semi-quantitative RT-PCR analysis of mRNA abundance in the respective lines tested for protein. 1x and 3x cDNA amounts were used for PCR from each genotype. The α-tubulin transcript was used as an internal control. Fold change in the relative *Smn* transcript abundance in *the Smne33* mutant group *(*Lanes 3 &4) and *Serf* overexpression in the *Smne33* mutant group (Act5cGAL4>*Serf*, Smne33; Lanes 5&6) with respect to the control group (Act5cgal4/+, Lanes 1&2) has been shown below the respective bands.

5.2.2.4 The *Serf* gene is necessary for maximum α-synuclein protein accumulation in a fly model of Parkinson's disease.

Serf has been shown to promote α-synuclein aggregate formation in *C. elegans* model of Parkinson's disease and in-vitro (Van-Ham *et al*., 2010, Falsone *et al*., 2012). Here, I have shown that Serf expression in *Drosophila* is necessary for maximum Smn protein abundance in wild type and *Smn* mutants. In *C. elegans* that loss of *Serf* does not impact α-synuclein protein abundance (Van-Ham *et al*., 2010), only aggregate size. Here I investigated the impact of Serf on α-synuclein protein and transcript levels in a Parkinson's fly model.

Figure 5.12A shows a western blot of α-synuclein in brain extracts. In each case, a human mutant form of α-synuclein A30P in a pan-neuronal manner under the Elav-GAL4 driver (Feany, M.B. 2000 Nature).*Drosophila* genome does not have an endogenous α-synuclein gene and in an otherwise wild type background the transgenic human α-

synuclein expressing flies show a unique protein band (lanes 1&2). I introduced the *Serf*Δ*10a* null deletion allele either in combination with the P-element insertion mutant, $Serf^{EY09918}$ (lanes 3&4) or a different null mutant *Serf*Δ*6c* (lanes 5&6) or as a homozygous null (lanes 7&8) in the α-synuclein expressing transgenic line. In all cases, the human α-synuclein proteins decreases roughly 3 to 8 fold when Serf expression is compromised.

As the P element insertion site is outside of the ORF, some level of *Serf* activity might persist and contribute to the milder impact of this construct on the α-synuclein protein abundance. In contrast, the *Serf*Δ*10a/Serf*Δ*6c* and homozygous *Serf*Δ*10a* are both complete null and shows a more robust effect. However, there was no notable changes in α-synuclein transcript abundance with or without Serf expression. While contrasting with the *C. elegans* results (Van-Ham *et al*., 2010) these data are consistent with *Serf*'s impact on Smn abundance, suggesting that *Serf* might regulate the expression of these two proteins (Smn and α-synuclein) at the level of protein synthesis or stability.

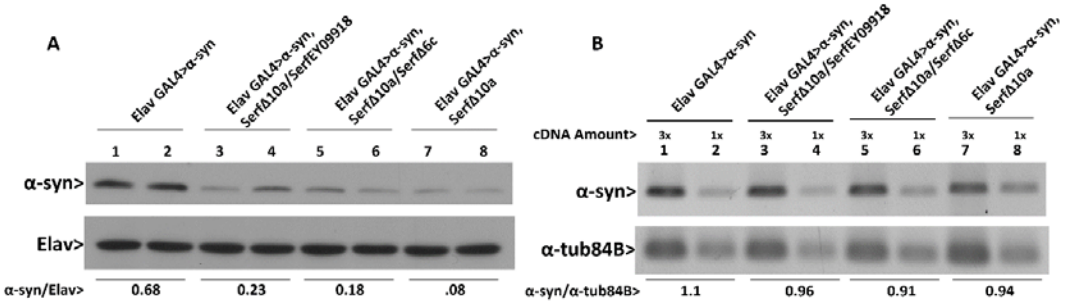

Fig 5.12 The loss of *Serf* in a fly model of Parkinson's disease correlates with the reduction of α- synuclein protein abundance but not the transcript levels. A) Western blot image showing α-synuclein protein levels in flies expressing human α-synuclein in neuronal tissue with wild type *Serf* (Elav GAL4> α-synuclein) or with different combinations of *Serf* alleles (*Serf*Δ*10a* and *Serf*Δ*6c* are null alleles whereas $Serf^{EY09918}$ represents the P element insertion allele). Two biological replicates for each genotype are shown. Elav protein in the corresponding lanes are shown as loading control. The values under the lanes corresponding to the genotypes indicate the mean α-synuclein protein levels relative to Elav between the two replicates. B) Semi-quantitative RT-PCR image showing α-synuclein transcript levels from flies with the same genotypes as used for the protein analysis. 3x and 1x amount of cDNAs were used for each genotype. The level of α-tub84B transcript serves as the internal control. The numbers indicate the mean α-synuclein transcript levels relative to α-tub84B between the two reactions for each genotype.

5.3 Conclusions and discussion

The major conclusion from this portion of my dissertation is that the *Serf* gene is a genetic modifier of SMA in the *Drosophila melanogaster* disease model. Similar to what was proposed in humans, reduced *Serf* expression enhances the mutant phenotype. And, while experimentally increased *Serf* gene expression cannot compensate for the absence of Smn activity, it does partially suppress some phenotypic defects associated with diminished Smn activity. While my study did not address the molecular basis for this interaction, our data is consistent with the view that the *Serf* gene is required for the maximal Smn protein abundance, the protein which is limiting in SMA patients. Furthermore our data rule out a mechanism acting through transcription or RNA stability and argue for Serf having a direct impact on protein synthesis or, more likely (see below), Smn protein stability.

The fly SMA disease model established by Praveen *et al*. served as a valuable system for testing genetic interaction between *Serf* and *Smn*. Here, the very same Smn amino acid substitutions found in human SMA patients are expressed in *Drosophila* through mutation of the endogenous fly gene. The mutations reside in distinct functional domains and represent a wide range of phenotypic severities providing the scope for easily and quantitatively scoring exacerbation and suppression of phenotypes. In my study, I found that the mild mutant alleles Smn^{D20V} and Smn^{T205I} proved most valuable to quantify the impact of diminished *Serf* expression on growth and development, since with normal *Serf* expression, these Smn mutants progress through all developmental stages. In contrast, the more severe mutants, Smn^{G206S} and Smn^{Y203C} provided a more sensitive background for monitoring the impact of *Serf* overexpression on growth and larval

mobility as the weaker Smn mutants were phenotypically normal in these assays. Interestingly, the Smn^{D20V} mutant was the most sensitive in the viability assays performed with knocking down and overexpressing *Serf*. While *Serf* overexpression could not rescue the larval lethality associated with Smn^{G206S} and Smn^{Y203C} mutants, it improved the proportion of larvae pupating, modestly but significantly, only in the Smn^{D20V} line. This is consistent with the observation that knocking down *Serf* showed the greatest reduction in viability at the larval and pupal stages in the Smn^{D20V} mutant.

Since, the point mutations reside in the distinct functional domains of the Smn protein, it allows us to hypothesize a basis for the exacerbation and amelioration of associated phenotypes that we observed with manipulating Serf abundance. The severe larval lethal mutations Smn^{G206S} and Smn^{Y203C} reside in the YG box domain necessary for self-association and complex formation with the Gemins and other proteins. It has been shown by Praveen *et al*. that the amount of Smn protein is greatly reduced in these lines giving rise to a more severe phenotype. The Smn^{T205I} mutation, although present within the YG box domain, has been shown to only slightly reduce the amount of Smn protein (Praveen *et al*., 2014), which is consistent with a less severe mutant phenotype. On the other hand the Smn^{D20V} mutation is located in the Gemin2 binding domain and does not associate with diminished Smn protein abundance, thereby explaining a weaker impact on the mutant phenotype. Our data show that while increased Serf protein could not restore normal level of Smn protein and associated larval lethality in the Smn^{G206S} and Smn^{Y203C} mutants it increased the Smn protein abundance in the Smn^{D20V} and Smn^{T205I} flies. At least for the Smn^{D20V} mutant, this increased Smn protein level correlate with an improvement of pupation. However, reduced level of Serf in the Smn^{D20V} and Smn^{T205I}

mutants associated with an exacerbation of mutant phenotypes in both cases, which correlates with a further reduction in the Smn protein level. Therefore, together the data support the hypothesis that Serf driven changes in the SMA phenotypes is caused, at least partly due to altered Smn protein abundance. Why Serf improves Smn protein in the milder allelic background but not in the severe mutants is not understood clearly. One possibility is that, since the YG box mutant Smn^{G206S} and Smn^{Y203C} are impaired in self-oligomerization, making more Serf would not help in stabilizing these mutant proteins, if Serf does so by promoting Smn self-association. Conversely, Smn^{D20V} and Smn^{T205I} mutants produce Smn protein capable of self-oligomerization and in these backgrounds increased Serf protein might act on stabilizing the Smn protein. Moreover, the fact that increased Smn level phenotypically benefit Smn^{D20V} but not Smn^{T205I} possibly points to Serf's relevance in the mechanism by which Smn^{D20V} mutation function. Praveen *et al*. showed that Smn^{D20V} protein is deficient in Gemin2 binding. Therefore it is possible that increased Serf protein promotes Smn^{D20V} self-association into multimeric complex which is more efficient in Gemin2 binding. On the other hand, the Smn^{T205I} protein has been shown to self-associate and interact with Gemin3 (Praveen *et al*., 2014), and the reason behind the reduced viability in this mutant is unclear. The observation that the increased Smn^{T205I} protein with *Serf* overexpression does not correlate with a viability improvement in this mutant might imply that the effect of this mutation does not depend on the amount of available Smn protein.

The other interesting thing we learned from the genetic interaction test is that the larval growth and locomotion of the Smn^{G206S} and Smn^{Y203C} mutants significantly improved with *Serf* overexpression although the larval lethality is not rescued. From our

mouth hook assay we learned that 90% of the small size *Smn*^{G206S} and *Smn*^{Y203C} larvae correspond to 3rd instar stage, although the remaining 10% showed 2nd instar specific mouth hook features. This implies that the severe *Smn* mutations possibly give rise to developmental delay or arrest in a certain proportion of the mutant population. The proportion that reaches 3rd instar stage within specified time are growth impaired since they do not reach the wild type third instar size and die before pupation. With *Serf* overexpression in these severe mutants we still see about equivalent proportion of larvae in the second instar stage, however, the proportion that reach 3rd instar stage grow significantly bigger than the mutants with normal level of Serf. It is known that in order for the larva to undergo the metamorphic molt (pupation), the larva is required to attain a critical weight (Mirth *et al*.,2005). Since the *Smn*^{G206S} and *Smn*^{Y203C} mutants are smaller in size and die as 3rd instar, it is conceivable that they fail to attain the critical weight and hence cannot undergo metamorphosis. *Serf* overexpression in these mutants significantly improve their growth but that is probably not sufficient for initiating the metamorphic molt. However, the positive correlation between *Serf* expression and the larval growth of Smn mutants is corroborated by the observation that reduced level of Serf in the milder *Smn* mutants, *Smn*^{D20V}and *Smn*^{T205I}, corresponds to reduced larval body size.

The improvement of larval growth in the severe *Smn* mutants, the *Smn*^{G206S} and *Smn*^{Y203C}, also associates with improved locomotion with *Serf* overexpression. Whether or not the locomotion impairment in these Smn mutants correspond to abnormal synaptic transmission or morphology at the larval NMJ, has not been described by Praveen et.al. However, the *Smn*^{73Ao} null mutant, first described by Chan *et al*., 2013, is known to have locomotion defect that correlates with reduced excitatory post synaptic current and

disorganized synaptic boutons at the larval NMJ. In contrast, the locomotion impairment associated with the neuronal and muscle specific *Smn* knockdown in flies do not directly correlate with diminished synaptic transmission, but associates with aberrations in the long-term homeostasis of the synaptic activity (Timmerman *et al*., 2012). This is consistent with the mice report where motor neuron specific SMN knockdown caused reduced synaptic transmission in mice at post-natal day 8 (PND-8) but got overcompensated by PND 10-12 to show increased end-plate potentials and quantal content than the control (Park *et al.*, 2010). Thus this implies that the homeostatic compensation of the synaptic transmission defect that occurs over developmental period is disrupted upon reduced SMN level in the motor neuron in mice (Park *et al*., 2010). The observation that Serf modulates the locomotion phenotype in *Smn* mutants raises the possibility that it affects some of the NMJ properties in these mutants. Although I did not study the NMJ morphology and activity in the *Smn* missense mutants with or without altered *Serf*, I attempted to study synaptic transmission in the *Serf* mutants as well as the Smn^{E33} mutant (Rajendra *et al*., 2007) with and without *Serf* knockdown (Appendix fig. A-3). My preliminary data showed that the Smn^{E33} mutant and the global *Serf* knockdown mutant display significantly increased EPSPs at the larval NMJ, while *Serf* knockdown in the Smn^{E33} mutant rescues the defect to normal. Such a complex genetic interaction is difficult to interpret. I suspect that the increased EPSPs observed in the *Smn* mutant and the *Serf* knockdown larvae at late 3rd instar stage could be due to aberrant homeostatic compensation as observed in mice (Park *et al*., 2010). However, the *Serf* null mutant did not result in the same phenotype and looked almost identical to the control. Homeostatic compensation in the null mutant might explain this apparently discrepancy between the

null and the knockdown allele. Nevertheless, these preliminary observation might suggest potential impact of Serf on larval NMJ thereby affecting Smn activity at the synapse in a SMA model. Whether locomotion impairment in the *Smn*^{G206S} and *Smn*^{Y203C} model correspond to similar NMJ defects and Serf driven rescue of the mobility phenotype correlates with an alteration of the NMJ properties, therefore becomes an important question to address.

Consistent with the phenotypic improvement with enhanced Serf in the *Smn*^{G206S} we found a partial restoration of Smn protein, however, the impact of Serf on Smn^{Y203C} mutant protein could not be determined as it is undetectable on a western blot, with or without *Serf* over expression. Since the Smn^{G206S} mutant protein is oligomerization deficient, it is curious to imagine how enhanced Serf might be impacting its abundance. One possibility is that it stabilizes the mutant protein by preventing its degradation through the Ubiquitin proteasome system. Alternatively, Serf could also stabilize the maternally deposited wild type Smn protein by either promoting its oligomerization or preventing its degradation.

The underlying mechanism of *Serf* dependent changes in Smn protein abundance is unknown. Our data shows that in the *Serf* mutant *Smn* gene expression is not reduced but the protein expression is diminished. In addition, Serf driven restoration of Smn protein in the *Smn*^{E33} mutant is not associated with increase in the RNA level. Our data on Serf's impact on protein abundance also extend beyond the Smn protein and shows that for at least another protein α-Syn, associated with the Parkinson's disease, loss of *Serf* greatly diminishes its protein abundance without correlated changes in the transcript levels. Together these data suggest that Serf dependent changes in the protein level likely acts

through protein synthesis or stability. Given Serf's previously described involvement in the amyloid protein assembly in *C. elegans* and *in vitro* (Van-Ham *et al*.,2010; Falsone *et al*.,2012) it is possible that Serf positively impact Smn and α-Syn protein stability by promoting their oligomeric assembly. Alternatively Serf might directly impact the half-lives of these proteins by either preventing their ubiquitination or their delivery to the proteasome, since both the Smn and α-Syn are known to be degraded by the UPS (Burnett *et al.,* 2008; Liu *et al.,* 2003). It is known from the α-Syn study that Serf does not itself incorporate into the amyloids but promote their growth, so we think that it might act like a chaperone protein to promote multimeric assembly of these proteins, hence rendering them more stable. Although our Smn self-association assay was not successful, we have seen Serf dependent changes in Smn post translational modification by phosphorylation (Appendix Fig. A-1), which might be relevant for assembly into the huge protein complex. Therefore, modulation of Smn interaction with the Gemins by altered level of Serf might provide an alternate hypothesis to Serf and Smn interaction in the cells. The idea here is that Serf driven stabilization of Smn protein might result from accelerated Smn complex formation by increased interaction with the Gemins. All these ideas can be tested and requires future attention for a better understanding about how Serf and Smn interact within cells to modify SMA phenotypes.

5.4 Materials and Methods

5.4.1 Fly strains and maintenance

The following genotypes are used in this chapter: (i) w^{1118}; (Xia, Fakler *et al*.) y w; {Act5C-GAL}25FO1/ CyO, y+ (Xia, Fakler *et al*.) [(i) & (Xia, Fakler *et al*.) are obtained from Bloomington Stock Center] (iii) UAS-*Serf* cDNA (generated in lab);

(Ruan, Tang *et al*.){UAS-hp-*Serf*}100894 (Xia, Fakler *et al*.) (*Serf* RNAi line- Vienna *Drosophila* RNAi Center); (v) Smn^{X7}/TM6.tb.GFP; (vi) Smn^{x7} , Smn^{WT}/TM6.tb.GFP; (vii) Smn^{x7} , Smn^{D20V}/TM6.tb.GFP; (viii) Smn^{x7} , Smn^{T205I}/TM6.tb.GFP; (ix) Smn^{x7} , Smn^{V72G}/TM6.tb.GFP; (x)Smn^{x7}, Smn^{G206S}/TM6.tb.GFP; (x) Smn^{x7} , Smn^{WT}/TM6.tb.GFP; (Zhang, Xing *et al*.) Smn^{E33} [(v)-(Zhang, Xing *et al*.) are generously gifted by Dr. Gregory Matera, University of North Carolina, Chapel Hill]. Flies were cultured in 25C humidified chamber under constant light condition. Vials or bottles containing semi defined medium, as described by Bloomington *Drosophila* Stock Center (Backhaus *et al*.,, 1984), were used for all experiments in this study. The description of the crosses performed to obtain the required genotypes used in this chapter is provided in table 5.5 - 5.8

Table 5.5 describes the generation of Act5c-GAL4-Smn^{X7} recombinant line.

Step	Cross	Progeny selected
1.	♀w^{1118}, Act5c GAL4/+ x ♂ w^{1118}, Smn^{X7}/TM3	w^{1118}, Smn^{X7}/Act5c-GAL4
2.	♀ w^{1118}, Smn^{X7}/Act5c-GAL4 x ♂ w^{1118}, Ly/TM3	w^{1118}, Act5c-GAL4-Smn^{X7}/TM3 (Red eye)
3.	w^{1118}, Act5c-GAL4- Smn^{X7}/TM3 (40 individual fly) x w^{1118}, Ly/TM3	w^{1118}, Act5c-GAL4-Smn^{X7}/TM3
4.	w^{1118}, Act5c-GAL4- Smn^{X7}/TM3 x Smn^{x7}/TM6 tb GFP	select lines producing no non-TM3 and non-TM6 flies (Lethal)

Table 5.6 describes the generation of w^{1118}, UAS-Serf (cDNA)/Cyo GFP, Act5c-GAL4- Smn^{X7}/TM3 Ser GFP line.

Step	Cross	Progeny selected
1.	♀ w^{1118}, Act5c-GAL4- Smn^{X7}/TM3 x ♂ w^{1118}, Sp/Cyo-GFP, Di/TM3 Ser GFP	w^{1118}, +/Cyo-GFP, Act5c-GAL4- Smn^{X7}/Di
2.	♀ w^{1118}, UAS-Serf (cDNA) x ♂ w^{1118}, Sp/Cyo-GFP, Di/TM3 Ser GFP	w^{1118}, UAS-Serf (cDNA)/Sp, TM3 Ser GFP/+
3.	♀w^{1118}, +/Cyo-GFP, Act5c-GAL4- Smn^{X7}/Di x ♂ w^{1118}, UAS-Serf (cDNA)/Sp, TM3 Ser GFP/+	w^{1118}, UAS-Serf (cDNA) /Cyo-GFP, Act5c-GAL4- Smn^{X7}/TM3 Ser GFP
4.	w^{1118}, UAS-Serf (cDNA) /Cyo-GFP, Act5c-GAL4- Smn^{X7}/TM3 Ser GFP (individual fly) x w^{1118}, Sp/Cyo-GFP, Di/TM3 Ser GFP	Make a stock from each single fly

Table 5.7 describes the generation of w^{1118}, UAS-hp-Serf (RNAi)/Cyo GFP, Smn^{Tg}/TM3 Ser GFP line (Tg represents Smn transgene, either wt or the various point mutants -D20V/T205I/V72G).

Step	Cross	Progeny selected
1.	♀ w^{1118}, Smn^{Tg}/TM3 x ♂ w^{1118}, Sco/Cyo-GFP, Sb/TM3 Ser GFP	w^{1118}, +/Cyo-GFP, Smn^{Tg}/TM3 Ser GFP
2.	♀ w^{1118}, UAS-hp-Serf (RNAi) x ♂ w^{1118}, Sco/Cyo-GFP, Sb/TM3 Ser GFP	w^{1118}, UAS-hp-Serf (RNAi)/Cyo GFP, +/TM3 Ser GFP
3.	♀ w^{1118}, +/Cyo-GFP, Smn^{Tg}/TM3 Ser GFP x w^{1118}, ♂ UAS-hp-Serf/Cyo GFP, +/TM3 Ser GFP	♀ w^{1118}, UAS-hp-Serf (RNAi) /Cyo-GFP, Smn^{Tg}/TM3 Ser GFP

Table 5.8 describes the specific crosses performed, to obtain the progeny of required genotypes for the different assays conducted in this chapter. (Tg represents *Smn* transgene either wildtype or the various point mutants- /D20V/T205I/V72G/Y203C/G206S)

Stage collected	Cross description	Progeny genotype collected
1st instar larva	Act5c GAL4/TM3 Ser GFP x w^{1118}	Act5c GAL4/+
	Act5c-GAL4/TM3 Ser GFP x UAS-Serf (cDNA)	UAS-Serf (cDNA)/+, Act5c-GAL4/+
	Act5c-GAL4/TM3 Serf GFP x UAS-hp-Serf (RNAi)	UAS-hp-Serf(RNAi)/+, Act5c GAL4/+
	Smn^{x7} , Smn^{Tg}/TM6.tb.GFP x Smn^{x7}/ TM6.tb.GFP	Smn^{x7} , Smn^{Tg}/ Smn^{x7}
	w^{1118}, UAS-Serf (cDNA) /Cyo-GFP, Act5c-GAL4- Smn^{X7}/TM3 Ser GFP x Smn^{x7} , Smn^{Tg}/TM6.tb.GFP	w^{1118}, UAS-Serf (cDNA)/+, Act5c-GAL4- Smn^{X7}/ Smn^{x7} , Smn^{Tg}
	w^{1118}, UAS-hp-Serf (RNAi) /Cyo-GFP, $Smn^{x7,}$ Smn^{Tg}/TM3 Ser GFP x w^{1118}, Act5c-GAL4- Smn^{X7}/TM3 Ser GFP	w^{1118}, UAS-hp-Serf (RNAi)/+, Smn^{x7} , Smn^{Tg}/ Act5c-GAL4- Smn^{X7}

Table 5.8 continued..

Adult	**Act5c-GAL4/Cyo x w^{1118}**	**Act5c-GAL4/+**
	Act5c-GAL4/Cyo x UAS-Serf (cDNA)	UAS-Serf (cDNA)/Act5c-GAL4
	Act5c-GAL4/Cyo x UAS-hp-Serf (RNAi)	UAS-hp-Serf(RNAi)/ Act5c GAL4
	Act5c-GAL4/Cyo GFP x w^{1118}	Act5c-GAL4/+
	Act5c-GAL4/Cyo GFP, Smn^{e33} x UAS-Serf (cDNA), Smn^{e33}	Act5c-GAL4/ UAS-Serf (cDNA), Smn^{e33}
	Act5c-GAL4/Cyo GFP, Smn^{e33} x Smn^{e33}	Act5c-GAL4/+, Smn^{e33}

5.4.2 Viability and growth assay

Viability assay was performed as described in chapter 2, section 2.4.5. In short, At least 100 synchronized 1st instar larvae of required genotype were collected on a small amount of the standard fly cornmeal food which was then carefully placed inside fly food vials for letting the larvae to develop into pupae and adults. The total number of pupae and adult formed per genotype is calculated and expressed as a proportion of the total number of larvae (% pupation, % larvae reaching adulthood) and pupae (% pupae eclosed). To monitor growth, food containing the staged larvae were scooped out from vials with a spatula at 96 and 120 hours post egg laying. The larvae were then carefully separated from the food on a small petri dish, washed in 1X PBS briefly and transferred in 100% ethanol for 10 minutes to kill them. Staged larvae were then aligned on glass slides for

imaging under 10X magnification. Larval body area measurements were performed using Image-J software as described in 5.4.6 and statistical analysis is described in 5.4.8.

5.4.3 Larval mobility assay

Larval mobility assay is performed as described in chapter 2, section 2.4.6. In short, synchronized (96 hrs post egg laying) 3rd instar larvae were collected and placed on apple juice agar plates for 1 minute of acclimatization followed by the counting of the body wall contractions for another 1 minute. At least 15 larvae for each genotype were assayed and the average body wall contractions/minute were measured and statistically analyzed (5.4.8).

5.4.4 SDS PAGE and western blots

SDS PAGE and western blots were performed following the procedure as described in chapter 2, section 2.4.4. 1 week old adult flies, males and females separately (12-15 flies for each) and synchronized 3rd instar larvae (96 hrs post egg laying) were used for extracting total protein. Mouse monoclonal anti-fly Smn (Chang *et al*., 2008) (1:1000 dilution, generous gift from Dr. Anindya Sen, UMASS), mouse monoclonal α-tubulin (1:1000 dilution; Developmental Studies Hybridoma Bank 12G10 anti-alpha tubulin -s) and mouse monoclonal anti-β tubulin (1:1000 dilution; Developmental Studies Hybridoma Bank, E7-s), mouse monoclonal anti-human alpha synuclein (Feany *et al*., 2000) (1:1250; BD Biosciences) and rat anti-Elav (1:5000; Developmental Studies Hybridoma Bank, 7E8A10) primary antibodies were used. Alkaline phosphatase conjugated polyclonal goat anti-mouse IgG (1:5000 dilution, Life Technologies) and horseradish peroxidase conjugated goat anti-rat IgG (1:5000 dilution, Santa Cruz) secondary antibodies were used. Alkaline phosphatase based signals were detected by

BCIP/NBT color development substrate (Promega) or Amersham^{TM} ECF substrate (GE Healthcare, Life Sciences) based detection of the fluorescence signal. HRP based signals were detected by SuperSignal West Pico reagents (Thermo Fisher Scientific) followed by development on X-ray films (CL-XPosure^{TM} Film, 5 x 7 inches, Thermo Scientific). Colored membranes and developed X-ray films are scanned using HP G4050 scanning machine and fluorescence signals are scanned by the Typhoon scanner (Emission Filter526 SP Fluorescein, Cy2, AlexaFluor 488, PMT-600, Sensitivity-high) followed by densitometric analysis with Image Quant 5.2 software.

5.4.5 Semi-quantitative RT-PCR

Reverse transcriptase PCR was done to analyze the expression level of *Smn* and α-synuclein transcript in flies with various *Serf* alleles in otherwise wild type or in Smn mutant background. The Total RNA extracted (for RNA extraction procedure see chapter 2, section 2.4.3) was DNase treated and 0.8 ug was subjected to reverse transcription using the MMLV Reverse Transcriptase 1st-Strand cDNA Synthesis Kit (Epicentre), and the levels of gene expression were then examined by PCR using first-strand cDNA as template. The α-tub84B transcript was used as an internal control. The primer pairs are described in table 5.9.

Table 5.9 describes the primer pairs used in semi-quantitative RT-PCR.

Genes	Primer Pairs
SMN	5'-TTCTGGATGACTTGGGAGTCT-3' and 5'-CGGAACCAGTATCCTTCAAAG-3'
α-synuclein	5'-ATGGATGTATTCATGAAAGGACT-3' and 5'-TTAGGCTTCAGGTTCGTAGTCT-3'
α-tubulin 84B	5'-GCTGTTCCACCCCGAGCAGCTGATC-3' and 5'-GGCGAACTCCAGCTTGGACTTCTTGC-3'

5.4.6 Image J analyses

Image J software was used to perform larval body area measurements. Following are the sets of action performed to obtain the measurements- file>open image> select the straight line tool to draw a straight line following the traces on the graph sheet (each side of the square=1 mm) in the background of each image> analyze> set scale by putting the known distance an unit corresponding to the pixels selected by the straight line and then hit global> select the 'freehand selection' tool to mark the outline of the larva>analyze>measure- this will produce a datasheet with the larval body area measurement.

5.4.7 Statistical analyses

The viability assay dataset were analyzed for statistical significance by the two sample t-test between percent. Rest of the data in this chapter are analyzed for statistical

significance calculations using two-tailed Unpaired Student's *t*-test. For all statistical tests $P<0.05$ were considered significant. For all graphs, data are represented as the mean ± the standard deviation of mean (Becker, Semler *et al*.) and significant difference is expressed as: '*'- P value between 0.01-0.05; '**'- P value between 0.001-0.01; '***' P value<.001.

Chapter 6: Discussion

SMA is an untreatable devastating disease affecting numerous children worldwide. In spite of our significant progress in unravelling the cause and the mechanism of SMA pathogenesis, we are still lacking understanding about many critical questions. Why diminished SMN is specifically detrimental to motor neuron survival? Why different forms of SMA exist? The *Drosophila* model of SMA has proven to be a powerful invertebrate system to address these questions and major discoveries were made concerning the molecular pathogenesis of the disease.

The *Drosophila* SMA model significantly contributed to the understanding of SMN dependent NMJ abnormalities in the pathogenesis of the disease (Chan, Miguel-Aliaga et al. 2003). Some of the key features of the SMA NMJs were first discovered in the fly model. For instance, the disorganized and reduced number of synaptic motor neuron boutons, reduced clustering of the neurotransmitter receptor subunit GluRIIA and reduction in the excitatory post synaptic current were identified as the hallmark of the disease, the rescue of which requires SMN activity in both neurons and muscles (Chan, Miguel-Aliaga et al. 2003). The abnormal architecture and activity of SMA NMJs correlate with greatly impaired motor functioning, slow growth and developmental defects in late developmental stages (late larval and pupal), (Chan, Miguel-Aliaga et al. 2003, Chang, Dimlich et al. 2008, Praveen, Wen et al. 2014).These mutant phenotypes serve as useful quantitative means for studying genetic modifiers and for conducting large scale screening to test therapeutic compounds (Yankner, Lu et al. 2008).

The discovery of 17 enhancers and 10 suppressors of SMA using the Exelixis Collection of transposon-induced mutations in *Drosophila* (Parks, Cook et al. 2004, Thibault, Singer et al. 2004) demonstrates the power of this invertebrate model to predict previously unknown genetic interactions of *SMN* (Chang, Dimlich et al. 2008). Sixteen out of these 27 modifiers (Table 6.1) showed cross species conservation in *C. elegans* SMA model demonstrating parallel enhancement or suppression of phenotypes pointing at the conserved features of the genetic network pertinent to the development of the disease (Dimitriadi, Sleigh et al. 2010). For instance increased BMP signaling improves the NMJ defects in SMA flies (Chan, Miguel-Aliaga et al. 2003) with correlated increase in the neuromuscular activity in terms of pharyngeal pumping in *C. elegans* SMA model (Dimitriadi, Sleigh et al. 2010). As another example, the protective SMA modifier *PLS3* identified initially in SMA patients (Dent and Gertler 2003, Oprea, Krober et al. 2008), when knocked down in SMA flies, reduces the number of synaptic motor neuron bouton numbers at the larval NMJ demonstrating the conservation of this SMA modifier between flies and humans. A recent study by the Matera group showed that specific *Smn* point mutations exert similar effects on humans and flies in terms of reduced viability and locomotion impairment and show a consistent corresponding range of phenotypic severities in the two systems (Praveen, Wen et al. 2014).

Adding to the value of using the *Drosophila* SMA model for studying the genetic modifiers, my study have shown that the *Serf* gene modifies the SMA phenotypes associated with disease severity in flies. This finding supports the human data that *SERF* deletion exacerbates the effects of *SMN1* mutation in the most severe forms of SMA. In addition my data show that increased *Serf* expression improves certain SMA-associated

phenotypes like decreased growth and locomotion. I propose that the genetic interactions between *Serf* and *Smn* in flies parallel their interaction in humans.

6.1 The SMN biology and potential impact of Serf

The mammalian SMN protein resides within a large (>1 mDa) multimeric complex, the core of which is made up of SMN tetramer that directly or indirectly interacts with eight other proteins including Gemins and Unrip (Meister, Buhler et al. 2000, Otter, Grimmler et al. 2007). The N terminal region of SMN (codons 13-44) binds Gemin 2 (Liu, Fischer et al. 1997) while Smn domains coded by exon 2b (52-91) and exon 6 (242-279) form the domain required for Smn dimerization and further oligomerization (Lorson, Strasswimmer et al. 1998) (Young, Man et al. 2000)). *Drosophila* contains a single copy *SMN* gene that codes for a highly conserved homologue (Miguel-Aliaga, Chan et al. 2000). It forms a very simple SMN complex in the cell comprised of only Gemin2, 3 and 5 and the Smn tetramer, sufficient for mediating the conserved steps of spliceosomal snRNP assembly function (Kroiss, Schultz et al. 2008).

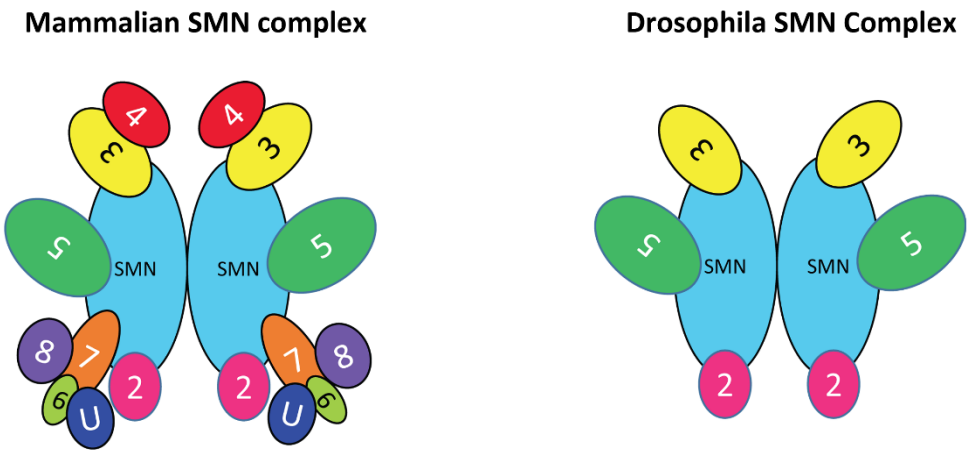

Fig 6.1 The SMN complexes in mammals and Drosophila. The numbers represent specific Gemin proteins (eg 2: Gemin 2, 3: Gemin 3 etc.). U: Unrip.

Diminished SMN protein abundance impairs SMN-directed function but which SMN activity is the most critical for development of SMA is unknown. A lot of attention has been given to its best characterized function in spliceosomal snRNP assembly and it is thought that aberrant splicing of disease-relevant transcript(s) (isoforms specific to motor neurons) could be causative to neuronal selectivity in SMA. Reduced snRNP levels and impaired snRNP assembly has been documented in SMA patient derived cells as well as in animal models (Pellizzoni, Yong et al. 2002, Gabanella, Butchbach et al. 2007). Biochemical assays testing the ability of SMN to assemble Sm proteins onto snRNA has been used to show strong correlation between the disease severity and the extent of snRNP assembly impairment (Gabanella, Butchbach et al. 2007). In addition, defective SMN complex function in SMA mice tissues has been shown to preferentially reduce the accumulation of a minor class U11-snRNP (Gabanella 2007). More recently, Lotti and colleagues identified a U12 intron containing conserved gene *Stasimon* in *Drosophila* as being a SMN target which has essential function in the motor circuit

(Lotti, Imlach et al. 2012). However, a more broad spectrum and non-uniform alteration of the stoichiometry of snRNA and splicing of numerous genes due to SMN deficiency has been documented in all cells including motor neurons (Zhang, Lotti et al. 2008).

Whether or not Serf, as a modifier of SMA phenotype, influences the SMN dependent splicing changes is unknown. The yeast *ySERF*, although co-purifies with two essential splicing factors, Prp8 & Brr2, does not have obvious impact on general splicing (Ghosh and Rymond, unpublished). However importantly, yeast does not have SMN homologue; therefore if *SERF* genetically interacts with *SMN* to influence cellular splicing could not be tested. Studies in *Drosophila* has shown that levels of spliceosomal snRNA do not change in larval-lethal Smn-null mutants, suggesting that larval lethality is not associated with global depletion of spliceosomal snRNP and splicing (Rajendra, Gonsalvez et al. 2007). Furthermore, transgenic expression of low levels of wild type SMN fully rescued the larval mobility and viability of *Smn* null mutants but not the snRNA levels (Praveen, Wen et al. 2012; Garcia et al. 2016). The expression level of four minor-class intron containing gene, reduced in *Smn*-null did not correlate with transgenic expression of wild type Smn (Praveen, Wen et al. 2012). Moreover, a RNA-seq based study showed that the bulk changes in the expression of minor intron containing transcripts in Smn-null larvae is contributed by the developmental arrest of this mutant, thus arguing against a minor-intron splicing dependent etiology of SMA (Praveen, Wen et al. 2012, Garcia, Lu et al. 2013). Together, these studies in *Drosophila* suggest that the snRNP assembly function of Smn can be uncoupled from the reduced organismal motility and viability observed with reduced Smn activity (Praveen, Wen et al. 2012, Garcia, Lu et al. 2013). Based on these observations, I predict that the *Serf* dependent modulation of SMA phenotype,

especially the mobility and viability defects, are not mediated by broad defects in splicing in flies.

Non-canonical functions of SMN protein have also been postulated providing hypothesis for motor neuron specificity in SMA. The finding that SMN localizes to the ribonucleoprotein granules (Fan and Simard 2002, Zhang, Xing et al. 2006) undergoing bidirectional transport along the long neurons (Zhang, Xing et al. 2006) led to the hypothesis that SMN functions in localized RNA processing and translation within neurons, necessary for proper neuronal development and NMJ function. In support of this idea, reduced SMN protein that co-localizes with β-actin containing RNA-protein complexes (Rossoll, Kroning et al. 2002, Rossoll, Jablonka et al. 2003) was shown to diminish β-actin mRNA and protein levels in axons and growth cones with correlated axonal outgrowth and pathfinding defects (Zhang, Pan et al. 2003).

It is conceivable that Smn contribution to NMJ activity could be modulated by Serf. Although I did not test the effect of *Serf* on NMJ morphology, limited studies were performed to test the electrophysiological properties of the *Smn* mutant and wild type NMJs with and without altered *Serf* expression (Appendix Fig. 3). We found that the hypomorphic Smn^{e33} mutant and the *Serf* RNAi knockdown mutant displays increased excitatory post synaptic potential (EPSP) at the larval NMJ. Paradoxically however, *Serf* knockdown in the Smn^{e33} mutant background brought the EPSPs back to the wild type range. Such a response is hard to interpret. In addition, I saw an inconsistency in the EPSP responses of the *Serf* knockdown and *Serf* null mutant where the knockdown showed hyperactivity while the deletion mutant displayed wild type like activity.

Therefore, *Serf* dependent changes in the larval NMJ, both morphology and activity, needs to be characterized more critically

In spite of the controversy about the features of SMN function most pertinent to the disease pathogenesis, it is a known fact that amount of available active SMN protein is critical for the motor neuron survival. The SMN protein is known to be ubiquitinated and degraded by the proteasome (Burnett, 2008). The major product of the *SMN2* gene, SMNΔ7, is deficient in oligomerization activity (Lorson et.al 1999, Young et.al 2000b) and binding to Sm core proteins (Pellizzoni, Charroux et al. 1999) and is known to have a two-fold shorter half-life in the cell compared to the full length protein (Burnett, Munoz et al. 2009). Incorporation of the SMN protein into oligomers and association with the Gemin complex reduce its rate of turn-over (Burnett, Munoz et al. 2009). In fact, SMNΔ7 can be stabilized by co-expressing the full length SMN suggesting that this derivative may be stabilized by its inefficient association with the full length protein (Le, Pham et al. 2005). In general, mutations that inhibit Smn protein oligomerization or Gemin complex assembly shorten SMN protein half-life (Burnett, Munoz et al. 2009). All these results strongly establish the idea that oligomerization and complex formation is the key to regulating SMN protein stability in cell.

I have shown that the level of Smn protein in flies is sensitive to the level of *Serf* expression, such that the Smn protein level changes with manipulating *Serf* without correlated change in the mRNA level. This suggested that *Serf* impact Smn protein expression post-transcriptionally, possibly at the level of synthesis or stability. Similar to its effect on Smn, we have also shown that the loss of Serf activity in flies greatly reduces the level of the α-synuclein peptide in vivo acting through a post-transcriptional event.

The α-synuclein, similar to Smn, self-oligomerizes to form long fibrillar amyloid complexes which renders them stable inside the cells. Therefore, one possibility is that Serf enhances stability of these proteins by promoting their assembly into complexes.

The proteins that are known to be involved in the process of protein complex assembly are the molecular chaperones (Makhnevych, Houry 2011). The HSP90 protein, for instance, functions in the assembly of seven different protein complexes- snoRNP, RNA polymerase II, phosphatidylinositol-3 kinase related protein kinase, telomere complex, kinetochore, RNA induced silencing complex (RISC) and 26S proteasome (Makhnevych, Houry 2011). More than 20 different co-chaperones and cofactors regulate the activity of HSP90 in these processes (Makhnevych, Houry 2011). In addition HSP90 has also been suggested in modulating the growth of α-synuclein amyloid fibril in an ATP dependent manner (Falsone *et al*. 2009). It has been shown that in presence of ATP, HSP90 favors the fibrillar growth of the α-synuclein protein over oligomeric species in an *in vitro* assay system. Other chaperone proteins have also been identified to have positive impact on the amyloid assembly process. For example, the formation of amyloid inclusions of expanded polyQ huntingtin protein was found to be increased in mammalian cells with increased expression of human HSP40, Hdj2 (Wyttenbach et al., 2000). In a follow up in-vitro study, the chaperones HSP70 and HSP40 were found to suppress oligomeric assembly of expanded polyQ peptide while promoting its fibrillar growth (Wacker et.al 2004). Given Serf's implication in promoting polyQ peptide and α-synuclein assembly into amyloid complexes (Van Ham et al. 2010; Falsone et al. 2012), together with our finding that it contributes in stabilizing cellular proteins (Smn and α-synuclein), imply that Serf could function as a molecular chaperone in the cell thereby affecting protein

complex assembly and stability. Such a cellular function of Serf could explain its relevance in SMA as well as its potential to impact neurodegenerative protein toxicity diseases in humans. It is important to note here that the *C. elegans* report on Serf has shown that the suppression of polyQ aggregation by Serf/MOAG4 deletion is not mediated by the HSF1 protein- the activator of a number of heat shock protein genes, including HSP70 (Van Ham et al. 2010). This study hypothesized that Serf in *C. elegans* might function downstream of HSF1 protein as loss of *HSF1* could not suppress the effect of *Serf/MOAG4* deletion on polyQ aggregation. Alternatively Serf/MOAG4 could be part of a parallel chaperone system, yet to be identified.

Stabilization of cellular proteins could also be achieved by inhibiting their degradation pathways. The SMN protein is degraded by the UPS (Burnett, Munoz et al. 2009) while the α-synuclein protein is targeted to both UPS or autophagy pathway for degradation (Pan et al. 2008). Therefore, antagonistic effect of Serf on these pathways or to the process of ubiquitination that tags the substrates for pathway specific turn over might explain Serf's impact on protein stability. According to my analysis *Serf* expression positively correlates with increased autophagy although it stabilizes the amount for cellular SMN and α-synuclein protein. Therefore, Serf might negatively impact UPS either by inhibiting ubiquitination or by preventing the delivery of the targets to proteasome.

Consistent with this idea, Boone and Rymond found in yeast that deletions of the *Serf* gene partially suppressed null mutations in the *UBP6*, the proteasomal ubiquitin protease and null mutations in the *BRE5*-encoded ubiquitin protease interacting protein, active in autophagy, suggesting that Serf activity might antagonize these catabolic pathways. That

is, if ubiquitin-directed protein turnover is compromised, the presence of Serf may further stabilize the residual complexes while Serf removal may promote enhanced turnover of selective proteins as appears to be the case with α synuclein and Smn in flies. The interpretation of the yeast results may be a bit more nuanced, however, since the *serf, ubp6* and *bre5* mutants show only mild growth defects and prior work has established that the intrinsic proteasome activity actually increases in the absence of the Ubp6 ubiquitin hydrolase (Hanna et al. 2006) although the resulting catabolism of ubiquitin results in a ubiquitin starvation phenotype with consequences on all ubiquitin-directed cellular events including proteasome-directed protein turnover. In addition, while Serf may antagonize ubiquitin-mediated proteolysis, the Serf protein itself appears to be a target for modification by the ubiquitin-like molecule, SUMO (Sung, Lim et al. 2013), a protein modification often associated with protein stabilization. While similar in size to both ubiquitin and SUMO, we find no evidence to suggest that Serf itself is covalently ligated to other proteins. A single band of predicted size is found in yeast when Serf is epitope tagged (Rymond, unpublished) and while the antibody raised against Serf binds Serf and multiple background bands in both flies and yeast, in the serf deletion background only the actual Serf band is lost. Nonetheless, the genetic interaction of Serf with the ubiquitin dependent proteolytic pathway factors supports the potential link between Serf and the protein turn-over processes and hence raises the possibility that Serf dependent protein stabilization could involve antagonistic effect on these pathways.

Total cellular ubiquitinated proteins include substrates of autophagy and UPS as well as stable proteins that acquire this posttranslational mark for regulatory purposes (Reviewed in Hochstrasser, 1996; Dunn and Hickey, 2003). I have presented evidence that

autophagy decreases after *Serf* deletion consistent with observed general accumulation of ubiquitinated proteins. But whether specific UPS substrates such as Smn are more heavily ubiquitinated in the Serf deletion background was not tested. Pharmacological (Belozerov, Ratkovic et al. 2014) or genetic approaches (Belote & Fortier 2002; Nezis, Simonsen et al. 2008) could be employed for investigating the possible link between Serf and the proteasome using fly in-vivo system or cell culture.

6.2 Serf function in protein homeostasis

The implication of Serf in the fibrillar aggregation of disease associated proteins *in vivo* and *in vitro* (Van Ham et al. 2010; Falsone et al. 2012), together with the finding that Serf in flies impacts specific protein abundance potentially by influencing their stability, makes it a likely candidate for functioning in the protein homeostasis network. The pathways governing the protein homeostasis network has been studied extensively for elucidating the mechanisms of protein toxicity diseases. The implications from my findings point to the possibility that protein homeostasis factors could also be important players in the modulation of an apparently unrelated disease like SMA.

Our knowledge of the cellular factors and processes that contribute to the formation, regulation and clearance of protein aggregates in protein toxicity diseases is far from complete. The identification of modifiers of amyloid aggregation has contributed to our understanding of this topic. For instance, an RNAi screen in a poly-Q expansion disease model in *C. elegans* identified 180 genes that, when suppressed, increased the accumulation of intracellular inclusions (Nollen, Garcia et al. 2004). These genes were clustered into five major groups based on their cellular function. These include genes involved in RNA metabolism, protein synthesis, protein folding, protein degradation and

protein trafficking - pathways proposed to underlie a homeostatic system that buffers the impact of toxic protein aggregates (Nollen, Garcia et al. 2004). A similar study in *C. elegans* using an aggregation-prone version of the human α-synuclein protein identified 80 genes that when knocked down increased aggregate formation. Majority of these modifiers were vesicle trafficking genes that are expressed in ER/Golgi complex and vesicular compartments, suggesting a protective role for endomembrane transport system in α-synuclein toxicity (van Ham, Thijssen et al. 2008). These genes are also relevant to autophagy which is a membrane dependent process and is active in the clearance of the terminal insoluble aggregates in cells (Ref from defense powerpoint). Surprisingly very few of these modifier genes were components of the proteasome or protein chaperones and also did not show a general overlap (except for one gene that overlapped, mentioned but not described in the Van Ham 2008 article) with the modifiers identified in the poly-Q aggregation screen by Nolen et al, suggesting that the detoxification of the poly-Q expansion proteins and α-synuclein may be handled differently, at least in *C. elegans.*

While speculation is abundant, comparatively little is truly known about the proteins that naturally contribute to protein aggregation. SERF/MOAG-4 is therefore amongst the rare modifiers of aggregation that assists in the formation of larger insoluble aggregates in *C. elegans* and *in vitro* (Van-Ham et al. 2010; Falsone et al. 2012). The fact that it impacts a variety of aggregation prone proteins in a similar manner indicates that common cellular processes are involved in the assembly of amyloid complexes (Van-Ham et al. 2010; Falsone et al. 2012). The reduction of cellular inclusion formation upon loss of SERF/MOAG-4 activity with correlated rescue of toxicity suggests that the natural

SERF/MOAG-4 function contributes to the disease phenotype. Contrary to this idea, Van Ham et al. argued that since loss of SERF/MOAG-4 inhibited the formation of toxic soluble aggregate intermediates, it resulted in the suppression of the associated cytotoxicity while reducing the assembly of larger complexes (Van Ham et al. 2010). In the follow up *in vitro* biochemical study Falsone et al. showed consistent results where Serf accelerated the nucleation of the fibrillar precursors (oligomeric intermediates) resulting in the rapid growth of larger fibrils (Falsone et al. 2012). Studies associated with Alzheimer's disease have shown that the soluble oligomeric forms of the Aβ peptide exerts neurotoxicity, both in animal model and cell culture system, while the large amyloid fibrils are phenotypically benign (He, Zheng et al. 2012) (Shankar, Li et al. 2008). A G-protein coupled receptor, Gprk-2, has been shown to reduce α-synuclein inclusion formation in *Drosophila* while increasing the neurotoxicity suggesting the protective role of inclusion formation under disease condition (Chen and Feany 2005). Thus it was hypothesized that SERF could be a factor involved in the protein homeostasis network that functions to actively aggregate misfolded proteins as part of a cellular strategy to protect itself from the increased load of toxic oligomeric misfolded proteins. A chaperone like activity therefore fits the model of conserved cellular function of SERF. As discussed in the section before, specific chaperone systems has been shown to promote cellular inclusion formation in the protein toxicity disease models (Wyttenbach et al., 2000).

Contrary to the observations in *C. elegans*, where *SERF/MOAG-4* did not impact organismal survival, I find that in *Drosophila* the loss of *Serf* activity results in a 25-30% reduction in adult lifespan while increased *Serf* expression extend *Drosophila* lifespan by

roughly the same value. Another longevity factor *AGE-1* has been identified in nematodes to impact Poly-Q aggregation, however, its functions is opposite to that of *SERF* in impacting lifespan. The inactivation of *AGE-1* extends lifespan and delays the formation of intracellular inclusions in a Poly-Q expansion model (Morley, Brignull et al. 2002). *AGE-1* encodes a PI3 kinase in the insulin signaling (IIS) pathway that negatively regulates the DAF-16/FOXO and HSF1 transcription factors (Hsu, Murphy et al. 2003). The *age-1* mutation activates DAF-16/FOXO that thereby upregulates a number of longevity promoting genes, including chaperones having protective influence on proteotoxic stress. When Van Ham et.al enquired the genetic interaction between *SERF/MOAG4* and IIS pathway effectors, *DAF16/FOXO* and *HSF1*in modifying inclusion formation, they found that suppression of aggregation by *moag-4* deletion does not require DAF16 or HSF1 activity (van Ham, Holmberg et al. 2010). Thus they predicted that SERF/MOAG4 either functions downstream or independent of DAF16/FOXO mediated IIS pathway.

The muscle specific activation of DAF16/FOXO in flies have been documented to extend lifespan, at least partially by enhancing the autophagy mediated clearance of naturally occurring age related aggregates (Demontis and Perrimon 2010). Similar to that, my data show that the reduction and extension of fly lifespan correlates with an apparent decrease in autophagy in the absence of *Serf* and an increase in autophagy when Serf activity is enhanced, respectively. The Serf related changes in autophagy also correlates with the clearance of the age-related poly-ubiquitinated aggregates from the adult muscles such that enhanced autophagy could partly be responsible for the rapid removal of the aggregates by Serf activation. There is compelling evidence that the induction of

autophagy functions as a protective quality control response to increased aggregation prone proteins in disease conditions (Williams, Jahreiss et al. 2006, Rubinsztein, Gestwicki et al. 2007). Therefore it is conceivable that a protein homeostasis factor like Serf might operate like a chaperone to assemble selective proteins into larger complex, naturally or under disease condition, thereby inducing autophagy that acts, at least in part, to remove protein aggregates from tissues and extend lifespan.

The loss of *SERF/MOAG-4* in *C. elegans* reduces the aggregation but apparently not the stability of α-synuclein expressed from an ectopic human disease gene. In flies, I observe that the protein accumulation of the same α-synuclein is greatly diminished in the absence of Serf. While I do not know the basis for this difference, the results are not necessarily contradictory since it is possible that the fly system is simply more efficient in removing the ectopically expressed α-synuclein when not stabilized through Serf-mediated oligomerization. For SMN protein, lack of oligomerization and assembly into larger complex prompts it towards its UPS mediated degradation (Burnett, Munoz et al. 2009). Since both SMN and α-synuclein is destabilized with Serf deletion, one possibility is that they are rapidly turned over by the UPS when they are not assembled into complexes in absence of Serf. Intriguingly, this is opposite to the impact of *Serf* deletion on natural poly-ubiquitinated aggregates which gets stabilized, at least partly, due to inhibition of autophagy. However, the hypothesis that Serf acts to promote assembly of protein complexes, may be by a chaperone like activity might explain its antagonistic effect on UPS and autophagy mediated degradation of proteins. It is thought that amyloid assembly is an active homeostatic response to increased load of misfolded proteins that induces autophagy for the subsequent clearance of the terminal aggregates (Williams,

Jahreiss et al. 2006, Rubinsztein, Gestwicki et al. 2007) (Kaganovich et al. 2009; Watanabe et al. 2011). So, Serf driven amyloid aggregation under disease condition or assembly of functional protein complexes under normal condition might relate to autophagy induction. In fact larger multiprotein complexes are required to be formed at different steps in the autophagy pathway (Levine & Klionsky, 2004) where Serf function could be important. On the other hand, inhibition of proteasome function has been shown to increase the accumulation of amyloid complexes (Wooten et al. 2006). Since Serf promotes aggregate formation, it might have a negative impact on UPS activity. So, in effect my hypothesis is that Serf promotes assembly of protein complexes that counteracts UPS while inducing autophagy that acts, at least in part, to remove protein aggregates from tissues and extend lifespan.

Increasing pool of studies are pointing at the integration of the two apparently disparate cellular proteolytic pathways- the UPS and autophagy. For instance, pharmacological inhibition of the proteasome has been shown to induce compensatory increase in the autophagic pathway (Du et al. 2009; Zhu et al. 2010, Pandey et al. 2007). There are co-chaperone and adaptor molecules like CHIP, BAG and p62 proteins that are known to interact with both pathways and determine the fate of the substrate proteins for degradation through one pathway versus the other (Shin et al. 2005; Gamerdinger et al. 2011; Wooten et al. 2006). In addition, cellular processes like the unfolded protein response in the ER has been shown to suppress UPS activity and favor autophagic pathway (Ding et.al, 2007). Therefore, it is not hard to imagine that cellular function of Serf might antagonistically affect UPS and autophagy. Future determination of how Serf

functions at a biochemical level may enrich our understanding of how autophagy and UPS are coordinated within the cell.

6.3 Limitations and future prospects

SERF, the phylogenetically highly conserved gene, when deleted in *Drosophila* is phenotypically benign. Loss of function mutants of this non-essential gene are viable through all developmental stages. This is not unusual, however, as only about 3600 genes out of approximately 17000 annotated genes (21.17%) in the *Drosophila* genome are projected to be essential for viability (Brizuela, Elfring et al. 1994, Miklos and Rubin 1996). One reason for the non-essential role of a gene in an organism is functional redundancy. Whether loss of *Serf* function is compensated in flies is not known, but two other Serf like proteins are encoded by fly genome. These two proteins are encoded by two adjacent genes CG18081 and CG15715 on chromosome 3L (Fig 6.2A). Their biological functions are not known. These two proteins contain C-terminal zinc finger domain and similar proteins are also found in humans and *C. elegans*. At least the human Serf-like protein named ZNF706 or HSPC038 has been shown to physically interact with a chloride channel protein ICln and is speculated to direct its membrane translocation in response to cell swelling necessary for the regulation of cell volume (Dossena, Gandini et al. 2011). Figure 6.1 shows the multiple sequence alignment of these Serf like proteins from human, *C. elegans*, *Drosophila* together with Serf proteins from different organisms.

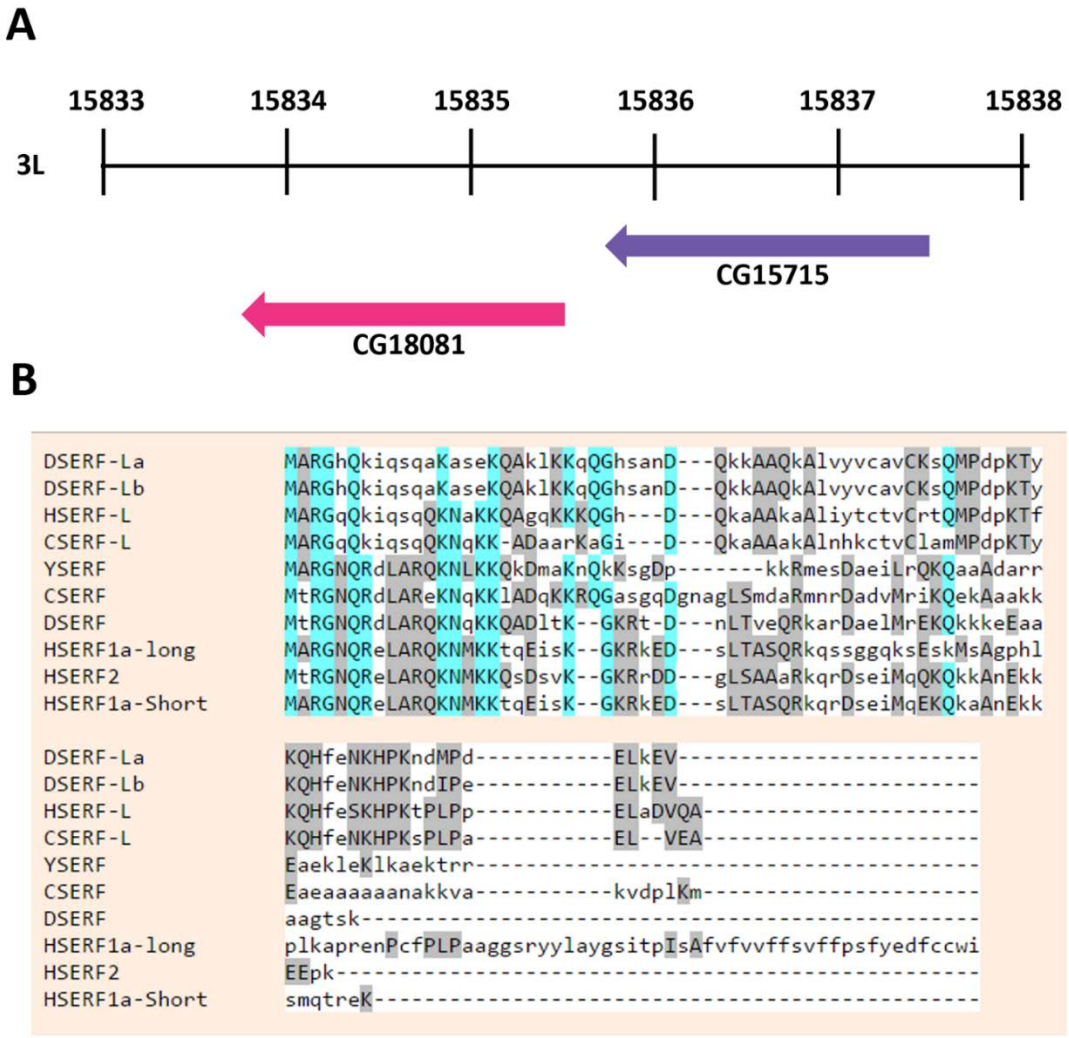

Fig: 6.2 The Serf like genes. A) The Genetic locus of the Serf like genes CG18081 and CG15715. The genes are located on the left arm of chromosome 3 (3L). The scale presented here correspond to the molecular map of chromosome 3L. B) Multiple sequence alignment of Serf like proteins and Serf from different organisms using Muscle multiple alignment program. Y=yeast, D=*Drosophila*, C=*C. elegans*, H= human; the –L designation is for Serf-like, a: CG18081 and b: CG15715.

Both of these proteins show similar level of homology with the *Drosophila* Serf protein (65% similarity and 43% identity within 29% query coverage), the human SERF1a

longer isoform (55% similarity and 32% identity within 32% query coverage) and the SERF2 protein (68% similarity and 43% identity within 38% percent covered alignment). Therefore, we cannot rule out the possibility that there could be certain levels of functional overlap between Serf and these Serf like proteins compensating for the impact of loss of Serf. However, both the proteins show differences in the highly conserved N-terminal region of the Serf protein. They also show only low level of homology with the shorter isoform of the Serf protein (aligns with only 11% of the human Serf shorter isoform) which is more commonly found among species. Therefore, these two genes cannot be considered as the human *Serf* homologue in flies.

My study, being the first line of investigation on Serf function in any model system, provides information about a variety of phenotypes. Although non-essential for viability, I have shown that Serf activity in flies is necessary for normal locomotor function, adult lifespan and survival under oxidative stress. The mechanisms behind the manifestations of lack or excess amount of Serf is not clearly understood. For instance, whether abnormality in the neuronal, muscular or neuromuscular junction properties underlie the climbing deficiency in *Serf* deletion flies is not known. My data points to the possibility that accelerated muscle aging could be responsible partly for the loss of muscle activity and climbing deficiency in the *Serf* deletion flies. However, whether Serf is directly affecting neuronal and muscle activity or has a more direct influence on the sensory function are still open questions. Furthermore, we do not know if these activities contribute to maintaining normal lifespan or survival under stress. My preliminary attempt to get mechanistic understanding of Serf's effect on longevity pointed at the autophagy pathway modulation as a potential basis for the altered tissue aging and

lifespan in *Serf* deletion and overexpression flies. In order to find out the degree to which autophagy contributes to Serf mediated life span extension further experiments need to be done. It would be informative to know if inhibiting autophagy pathway (Li, Hou et al. 2009; Denton, Shravage et al. 2009) abrogates Serf's life extending impact, for instance. In addition to autophagy, my data have also implied potential Serf dependent changes in the mitochondrial structure and function pertinent to lifespan determination and oxidative stress response. The finding that the mitochondrial marker protein Mfn is stabilized in the long lived flies with excess Serf is intriguing since the level of Mfn is indicative of the degree of mitochondrial fusion versus fission and determine the structure of cellular mitochondrial network (Detmer & Chan 2007). It is very likely therefore that cells with altered level of Serf would have alteration in the mitochondrial dynamics and the resulting morphology. Whether this is true and how that relates to functional changes in the cellular activity and organismal lifespan, requires future experimentation. Given that the mitochondrial quality control (MQC) is governed by both UPS and autophagy pathways (Twig, Hyde et al. 2008; Taylor & Rutter 2011) it will be very interesting to know whether Serf activity influences MQC to modulate organismal survival under normal and oxidative stress condition.

My study has generated a refined hypothesis about cellular function of Serf. The idea that Serf promotes assembly of protein complexes like a molecular chaperone/cofactor which induces autophagy and counteracts UPS activity demands rigorous experimental testing. In the context of SMA the first essential thing to test is whether Serf influences SMN complex formation by promoting SMN-SMN interaction or interaction with other partners like Gemins. A cell culture based approach where differentially tagged SMN

proteins could be co-immuno-precipitated with itself or with Gemins (Praveen et al. 2014), with and without Serf knocked down, can be used to address the question. This is an important question to address for a complete understanding of the genetic interaction between Serf and SMN. In addition, I proposed that destabilization of SMN and α-synuclein in absence of Serf requires proteasome. If this is true, pharmacological inhibition of proteasome (Belozerov, Ratkovic et al. 2014) in absence of Serf should stabilize both proteins. How Serf activity relates to autophagy induction is a harder question to answer. Specifically whether Serf driven protein complex assembly induces autophagy would be difficult to test. One way could be using a Serf deletion protein toxicity disease background where inclusion formation is inhibited and test the level of autophagy gene expression as a marker for basal level autophagy as compared to when Serf activity is intact. Relative to a completely normal animal, inclusion forming model should have upregulation of autophagy genes when Serf is wild type. However when Serf is deleted and inclusion formation is abrogated, relative level of autophagy would decrease in these animals. This would be supportive of the idea that autophagy induction is a homeostatic response to inclusion formation and when Serf deletion reduces inclusion formation the autophagic response is also inhibited. Although, it is important to remember that multi-protein complexes are involved in autophagy pathway and Serf might influence it directly to modulate the pathway. Therefore, my findings and their implications with regard to Serf's involvement in autophagy clearly opens up a variety of avenues for further research.

The studies related to Serf's role in protein toxicity diseases in flies were limited in my dissertation. Although preliminary, but the data are consistent with the notion that Serf in

flies might modulate neuro-toxicity diseases. A variety of these amyloid diseases have been successfully modelled in the fly system. Using my Serf deletion, overexpression or knockdown fly models, one could test if Serf has a general role in modifying these diseases for a better understanding of the conserved nature of such predicted function. In conclusion, it is evident that our understanding about the natural function of Serf and the molecular basis for its SMA modifying effect is far from complete. Further investigation about Serf function has a lot of potential to increase our understanding about different aspects of cellular processes involved in the pathogenesis of human diseases.

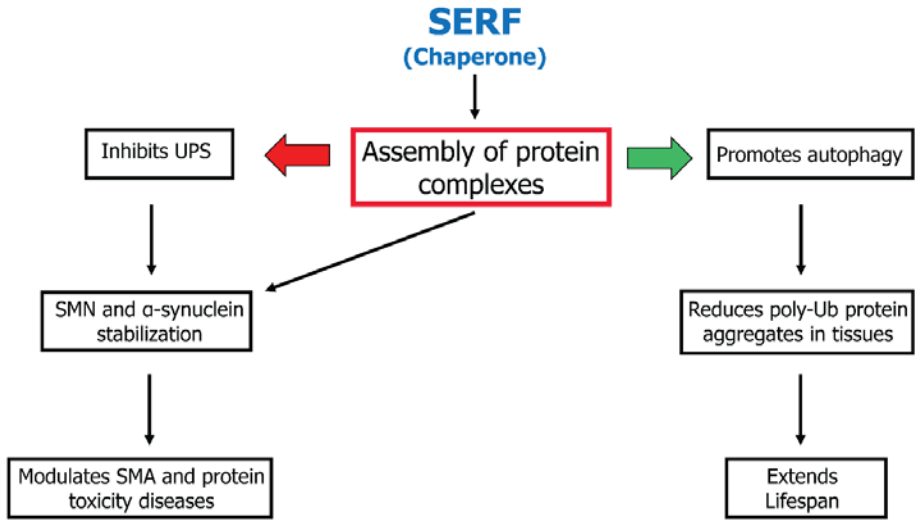

Fig 6.3 A Model for cellular function of Serf. Based on our analysis of Serf in Drosophila melanogaster and previous knowledge it is proposed that Serf protein functions like a chaperone in cell to promote the assembly of larger protein complexes. This process is thought to positively impact autophagy mediated protein turnover, which is, at least partly, responsible for reducing the natural accumulation of poly-ubiquitinated proteins in aging tissues and extend lifespan. On the other hand, protein complex assembly might counteract UPS activity and help to stabilize specific proteins like SMN

and α-synuclein thereby modifying SMA and Parkinson's disease (protein toxicity diseases).

Table 6.1 List of SMA modifier genes (Dimitriadi et.al, 2010).

***Ce* Gene**	***Dm* Gene**	***Hs* Gene**	**Change/Affect *Ce***	**Change/Affect *Dm***
Plst-1	*Fim*	Plastin 3 (*PLS3*)	RNAi/Cmpx Gr, Enh pump	Lof/Enh
daf-4	*Wit*	TGFβ Receptor (*BMPRII*)	RNAi/Enh Pump	Lof/Enh
kcnl-2	*SK*	SK Channel (*KCNN3*)	RNAi/Enh Gr, Sup Pump	Lof/Enh
nhr-25	*Usp*	NHR LRH-1 (*NR5A2*)	RNAi/Sup Pump	OE/Enh
uso-1	*p115*	Vesicle docking (*USO1*)	RNAi/Enh Gr	OE/Sup
nhr-85	*Eip75B*	NHR RevErb (*NR1D2*)	RNAi/Enh Gr	Lof/Enh
atf-6	*Atf6*	Atf6 trans. Factor (*ATF6*)	RNAi/Enh Gr	?/Sup
egl-15	*Btl*	FGF receptor (*FGFR3*)	RNAi/Enh Gr	Lof/Enh
ape-1	CG18375	p53 inhibition (PPP1R13)	RNAi/Enh Gr	?/Enh
nekl-3	*Nek2*	NIMA Family Kinase (*NEK7*)	RNAi/Enh Gr	OE/Sup
atn-1	*Actinin*	a-actinin (*ACTN*)	RNAi/Sup Gr	OE/Enh
cash-1	*CG33172*	Striatin (*STRN*)	RNAi/Cmpx Gr	Lof/Enh
dlc-1	*Cut up*	Dynein light chain (*DYNLL2*)	RNAi/Cmpx Gr	Lof/Sup
ncbp-2	*CBC20*	Cap binding (*CBP20*)	RNAi/Enh Gr & Pump	Lof/Enh
grk-2	*Gprk*	GRK Kinase (*ADRBK1*)	RNAi/Enh Gr & Pump	nd
flp-4	*FMRF*	Neuropeptide (*NPFF*)	RNAi/Enh Gr	Lof/Enh
T02G5.3	none	none	RNAi/Enh Gr, Sup Pump	nd

The list is divided into three sections corresponding to SMA modifiers identified originally in humans, *Drosophila* and *C. elegans.* The species and the gene names are indicated in first three columns. The effect of RNAi mediated knockdown of the genes in *C. elegans* are indicated in column 4. The effect of changes in the gene expression in *Drosophila* transposon insertion lines are mentioned in column 5. RNAi: RNAi knockdown; Lof: Loss of function, decreased function or antisense; OE: overexpression, ?: Unclear; Enh: Enhanced *Smn* loss of function defects; Sup: Suppressed *Smn* loss of function defects; Cmpx: Complex genetic interaction; nd: Not determined. Column 4 includes *C. elegans* assays used to test SMA modifier activity- Gr: Growth defect; Pump: Pharyngeal pumping activity defect.

Table 6.2 A: Insertion mutants of *Drosophila* that enhances *Smn^{73A0}* dependent lethality, adopted from Chang et.al 2008.

Enhancers			
Exelixis insertion	**Corresponding gene(s)**	**Gene Name (Symbol)**	**Annotated function of the human homolog**
d00712	CG4376	*a-actinin (Actn)*	F actin binding protein
	CG4380	*ultraspiracle (usp)*	Nuclear hormone receptor
	CG4325	NA	Contains a ring domain
d03336	CG10706	*small conductance calcium activated potassium channel (SK)*	Calcium dependent K+ channel
d04197	CG32796	*brother of iHog (boi)*	Binds and mediates response to hedgehog
	CG33950	*terribly reduced optic lobes (trol)*	Neuroblast proliferation
d05295	CG34414	*sprint (sprint)*	Ras GTPase binding
f01369	CG6414	N/A	Contains Esterase lipase domain
f04448	CG33172	N/A	Contains WD repeats
f05849	CG1835	N/A	Localized to the preacrosome regions of spermatids
d00698	CG17323	N/A	Glucronosyltransferase
	CG17322	N/A	Glucronosyltransferase
	CG17324	N/A	Glucronosyltransferase
d05779	CG18375	N/A	p53 binding protein apoptosis
d00985	CG34379	N/A	F actin binding
	CG8589	N/A	Nucleic acid binding
f04249	CG11450	*net*	Transcription factor

Table 6.2A Continued.

d02492	CG10776	*wishful thinking (wit)*	BMP type II receptor
d09170	CG5361	N/A	Alkaline phosphatase
	CG6203	*(Fmr1)*	mRNA binding
d09801	CG8127	*Ecdysone-induced protein 75B (Eip75B)*	Nuclear hormone receptor
f02477	CG1927	N/A	N/A
f06201	CG1927	N/A	N/A
f02864	CG32134	*breathless (btl)*	FGF receptor

Table 6.2B The *Drosophila* insertion mutants that suppressors of Smn73Ao dependent lethality, adopted from Chang et.al 2008.

Supressors			
Exelixis insertion	**Corresponding gene(s)**	**Gene Name (Symbol)**	**Annotated function of the human homolog**
D00184	CG4320	*raptor*	mTOR binding protein
	CG4717	*Multiple inositol polyphosphate phosphatase 2 (Mipp2)*	Phosphatidyl inositol phosphatase
	CG5905	*Neprilysin 1 (Nep1)*	Metalloendopeptidase
E02369	CG10701	*Moesin* (Moe)	Cytoskeleton association
D03478	CG17256	*Nek2*	Mitosis/meiosis, cell cycle
	CG1422	*p115*	Protein transport, vesicle docking
F02345	CG6998	*cut up*	Cytoskeleton motor
D10763	CG1697	*rhomboid-4 (rho-4)*	EGK signaling activation
	CG1561	N/A	Contains a kinase domain
C05057	CG3136	*Atf6*	Transcription factor responsive to ER stress
D02302	CG11200	N/A	Calbonyl reductase (NADPH)
	CG8920	N/A	Tudor domain/nucleic acid binding
	CG13868	N/A	N/A

Table 6.2B Continued.

E00818	CG12214	N/A	Tubulin polymerization
F05549	CG13775	N/A	GTPase activity
F06260	CG10561	N/A	Polyamine oxidase

For both tables (6.2A and 6.2B), gene assignments are ambiguous in some cases due to the site of transposon insertion. ‘d’ or ‘f’ designated strains represent GAL4 inducible lines; ‘c’ or ‘e’ designated strains are not GAL4 inducible. *Drosophila* candidate SMA modifier genes, respective human homologues and their annotated functions are depicted in columns 2, 3 & 4 of tables 6.2A & B.

APPENDIX

A hyper-phosphorylated form of Smn protein appears to accumulate in the *Serf* deletion mutant.

The Smn protein is known to be post translationally modified by phosphorylation (Bella, V.L. 2004, Biochemical and Biophysical Research communications) and Smn phosphorylation by enzyme Protein Kinase A (PKA) is known to regulate its complex formation (Burnett, B.G. 2009, Mol Cell). In our western blot assays for Smn protein, we observed a smeary doublet pattern that varied between genotypes. To address this, I used alkaline Lambda phosphate to investigate which bands were sensitive to dephosphorylation and how the phosphorylation pattern may differ in the presence of absence of Serf. This assay was performed on Smn protein extracted from adult flies.

The *Serf* deletion mutant (*Serf*Δ*10a*) and the precise excision control (PE26B) flies were used to extract protein under non-denaturing condition (0.1% NP40, 1X protease inhibitor cocktail in 1X PBS, 20ul extraction buffer per fly), either in presence or absence of a phosphatase inhibitor mix (10mM sodium orthovandate+50mM Sodium fluoride). 200 units of Lambda PP enzyme was used to treat 40 ul of protein extract in 50ul reaction mix (1X NEBuffer for PMP, 1mM $MnCl_2$) for 45 minutes at 30℃. Western blotting of the Smn protein was used to monitor the effect of phosphatase treatment on band migration (mouse monoclonal anti-Smn antibody- a generous gift from Dr. Anindya Sen, UMASS, 1:1000 dilution and alkaline phosphatase conjugated goat anti-mouse secondary, 1:5000

dilution, Life Technologies; Amersham™ ECF substrate for western blotting, GE Healthcare, Life Sciences).

Figure 1 shows that the Smn protein forms a doublet of two very closely migrating bands where the upper band is predominant in both the wild type and *Serf* deletion lines. It is important to mention here that such a banding pattern is not typically seen in the literature, where an affinity purified rabbit anti-fly Smn antibody (Rajendra et.al, 2007; Praveen et.al 2014) has been used instead of the mouse monoclonal anti-fly Smn antibody used in this study. The mouse monoclonal anti-fly Smn antibody (Chang et.al 2008) has only been used in tissue immunostaining experiments before. Smn protein from the *Serf* deletion mutant (SerfΔ10a: lanes 3,4,7 & 8), however, shows slightly different banding pattern compared to the precise excision control (PE26B: lanes 1, 2, 5 & 6). In the *Serf* deletion line, both the upper and lower bands of Smn migrate slightly slower compared to the bands observed in the wild type sample (compare lanes 1-3 and 5-7 where 1 & 5 represents wild type and 3&7 represents *Serf* deletion). Upon Lambda PP treatment, the Smn bands are re-distributed almost equally between the upper and lower bands for both the genotypes (compare 5-6 for wild type and 7-8 for *Serf* deletion where 5 & 7 represents samples before treatment and 6 & 8 represents samples after phosphatase treatment). In addition, the enzyme treatment also causes the Smn bands in the precise excision control and the Serf deletions to co-migrate (Compare 8-9 where 8 represents Serf deletion and 9 precise excision, both enzyme treated). This effect of phosphatase treatment is abolished when the protein extracts contain phosphatase inhibitor (compare 1-2 for wild type and 3-4 for *Serf* deletion where 1 & 3 represents samples before treatment and 2& 4 represents samples after phosphatase treatment)

confirming the alterations in Smn banding observed in presence of phosphatase is specifically due to the presence of this enzyme.

These data show that the slightly upward shift of Smn bands in the *Serf* deletion mutant is due to phosphorylation. In addition, consistent with our previous observation, based on mass loading, I observe reduced levels of Smn protein in the *Serf* deletion line compared to the precise excision control. Both the reduced abundance and the mobility shift of Smn protein observed in the *Serf* mutant line could be restored upon *Serf* cDNA expression in the mutant line (Chapter 5, Fig. 5.9A). Therefore, hyper-phosphorylation of Smn observed in the Serf deletion background may reflect a change other than total Serf abundance.

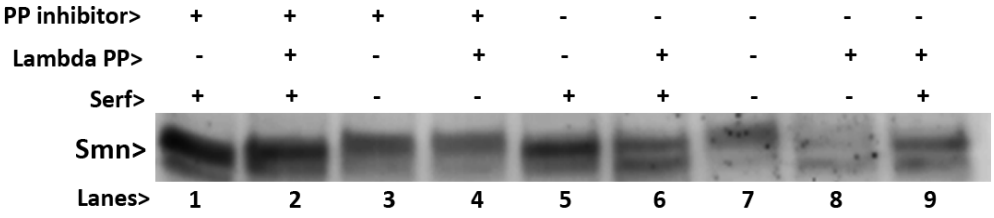

Figure A-1. Phosphatase treatment changes the banding pattern on *Smn* in *Drosophila*. Analysis of Smn protein with mouse anti-Smn antibody in adult whole fly extracts, prepared in presence or absence of phosphatase inhibitor. Western blot image shows the effect of Lambda protein phosphatase (Lambda PP) treatment in fly extracts with and without wild type Serf.

The detection of Smn-EYFP - Smn protein interaction is inefficient and inconsistent by co-immunoprecipitation.

Since Smn certain Smn mutations are known to influence oligomerization (and hence Smn stability), I attempted to assay Smn-Smn interaction by co-immuno precipitation.

Smn-EYFP expressing flies with wild type, enhanced and reduced levels of Serf were assayed. (lysis/binding buffer-50 mM Tris-HCl pH 8.5, 150 mM Nacl, 1% NP-40 and 1X protease inhibitor cocktail, 100 flies in 1 ml buffer). About 3 mg total protein (300µl) was used to incubate with 100 µl antibody-bound protein-A agarose beads (6 µg mouse anti-GFP 4C9 antibody, Developmental Studies Hybridoma Bank, per 300 µl beads in) at 4°C for overnight. The beads were precipitated (4000 rpm for 2 mins) and supernatant saved as unbound fraction. After washing the beads for 5 times with the same buffer (1 ml each), the antibody precipitated protein complexes were extracted in 120µl of 1X SDS sample buffer (bound fraction). 10% of the total and unbound fraction and 30% of the bound fraction were used for western blot. Protein fractions were separated in 7.5% SDS PAGE for visualizing the SMN-EYFP fusion protein (mouse anti-GFP 4C9 antibody, DSHB,1:10,000 dilution) and 10% SDS PAGE for assessing the endogenous Smn protein (mouse monoclonal anti-Smn antibody 1:1000 dilution). Alpha tubulin in each fraction was detected as an internal control (mouse monoclonal α-tubulin, 1:1000 dilution; DSHB-12G10 anti-alpha tubulin).

Figure 2A & B shows the results of the assay, done with overexpression and knockdown of *Serf*, respectively. Flies expressing Smn-EYFP with wild type Serf serve as the control for both experiments. In both the experiments considerable proportion of the Smn-EYFP protein (that corresponds to the band which is absent in case of the non-Smn-GFP negative control) was precipitated as shown in the anti-GFP blot. The level of Smn-EYFP protein found in the bound fraction (30% bound fractions presented) is equivalent with that in the total fraction (10% total protein presented) for the *Serf* overexpression group (Fig 2A, compare lanes 2-5 and 3-6, where 2 & 3 represents total

protein and 5 & 6 represents bound fraction) as well as *Serf* knockdown group (Fig 2B, compare lanes 2-5 and 3-6, where 2 & 3 represents total protein and 5 & 6 represents bound fraction). This also suggests that approximately 1/3rd of the total Smn-EYFP protein got precipitated in both the experiments. The unbound fractions (Fig. 2A and 2B-lanes 7, 8, 9 for both) also show obvious de-enrichment of the Smn-EYFP protein, suggesting that most of the fusion protein got precipitated.

The anti-Smn blots show the band corresponding to the endogenous Smn protein but not the fusion protein, because the upper portion of the blot containing higher molecular weight Smn-EYFP was cut off. The total and unbound fractions from both the experiments show equivalent amount of endogenous Smn except for the wild type control in the knockdown group show reduced level of Smn in the unbound fraction (Fig 2A and 2B, compare lanes 1-7, 2-8 and 3-9 where 1, 2, 3 represent total protein fractions and 7,8 and 9 represent unbound protein fractions). The upward shift of the endogenous Smn band usually observed with Serf depletion (Appendix figure 1) is also not seen in Smn-EYFP expressing flies with *Serf* knockdown. The Smn protein observed in the bound fraction would indicate the fraction of the endogenous Smn that co-precipitates with Smn-EYFP fusion. In case of the overexpression group I identified a minor band specific to the Smn-EYFP expressing flies (Fig. 2A, lanes 5 and 6) showing that a very small proportion of endogenous Smn precipitated with the EYFP fused Smn. As predicted for flies with Serf overexpression with normal level of Smn, the co-precipitated fraction of Smn was roughly equivalent between the overexpression and the wild type control. However, for the *Serf* knockdown group, I could not specifically detect a band corresponding to the endogenous Smn in the bound fractions of the GFP expressing lines

(Fig. 2B, lanes 4,5 & 6). Therefore, I could not determine if knockdown of Serf alters in-vivo Smn-Smn self-interaction in this assay.

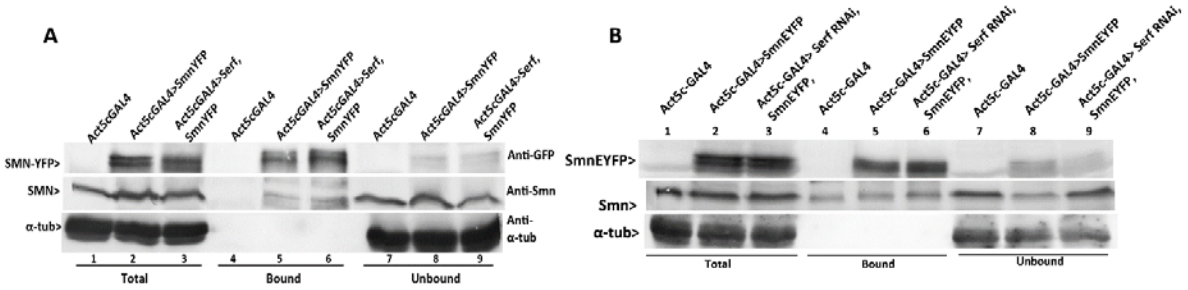

Fig. A-2. Co-immuno precipitation of Smn from Smn-EYFP expressing fly extract with wild type, enhanced or reduced levels of Serf. Anti-GFP, anti-Smn and anti-α-tubulin primary antibodies were used to detect Smn-EYFP fusion, endogenous Smn and α-tubulin protein from the same fractions as indicated below the lanes. A) Smn-EYFP flies with Serf knockdown were compared with wild type and no-GFP controls. B) Smn-EYFP flies with Serf overexpression were compared with wild type and no-GFP controls.

Altered levels of Serf might modify the neuromuscular defect of *Smn* mutants.

Imlach et.al has shown that a Smn null mutant has aberrant neurotransmitter release at the larval neuromuscular junction (NMJ). Stimulation of the motor neuron innervating the 6th muscle of the 3rd segment of 3rd instar *Smn* mutant larvae shows significant increase in the evoked excitatory post synaptic potential (EPSP) (Imlach W.L. 2012 Cell). This finding is consistent with a presynaptic change in the neurotransmitter release from the motor neurons of the NMJs of Smn mutants (Imlach W.L. 2012 Cell). I wanted to know if *Serf* mutants show similar aberration in neuromuscular function. In addition, I seeked to learn if altered Serf levels in Smn mutants modifies the larval NMJ phenotype.

We measured the evoked EPSPs at the larval NMJ according to the protocol described by Imlach et.al, 2012; Imlach & McCabe 2009. Figure 3A shows the average EPSPs from larvae that express the various *Serf* alleles. I find that the *Serf* overexpression (Act5c-GAL4>Serf) and *Serf* deletion (*Serf*Δ*10a*) larvae show average EPSPs very similar to the Act5c-GAL4 control, however, the *Serf* knockdown larvae (Act5c GAL4> Serf RNAi) show a significant increase in EPSP response (P=.03, n=10), similar to the *Smn* mutants. Although, the *Serf* deletion larvae behave differently than the knockdown larvae it is important to note that the *Serf* deletions were not compared with their isogenic precise excision control PE26B. Without this comparison we cannot conclude whether the *Serf* deletion larvae truly behave like wild type or not. If this is true, then the aberration in the knockdown line might have resulted from potential off-target effect of the RNAi construct or it is possible that the null allele shows an adaptation response to the altered neuromuscular activity that might occur due to loss of Serf.

When the hypomorphic Smn^{E33} homozygous and hemizygous (Smn^{E33}/Smn^{73Ao}, where Smn^{73Ao} is a null allele) larvae were tested, they exhibited the anticipated increased evoked EPSPs at their NMJ (Fig. 3B), consistent with the previous report (Imlach et.al 2012). Ubiquitous overexpression of *Serf* in the Smn^{E33} larvae did not impact this phenotype (Fig. 3B), however, knockdown of *Serf* in the hemizygous Smn^{E33} larvae (Act5c-GAL4>*Serf* RNAi, Smn^{E33}/Smn^{73Ao}) reverted their EPSPs back to the normal level (P=.03, n=10). This suppression of NMJ defect by *Serf* knockdown in the Smn mutants is difficult to understand, especially when flies with *Serf* knockdown by itself appears to increase the EPSP response. Nonetheless, this observation might reflect a complex genetic interaction between *Serf* and *Smn* to modify the neuromuscular junction

properties when Serf is lost and Smn levels are presumably further reduced. Additional work is required to better understand this issue.

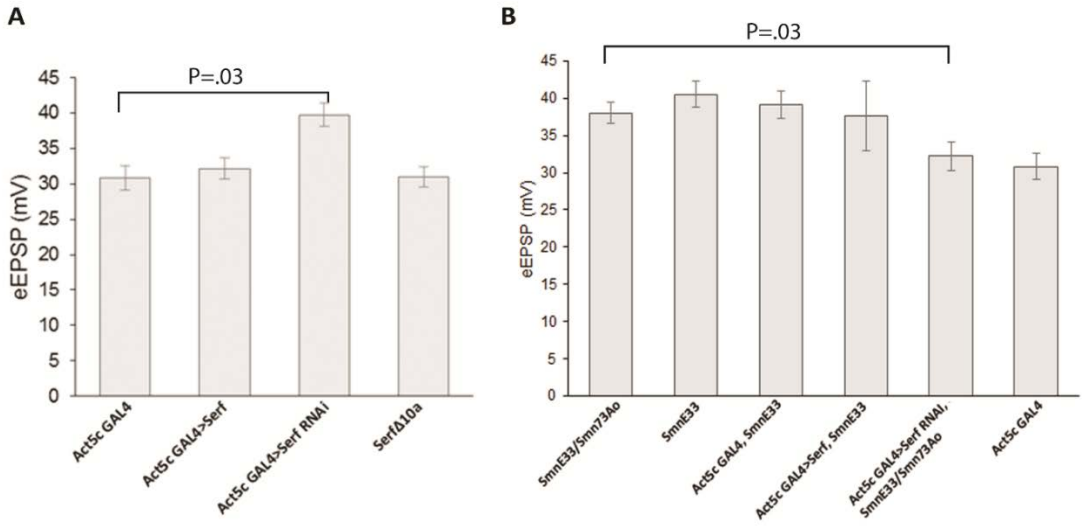

Figure A-3. The *Smn* and *Serf* mutants display aberrant EPSPs at the larval NMJ. Wandering 3rd instar stage larvae containing various *Serf* and *Smn* alleles (n=10 for each genotype) were used for measuring voked EPSPs at the 6th muscle of their 3rd body segment. A) Average EPSPs from *Serf* overexpression (Act5c GAL4> *Serf*), knockdown (Act5c GAL4> *Serf* RNAi) and null larvae (*SerfΔ10a*) are compared with a wild type (Act5c-GAL4) driver only control. Statistical significance values as measured by two tailed Student's t-test are indicated for genotypes being compared. B) Average EPSPs from Smn^{E33} homozygous (Smn^{E33}) and hemizygous (Smn^{E33} / Smn^{73Ao}) larvae were measured and compared with when *Serf* is overexpressed (Act5c GAL4> *Serf*, Smn^{E33}), and knocked down (Act5c GAL4> *Serf* RNAi, Smn^{E33} / Smn^{73Ao}) in them. Statistical significance value, as measured by two tailed Student's t-test, is indicated for genotypes being compared.

References:

Ackermann, B., S. Krober, L. Torres-Benito, A. Borgmann, M. Peters, S. M. Hosseini Barkooie, R. Tejero, M. Jakubik, J. Schreml, J. Milbradt, T. F. Wunderlich, M. Riessland, L. Tabares and B. Wirth (2013). "Plastin 3 ameliorates spinal muscular atrophy via delayed axon pruning and improves neuromuscular junction functionality." Hum Mol Genet **22**(7): 1328-1347.

Alias, L., S. Bernal, M. J. Barcelo, E. Also-Rallo, R. Martinez-Hernandez, F. J. Rodriguez-Alvarez, C. Hernandez-Chico, M. Baiget and E. F. Tizzano (2011). "Accuracy of marker analysis, quantitative real-time polymerase chain reaction, and multiple ligation-dependent probe amplification to determine SMN2 copy number in patients with spinal muscular atrophy." Genet Test Mol Biomarkers **15**(9): 587-594.

Arnold, W. D. and A. H. Burghes (2013). "Spinal muscular atrophy: development and implementation of potential treatments." Ann Neurol **74**(3): 348-362.

Ashrafi, G. and T. L. Schwarz (2013). "The pathways of mitophagy for quality control and clearance of mitochondria." Cell Death Differ **20**(1): 31-42.

Avila, A. M., B. G. Burnett, A. A. Taye, F. Gabanella, M. A. Knight, P. Hartenstein, Z. Cizman, N. A. Di Prospero, L. Pellizzoni, K. H. Fischbeck and C. J. Sumner (2007). "Trichostatin A increases SMN expression and survival in a mouse model of spinal muscular atrophy." J Clin Invest **117**(3): 659-671.

Baccon, J., L. Pellizzoni, J. Rappsilber, M. Mann and G. Dreyfuss (2002). "Identification and characterization of Gemin7, a novel component of the survival of motor neuron complex." J Biol Chem **277**(35): 31957-31962.

Baughan, T., M. Shababi, T. H. Coady, A. M. Dickson, G. E. Tullis and C. L. Lorson (2006). "Stimulating full-length SMN2 expression by delivering bifunctional RNAs via a viral vector." Mol Ther **14**(1): 54-62.

Becker, J., O. Semler, C. Gilissen, Y. Li, H. J. Bolz, C. Giunta, C. Bergmann, M. Rohrbach, F. Koerber, K. Zimmermann, P. de Vries, B. Wirth, E. Schoenau, B. Wollnik, J. A. Veltman, A. Hoischen and C. Netzer (2011). "Exome sequencing identifies truncating mutations in human SERPINF1 in autosomal-recessive osteogenesis imperfecta." Am J Hum Genet **88**(3): 362-371.

Bellare, P., A. K. Kutach, A. K. Rines, C. Guthrie and E. J. Sontheimer (2006). "Ubiquitin binding by a variant Jab1/MPN domain in the essential pre-mRNA splicing factor Prp8p." RNA **12**(2): 292-302.

Bellare, P., E. C. Small, X. Huang, J. A. Wohlschlegel, J. P. Staley and E. J. Sontheimer (2008). "A role for ubiquitin in the spliceosome assembly pathway." Nat Struct Mol Biol **15**(5): 444-451.

Bellen, H. J., R. W. Levis, Y. He, J. W. Carlson, M. Evans-Holm, E. Bae, J. Kim, A. Metaxakis, C. Savakis, K. L. Schulze, R. A. Hoskins and A. C. Spradling (2011). "The Drosophila gene disruption project: progress using transposons with distinctive site specificities." Genetics **188**(3): 731-743.

Bjorkoy, G., T. Lamark, A. Brech, H. Outzen, M. Perander, A. Overvatn, H. Stenmark and T. Johansen (2005). "p62/SQSTM1 forms protein aggregates degraded by autophagy and has a protective effect on huntingtin-induced cell death." J Cell Biol **171**(4): 603-614.

Bokov, A., A. Chaudhuri and A. Richardson (2004). "The role of oxidative damage and stress in aging." Mech Ageing Dev **125**(10-11): 811-826.

Brichta, L., Y. Hofmann, E. Hahnen, F. A. Siebzehnrubl, H. Raschke, I. Blumcke, I. Y. Eyupoglu and B. Wirth (2003). "Valproic acid increases the SMN2 protein level: a well-known drug as a potential therapy for spinal muscular atrophy." Hum Mol Genet **12**(19): 2481-2489.

Briese, M., B. Esmaeili, S. Fraboulet, E. C. Burt, S. Christodoulou, P. R. Towers, K. E. Davies and D. B. Sattelle (2009). "Deletion of smn-1, the Caenorhabditis elegans ortholog of the spinal

muscular atrophy gene, results in locomotor dysfunction and reduced lifespan." Hum Mol Genet **18**(1): 97-104.
Brizuela, B. J., L. Elfring, J. Ballard, J. W. Tamkun and J. A. Kennison (1994). "Genetic analysis of the brahma gene of Drosophila melanogaster and polytene chromosome subdivisions 72AB." Genetics **137**(3): 803-813.
Brzustowicz, L. M., T. Lehner, L. H. Castilla, G. K. Penchaszadeh, K. C. Wilhelmsen, R. Daniels, K. E. Davies, M. Leppert, F. Ziter, D. Wood and et al. (1990). "Genetic mapping of chronic childhood-onset spinal muscular atrophy to chromosome 5q11.2-13.3." Nature **344**(6266): 540-541.
Burghes, A. H. (1997). "When is a deletion not a deletion? When it is converted." Am J Hum Genet **61**(1): 9-15.
Burglen, L., S. Lefebvre, O. Clermont, P. Burlet, L. Viollet, C. Cruaud, A. Munnich and J. Melki (1996). "Structure and organization of the human survival motor neurone (SMN) gene." Genomics **32**(3): 479-482.
Burnett, B. G., E. Munoz, A. Tandon, D. Y. Kwon, C. J. Sumner and K. H. Fischbeck (2009). "Regulation of SMN protein stability." Mol Cell Biol **29**(5): 1107-1115.
Butchbach, M. E., J. Singh, M. Thorsteinsdottir, L. Saieva, E. Slominski, J. Thurmond, T. Andresson, J. Zhang, J. D. Edwards, L. R. Simard, L. Pellizzoni, J. Jarecki, A. H. Burghes and M. E. Gurney (2010). "Effects of 2,4-diaminoquinazoline derivatives on SMN expression and phenotype in a mouse model for spinal muscular atrophy." Hum Mol Genet **19**(3): 454-467.
Cai, J., D. Ash, L. E. Kotch, E. W. Jabs, T. Attie-Bitach, J. Auge, G. Mattei, H. Etchevers, M. Vekemans, Y. Korshunova, R. Tidwell, D. N. Messina, J. B. Winston and M. Lovett (2005). "Gene expression in pharyngeal arch 1 during human embryonic development." Hum Mol Genet **14**(7): 903-912.
Chan, Y. B., I. Miguel-Aliaga, C. Franks, N. Thomas, B. Trulzsch, D. B. Sattelle, K. E. Davies and M. van den Heuvel (2003). "Neuromuscular defects in a Drosophila survival motor neuron gene mutant." Hum Mol Genet **12**(12): 1367-1376.
Chang, H. C., D. N. Dimlich, T. Yokokura, A. Mukherjee, M. W. Kankel, A. Sen, V. Sridhar, T. A. Fulga, A. C. Hart, D. Van Vactor and S. Artavanis-Tsakonas (2008). "Modeling spinal muscular atrophy in Drosophila." PLoS One **3**(9): e3209.
Chang, H. C., W. C. Hung, Y. J. Chuang and Y. J. Jong (2004). "Degradation of survival motor neuron (SMN) protein is mediated via the ubiquitin/proteasome pathway." Neurochem Int **45**(7): 1107-1112.
Chen, B., M. Retzlaff, T. Roos and J. Frydman (2011). "Cellular strategies of protein quality control." Cold Spring Harb Perspect Biol **3**(8): a004374.
Chen, L. and M. B. Feany (2005). "Alpha-synuclein phosphorylation controls neurotoxicity and inclusion formation in a Drosophila model of Parkinson disease." Nat Neurosci **8**(5): 657-663.
Chiti, F. and C. M. Dobson (2006). "Protein misfolding, functional amyloid, and human disease." Annu Rev Biochem **75**: 333-366.
Clancy, D. J., D. Gems, L. G. Harshman, S. Oldham, H. Stocker, E. Hafen, S. J. Leevers and L. Partridge (2001). "Extension of life-span by loss of CHICO, a Drosophila insulin receptor substrate protein." Science **292**(5514): 104-106.
Coady, T. H. and C. L. Lorson (2010). "Trans-splicing-mediated improvement in a severe mouse model of spinal muscular atrophy." J Neurosci **30**(1): 126-130.
Demontis, F. and N. Perrimon (2010). "FOXO/4E-BP signaling in Drosophila muscles regulates organism-wide proteostasis during aging." Cell **143**(5): 813-825.
Demontis, F., R. Piccirillo, A. L. Goldberg and N. Perrimon (2013). "Mechanisms of skeletal muscle aging: insights from Drosophila and mammalian models." Dis Model Mech **6**(6): 1339-1352.
Dent, E. W. and F. B. Gertler (2003). "Cytoskeletal dynamics and transport in growth cone motility and axon guidance." Neuron **40**(2): 209-227.

Dickson, A., E. Osman and C. L. Lorson (2008). "A negatively acting bifunctional RNA increases survival motor neuron both in vitro and in vivo." Hum Gene Ther **19**(11): 1307-1315.
Dimitriadi, M., J. N. Sleigh, A. Walker, H. C. Chang, A. Sen, G. Kalloo, J. Harris, T. Barsby, M. B. Walsh, J. S. Satterlee, C. Li, D. Van Vactor, S. Artavanis-Tsakonas and A. C. Hart (2010). "Conserved genes act as modifiers of invertebrate SMN loss of function defects." PLoS Genet **6**(10): e1001172.
Ding, W. X., H. M. Ni, W. Gao, T. Yoshimori, D. B. Stolz, D. Ron and X. M. Yin (2007). "Linking of autophagy to ubiquitin-proteasome system is important for the regulation of endoplasmic reticulum stress and cell viability." Am J Pathol **171**(2): 513-524.
Dossena, S., R. Gandini, G. Tamma, V. Vezzoli, C. Nofziger, M. Tamplenizza, E. Salvioni, E. Bernardinelli, G. Meyer, G. Valenti, M. Wolf-Watz, J. Furst and M. Paulmichl (2011). "The molecular and functional interaction between ICln and HSPC038 proteins modulates the regulation of cell volume." J Biol Chem **286**(47): 40659-40670.
Duffy, J. B. (2002). "GAL4 system in Drosophila: a fly geneticist's Swiss army knife." Genesis **34**(1-2): 1-15.
Evans, D. S., P. Kapahi, W. C. Hsueh and L. Kockel (2011). "TOR signaling never gets old: aging, longevity and TORC1 activity." Ageing Res Rev **10**(2): 225-237.
Falsone, S. F., N. H. Meyer, E. Schrank, G. Leitinger, C. L. Pham, M. T. Fodero-Tavoletti, M. Holmberg, M. Dulle, B. Scicluna, B. Gesslbauer, H. M. Ruckert, G. E. Wagner, D. A. Merle, E. A. Nollen, A. J. Kungl, A. F. Hill, R. Cappai and K. Zangger (2012). "SERF protein is a direct modifier of amyloid fiber assembly." Cell Rep **2**(2): 358-371.
Fan, L. and L. R. Simard (2002). "Survival motor neuron (SMN) protein: role in neurite outgrowth and neuromuscular maturation during neuronal differentiation and development." Hum Mol Genet **11**(14): 1605-1614.
Feany, M. B. and W. W. Bender (2000). "A Drosophila model of Parkinson's disease." Nature **404**(6776): 394-398.
Feldkotter, M., V. Schwarzer, R. Wirth, T. F. Wienker and B. Wirth (2002). "Quantitative analyses of SMN1 and SMN2 based on real-time lightCycler PCR: fast and highly reliable carrier testing and prediction of severity of spinal muscular atrophy." Am J Hum Genet **70**(2): 358-368.
Figge, M. T., H. D. Osiewacz and A. S. Reichert (2013). "Quality control of mitochondria during aging: is there a good and a bad side of mitochondrial dynamics?" Bioessays **35**(4): 314-322.
Figge, M. T., A. S. Reichert, M. Meyer-Hermann and H. D. Osiewacz (2012). "Deceleration of fusion-fission cycles improves mitochondrial quality control during aging." PLoS Comput Biol **8**(6): e1002576.
Friesen, W. J., S. Paushkin, A. Wyce, S. Massenet, G. S. Pesiridis, G. Van Duyne, J. Rappsilber, M. Mann and G. Dreyfuss (2001). "The methylosome, a 20S complex containing JBP1 and pICln, produces dimethylarginine-modified Sm proteins." Mol Cell Biol **21**(24): 8289-8300.
Fukuto, H. S., D. M. Ferkey, A. J. Apicella, H. Lans, T. Sharmeen, W. Chen, R. J. Lefkowitz, G. Jansen, W. R. Schafer and A. C. Hart (2004). "G protein-coupled receptor kinase function is essential for chemosensation in C. elegans." Neuron **42**(4): 581-593.
Gabanella, F., M. E. Butchbach, L. Saieva, C. Carissimi, A. H. Burghes and L. Pellizzoni (2007). "Ribonucleoprotein assembly defects correlate with spinal muscular atrophy severity and preferentially affect a subset of spliceosomal snRNPs." PLoS One **2**(9): e921.
Ganetzky, B. and J. R. Flanagan (1978). "On the relationship between senescence and age-related changes in two wild-type strains of Drosophila melanogaster." Exp Gerontol **13**(3-4): 189-196.
Garbes, L., M. Riessland, I. Holker, R. Heller, J. Hauke, C. Trankle, R. Coras, I. Blumcke, E. Hahnen and B. Wirth (2009). "LBH589 induces up to 10-fold SMN protein levels by several independent mechanisms and is effective even in cells from SMA patients non-responsive to valproate." Hum Mol Genet **18**(19): 3645-3658.

Garcia, E. L., Z. Lu, M. P. Meers, K. Praveen and A. G. Matera (2013). "Developmental arrest of Drosophila survival motor neuron (Smn) mutants accounts for differences in expression of minor intron-containing genes." RNA **19**(11): 1510-1516.
Giannakou, M. E. and L. Partridge (2007). "Role of insulin-like signalling in Drosophila lifespan." Trends Biochem Sci **32**(4): 180-188.
Glabe, C. G. (2006). "Common mechanisms of amyloid oligomer pathogenesis in degenerative disease." Neurobiol Aging **27**(4): 570-575.
Guarente, L. and C. Kenyon (2000). "Genetic pathways that regulate ageing in model organisms." Nature **408**(6809): 255-262.
Gubitz, A. K., W. Feng and G. Dreyfuss (2004). "The SMN complex." Exp Cell Res **296**(1): 51-56.
Gunadi, T. H. Sasongko, S. Yusoff, M. J. Lee, E. Nishioka, M. Matsuo and H. Nishio (2008). "Hypomutability at the polyadenine tract in SMN intron 3 shows the invariability of the a-SMN protein structure." Ann Hum Genet **72**(Pt 2): 288-291.
Gupta, K., R. Martin, R. Sharp, K. L. Sarachan, N. S. Ninan and G. D. Van Duyne (2015). "Oligomeric Properties of Survival Motor Neuron.Gemin2 Complexes." J Biol Chem **290**(33): 20185-20199.
Hahnen, E., I. Y. Eyupoglu, L. Brichta, K. Haastert, C. Trankle, F. A. Siebzehnrubl, M. Riessland, I. Holker, P. Claus, J. Romstock, R. Buslei, B. Wirth and I. Blumcke (2006). "In vitro and ex vivo evaluation of second-generation histone deacetylase inhibitors for the treatment of spinal muscular atrophy." J Neurochem **98**(1): 193-202.
Hahnen, E., R. Forkert, C. Marke, S. Rudnik-Schoneborn, J. Schonling, K. Zerres and B. Wirth (1995). "Molecular analysis of candidate genes on chromosome 5q13 in autosomal recessive spinal muscular atrophy: evidence of homozygous deletions of the SMN gene in unaffected individuals." Hum Mol Genet **4**(10): 1927-1933.
Hales, K. G. and M. T. Fuller (1997). "Developmentally regulated mitochondrial fusion mediated by a conserved, novel, predicted GTPase." Cell **90**(1): 121-129.
Hanna, J., D. S. Leggett and D. Finley (2003). "Ubiquitin depletion as a key mediator of toxicity by translational inhibitors." Mol Cell Biol **23**(24): 9251-9261.
Hao le, T., M. Wolman, M. Granato and C. E. Beattie (2012). "Survival motor neuron affects plastin 3 protein levels leading to motor defects." J Neurosci **32**(15): 5074-5084.
Harper, J. M., A. B. Salmon, Y. Chang, M. Bonkowski, A. Bartke and R. A. Miller (2006). "Stress resistance and aging: influence of genes and nutrition." Mech Ageing Dev **127**(8): 687-694.
Hars, E. S., H. Qi, A. G. Ryazanov, S. Jin, L. Cai, C. Hu and L. F. Liu (2007). "Autophagy regulates ageing in C. elegans." Autophagy **3**(2): 93-95.
Hauke, J., M. Riessland, S. Lunke, I. Y. Eyupoglu, I. Blumcke, A. El-Osta, B. Wirth and E. Hahnen (2009). "Survival motor neuron gene 2 silencing by DNA methylation correlates with spinal muscular atrophy disease severity and can be bypassed by histone deacetylase inhibition." Hum Mol Genet **18**(2): 304-317.
He, Y. and H. Jasper (2014). "Studying aging in Drosophila." Methods **68**(1): 129-133.
He, Y., M. M. Zheng, Y. Ma, X. J. Han, X. Q. Ma, C. Q. Qu and Y. F. Du (2012). "Soluble oligomers and fibrillar species of amyloid beta-peptide differentially affect cognitive functions and hippocampal inflammatory response." Biochem Biophys Res Commun **429**(3-4): 125-130.
Heckscher, E. S., S. R. Lockery and C. Q. Doe (2012). "Characterization of Drosophila larval crawling at the level of organism, segment, and somatic body wall musculature." J Neurosci **32**(36): 12460-12471.
Hermann, G. J., J. W. Thatcher, J. P. Mills, K. G. Hales, M. T. Fuller, J. Nunnari and J. M. Shaw (1998). "Mitochondrial fusion in yeast requires the transmembrane GTPase Fzo1p." J Cell Biol **143**(2): 359-373.

Hermann, H., P. Fabrizio, V. A. Raker, K. Foulaki, H. Hornig, H. Brahms and R. Luhrmann (1995). "snRNP Sm proteins share two evolutionarily conserved sequence motifs which are involved in Sm protein-protein interactions." EMBO J **14**(9): 2076-2088.
Hsu, A. L., C. T. Murphy and C. Kenyon (2003). "Regulation of aging and age-related disease by DAF-16 and heat-shock factor." Science **300**(5622): 1142-1145.
Iwata, A., B. E. Riley, J. A. Johnston and R. R. Kopito (2005). "HDAC6 and microtubules are required for autophagic degradation of aggregated huntingtin." J Biol Chem **280**(48): 40282-40292.
Kaganovich, D., R. Kopito and J. Frydman (2008). "Misfolded proteins partition between two distinct quality control compartments." Nature **454**(7208): 1088-1095.
Kapahi, P., B. M. Zid, T. Harper, D. Koslover, V. Sapin and S. Benzer (2004). "Regulation of lifespan in Drosophila by modulation of genes in the TOR signaling pathway." Curr Biol **14**(10): 885-890.
Karpac, J. and H. Jasper (2009). "Insulin and JNK: optimizing metabolic homeostasis and lifespan." Trends Endocrinol Metab **20**(3): 100-106.
Kastenmayer, J. P., L. Ni, A. Chu, L. E. Kitchen, W. C. Au, H. Yang, C. D. Carter, D. Wheeler, R. W. Davis, J. D. Boeke, M. A. Snyder and M. A. Basrai (2006). "Functional genomics of genes with small open reading frames (sORFs) in S. cerevisiae." Genome Res **16**(3): 365-373.
Keen, J. E., R. Khawaled, D. L. Farrens, T. Neelands, A. Rivard, C. T. Bond, A. Janowsky, B. Fakler, J. P. Adelman and J. Maylie (1999). "Domains responsible for constitutive and Ca(2+)-dependent interactions between calmodulin and small conductance Ca(2+)-activated potassium channels." J Neurosci **19**(20): 8830-8838.
Kenyon, C. (2005). "The plasticity of aging: insights from long-lived mutants." Cell **120**(4): 449-460.
Kenyon, C. J. (2010). "The genetics of ageing." Nature **464**(7288): 504-512.
Khoo, B. and A. R. Krainer (2009). "Splicing therapeutics in SMN2 and APOB." Curr Opin Mol Ther **11**(2): 108-115.
Klionsky, D. J., Z. Elazar, P. O. Seglen and D. C. Rubinsztein (2008). "Does bafilomycin A1 block the fusion of autophagosomes with lysosomes?" Autophagy **4**(7): 849-850.
Koga, H., S. Kaushik and A. M. Cuervo (2011). "Protein homeostasis and aging: The importance of exquisite quality control." Ageing Res Rev **10**(2): 205-215.
Komatsu, M. and Y. Ichimura (2010). "Physiological significance of selective degradation of p62 by autophagy." FEBS Lett **584**(7): 1374-1378.
Kong, L., X. Wang, D. W. Choe, M. Polley, B. G. Burnett, M. Bosch-Marce, J. W. Griffin, M. M. Rich and C. J. Sumner (2009). "Impaired synaptic vesicle release and immaturity of neuromuscular junctions in spinal muscular atrophy mice." J Neurosci **29**(3): 842-851.
Kraft, C., A. Deplazes, M. Sohrmann and M. Peter (2008). "Mature ribosomes are selectively degraded upon starvation by an autophagy pathway requiring the Ubp3p/Bre5p ubiquitin protease." Nat Cell Biol **10**(5): 602-610.
Krogan, N. J., G. Cagney, H. Yu, G. Zhong, X. Guo, A. Ignatchenko, J. Li, S. Pu, N. Datta, A. P. Tikuisis, T. Punna, J. M. Peregrin-Alvarez, M. Shales, X. Zhang, M. Davey, M. D. Robinson, A. Paccanaro, J. E. Bray, A. Sheung, B. Beattie, D. P. Richards, V. Canadien, A. Lalev, F. Mena, P. Wong, A. Starostine, M. M. Canete, J. Vlasblom, S. Wu, C. Orsi, S. R. Collins, S. Chandran, R. Haw, J. J. Rilstone, K. Gandi, N. J. Thompson, G. Musso, P. St Onge, S. Ghanny, M. H. Lam, G. Butland, A. M. Altaf-Ul, S. Kanaya, A. Shilatifard, E. O'Shea, J. S. Weissman, C. J. Ingles, T. R. Hughes, J. Parkinson, M. Gerstein, S. J. Wodak, A. Emili and J. F. Greenblatt (2006). "Global landscape of protein complexes in the yeast Saccharomyces cerevisiae." Nature **440**(7084): 637-643.
Kroiss, M., J. Schultz, J. Wiesner, A. Chari, A. Sickmann and U. Fischer (2008). "Evolution of an RNP assembly system: a minimal SMN complex facilitates formation of UsnRNPs in Drosophila melanogaster." Proc Natl Acad Sci U S A **105**(29): 10045-10050.

Kuwahara, T., A. Koyama, S. Koyama, S. Yoshina, C. H. Ren, T. Kato, S. Mitani and T. Iwatsubo (2008). "A systematic RNAi screen reveals involvement of endocytic pathway in neuronal dysfunction in alpha-synuclein transgenic C. elegans." Hum Mol Genet **17**(19): 2997-3009.
Lambrechts, A., A. Braun, V. Jonckheere, A. Aszodi, L. M. Lanier, J. Robbens, I. Van Colen, J. Vandekerckhove, R. Fassler and C. Ampe (2000). "Profilin II is alternatively spliced, resulting in profilin isoforms that are differentially expressed and have distinct biochemical properties." Mol Cell Biol **20**(21): 8209-8219.
Le, T. T., L. T. Pham, M. E. Butchbach, H. L. Zhang, U. R. Monani, D. D. Coovert, T. O. Gavrilina, L. Xing, G. J. Bassell and A. H. Burghes (2005). "SMNDelta7, the major product of the centromeric survival motor neuron (SMN2) gene, extends survival in mice with spinal muscular atrophy and associates with full-length SMN." Hum Mol Genet **14**(6): 845-857.
Lefebvre, S., L. Burglen, S. Reboullet, O. Clermont, P. Burlet, L. Viollet, B. Benichou, C. Cruaud, P. Millasseau, M. Zeviani and et al. (1995). "Identification and characterization of a spinal muscular atrophy-determining gene." Cell **80**(1): 155-165.
Libert, S., Y. Chao, J. Zwiener and S. D. Pletcher (2008). "Realized immune response is enhanced in long-lived puc and chico mutants but is unaffected by dietary restriction." Mol Immunol **45**(3): 810-817.
Lilienbaum, A. (2013). "Relationship between the proteasomal system and autophagy." Int J Biochem Mol Biol **4**(1): 1-26.
Lin, Y. J., L. Seroude and S. Benzer (1998). "Extended life-span and stress resistance in the Drosophila mutant methuselah." Science **282**(5390): 943-946.
Lindner, A. B. and A. Demarez (2009). "Protein aggregation as a paradigm of aging." Biochim Biophys Acta **1790**(10): 980-996.
Lints, F. A., M. Bourgois, A. Delalieux, J. Stoll and C. V. Lints (1983). "Does the female life span exceed that of the male? A study in Drosophila melanogaster." Gerontology **29**(5): 336-352.
Liu, Q., U. Fischer, F. Wang and G. Dreyfuss (1997). "The spinal muscular atrophy disease gene product, SMN, and its associated protein SIP1 are in a complex with spliceosomal snRNP proteins." Cell **90**(6): 1013-1021.
Lorson, C. L. and E. J. Androphy (2000). "An exonic enhancer is required for inclusion of an essential exon in the SMA-determining gene SMN." Hum Mol Genet **9**(2): 259-265.
Lorson, C. L., E. Hahnen, E. J. Androphy and B. Wirth (1999). "A single nucleotide in the SMN gene regulates splicing and is responsible for spinal muscular atrophy." Proc Natl Acad Sci U S A **96**(11): 6307-6311.
Lorson, C. L., J. Strasswimmer, J. M. Yao, J. D. Baleja, E. Hahnen, B. Wirth, T. Le, A. H. Burghes and E. J. Androphy (1998). "SMN oligomerization defect correlates with spinal muscular atrophy severity." Nat Genet **19**(1): 63-66.
Lotti, F., W. L. Imlach, L. Saieva, E. S. Beck, T. Hao le, D. K. Li, W. Jiao, G. Z. Mentis, C. E. Beattie, B. D. McCabe and L. Pellizzoni (2012). "An SMN-dependent U12 splicing event essential for motor circuit function." Cell **151**(2): 440-454.
Lunn, M. R. and C. H. Wang (2008). "Spinal muscular atrophy." Lancet **371**(9630): 2120-2133.
Madeo, F., A. Zimmermann, M. C. Maiuri and G. Kroemer (2015). "Essential role for autophagy in life span extension." J Clin Invest **125**(1): 85-93.
Markowitz, J. A., M. B. Tinkle and K. H. Fischbeck (2004). "Spinal muscular atrophy in the neonate." J Obstet Gynecol Neonatal Nurs **33**(1): 12-20.
Martin, R., K. Gupta, N. S. Ninan, K. Perry and G. D. Van Duyne (2012). "The survival motor neuron protein forms soluble glycine zipper oligomers." Structure **20**(11): 1929-1939.
Martinez, V. G., C. S. Javadi, E. Ngo, L. Ngo, R. D. Lagow and B. Zhang (2007). "Age-related changes in climbing behavior and neural circuit physiology in Drosophila." Dev Neurobiol **67**(6): 778-791.

Mattson, M. P. and T. Magnus (2006). "Ageing and neuronal vulnerability." Nat Rev Neurosci **7**(4): 278-294.
Mauvezin, C., C. Ayala, C. R. Braden, J. Kim and T. P. Neufeld (2014). "Assays to monitor autophagy in Drosophila." Methods **68**(1): 134-139.
McWhorter, M. L., U. R. Monani, A. H. Burghes and C. E. Beattie (2003). "Knockdown of the survival motor neuron (Smn) protein in zebrafish causes defects in motor axon outgrowth and pathfinding." J Cell Biol **162**(5): 919-931.
Meister, G., D. Buhler, B. Laggerbauer, M. Zobawa, F. Lottspeich and U. Fischer (2000). "Characterization of a nuclear 20S complex containing the survival of motor neurons (SMN) protein and a specific subset of spliceosomal Sm proteins." Hum Mol Genet **9**(13): 1977-1986.
Meister, G., D. Buhler, R. Pillai, F. Lottspeich and U. Fischer (2001). "A multiprotein complex mediates the ATP-dependent assembly of spliceosomal U snRNPs." Nat Cell Biol **3**(11): 945-949.
Meister, G. and U. Fischer (2002). "Assisted RNP assembly: SMN and PRMT5 complexes cooperate in the formation of spliceosomal UsnRNPs." EMBO J **21**(21): 5853-5863.
Melki, J., S. Abdelhak, P. Sheth, M. F. Bachelot, P. Burlet, A. Marcadet, J. Aicardi, A. Barois, J. P. Carriere, M. Fardeau and et al. (1990). "Gene for chronic proximal spinal muscular atrophies maps to chromosome 5q." Nature **344**(6268): 767-768.
Miguel-Aliaga, I., Y. B. Chan, K. E. Davies and M. van den Heuvel (2000). "Disruption of SMN function by ectopic expression of the human SMN gene in Drosophila." FEBS Lett **486**(2): 99-102.
Miguel-Aliaga, I., E. Culetto, D. S. Walker, H. A. Baylis, D. B. Sattelle and K. E. Davies (1999). "The Caenorhabditis elegans orthologue of the human gene responsible for spinal muscular atrophy is a maternal product critical for germline maturation and embryonic viability." Hum Mol Genet **8**(12): 2133-2143.
Miklos, G. L. and G. M. Rubin (1996). "The role of the genome project in determining gene function: insights from model organisms." Cell **86**(4): 521-529.
Morley, J. F., H. R. Brignull, J. J. Weyers and R. I. Morimoto (2002). "The threshold for polyglutamine-expansion protein aggregation and cellular toxicity is dynamic and influenced by aging in Caenorhabditis elegans." Proc Natl Acad Sci U S A **99**(16): 10417-10422.
Mortillaro, M. J. and R. Berezney (1998). "Matrin CYP, an SR-rich cyclophilin that associates with the nuclear matrix and splicing factors." J Biol Chem **273**(14): 8183-8192.
Nichols, C. D., J. Becnel and U. B. Pandey (2012). "Methods to assay Drosophila behavior." J Vis Exp(61).
Nlend Nlend, R., K. Meyer and D. Schumperli (2010). "Repair of pre-mRNA splicing: prospects for a therapy for spinal muscular atrophy." RNA Biol **7**(4): 430-440.
Nollen, E. A., S. M. Garcia, G. van Haaften, S. Kim, A. Chavez, R. I. Morimoto and R. H. Plasterk (2004). "Genome-wide RNA interference screen identifies previously undescribed regulators of polyglutamine aggregation." Proc Natl Acad Sci U S A **101**(17): 6403-6408.
O'Brochta, D. A., S. P. Gomez and A. M. Handler (1991). "P element excision in Drosophila melanogaster and related drosophilids." Mol Gen Genet **225**(3): 387-394.
Ogino, S., D. G. Leonard, H. Rennert, W. J. Ewens and R. B. Wilson (2002). "Genetic risk assessment in carrier testing for spinal muscular atrophy." Am J Med Genet **110**(4): 301-307.
Oprea, G. E., S. Krober, M. L. McWhorter, W. Rossoll, S. Muller, M. Krawczak, G. J. Bassell, C. E. Beattie and B. Wirth (2008). "Plastin 3 is a protective modifier of autosomal recessive spinal muscular atrophy." Science **320**(5875): 524-527.
Orr, W. C. and R. S. Sohal (2003). "Does overexpression of Cu,Zn-SOD extend life span in Drosophila melanogaster?" Exp Gerontol **38**(3): 227-230.
Otter, S., M. Grimmler, N. Neuenkirchen, A. Chari, A. Sickmann and U. Fischer (2007). "A comprehensive interaction map of the human survival of motor neuron (SMN) complex." J Biol Chem **282**(8): 5825-5833.

Pacifici, R. E. and K. J. Davies (1991). "Protein, lipid and DNA repair systems in oxidative stress: the free-radical theory of aging revisited." Gerontology **37**(1-3): 166-180.
Pandey, U. B. and C. D. Nichols (2011). "Human disease models in Drosophila melanogaster and the role of the fly in therapeutic drug discovery." Pharmacol Rev **63**(2): 411-436.
Pankiv, S., T. H. Clausen, T. Lamark, A. Brech, J. A. Bruun, H. Outzen, A. Overvatn, G. Bjorkoy and T. Johansen (2007). "p62/SQSTM1 binds directly to Atg8/LC3 to facilitate degradation of ubiquitinated protein aggregates by autophagy." J Biol Chem **282**(33): 24131-24145.
Parks, A. L., K. R. Cook, M. Belvin, N. A. Dompe, R. Fawcett, K. Huppert, L. R. Tan, C. G. Winter, K. P. Bogart, J. E. Deal, M. E. Deal-Herr, D. Grant, M. Marcinko, W. Y. Miyazaki, S. Robertson, K. J. Shaw, M. Tabios, V. Vysotskaia, L. Zhao, R. S. Andrade, K. A. Edgar, E. Howie, K. Killpack, B. Milash, A. Norton, D. Thao, K. Whittaker, M. A. Winner, L. Friedman, J. Margolis, M. A. Singer, C. Kopczynski, D. Curtis, T. C. Kaufman, G. D. Plowman, G. Duyk and H. L. Francis-Lang (2004). "Systematic generation of high-resolution deletion coverage of the Drosophila melanogaster genome." Nat Genet **36**(3): 288-292.
Partridge, L. and D. Gems (2002). "Mechanisms of ageing: public or private?" Nat Rev Genet **3**(3): 165-175.
Paushkin, S., B. Charroux, L. Abel, R. A. Perkinson, L. Pellizzoni and G. Dreyfuss (2000). "The survival motor neuron protein of Schizosacharomyces pombe. Conservation of survival motor neuron interaction domains in divergent organisms." J Biol Chem **275**(31): 23841-23846.
Paushkin, S., A. K. Gubitz, S. Massenet and G. Dreyfuss (2002). "The SMN complex, an assemblyosome of ribonucleoproteins." Curr Opin Cell Biol **14**(3): 305-312.
Pearn, J. (1980). "Classification of spinal muscular atrophies." Lancet **1**(8174): 919-922.
Pellizzoni, L., J. Baccon, J. Rappsilber, M. Mann and G. Dreyfuss (2002). "Purification of native survival of motor neurons complexes and identification of Gemin6 as a novel component." J Biol Chem **277**(9): 7540-7545.
Pellizzoni, L., B. Charroux and G. Dreyfuss (1999). "SMN mutants of spinal muscular atrophy patients are defective in binding to snRNP proteins." Proc Natl Acad Sci U S A **96**(20): 11167-11172.
Pellizzoni, L., J. Yong and G. Dreyfuss (2002). "Essential role for the SMN complex in the specificity of snRNP assembly." Science **298**(5599): 1775-1779.
Praveen, K., Y. Wen, K. M. Gray, J. J. Noto, A. R. Patlolla, G. D. Van Duyne and A. G. Matera (2014). "SMA-causing missense mutations in survival motor neuron (Smn) display a wide range of phenotypes when modeled in Drosophila." PLoS Genet **10**(8): e1004489.
Praveen, K., Y. Wen and A. G. Matera (2012). "A Drosophila model of spinal muscular atrophy uncouples snRNP biogenesis functions of survival motor neuron from locomotion and viability defects." Cell Rep **1**(6): 624-631.
Pyo, J. O., S. M. Yoo, H. H. Ahn, J. Nah, S. H. Hong, T. I. Kam, S. Jung and Y. K. Jung (2013). "Overexpression of Atg5 in mice activates autophagy and extends lifespan." Nat Commun **4**: 2300.
Rajendra, T. K., G. B. Gonsalvez, M. P. Walker, K. B. Shpargel, H. K. Salz and A. G. Matera (2007). "A Drosophila melanogaster model of spinal muscular atrophy reveals a function for SMN in striated muscle." J Cell Biol **176**(6): 831-841.
Raker, V. A., K. Hartmuth, B. Kastner and R. Luhrmann (1999). "Spliceosomal U snRNP core assembly: Sm proteins assemble onto an Sm site RNA nonanucleotide in a specific and thermodynamically stable manner." Mol Cell Biol **19**(10): 6554-6565.
Raker, V. A., G. Plessel and R. Luhrmann (1996). "The snRNP core assembly pathway: identification of stable core protein heteromeric complexes and an snRNP subcore particle in vitro." EMBO J **15**(9): 2256-2269.
Rana, A., M. Rera and D. W. Walker (2013). "Parkin overexpression during aging reduces proteotoxicity, alters mitochondrial dynamics, and extends lifespan." Proc Natl Acad Sci U S A **110**(21): 8638-8643.

Rapaport, D., M. Brunner, W. Neupert and B. Westermann (1998). "Fzo1p is a mitochondrial outer membrane protein essential for the biogenesis of functional mitochondria in Saccharomyces cerevisiae." J Biol Chem **273**(32): 20150-20155.
Renvoise, B., K. Khoobarry, M. C. Gendron, C. Cibert, L. Viollet and S. Lefebvre (2006). "Distinct domains of the spinal muscular atrophy protein SMN are required for targeting to Cajal bodies in mammalian cells." J Cell Sci **119**(Pt 4): 680-692.
Richardson, A., F. Liu, M. L. Adamo, H. Van Remmen and J. F. Nelson (2004). "The role of insulin and insulin-like growth factor-I in mammalian ageing." Best Pract Res Clin Endocrinol Metab **18**(3): 393-406.
Riessland, M., B. Ackermann, A. Forster, M. Jakubik, J. Hauke, L. Garbes, I. Fritzsche, Y. Mende, I. Blumcke, E. Hahnen and B. Wirth (2010). "SAHA ameliorates the SMA phenotype in two mouse models for spinal muscular atrophy." Hum Mol Genet **19**(8): 1492-1506.
Riessland, M., L. Brichta, E. Hahnen and B. Wirth (2006). "The benzamide M344, a novel histone deacetylase inhibitor, significantly increases SMN2 RNA/protein levels in spinal muscular atrophy cells." Hum Genet **120**(1): 101-110.
Rogina, B. and S. L. Helfand (2004). "Sir2 mediates longevity in the fly through a pathway related to calorie restriction." Proc Natl Acad Sci U S A **101**(45): 15998-16003.
Rogina, B. and S. L. Helfand (2013). "Indy mutations and Drosophila longevity." Front Genet **4**: 47.
Rossoll, W., S. Jablonka, C. Andreassi, A. K. Kroning, K. Karle, U. R. Monani and M. Sendtner (2003). "Smn, the spinal muscular atrophy-determining gene product, modulates axon growth and localization of beta-actin mRNA in growth cones of motoneurons." J Cell Biol **163**(4): 801-812.
Rossoll, W., A. K. Kroning, U. M. Ohndorf, C. Steegborn, S. Jablonka and M. Sendtner (2002). "Specific interaction of Smn, the spinal muscular atrophy determining gene product, with hnRNP-R and gry-rbp/hnRNP-Q: a role for Smn in RNA processing in motor axons?" Hum Mol Genet **11**(1): 93-105.
Ruan, H., X. D. Tang, M. L. Chen, M. L. Joiner, G. Sun, N. Brot, H. Weissbach, S. H. Heinemann, L. Iverson, C. F. Wu and T. Hoshi (2002). "High-quality life extension by the enzyme peptide methionine sulfoxide reductase." Proc Natl Acad Sci U S A **99**(5): 2748-2753.
Rubinsztein, D. C., J. E. Gestwicki, L. O. Murphy and D. J. Klionsky (2007). "Potential therapeutic applications of autophagy." Nat Rev Drug Discov **6**(4): 304-312.
Russman, B. S. (2007). "Spinal muscular atrophy: clinical classification and disease heterogeneity." J Child Neurol **22**(8): 946-951.
Rzezniczak, T. Z., L. A. Douglas, J. H. Watterson and T. J. Merritt (2011). "Paraquat administration in Drosophila for use in metabolic studies of oxidative stress." Anal Biochem **419**(2): 345-347.
Salgado-Garrido, J., E. Bragado-Nilsson, S. Kandels-Lewis and B. Seraphin (1999). "Sm and Sm-like proteins assemble in two related complexes of deep evolutionary origin." EMBO J **18**(12): 3451-3462.
Santel, A. and M. T. Fuller (2001). "Control of mitochondrial morphology by a human mitofusin." J Cell Sci **114**(Pt 5): 867-874.
Scharf, J. M., M. G. Endrizzi, A. Wetter, S. Huang, T. G. Thompson, K. Zerres, W. F. Dietrich, B. Wirth and L. M. Kunkel (1998). "Identification of a candidate modifying gene for spinal muscular atrophy by comparative genomics." Nat Genet **20**(1): 83-86.
Schmelzle, T. and M. N. Hall (2000). "TOR, a central controller of cell growth." Cell **103**(2): 253-262.
Scholz, S. and A. Singleton (2008). "Susceptibility genes in movement disorders." Mov Disord **23**(7): 927-934; quiz 1064.
Schrank, B., R. Gotz, J. M. Gunnersen, J. M. Ure, K. V. Toyka, A. G. Smith and M. Sendtner (1997). "Inactivation of the survival motor neuron gene, a candidate gene for human spinal

muscular atrophy, leads to massive cell death in early mouse embryos." Proc Natl Acad Sci U S A **94**(18): 9920-9925.
Schumacher, M. A., A. F. Rivard, H. P. Bachinger and J. P. Adelman (2001). "Structure of the gating domain of a Ca2+-activated K+ channel complexed with Ca2+/calmodulin." Nature **410**(6832): 1120-1124.
Shakkottai, V. G., C. H. Chou, S. Oddo, C. A. Sailer, H. G. Knaus, G. A. Gutman, M. E. Barish, F. M. LaFerla and K. G. Chandy (2004). "Enhanced neuronal excitability in the absence of neurodegeneration induces cerebellar ataxia." J Clin Invest **113**(4): 582-590.
Shankar, G. M., S. Li, T. H. Mehta, A. Garcia-Munoz, N. E. Shepardson, I. Smith, F. M. Brett, M. A. Farrell, M. J. Rowan, C. A. Lemere, C. M. Regan, D. M. Walsh, B. L. Sabatini and D. J. Selkoe (2008). "Amyloid-beta protein dimers isolated directly from Alzheimer's brains impair synaptic plasticity and memory." Nat Med **14**(8): 837-842.
Sharma, A., A. Lambrechts, T. Hao le, T. T. Le, C. A. Sewry, C. Ampe, A. H. Burghes and G. E. Morris (2005). "A role for complexes of survival of motor neurons (SMN) protein with gemins and profilin in neurite-like cytoplasmic extensions of cultured nerve cells." Exp Cell Res **309**(1): 185-197.
Skordis, L. A., M. G. Dunckley, B. Yue, I. C. Eperon and F. Muntoni (2003). "Bifunctional antisense oligonucleotides provide a trans-acting splicing enhancer that stimulates SMN2 gene expression in patient fibroblasts." Proc Natl Acad Sci U S A **100**(7): 4114-4119.
Sofola, O., F. Kerr, I. Rogers, R. Killick, H. Augustin, C. Gandy, M. J. Allen, J. Hardy, S. Lovestone and L. Partridge (2010). "Inhibition of GSK-3 ameliorates Abeta pathology in an adult-onset Drosophila model of Alzheimer's disease." PLoS Genet **6**(9): e1001087.
Sumner, C. J., T. N. Huynh, J. A. Markowitz, J. S. Perhac, B. Hill, D. D. Coovert, K. Schussler, X. Chen, J. Jarecki, A. H. Burghes, J. P. Taylor and K. H. Fischbeck (2003). "Valproic acid increases SMN levels in spinal muscular atrophy patient cells." Ann Neurol **54**(5): 647-654.
Sun, D., A. R. Muthukumar, R. A. Lawrence and G. Fernandes (2001). "Effects of calorie restriction on polymicrobial peritonitis induced by cecum ligation and puncture in young C57BL/6 mice." Clin Diagn Lab Immunol **8**(5): 1003-1011.
Suzuki, T., A. Kashiwagi, K. Mori, I. Urabe and T. Yomo (2004). "History dependent effects on phenotypic expression of a newly emerged gene." Biosystems **77**(1-3): 137-141.
Talbot, K., C. P. Ponting, A. M. Theodosiou, N. R. Rodrigues, R. Surtees, R. Mountford and K. E. Davies (1997). "Missense mutation clustering in the survival motor neuron gene: a role for a conserved tyrosine and glycine rich region of the protein in RNA metabolism?" Hum Mol Genet **6**(3): 497-500.
Tatar, M., A. Bartke and A. Antebi (2003). "The endocrine regulation of aging by insulin-like signals." Science **299**(5611): 1346-1351.
Taylor, J. P., F. Tanaka, J. Robitschek, C. M. Sandoval, A. Taye, S. Markovic-Plese and K. H. Fischbeck (2003). "Aggresomes protect cells by enhancing the degradation of toxic polyglutamine-containing protein." Hum Mol Genet **12**(7): 749-757.
Thibault, S. T., M. A. Singer, W. Y. Miyazaki, B. Milash, N. A. Dompe, C. M. Singh, R. Buchholz, M. Demsky, R. Fawcett, H. L. Francis-Lang, L. Ryner, L. M. Cheung, A. Chong, C. Erickson, W. W. Fisher, K. Greer, S. R. Hartouni, E. Howie, L. Jakkula, D. Joo, K. Killpack, A. Laufer, J. Mazzotta, R. D. Smith, L. M. Stevens, C. Stuber, L. R. Tan, R. Ventura, A. Woo, I. Zakrajsek, L. Zhao, F. Chen, C. Swimmer, C. Kopczynski, G. Duyk, M. L. Winberg and J. Margolis (2004). "A complementary transposon tool kit for Drosophila melanogaster using P and piggyBac." Nat Genet **36**(3): 283-287.
Ulgherait, M., A. Rana, M. Rera, J. Graniel and D. W. Walker (2014). "AMPK modulates tissue and organismal aging in a non-cell-autonomous manner." Cell Rep **8**(6): 1767-1780.
Urbe, S. (2005). "Ubiquitin and endocytic protein sorting." Essays Biochem **41**: 81-98.
van Ham, T. J., M. A. Holmberg, A. T. van der Goot, E. Teuling, M. Garcia-Arencibia, H. E. Kim, D. Du, K. L. Thijssen, M. Wiersma, R. Burggraaff, P. van Bergeijk, J. van Rheenen, G.

Jerre van Veluw, R. M. Hofstra, D. C. Rubinsztein and E. A. Nollen (2010). "Identification of MOAG-4/SERF as a regulator of age-related proteotoxicity." Cell **142**(4): 601-612.
van Ham, T. J., K. L. Thijssen, R. Breitling, R. M. Hofstra, R. H. Plasterk and E. A. Nollen (2008). "C. elegans model identifies genetic modifiers of alpha-synuclein inclusion formation during aging." PLoS Genet **4**(3): e1000027.
Vendruscolo, M., T. P. Knowles and C. M. Dobson (2011). "Protein solubility and protein homeostasis: a generic view of protein misfolding disorders." Cold Spring Harb Perspect Biol **3**(12).
Vernace, V. A., L. Arnaud, T. Schmidt-Glenewinkel and M. E. Figueiredo-Pereira (2007). "Aging perturbs 26S proteasome assembly in Drosophila melanogaster." FASEB J **21**(11): 2672-2682.
Wallace, D. C. (2005). "A mitochondrial paradigm of metabolic and degenerative diseases, aging, and cancer: a dawn for evolutionary medicine." Annu Rev Genet **39**: 359-407.
Wan, L., D. J. Battle, J. Yong, A. K. Gubitz, S. J. Kolb, J. Wang and G. Dreyfuss (2005). "The survival of motor neurons protein determines the capacity for snRNP assembly: biochemical deficiency in spinal muscular atrophy." Mol Cell Biol **25**(13): 5543-5551.
Wang, C. H., R. S. Finkel, E. S. Bertini, M. Schroth, A. Simonds, B. Wong, A. Aloysius, L. Morrison, M. Main, T. O. Crawford, A. Trela and S. M. A. S. o. C. Participants of the International Conference on (2007). "Consensus statement for standard of care in spinal muscular atrophy." J Child Neurol **22**(8): 1027-1049.
Wang, H., L. J. Wu, S. S. Kim, F. J. Lee, B. Gong, H. Toyoda, M. Ren, Y. Z. Shang, H. Xu, F. Liu, M. G. Zhao and M. Zhuo (2008). "FMRP acts as a key messenger for dopamine modulation in the forebrain." Neuron **59**(4): 634-647.
Wang, M. C., D. Bohmann and H. Jasper (2003). "JNK signaling confers tolerance to oxidative stress and extends lifespan in Drosophila." Dev Cell **5**(5): 811-816.
Wang, P. Y., N. Neretti, R. Whitaker, S. Hosier, C. Chang, D. Lu, B. Rogina and S. L. Helfand (2009). "Long-lived Indy and calorie restriction interact to extend life span." Proc Natl Acad Sci U S A **106**(23): 9262-9267.
Webb, J. L., B. Ravikumar, J. Atkins, J. N. Skepper and D. C. Rubinsztein (2003). "Alpha-Synuclein is degraded by both autophagy and the proteasome." J Biol Chem **278**(27): 25009-25013.
Welchman, R. L., C. Gordon and R. J. Mayer (2005). "Ubiquitin and ubiquitin-like proteins as multifunctional signals." Nat Rev Mol Cell Biol **6**(8): 599-609.
Williams, A., L. Jahreiss, S. Sarkar, S. Saiki, F. M. Menzies, B. Ravikumar and D. C. Rubinsztein (2006). "Aggregate-prone proteins are cleared from the cytosol by autophagy: therapeutic implications." Curr Top Dev Biol **76**: 89-101.
Winkler, C., C. Eggert, D. Gradl, G. Meister, M. Giegerich, D. Wedlich, B. Laggerbauer and U. Fischer (2005). "Reduced U snRNP assembly causes motor axon degeneration in an animal model for spinal muscular atrophy." Genes Dev **19**(19): 2320-2330.
Wirth, B., L. Brichta and E. Hahnen (2006). "Spinal muscular atrophy and therapeutic prospects." Prog Mol Subcell Biol **44**: 109-132.
Wirth, B., L. Brichta, B. Schrank, H. Lochmuller, S. Blick, A. Baasner and R. Heller (2006). "Mildly affected patients with spinal muscular atrophy are partially protected by an increased SMN2 copy number." Hum Genet **119**(4): 422-428.
Workman, E., L. Saieva, T. L. Carrel, T. O. Crawford, D. Liu, C. Lutz, C. E. Beattie, L. Pellizzoni and A. H. Burghes (2009). "A SMN missense mutation complements SMN2 restoring snRNPs and rescuing SMA mice." Hum Mol Genet **18**(12): 2215-2229.
Xia, X. M., B. Fakler, A. Rivard, G. Wayman, T. Johnson-Pais, J. E. Keen, T. Ishii, B. Hirschberg, C. T. Bond, S. Lutsenko, J. Maylie and J. P. Adelman (1998). "Mechanism of calcium gating in small-conductance calcium-activated potassium channels." Nature **395**(6701): 503-507.

Yankner, B. A., T. Lu and P. Loerch (2008). "The aging brain." Annu Rev Pathol **3**: 41-66.
Youle, R. J. and A. M. van der Bliek (2012). "Mitochondrial fission, fusion, and stress." Science **337**(6098): 1062-1065.
Young, P. J., N. T. Man, C. L. Lorson, T. T. Le, E. J. Androphy, A. H. Burghes and G. E. Morris (2000). "The exon 2b region of the spinal muscular atrophy protein, SMN, is involved in self-association and SIP1 binding." Hum Mol Genet **9**(19): 2869-2877.
Zhang, H., L. Xing, W. Rossoll, H. Wichterle, R. H. Singer and G. J. Bassell (2006). "Multiprotein complexes of the survival of motor neuron protein SMN with Gemins traffic to neuronal processes and growth cones of motor neurons." J Neurosci **26**(33): 8622-8632.
Zhang, H. L., F. Pan, D. Hong, S. M. Shenoy, R. H. Singer and G. J. Bassell (2003). "Active transport of the survival motor neuron protein and the role of exon-7 in cytoplasmic localization." J Neurosci **23**(16): 6627-6637.
Zhang, Z., F. Lotti, K. Dittmar, I. Younis, L. Wan, M. Kasim and G. Dreyfuss (2008). "SMN deficiency causes tissue-specific perturbations in the repertoire of snRNAs and widespread defects in splicing." Cell **133**(4): 585-600.

VITA

Swagata Ghosh

Born: 1985, Maldah, West Bengal, India.

Education:

August 2008- December 2016:	Ph. D, Biology, University of Kentucky
July 2005-June 2007:	MS, Biochemistry, Department of Biochemistry, Calcutta University, India.
July 2002-June 2005:	BS, Zoology, Calcutta University, India.

Awards:

Kentucky Opportunity Fellowship, University of Kentucky	Fall 2015
Gertrude Flora Ribble Mini Grant, Department of Biology, University of Kentucky	2012-2013
Gertrude Flora Ribble Mini Grant, Department of Biology, University of Kentucky	2011-2012
Gertrude Flora Ribble Mini Grant, Department of Biology, University of Kentucky	2010-2011
Indira Gandhi Scholarship, University Grants Commission, New Delhi	2005-2007
5th Rank, BS, Zoology, Calcutta University (out of ~2000 students)	2002-2005

Manuscripts in Preparation:

1. *The Serf gene contributes to SMA severity by altering SMN protein abundance in Drosophila disease model*. **Swagata Ghosh**, Douglas Harrison & Brian C. Rymond.

2. *The Serf gene expression promotes fruit fly longevity and delays tissue aging by upregulating autophagy during early life*. **Swagata Ghosh**, Douglas Harrison & Brian C. Rymond.